CRANFIELD UNIVERSITY

Matthew A. Upson

THE CARBON STORAGE BENEFITS OF AGROFORESTRY AND FARM WOODLANDS

SCHOOL OF APPLIED SCIENCES

Doctor of Philosophy
Academic Year: 2011 - 2014

Supervisor:
Dr. Paul Burgess
July 2014

CRANFIELD UNIVERSITY

Matthew A. Upson

THE CARBON STORAGE BENEFITS OF AGROFORESTRY AND FARM WOODLANDS

School of Applied Sciences

This thesis is submitted in partial fulfilment of the requirements for the degree of Doctor of philosophy.

Doctor of Philosophy
Academic Year 2011 - 2014

Supervisor:
Dr. Paul Burgess
July 2014

ABSTRACT

Planting trees on agricultural land either as farm woodlands or agroforestry (trees integrated with farming) is one option for reducing the level of atmospheric carbon dioxide. Trees store carbon as biomass, and may increase carbon storage in the ground.

A review of the literature outlined uncertainty relating to changes in carbon storage after planting trees on agricultural land. The aim of this thesis is to determine the impact of tree planting on arable and pasture land in terms of above and belowground carbon storage and thereby address these uncertainties, and assess the implications for the Woodland Carbon Code: a voluntary standard for carbon storage in UK woodlands.

Measurements of soil organic carbon to a depth of 1.5 m were taken at two field sites in Bedfordshire in the UK: a 19 year old silvoarable trial, and a 14 year old silvopasture and farm woodland. On average 60% and 40% of the soil carbon (relative to 1.5 m) was found beneath 0.2 and 0.4 m in depth respectively. Whilst tree planting in the arable system showed gains in soil organic carbon (12.4 t C ha^{-1} at 0–40 cm), tree planting in the pasture was associated with losses of soil organic carbon (6.1–13.4 t C ha^{-1} at 0–10 cm). Evidence from a nearby mature grazed woodland indicate that these losses may be recovered. No differences associated with tree planting were found to the full 1.5 m, though this may be due to a lack of statistical power.

Measurements of above and belowground biomass, and the root distribution of 19 year old poplar (*Populus* spp.) trees (at the silvoarable trial) and ash (*Fraxinus excelsior*) trees ranging from 7 to 21 years (at several field sites across Bedfordshire) were made, involving the destructive harvest of 48 trees. These measurements suggest that Forestry Commission yield tables overestimate yield for poplar trees grown in a silvoarable system. An allometric relationship for determining ash tree biomass from diameter measurements was established.

The biophysical model Yield-SAFE was updated to take into account root growth, and was parameterised using field measurements. It was successfully used to describe existing tree growth at two sites, and was then used to predict future biomass carbon storage at the silvoarable trial.

Measurements indicate that losses in soil carbon at relatively shallow depths can offset a large proportion of the carbon stored in tree biomass, but assessing changes on a site by site basis may be prohibitively expensive for schemes such as the Woodland Carbon Code.

KEYWORDS:
Agroforestry, Soil organic carbon, Woodland Carbon Code, Soil carbon fractionation, Yield tables, Modelling, Carbon storage

A philosopher, which is what I am supposed to be,
is a sort of intellectual yokel who gapes and
stares at what sensible people take for granted,
a person who cannot get rid of the feeling that
the barest facts of everyday life are unbelievably
odd. As Aristotle put it: the beginning of
philosophy is wonder.

— Alan Wilson Watts (1915 - 1973)

PUBLICATIONS

Some ideas and figures have appeared previously in the following publications:

Upson, MA, and Burgess, PJ (2013) Soil organic carbon and root distribution in a temperate arable agroforestry system, *Plant and Soil*, 373, 43–58.

COLOPHON

This document was produced using the typsetting language LaTeX using the typographical look-and-feel `classicthesis` developed by André Miede[1].

Data arrangement, statistical analysis, and the graphical presentation of results was completed in the statistical computing environment `R` (R Development Core Team, 2013). `R` code was combined with LaTeX using the package knitR (Xie, 2012). Coding and compilation of the pdf documents was completed using RStudio (RStudio, 2012). `R` and LaTeX code used to compile this thesis is available as a private github repository[2].

1 The style was inspired by Robert Bringhurst's seminal book on typography *"The Elements of Typographic Style"*: `http://code.google.com/p/classicthesis/`

2 `https://github.com/ivyleavedtoadflax`

ACKNOWLEDGMENTS

A piece of advice I was given in writing up my MSc thesis which has stuck with me, was that you should always include acknowledgements: firstly because it is the polite thing to do, and second because it may be the only place in a thesis that one may express some personality, and perhaps even some wit! With this sound advice in mind, I make no apologies for the lengthy thanks that follow.

Of course, my first thanks must go to my funders: Cranfield University (particularly William Stephens), the Silsoe heritage fund, Forest Research and the Forestry Commission, and the Scottish Forestry Trust. Without the financial support of these institutions, this PhD would not have happened, so my grateful acknowledgements to all involved.

In particular, my great thanks go to my supervisor Paul Burgess. Paul was instrumental in helping me to convert my MSc by Research into a PhD, and has unfailingly made himself available to offer guidance and support throughout, and certainly deserves no small credit for its successful completion. Paul, thank you.

I would also like to thank the other members of my thesis committee: associate supervisor Anil Graves, subject advisor Guy Kirk, and independent chairman Andrew Starr. Your constructive comments over drafts and presentations have been valuable.

Thank you also to James Morison of Forest Research for his help in securing funding, refining ideas, and the loan of vital equipment. To other researchers at Forest Research: Elena Vanguelova, and Eric Cassella, thank you also for your contribution.

A considerable amount of field and lab work was completed in the course of this PhD, and I have been very lucky to have had the support of four interns to complete the work. François Clavagnier assisted me for the first four months of my PhD in 2011 in conducting all of the fieldwork of my first year, and much of the lab work. François' help was indispensible – those were probably the most productive four months of the entire three years! Ellie Chandler, a local sixth form student (and now biology undergraduate it pleases me to say) assisted me for six weeks in 2012, during which time we measured some thousand ash trees. Claire Smith, another local sixth form student also helped me for six weeks in 2013, and bravely tackled some pretty tedious lab work. Finally Irene Friás-Hornillos helped me most recently for three months in 2014, very competently conducting the frustrating process of soil carbon fractionation, the results of which sadly did not make it into this thesis in time, but will make it into a resulting paper. Thanks to all four of you! Thanks also to Richard Andrews, Jan Bingham, and particularly Maria Biskupska for their patience in helping me, and my interns with laboratory work.

I have made use of several datasets which were presented by other students in their theses before me. In particular, acknowledgements are due to Julius Nkomaula and Pascal Pasturel, whose data were essential for observations of poplar roots.

In total, nine field sites were used throughout this PhD, my thanks to Bob Walker, Ian Froggatt, James Russell, Andy Lingard, Ed Burnett, and Doug and Charlie Tompkins for their co-operation in allowing me to use their sites.

On a personal note, my thanks to my friends, old and new, who have helped me through what can, at times, be a difficult process. In particular: Syd Howells and the other members of 'Height Club' who have joined me for many a fine day in the canopy of a beautiful beech tree; and Bruce Fitzsimons, Terry Howe, and my other training partners of the last three years, who have taught me at least as much about myself as about the *arte suave*. And to Lisa Fenton, soon to finish her own thesis, who helped put the whole crazy PhD notion in my head in the first place.

Finally my thanks to my girlfriend Marta, who has given me so much support in the closing months of my PhD; it was my great pleasure to support her while she wrote her thesis, and she has more than repaid me in kind. And to my parents, whose constant encouragement, support, and pride, has helped sustain me over the last three years, and indeed the last thirty.

CONTENTS

ACRONYMS

AM	arbuscular mycorrhizae
AIC	Aikake information criterion
ANOVA	analysis of variance
AOGCM	atmosphere-ocean global circulation model
BR	Buttons Ramsay
CAI	current annual increment
CAP	Common Agricultural Policy
C%	carbon content
CI	confidence interval
CP	Clapham Park
CV	coefficient of variation
D_{30}	diameter at 30 cm
D_{bh}	diameter at breast height
DOC	dissolvable organic carbon fraction
ESM	equivalent soil mass
AR4	Fourth Assessment Report
M	fresh mass
FRLD	fine root length density
FRMD	fine root mass density
FW	farm woodland
GHG	greenhouse gas
GMST	Global Mean Surface Temperature
IPCC	Intergovernmental Panel on Climate Change
LER	Land Equivalent Ratio
LOI	weight loss on ignition
LULUCF	land use, land use change and forestry
LSD	least significant difference
M_e	dry mass
MAFF	Ministry of Agriculture, Fisheries and Food
MAI	mean annual increment
mc	moisture content
MD	mass density
MP	Millennium Country Park
n_{adj}	number of adjacent trees
NTFP	non-timber forest product

nRMSE	normalised Root Mean Squared Error
C_o%	organic carbon content
PA	pasture
PES	Payments for Ecosystem Services
POM	particulate organic matter
PSD	particle size determination
RF	radiative forcing
RL	Randall's Farm
RY	Reynold's Wood
RW	Ridgeway Wood
rSOC	chemically resistant soil organic carbon
S_{130}	number of stems at 130 cm height
S_{30}	number of stems at 30 cm height
S+A	sand and stable aggregates
s+c	silt and clay fraction
SAB	sycamore, ash, and birch
SAFE	Silvoarable Agroforestry for Europe
SD	standard deviation
ρ_b	soil bulk density
SOC	soil organic carbon
SOM	soil organic matter
SOP	standard operating procedure
SP	silvopasture
TSI	total solar irradiance
UKMO	UK Met Office
VD	van Diemen's land
WCC	Woodland Carbon Code
WRB	World Reference Base for Soil Resources
YN	Yelnow New Wood

Part I

INTRODUCTION

Climate Change is the greatest threat
that human civilization has ever faced.

— Angela Merkel (1954 - Present)

1 INTRODUCTION

This chapter provides an introduction to the context of the research questions, the aim, the objectives, and the structure of the thesis.

1.1 CLIMATE CHANGE

During the twentieth century, measurements of global mean temperature began to indicate a strong warming trend. Between 1880 and 2012 global mean temperature[1] is estimated by the Intergovernmental Panel on Climate Change (IPCC) to have increased by $0.85 \pm 0.2°C$[2], and it is thought that 1983 to 2012 was the warmest period for the last 800 years in the northern hemisphere (Stocker et al., 2013, p.37). A number of factors can influence the Earth's climate, for instance perturbations of the Earth's orbit (Goosse, 2005; Hays et al., 1976), variations in the radiation output of the sun (Eddy, 1976; Labitzke and Matthes, 2003), and the amount of radiation reflected back from the Earth's surface (Kirschbaum et al., 2011; Winton, 2006). However, recent rises in global temperature have been directly linked to the rise of atmospheric concentrations of greenhouse gases, such as CO_2, CH_4, and N_2O (Foster et al., 2007).

Whilst the greenhouse effect, and the presence of greenhouse gases (GHGs) in the atmosphere is entirely natural, the rate of change in the concentrations of these gases is unprecedented in human history: concentrations of CO_2 in particular have increased by 36% over the last 250 years, whilst in the previous 8000 years, CO_2 concentrations increased by an equivalent 0.005% (Foster et al., 2007, p.137).

The first predictions about a rise in temperature caused by an increase in atmospheric CO_2 were published in 1896 (Arrhenius, 1896), and it is well understood that the burning of fossil fuels for electricity, heat, and transport are major sources of GHG release. Other sources of GHGs include the forestry and agricultural sectors where in particular, land use changes, and emissions from rice, and cattle are major contributors (IPCC, 2007; Nabuurs et al., 2007; UNEP, 2011).

Projections of the extent of climate change are typically divided into a number of scenarios relating to future emissions of GHGs, changes in human population, economic growth, and the adoption of 'greener' technologies (IPCC, 2000*a*). Based on the most recent predictions by the IPCC, global mean surface warming (relative to 1986–2005) is predicted to be between 1.0 °C to 2.0 °C by 2046–2065 (95% CIs: 0.4 °C to 2.6 °C), and between 1.0 °C to 3.7 °C by 2081–2100 (95% CIs: 0.3 °C to 4.8 °C) (Stocker et al., 2013, p.90).

The implications of unchecked increases in global mean temperature are severe. Broadly speaking it is expected that there will be an increase in hotter and longer heatwaves, more severe precipitation events, and conversely an increased likelihood of drought (Meehl et al., 2007). Globally, snow cover, sea ice, glaciers, and

1 Values given here are globally averaged combined land and ocean temperature.
2 90% confidence interval (CI).

ice caps are all expected to shrink leading to sea level rise, and a positive feedback loop owing to reduced reflection (albedo) of solar radiation due to reduced snow cover (Winton, 2006). A second positive feedback loop may also be initiated by the melting of perma-frost and the release of large amounts of stored carbon as CO_2 or CH_4 (Schuur et al., 2008).

Changes in ocean acidity owing to an increase in dissolved CO_2 are likely to affect marine wildlife, and the sea level rise is likely to increase flooding risk to coastal settlements (Meehl et al., 2007). Large numbers of species face extinction risk, whilst largely negative consequences are expected for food production over the long-term (IPCC, 2007).

1.2 MITIGATION

Despite this largely negative outlook, as recently as 2011, reports have indicated that it is within our means and technological capabilities to constrain temperature rises to 2°C by acting before 2020 (UNEP, 2011). Such an effort would require reductions in GHG emissions across a range of sectors, including forestry and agriculture. Such an approach is sometimes referred to as the 'climate wedge' approach: making achievable changes across a number of sectors ('wedges') can reduce the overall impact of climate change (Pacala and Socolow, 2004).

Reducing emissions from forestry and agriculture is a key part of this approach (UNEP, 2011). In the agricultural sector, substantial emissions come from CH_4 and N_2O either from enteric fermentation within the gut of livestock, or microbial processes in the soil, often the result of rice cultivation (Smith et al., 2007). Emissions related to the release of CO_2 from the soil are also important, and are likely to be accelerated by the warming trend. Jenkinson et al. (1991) suggest soil C emissions over the next 60 years could be almost a fifth of unmitigated fossil fuel use over the same period, whilst Bellamy et al. (2005) suggest that UK soil C losses may be equivalent to almost a tenth of national industrial C output. Strategies for mitigating emissions in the agricultural sector focus on three main areas: reducing emissions from land, improving the C sequestration potential of land, and avoiding emissions related to management practices (Koga et al., 2006; Paustian et al., 2004; Smith et al., 2007).

In the forestry sector, important steps to reduce emissions are increasing global forest area, increasing the C density of forested land (Nabuurs et al., 2007), increasing C storage in durable woody products, and importantly: substituting more C intensive materials for timber based products (Burgess et al., 2010; Gustavsson and Sathre, 2006; Perez-Garcia et al., 2005).

Tree planting within agricultural landscapes increases C density of the land, increases forested area, and provides scope for the displacement of more C intensive materials. However, all this must be weighed up in the context of a rising population, the expectation that global population will reach 9 billion by 2050 (UNESA, 2004), and the potentially negative changes to worldwide food production (IPCC, 2007). Food security and the reduction of emissions of GHGs are thus two challenges that must be faced simultaneously, and increasingly on the same areas of land (UNFAO, 2009).

1.3 AGROFORESTRY AND FARM WOODLANDS

'Agroforestry' is the practice of deliberately integrating woody vegetation (trees and shrubs) with crop and/or animal production systems to benefit from the resulting ecological and economic interactions (AGFORWARD, 2014).

By practicing 'agroforestry' and combining trees with agricultural practices, it is possible to maintain the GHG mitigation benefits of forestry whilst continuing to produce food on the same unit of land. In addition, agroforestry systems have been demonstrated to provide improved ecosystem services compared to tree-less agriculture, for instance: improved biodiversity, pest control, erosion control, and soil enrichment (Jose, 2009; Klaa et al., 2005; Peng and Sutton, 1996; Williams-Guillen et al., 2008). These are services which are likely to become increasingly important in a world impacted by climate change.

During the 20th Century, most trees planted on UK farms were planted as 'farm woodlands', typically on marginal land. Such woodlands provide a number of services to farmers, including woodfuel and timber, windbreaks, shelter and cover for game (Burgess et al., 2000). At the farm and landscape scale, farm woodlands may be considered agroforestry systems, and offer many of the benefits of more intimately mixed combinations.

Such woodlands can be registered by the Woodland Carbon Code (WCC), a voluntary scheme which offers procedures for quantifying C storage within new UK woodlands (Forestry Commission, 2013). Launched in 2012 by the Forestry Commission, the Woodland Carbon Code has, to date, registered over 200 woodlands equating to over 15 000 ha of land, and over a million metric tonnes of C expected to be stored in the lifetime of the registered woodlands (Darot, 2014).

Soil C storage typically is much larger than C stored in biomass on a per hectare basis (depending on soil depth, e.g. Peichl et al., 2006) and therefore the two must be considered in concert, as small negative changes in soil organic carbon (SOC) storage can negate gains in aboveground C storage (Carney et al., 2007). Sampling depth is therefore a critical consideration (Harper and Tibbett, 2013), and in the temperate environment few studies consider SOC storage at depths greater than 60 cm; this is recognised as an impediment to a comprehensive understanding of soil C dynamics (Shi et al., 2013). Furthermore, while many studies exist that examine land-use change from pure agricultural to forestry systems (and vice versa), few studies consider the establishment of agroforestry systems, fewer still consider such systems to any great depth, and almost no studies of this kind exist for the UK at all. Understanding SOC changes at depth however presents a statistical challenge that is not always recognised; quantifying the uncertainty, and developing techniques to adequately sample SOC in deep soil horizons should be considered a critical area of soil C research (Hungate et al., 1995; Kravchenko and Robertson, 2011).

Longevity of storage is also an important consideration, as each 'pool' has a different rate of C 'turnover' – sometimes referred to as a 'residence time'. Aboveground tree C turnover varies according to the rotation length (usually somewhere upwards of three decades depending on species (Hamilton, 1996)); the longevity of coarse root C can usually be measured in years rather than decades (Fahey and Arthur, 1994; Janzen, 2005), whilst the longevity of C stored in wooden products

may be as little as a few months, or as long as a century (Thompson and Matthews, 1989). The longevity of SOC is also important, and conceptually it can be useful to think of three 'pools': an active or labile pool which has a turnover rate measurable in months or years, a slow pool which is likely to persist for decades, and a passive or recalcitrant pool in which C may be stored for centuries or millennia (Gaudinski et al., 2000; Rumpel et al., 2002; Schöning and Kögel-Knabner, 2006). The relative longevity of biomass C and SOC should therefore be compared when attempting to assess the overall impact of tree planting on the C density of a site.

1.4 RESEARCH QUESTIONS AND HYPOTHESES

This research project was developed to address an applied and a strategic question:

1. **What is the effect of tree planting on arable and pasture land on above and belowground carbon stocks?**

2. **What are the implications for carbon sequestration standards such as the Woodland Carbon Code?**

In order to answer the applied question, a number of hypotheses were developed which are tested in the subsequent chapters. These are summarised here, but are developed within the wider literature context in the literature review.

Hypotheses

1. Establishing silvoarable agroforestry systems on arable land will increase soil organic carbon (SOC) stocks relative to a pure arable control.
2. The incorporation of trees into the arable environment will lead to increases in soil organic carbon (SOC) storage at depth.
3. Tree related SOC is more stable than arable crop or grass related SOC.
4. Planting trees on grassland will lead to a decline in SOC stock.
5. Losses of SOC from tree planting on grassland are dependent on the density of the tree planting.
6. Using traditional forestry yield tables to predict the growth of trees in agroforestry systems and farm woodlands (which are typically planted at much wider spacings) will over-estimate yield.
7. Small losses in SOC may offset a large proportion of gains of C in aboveground tree biomass.
8. Frequentist hypothesis testing is an appropriate tool to determine differences in SOC in newly planted woodlands.

The project began in May 2011, originally as an MSc by Research focused on the Silsoe experimental site, a poplar based silvoarable system. In May 2012, the research was extended to a PhD after receiving support from Forest Research and the Scottish Forestry Trust. Consequently, the scope was widened to incorporate

ash tree measurements at a variety of sites across Bedfordshire, and soil C measurements at Clapham Park, a silvopastoral site in Bedfordshire, UK.

1.5 THESIS STRUCTURE

The thesis is divided into four parts, containing a total of eleven chapters (Figure 1.1), followed by references and appendices.

The first part (Chapters 1–3) comprises the literature review, and the framing of the project objectives, followed by a general methodology section. The literature review is itself split into two; the first section offers a general review of climate change, the link with anthropogenic activity, and options for mitigation, particularly with reference to the forestry and agricultural sectors. The second section gives a description of agroforestry and tree planting on farms, and a more focused review on their role in the global carbon balance, the nature of soil carbon and methods for measuring it. The methodology section outlines the broad methods used in the thesis and provides a description of the two main field sites used in the subsequent chapters.

Part II (Chapters 4–6) contains two studies of SOC in relation to tree planting at the field sites described in the general methodology, and concludes with a chapter considering the statistical difficulties of sampling SOC, with recommendations arising from this work.

Part III (Chapters 7–9) contains two studies concerned with aboveground C stored in biomass at the two study sites described in the methodology, amongst others. Measurements from Silsoe, an experimental site at Silsoe, Bedfordshire, in the UK, are incorporated into a biophysical model called Yield-SAFE, and this model used to make predictions about future growth.

The final part of the thesis provides a synthesis of the results presented so far: results from biomass and soil C pools are combined, and discussed in the context of the Woodland Carbon Code.

An appendix to each section and a general miscellaneous appendix is included at the end of the thesis.

Each chapter is formulated as an extended journal paper, with a short introduction, independent methods, results, discussion, conclusions, and bullet point summary.

1.6 CONTRIBUTION

Data from a variety of sources was used in this thesis. Most datasets were generated in the course of the three years' research, however some data relating to the silvoarable trial at the Cranfield Experimental Farm at Silsoe was inherited from previous research. In addition, some samples collected by the author were analysed by other researchers either at Cranfield University or externally. Appendix H provides a comprehensive summary of which datasets have been used in which chapter, and where these datasets originated. A summary of that information is included in Table 1.1.

Data for which attribution has been clearly indicated in the text, for instance yield table and weather data has not been included here.

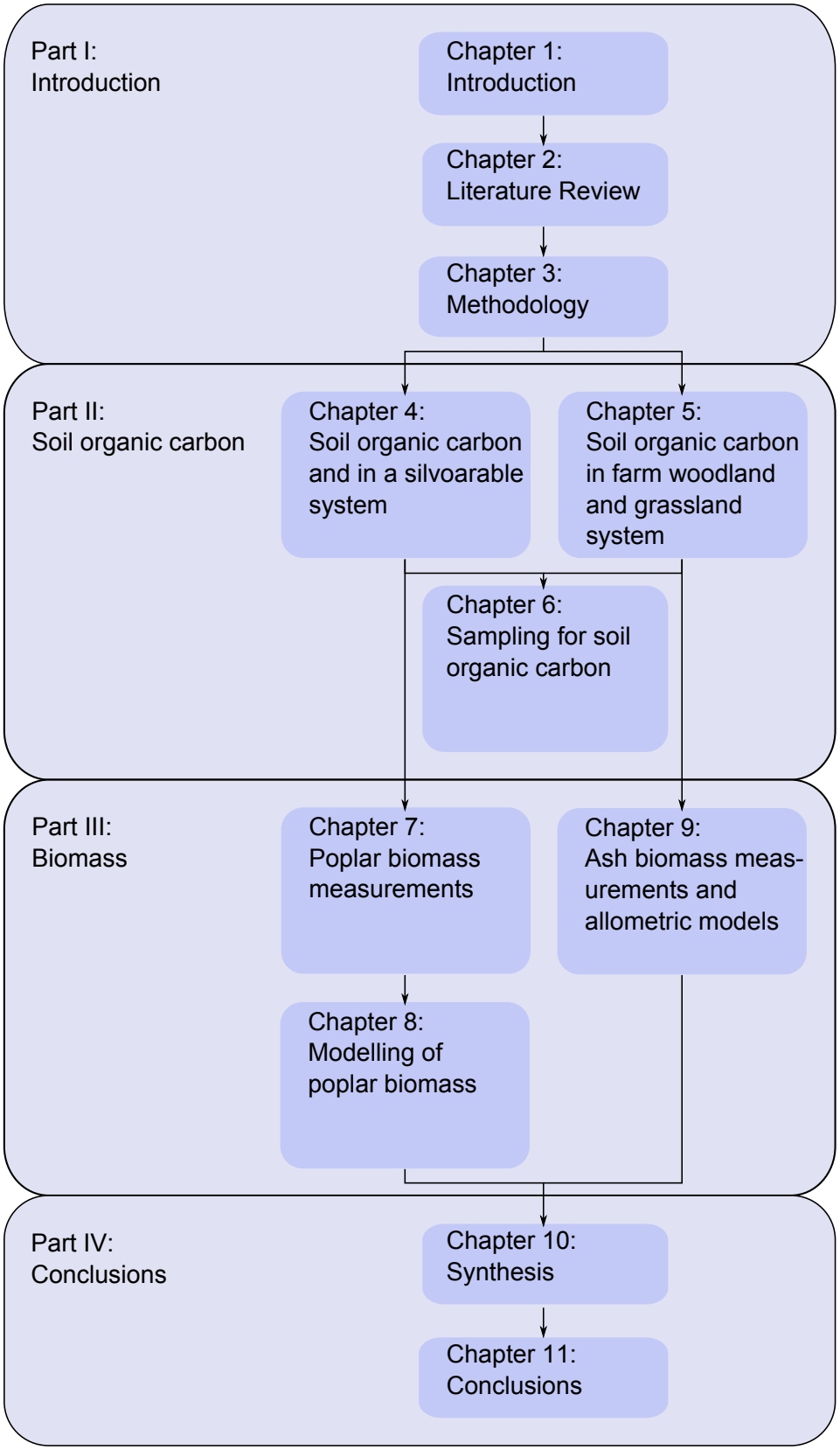

Figure 1.1: Thesis structure showing division of parts and chapters.

Table 1.1: Explanation of the sources of data used in each of the major chapters, and the approximate contribution of the author. Data originating from publications has not been included in this table, and is given the appropriate attribution in the text.

Chapter	Description	Contribution
4	New measurements of poplar root distribution, were completed with the help of François Clavagnier in addition to the collection of samples for soil bulk density (ρ_b) and organic carbon content ($C_o\%$) determination. Analysis of these samples was completed entirely by the author. Eighteen samples collected by the author were analysed by Andy Gregory of Rothamsted Research using the Zimmermann et al. (2007) fractionation procedure.	80%
5	Some particle size determination (PSD) analysis was completed by Claire Smith, but all other data presented in this chapter was generated by the author alone.	95%
6	This chapter used data presented in Chapter 5 in running simulations.	100%
7	Several new datasets relating to the biomass of different tree tissues were collected by the author with the help of Françcois Clavagnier. Historical mensuration data collected from the Silsoe silvoarable trial was also used.	80%
8	In this chapter, the model Yield-SAFE was parameterised with new data collected by the author (presented in Chapter 7). Historical data relating to crop yields at the Silsoe Leeds silvoarable trials presented by Burgess et al. (2003) were used for model calibration and validation, as were the most up-to-date poplar measurements from Leeds provided by Dr. David Pilbeam.	80%
9	The data presented in this chapter was entirely generated by the author with the assistance of interns Claire Smith, and Eleanor Chandler.	100%

2 LITERATURE REVIEW

This literature review is split into two sections. The first section gives a brief overview of the history and current understanding of climate change, including opportunities for mitigation in the agricultural and forestry sectors.

The second section gives a definition and history of agroforestry, a more in-depth examination of the potential of agroforestry for C sequestration, and the methods used to determine it. The key objectives of the thesis are framed in the literature context.

2.1 CLIMATE CHANGE

2.1.1 *The Earth's climate*

Climate can be defined as the average patterns of weather experienced over a time period, be it several millennia, a few months, or the nominal thirty years (Le Treut et al., 2007). It can be described for a specific location, region, or at the global level. At each scale climate is a complex system dependent on incoming solar radiation, the atmosphere, land surface, snow, ice, bodies of water, and flora and fauna (Le Treut et al., 2007).

Global climate is primarily driven by solar radiation, and the difference between the amount of solar radiation received and the amount of heat that is radiated back into space (Le Treut et al., 2007). Of the total solar radiation received by the earth, roughly a third is directly reflected back into space by clouds, atmospheric gasses and the ground (Figure 2.1). About half of the total solar radiation is absorbed by the earth's surface, whilst the remaining fifth is absorbed by the atmosphere. The energy absorbed by the earth is released back to the atmosphere over time, either as long-wave radiation, or through evapotranspiration, or the warming of air close to the earth's surface. From there, energy stored by the atmosphere is emitted directly into space, while a not insignificant portion is reflected back to earth in the so-called 'greenhouse effect' by the greenhouse gases (GHGs), including: water vapour (H_2O) carbon dioxide (CO_2), methane (CH_4), nitrous oxide (N_2O), ozone (O_3). Some of the energy absorbed by the earth is redistributed by the evaporation of water or the warming of air close to the earth's surface: each of these can also result in long wave radiation (Kleidon et al., 2000).

Global Mean Surface Temperature (GMST) has been increasing since the end of the 19th century, and in 2012 was around 0.9 ± 0.01°C[1] warmer than in 1880 (Hartmann et al., 2013, p.187). Consequently, the last 30 years (1983–2012) was most likely the warmest period in the northern hemisphere for the last 800, and possibly 1400 years (Stocker et al., 2013, p.37). In light of the above, the cause of

1 90% confidence intervals (CIs).

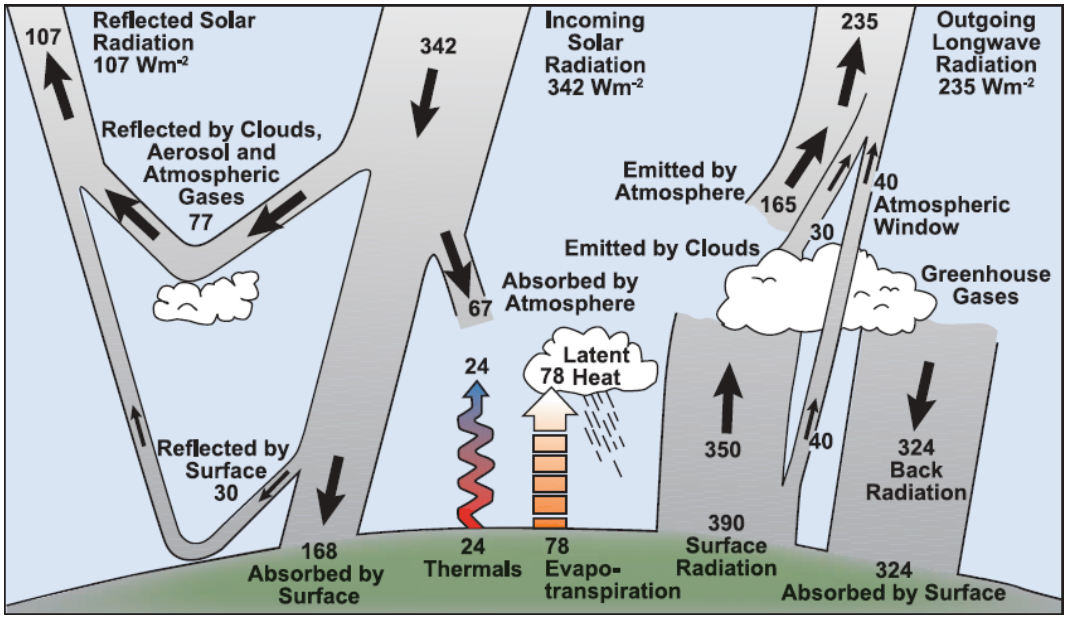

Figure 2.1: Estimate of the Earth's annual and global mean energy balance $\mathrm{W\,m^{-2}}$, from Kiehl and Trenberth (1997).

this recent climate change may have been caused by three factors (Le Treut et al., 2007):

1. Alterations to incoming solar radiation (i.e. by changes to the earth's orbit, or the intensity of radiation emitted by the sun

2. Changes to the fraction of solar radiation that is reflected back to space - so called 'albedo'. This can occur from, or example, changes in cloud cover, the size of ice caps, etc.)

3. Alterations to the emission of long-wave radiation back into space (e.g. by changing the atmospheric concentration of GHGs).

The sections that follow consider these three potential causes in turn.

2.1.1.1 *Radiative forcing*

In order to explain the causes behind the changes in the Earth's climate, scientists have attempted to quantify the key factors which may affect it. These are generally explained in terms of radiative forcing (RF). RF is the influence that a given factor can have on the earth's climate. *Radiative*: because ultimately factors which affect the climate are influencing the balance of incoming and outgoing radiation; and *forcing*: because these factors push the balance of the Earth's incoming and outgoing radiation away from the 'normal state' (Foster et al., 2007). RF is usually defined as the 'rate of energy change per unit area of the globe as measured at the top of the atmosphere' and is measured in units of $\mathrm{W\,m^{-2}}$ (Foster et al., 2007).

RF can either be positive or negative: when positive, more energy is retained in the Earth-atmosphere system leading to warming; when negative, more energy is radiated away, hence cooling will occur (Foster et al., 2007).

2.1.1.2 *Astronomical factors*

The Earth's orbit Variations in the amount of solar radiation that warms the earth have long been observed. One source of these variations are the changes in the earth's orbit. Much of our modern understanding of the subject comes from the work of Milankovitch in the early twentieth century. However, it was not until later in the century that Hays et al. (1976) were able to link 'Milankovitch' cycles with climate data extracted from ice cores, allowing them to conclude that Quaternary ice ages were a direct result of changes in the geometry of earth's orbit.

Orbital changes are not thought to have had a major influence on the earth's climate over the last thousand years. Nevertheless, changes in the order of 0.33 and 0.83 $W\,m^{-2}$ have been estimated for changes in summer and winter RF for 45° N (Goosse, 2005).

Solar irradiance Measurements of total solar irradiance (TSI) for the top of the atmosphere over the last century have settled on a figure of about 1365 $W\,m^{-2}$ (Le Treut et al., 2007). This value subject to cyclical variations on a number of timescales. Total solar irradiance varies on a 27-day rotational cycle, the 11-year (Schwabe) cycle, the 88-year (Gleisberg) cycle, a roughly 200 year cycle, and much longer variations over 20 000 and 40 000 years due to wider orbital changes (Labitzke and Matthes, 2003).

In the case of the 11-year cycle, these variations are a result of the interplay of different solar phenomena: solar faculae (essentially bright spots), sunspots, and groups of sunspots (Labitzke and Matthes, 2003). The 'Little Ice Age', a well documented cold period extending from the 16^{th} to the 19^{th} centuries has been linked to two sunspot minima: the 'Spörer Minimum' (c.1460-1550), and the 'Maunder Minimum' (c.1645-1715, Eddy, 1976). During the 'Little Ice Age', the River Thames froze 23 times, during which time Frost Fairs were sometimes held on the ice (Figure 2.2). Many other depictions of cold extremes were captured by artists during this period.

Despite these variations, the current rate of irradiance is considered to be similar to that of the last glacial maximum. It is thought therefore that changes in atmospheric composition and surface albedo, are the major factors contributing to changes in the earth's climate (Hegerl et al., 2007).

2.1.1.3 *Surface albedo*

Albedo is a measure of reflectivity – essentially how much energy (be it light, or heat) that a surface reflects; for example, an albedo of 0.2 means that 20% of the radiation is reflected. In the climatological context, surface albedo refers to the reflection of shortwave radiation to space due to changes in the earth's reflectivity – principally snow and ice cover (Winton, 2006).

Whereas the albedo of fresh snow may be as high as 90%, ocean, and other terrestrial environments may have significantly lower reflectance values. Woodlands for example, are considered to have an albedo of around 13%, whilst pasture is typically higher at 20% (Kirschbaum et al., 2011). Hence, there is a positive feedback effect when warming of the planet results in a loss of snow and ice cover, and a consequent decrease in albedo (Winton, 2006).

Figure 2.2: Frost Fair on the Thames (1683–1684) as depicted by Thomas Wycke (Public domain).

Radiative forcing as a result of surface albedo is thought to be relatively unimportant when compared to the effect of GHGs, hence the Third Assessment Report of the IPCC settled on change in RF of -0.2 ± 0.2 W m^{-2} since 1750 (Figure 2.4, Foster et al., 2007). The size of the uncertainty interval, indicates the relative lack of scientific understanding in this field at present.

Burning of biomass carbon has also been found to have a negative effect on the albedo of snow, due to the deposition of soot. The Fourth Assessment Report (AR4) of the IPCC adopts a RF estimate of $+0.10 \pm 0.10$ W m^{-2} (Figure 2.4), indicating the considerable uncertainty surrounding the phenomenon (Lemke et al., 2007).

Changes in land use may also have an influence on surface albedo; forest cover can be darker and less reflective than for example pasture. (Kirschbaum et al., 2011) report that a change in albedo from 20% to 13% associated with establishment of the darker forest canopy was been found to negate up to 24% of carbon storage benefits in woody biomass of *Pinus radiata* plantations (Kirschbaum et al., 2011). The impact of albedo changes therefore complicate the question of afforestation as a tool for carbon sequestration (Betts et al., 2007).

2.1.1.4 *The Greenhouse effect*

The greenhouse effect is a natural phenomenon, without which life as we know it would not be possible on Earth. Global mean surface temperatures would be well below freezing, if not for the action of complex molecules such as H_2O and CO_2 in absorbing and re-radiating escaping heat back to earth (Le Treut et al., 2007).

The idea that changes to atmospheric composition effected by human activity may influence the greenhouse effect, and thereby terrestrial temperatures, is not new. As early as 1896, attempts to quantify the contribution of CO_2 to the greenhouse effect appeared in the literature (Arrhenius, 1896). Arrhenius calculated that a two-fold increase in the concentration of atmospheric CO_2 would result in an in-

crease of global surface temperatures of about 4°C; and despite being aware of the link with fossil fuel consumption, he did not foresee this as being a concern for mankind (Fleming, 1998).

Recent measurements have confirmed that the atmospheric composition of CO_2 has increased from an average 280 ppm (pre-1750), to 379 ppm in 2005, a change of about 36% over the last 250 years (Foster et al., 2007). Measurements at the Mauna Loa observatory in Hawaii recorded CO_2 levels of greater than 400 ppm for the first time in May 2013 and levels are now routinely above 400 ppm. In the 8000 years prior to industrialisation, CO_2 concentrations increased by just 20 ppm, whilst the current (1965–2005) average rate of change stands at 1.7 ppm yr (Hartmann et al., 2013, Figure 2.3).

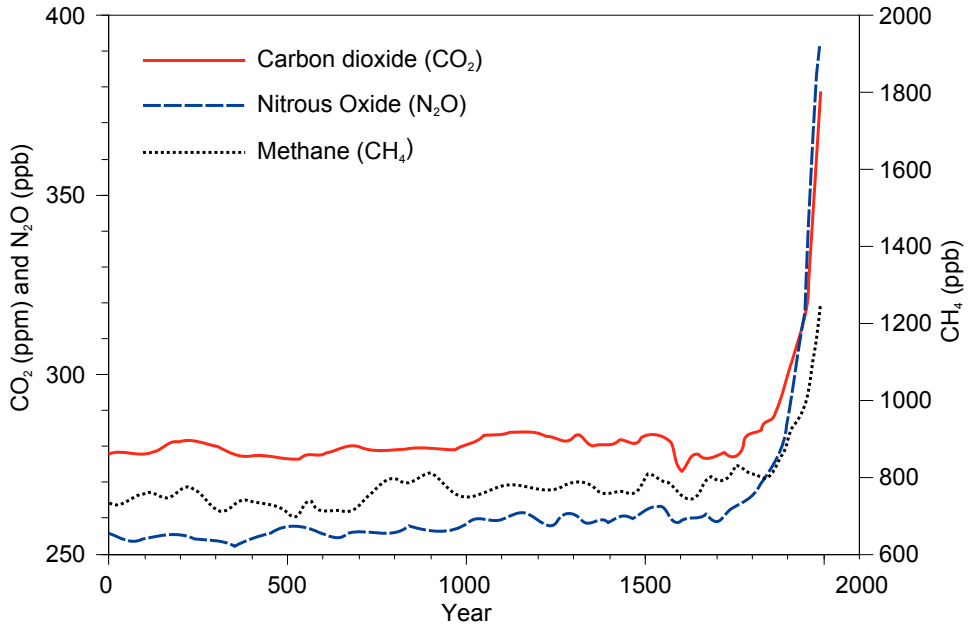

Figure 2.3: Atmospheric concentrations of important long-lived green-house gases over the last 2000 years. Increases since about 1750 are attributed to human activities in the industrial era. Adapted from Foster et al. (2007).

2.1.2 *Attributing climate change*

Attempting to attribute changes in global temperature to changes in GHGs has been an important field of study for the last 20 years. As recently as the first IPCC report in 1990, there was relatively little observational evidence of the influence of anthropogenic drivers on climate change, however by the publication by the IPCC of its Third Assessment Report in 2001, a substantial body of evidence had accrued which implicated them (Hegerl et al., 2007).

2.1.2.1 *Climate modelling*

Attributing climate change to anthropogenic drivers has generally been conducted with the use of computationally intensive computer simulations. More than 20 of these models – the most complicated of which are termed atmosphere-ocean

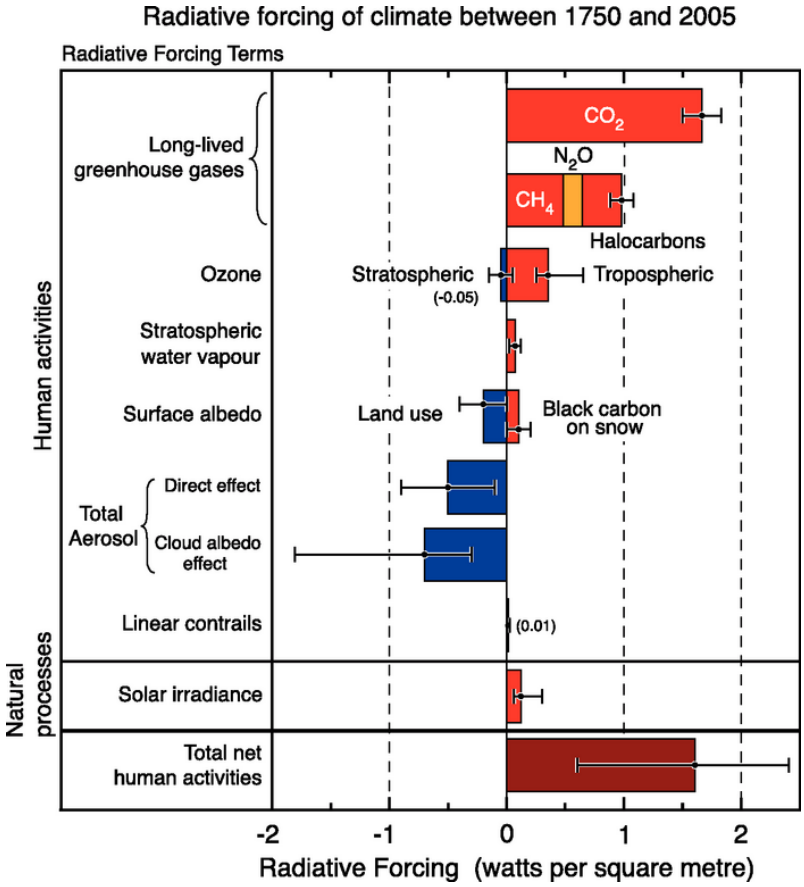

Figure 2.4: Summary of human influenced RF in 2005, relative to the start of the industrial era (about 1750). Whiskers indicate the 90% range of uncertainty for the respective value. From Foster et al. (2007)

global circulation models (AOGCMs) – are operated by research groups across the world (Hegerl et al., 2007) with the aim of explaining global temperature rises. Crowley (2000), for instance, was able to show using a climate model that successfully reconstructed northern hemisphere temperatures for the period 1000–1850 (using ^{14}C and ^{10}Be proxies), that only 25% of 20th century warming can be attributed to natural forcing.

Climate models typically include a wide range of forcings including increases in long-lived GHGs (CO_2, CH_4, N_2O, and halo-carbons), decreases in stratospheric O_3, increases in tropospheric O_3, sulphate aerosols, nitrate aerosols, black carbon and organic matter from fossil fuel burning, biomass burning aerosols, mineral dust aerosols, land use change, indirect aerosol effects on clouds, aircraft contrails and cloud effects, variation in solar irradiance, and stratospheric and tropospheric water vapour increases from CH_4 and irrigation (Hegerl et al., 2007).

The AR4 of the IPCC quotes values of 1.6 ($W\,m^{-2}$, (90% range: 0.6 to 2.4 $W\,m^{-2}$) for total anthropogenic RF (Figure 2.4) in 2005, relative to 1750. Models show that the majority of this forcing is caused by GHGs, in particular CO_2. By contrast, RF associated with changes in solar irradiance was only 0.12 (90% range: 0.06 to 0.3) $W\,m^{-2}$ over the same time period (Foster et al., 2007). Without this anthro-

pogenic RF, modelers have been unable to recreate the observed warming trend with simulations run on the major climate models (Figure 2.5).

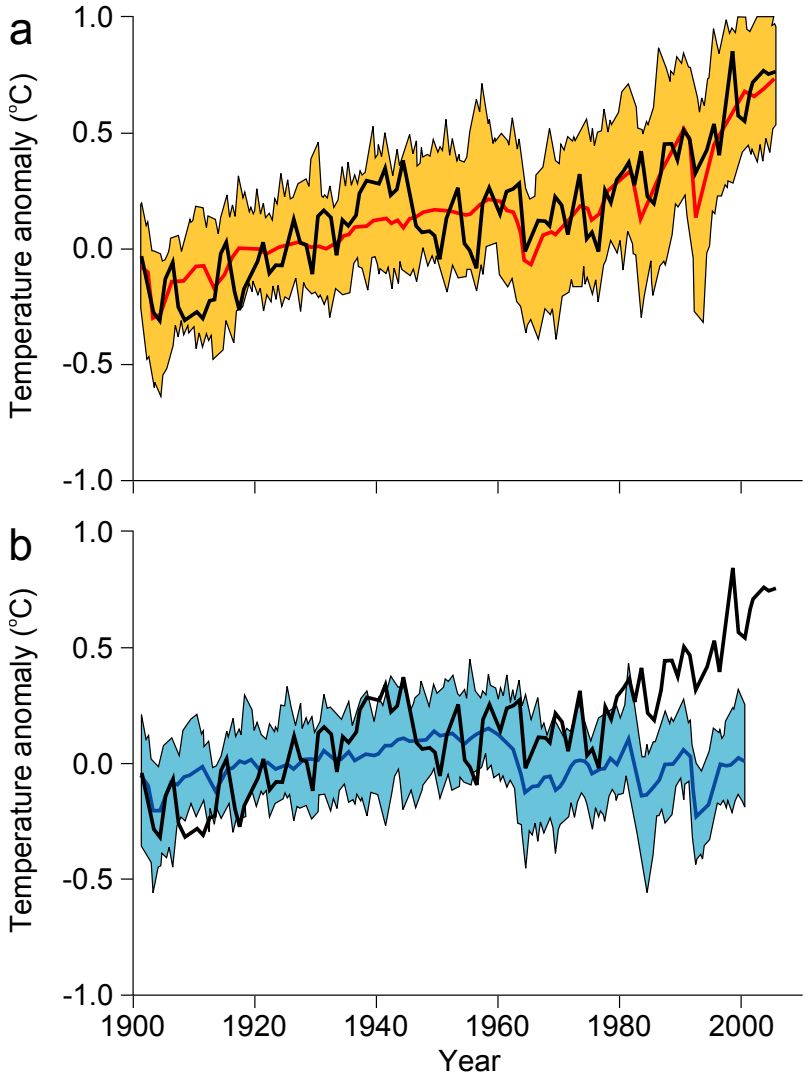

Figure 2.5: Comparison between Global Mean Surface Temperature (GMST) anomalies (°C) from observations (black) and AOGCM simulations forced with (a) both anthropogenic and natural forcings and (b) natural forcings only. Units in °C relative to the period 1901 to 1950. Reproduced from Hegerl et al. (2007).

2.1.2.2 *Climate projections*

Much effort has gone into the question of how the climate is likely to change in response to increased anthropogenic RF. Since anthropogenic emissions play the major role in shaping the future climate, any predictions of climate change must take into account socio-economic changes that may occur in future years.

With this in mind, the IPCC have typically provided climate projections based on a number of scenarios relating to the future emission of GHGs, trends in human population, economic growth, and the adoption of new, greener, technologies (IPCC, 2000*a*). Based on these scenarios, and the means of multiple models, the IPCC (Meehl et al., 2007), predict global mean surface air temperature warming of

between 0.64 and 0.69 °C) between 2011–2030, 1.3–1.8 °C) between 2046–2065 and 1.8–6.4°C) by the end of the century (2090–2099).

2.1.3 *Implications of rising temperature*

Based on the available knowledge, a wide range of effects to occur as a result of increases in global mean temperature. Almost all have major implications for the existence of mankind, and most other forms of terrestrial and oceanic life.

Temperature extremes It is expected that minimum daily temperatures across the globe will rise more quickly than daily maximum temperatures, leading to changes in temperature ranges, and a reduction in frost days. In addition, it is expected that heat waves will become more frequent, and last for longer (Meehl et al., 2007).

Precipitation It is expected that global climate change will bring an increase in mean precipitation as the higher temperatures allow air to store larger quantities of water vapour. Hence rainfall is generally expected to increase where it already occurs (e.e the tropics and high latitudes), but it may decrease in subtropical areas that are already dry. Alongside the increase in global precipitation means, the intensity of precipitation events is expected to increase in tropical and high latitude regions (Meehl et al., 2007).

Snow and ice Commensurate with global warming, it is expected that snow cover, the extent of sea ice, glaciers and ice caps will decline, leading to reductions to surface albedo (and thereby a positive feedback loop, Winton, 2006), and a rise in sea level. Thawing of sub-arctic permafrost may also play a significant role in further warming, as previously frozen soil organic carbon is made accessible to microbial decomposition; or worse still, anaerobic decomposition which can result in the release of CH_4. This is particularly undesirable as CH_4 has 25 times the global warming potential of CO_2 over the century timescale (Schuur et al., 2008).

Ocean acidification and sea level rise Although the potential effects are not well understood, increases in atmospheric CO_2 have been predicted to give rise to a pH reduction of between 0.14 and 0.35 for the 21 century (Meehl et al., 2007). These changes are likely to have implications for marine life. By the 2080s, it is expected that many millions more people will be at risk from floods due to sea level rises than are currently considered at risk, particularly in low lying areas and small islands (IPCC, 2007).

Biodiversity, and ecosystem services If temperatures exceed 1.5–2.0°C, the IPCC have estimated that 20–30% of plant and animal species may be at increased extinction risk.

Huge changes in ecosystem structure, function, and species' geographical ranges are likely to result in largely negative consequences for biodiversity and ecosystem service provision including food supply and water regulation (IPCC, 2007).

Food Whilst increases in atmospheric CO_2 concentrations, may lead to increases in water use efficiency, particularly for C_3 plants, and hence increased yields (Kirschbaum, 2004), crops currently growing at temperatures near their optimum will show decreased yields (IPCC, 2007).

Overall the IPCC (2007) predict that global food production is likely to increase initially, before declining at temperature increases greater than 3°C.

Human health Increased levels of malnutrition, death and disease due to extreme weather events, and increased prevalence of gastro-intestinal diseases are likely to affect the health of millions of people (Confalonieri et al., 2007). Increased O_3 concentrations in urban areas is also likely to increase the incidence of cardio-respiratory diseases (Confalonieri et al., 2007).

Reduced winter temperature extremes and the shifting ranges of infectious diseases like Malaria may outweigh the negative health effects in developing countries (IPCC, 2007).

2.1.4 *Anthropogenic sources of greenhouse gases*

Between 1970 and 2004 (Figure 2.6), the greatest growth in the emissions of anthropogenic GHGs has been in the energy, transport and industrial sectors; however emissions from forestry, agriculture, and commercial and residential buildings also rose (IPCC, 2007).

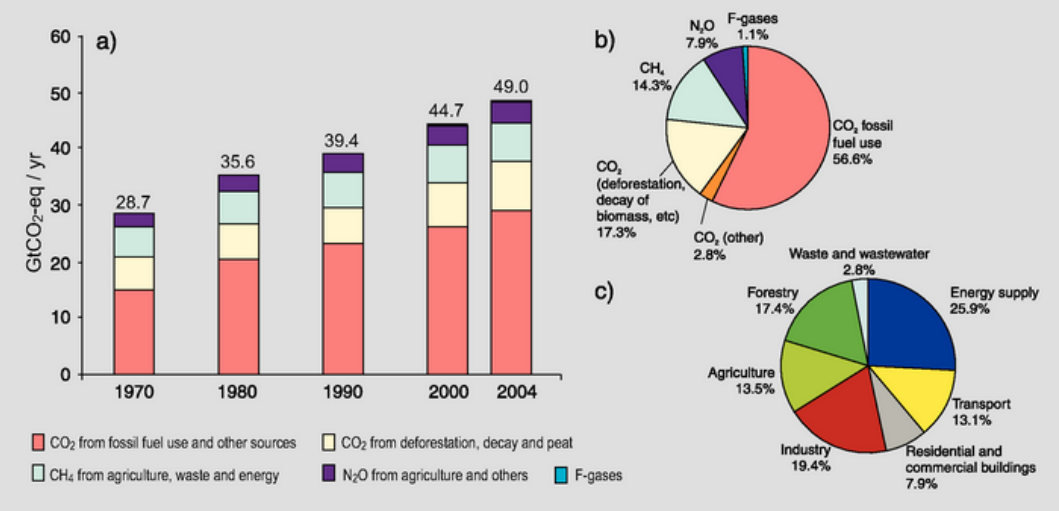

Figure 2.6: (a) Global annual emissions of anthropogenic GHGs from 1970 to 2004. (b) Share of different anthropogenic GHGs in total emissions in 2004 in terms of CO_2. (c) Share of different sectors in total anthropogenic GHG emissions in 2004 in terms of CO_2-eq. (Forestry includes deforestation). Reproduced from IPCC (2007).

The main GHGs are water vapour, carbon dioxide, methane, nitrogen oxides, and ozone. These are covered in turn.

2.1.4.1 *Water vapour*

Water vapour is the dominant GHG, responsible for about 60% of the natural greenhouse effect (Trenberth et al., 2007). There exists a strong link between temperature and the presence of water vapour in the atmosphere: relative humidity increases at a rate of about 7% $°C^{-1}$, meaning that a strong positive water vapour feedback exists (Dessler et al., 2008). However, human activity only has a small direct impact on the presence of water vapour in the atmosphere (Foster et al., 2007, p.135). Records of the presence of water vapour are relatively recent (the longest time-series was begun in 1980) and indicate a net increase up to 2012, but with low confidence in this trend (Hartmann et al., 2013, p.170).

2.1.4.2 *Carbon dioxide*

Fossil fuel use is by far and away the greatest sources of anthropogenic carbon dioxide (CO_2). Emission sources can broadly be divided into electricity generation, industrial processes, transport, waste management, and the building sector (including residential and commercial heating, lighting, etc.) (Figure 2.7, UNEP, 2011).

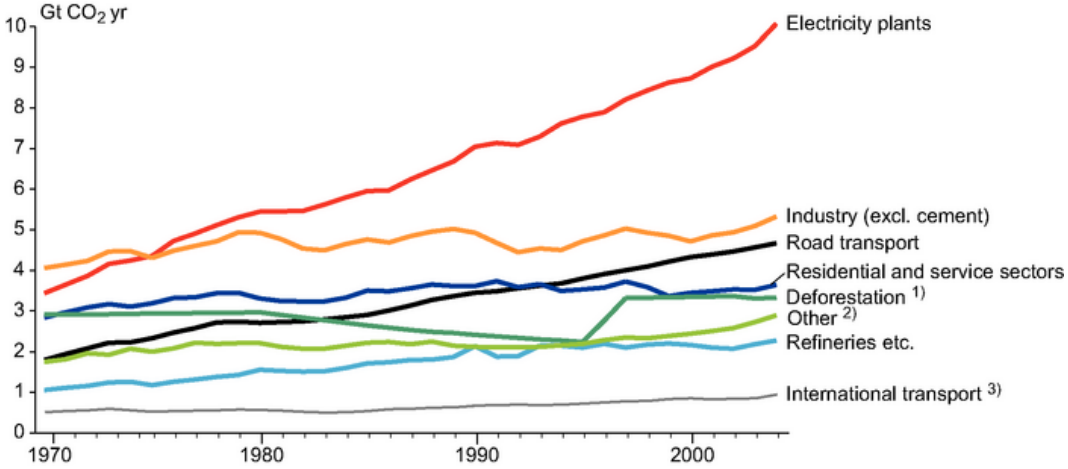

Figure 2.7: Sources of global CO_2 emissions by sector, 1970–2004. Reproduced from Rogner et al. (2007).

Indeed, there exists a gradient of CO_2 concentration from Northern to Southern Hemisphere, concomitant with greater fossil fuel emissions in the Northern Hemisphere (Denman et al., 2007).

Large amounts of CO_2 are also released to the atmosphere by the agricultural and forestry sectors. The reasons for these emissions are more complex than simple fossil fuel use, and are linked to land use changes, and in particular deforestation, unsustainable logging practices, and the clearing of forest land for agricultural production (Nabuurs et al., 2007).

2.1.4.3 *Methane*

Methane (CH_4) emissions originate from both biological and non-biological sources. The larger part of emissions, some 70%, originate from biological sources, mostly

through the process 'methanogenesis', mediated by 'methanogenic' Archaea (Denman et al., 2007). This may occur in wetlands, rice paddies, landfills, forests, or in the digestive system of animals, particularly ruminants (Denman et al., 2007). Non-biological sources of CH_4 include the burning of biomass, the extraction of fossil fuels, waste treatment, and seepage of natural gas.

Anthropogenic sources are thought to dominate CH_4 emissions, accounting for 60% of total emissions. A large percentage of this (as much as half in some budgets) is thought to be caused by agriculture – ruminants and rice production (Denman et al., 2007).

As much as 10% of the total anthropogenic methane emissions in the US are thought to be caused by so called 'coal bed methane' which is released during the process of coal extraction, unless intentionally removed prior to coal extraction (Sims et al., 2007).

2.1.4.4 *Nitrogen compounds*

Three nitrogen N containing gases have an impact on the atmosphere climate system: nitrous oxide (N_2O), ammonia (NH_3), and NO_x (nitrogen oxide (NO) and nitrogen dioxide (NO_2)) (Denman et al., 2007). Whilst short-lived in the atmosphere, N_2O is a significant contributor to RF. By contrast, NO_x has both positive and negative RF effects, positively by the formation of low level O_3 (a greenhouse gas when present in the stratosphere), negatively by shortening the atmospheric lifetime of CH_4 (Denman et al., 2007). At the time of the fifth report of the IPCC, the net effect of NO_x is thought to be negative (Alexander et al., 2013). NH_3 exerts a similar negative RF by assisting in the formation of aerosols (which act to reflect solar radiation away from the earth's surface) (Denman et al., 2007).

Anthropogenic sources of N containing gases include fossil fuel combustion, industrial processes, aircraft emissions, agriculture, burning of biomass, and human waste. In the case of N_2O, almost half of anthropogenic emissions are though to originate from agricultural deposition. Whilst human emissions of NO_x and NH_3 account for between 4 and 5 times the natural emissions (according to the fourth IPCC assessment report), anthropogenic N_2O emissions are thought to be comparable or less than natural sources (Denman et al., 2007).

Nitrogen fertiliser, often applied in the form of ammonia (NH_3) has a beneficial effect on carbon sequestration by terrestrial vegetation by increasing growth: as much as a fifth of all the carbon sequestered by terrestrial ecosystems between 1996 and 2005 is thought to be a result of the addition of nitrogen fertilizers. However, the net effect of applying nitrogen fertiliser is an increase in RF resulting from N_2O emissions Zaehle et al. (2011).

2.1.4.5 *Ozone*

Whilst stratospheric[2] ozone (O_3) plays an important role in blocking ultraviolet radiation from the atmosphere; in the troposphere O_3 is an important contributor to positive RF (Denman et al., 2007).

2 The stratosphere is an intermediate layer of the atmosphere, immediately above the troposphere, stretching from about 10 km to between 50 and 60 km above the earth's surface.

Ozone itself is not produced in large quantities by anthropogenic processes. Instead, O_3 is produced as a result of a chemical reaction with so-called 'ozone precursors' – notably CH_4 and NO_x. This reaction occurs in the presence of ultraviolet radiation from the sun; hence, concentrations of O_3 can vary greatly, and are greatest in metropolitan centres close to equatorial latitudes – notably Mexico city, Los Angeles, and Athens.

Emissions of ozone precursors by aircraft are thought to have the greatest impact on O_3 induced RF, perhaps as much as thirty times the impact of surface emissions (Johnson et al., 1992).

2.1.5 *Mitigating greenhouse gas emissions*

Despite the largely negative prognosis for climate change, as recently as 2011 the United Nations Environment Program reported that keeping global temperature increases below 2°C was feasible and achievable with a sustained commitment to cutting GHG emissions (UNEP, 2011). Cutting the expected emissions by 2020, include confidence intervals of 5 $GtCO_2e$, meaning that the size of the emissions gap is likely to be between 9 and 18 $GtCO_2e$of 56 $GtCO_2e$ to 44 $GtCO_2e$ would be sufficient to bridge the 'emissions gap'[3] (UNEP, 2011).

This gap could be bridged by making achievable changes in a number of major sectors; global GHG emissions could be reduced by as much as 17 $GtCO_2e$ (14–20). Of this, between 1.1 and 4.3 $GtCO_2e$, and 1.3 and 4.2 $GtCO_2e$, could be saved through changes in the agricultural and forestry sectors respectively (UNEP, 2011). The following sections consider these sectors in turn.

2.1.5.1 *The agricultural sector*

Emissions of CO_2 from agriculture are not normally calculated separately, but are included within land use, land use change and forestry (LULUCF); those estimates that do exist suggest that although fluxes of CO_2 may be very large, net CO_2 flux is small, around just 1% of global anthropogenic CO_2 emissions (about 40 Mt CO_2e) (Smith et al., 2007, p.503). Conversely, emissions of non-CO_2 GHGs from agriculture are reported to be of the order of 5–6 $GtCO_2e\ year^{-1}$ (Denman et al., 2007), and were in 2005 about 10–12% of total global anthropogenic emissions (Smith et al., 2007). About 47% and 58% of total man-made CH_4 and N_2O emissions are caused by agriculture respectively, the bulk of these emissions coming from enteric fermentation and microbial processes in the soil respectively (Smith et al., 2007), the remainder coming largely from burning of biomass (CO_2), rice production and manure management (CH_4 and N_2O).

Despite declines in NO_2 emissions since 1990, due to a reduction in N fertiliser use (Smith et al., 2007), emissions are predicted to increase with global food demand, resulting in an increase of up to 60% in the years leading up to 2030, largely due to the increase in nitrogen fertiliser use (FAO, 2003). Only in Western Europe are GHG emissions in agriculture predicted to decrease as a result of environmental policies instituted by the European Union (Smith et al., 2007).

3 Note that CO_2e – carbon dioxide equivalent – is a measure of the global warming potential of a mix of gases in equivalent terms of CO_2

There are a number of possible technologies and practices that could allow for some mitigation of agricultural GHG emissions, these fall into three broad categories:

Reducing emissions from the land Options for reducing GHG emissions associated with agriculture include rotations of N-fixing legumes, vegetative cover between crop rotations, and intercropping systems which add carbon (C) to the soil Tiessen et al., 1994, and remove N unused by the crop, (Smith et al., 2007). This is of particular relevance when inter-cropping with deeper rooting plants and trees – the so called 'safety-net' hypothesis (Cannell et al., 1996).

Reduced, and no-till agriculture reduce soil disturbance and the mineralisation of SOC (Madari et al., 2005), although the efficacy of the technique may be largely dependent on local conditions (Smith et al., 2007).

Precision methods such as the targeted and accurate application of inputs could also significantly reduce the volume of agricultural inputs, and the potential for (for example) N_2O emissions from N application in excess of the plant requirements (Smith et al., 2007). In addition, the application of fertiliser in slow-release forms or with compounds which inhibit N mineralisation have shown promise in reducing N_2O emissions (Delgado and Mosier, 1996; Shoji et al., 2001).

Since emissions from wetland rice soils make up a significant proportion of total agricultural GHG emissions, there is scope for changes in rice management practices to reduce emissions (Smith et al., 2007). Potential alterations to management practices include draining wetland areas periodically, and keeping the soil as dry as possible in the off-season (Smith et al., 2007), which may help reduce CH_4 emissions caused be anaerobic conditions.

Avoiding the burning of biomass on farms (not for energy) can reduce CO_2, CH_4, and N_2O emissions. Reducing the frequency and extent of fires can be beneficial, as can the introduction of mechanical harvesting techniques, which can reduce the need for pre-harvest burning, for example in sugarcane harvesting (Cerri et al., 2004; Smith et al., 2007).

The use of concentrated feed can reduce CH_4 emissions from enteric fermentation in the digestive system of livestock, although the efficacy of this practice depends on a number of other, inter-dependent factors (Smith et al., 2007). The addition of oils and other dietary additives, the improvement of pasture quality, the optimisation of protein intake, and the general improvement of management practices in the long term, all play a role in reducing CH_4 emissions from livestock (Smith et al., 2007).

Enhancing sequestration potential Increasing the amount of GHGs sequestered by agricultural ecosystems can also help to reduce the impact of agriculture on the climate. An increase in vegetated rather than bare fallows, and the incorporation of deeper rooting, and longer-lived perennials in the form of intercropping or agroforestry, is a major area of interest for the management of (in particular) soil carbon in agricultural environments (Mosquera-losada et al., 2011; Nair et al., 2009; Smith et al., 2007).

Where possible, the conversion or reversion of arable land to a more C dense land use, for instance hedgerow, shelter-belt, pasture, or native woodland, proba-

bly represents the most effective means of enhancing C storage both above, and belowground. Other measures include the use of reduced and no-till agriculture, and the better management of post-harvest residues (Smith et al., 2007).

Avoiding (or displacing) emissions related to management practices In the first case, emissions from agriculture can be avoided by the adoption of cropping systems which rely less heavily on fertilizers, pesticides, and other inputs which are GHG intensive in their production (Paustian et al., 2004). Emissions from agricultural machinery may also be avoided in the case of reduce and no-till agriculture (Koga et al., 2006).

Fossil fuels may also be displaced by the use of CH_4 as a fuel source, recovered from anaerobically digested manure, whilst bioenergy crops and residues are increasingly being seen as a potential energy source (Smith et al., 2007). Competition with other land-use priorities such as food production, conservation, and C sequestration, are likely to limit the efficacy of this approach as a means of reducing the overall impact of agriculture (Smith et al., 2007).

2.1.5.2 *The forestry sector*

The main cause of GHG emissions from forestry is losses of carbon stored in biomass and in the soil following deforestation due to human actions or other disturbance such as fire, insect attack, disease, and climatic events. Options options for mitigation of GHG emissions from forestry can be broadly grouped into three categories (Nabuurs et al., 2007):

Increase forest area Increasing the total forest area through afforestation, and reducing forest loss through deforestation and degradation is a clear and obvious goal in increasing (and preventing further loss of) C storage in forests. Deforestation alone was reported to be responsible for as much as 8.5 Gt CO_2e out of a global budget of 49 Gt CO_2e – equating to 17.4% of global anthropogenic GHG emissions in 2004 (Rogner et al., 2007). As Burgess et al. (2010) point out however, this value is subject to a very large level of uncertainty, not least because changes in albedo may mitigate some of deforestation related RF. Between 2000 and 2012, 2.3 million km^2 of a total 39.5 million km^2 (Nabuurs et al., 2007) of forest were lost to either deforestation or other disturbance, whilst only 0.8 million km^2 were established over the same period (Hansen et al., 2013).

Strategies for reducing deforestation include the reduction of agricultural rent, to reduce poverty and thereby alleviate the need for deforestation, whilst also increasing monetary benefits to landowners of maintaining forest cover, for example through Payments for Ecosystem Services (PES) (Angelsen et al., 2009). By supporting intensive agriculture and technology change, a shift away from upland and frontier (extensive) agriculture can be encouraged, thereby obviating the need for deforestation (Angelsen et al., 2009). Limiting road construction, reforming land tenure, and establishing protected areas may also impact the rate of deforestation (Angelsen et al., 2009).

Increase carbon density Maintaining or increasing the C density (t C ha^{-1}) through management is another option for abating emissions from forests. This might include preventing or reversing degradation caused by forest fires, pests and diseases: by capacity building of fire control and prevention, monitoring, and quarantine systems (Wenhua, 2004).

Pre-planting disturbance has been shown to reduce the quantity of C retained at a site; utilising less disruptive site preparation methods may therefore be beneficial C density (Laganiere et al., 2010; Lundmark-Thelin and Johansson, 1997; Piirainen et al., 2007).

Establishing uneven-aged stands (Nabuurs et al., 2007, p.549), and thereby selective rather than clear-felling, may help maintain aboveground C (and other ecosystem service benefits) without the periodicity of a clear-fell – re-establishment cycle, and the periodic loss of nutrients (Kubin, 1998).

Tree improvement programs and fertilisation, which maximise yield can increase the C density of a stand (Nabuurs et al., 2007, p.549), as would longer forest rotations (Jandl et al., 2007). This latter point is of particular interest for two reasons. Firstly Stephenson et al. (2014) has recently shown that the rate of tree growth (and by extension, carbon accretion) increases continually with tree age. This is contrary to the widely held belief that after a rapid period of carbon accretion early in life, the rate of increase in mass slows. Big, old trees may thus have a larger role to play in aboveground carbon storage than commonly presumed. Stephenson et al. (2014) found, for instance, in old-growth forest stands in the western USA, 6% of trees (those >100 cm diameter) were responsible for 33% of annual forest mass growth. Furthermore, short rotations may not maximise long-term C storage, as it takes time for soil C to accumulate over successive years, and (in the case of black carbon from charcoal) successive fires (Jandl et al., 2007; Schulze, 2000).

Increasing atmospheric concentrations of CO_2 are likely to increase forest productivity (Norby et al., 2005) and global wood supply is likely to increase (Easterling et al., 2007). However, the impact of atmospheric CO_2 changes can have negative effects on old stored soil C storage (Hoosbeek et al., 2004), and it is possible for soil C sinks to turn into sources despite increased plant growth (Carney et al., 2007)

Off-site stocks and substitution The final way to improve the balance of GHG emissions relating to forestry, is to increase the storage of C once it has been harvested in durable woody products, and further, to use these products to displace more C intensive products.

Storage of C in off-site stocks is only likely to be of great relevance if the retention of these stocks extends beyond the rotation length of the trees from which the wood is harvested, meaning that C stocks will increase year on year (Dewar, 1990). However, modelling of the longevity of C storage in woody products has assumed that the majority of wooden products persist for just a short period (Buchanan and Levine, 1999; Thompson and Matthews, 1989).

The displacement of more C intensive products and their substitution with timber based products offer substantial potential. Substituting timber for cement is a prime example (Gustavsson and Sathre, 2006; Perez-Garcia et al., 2005). Perez-

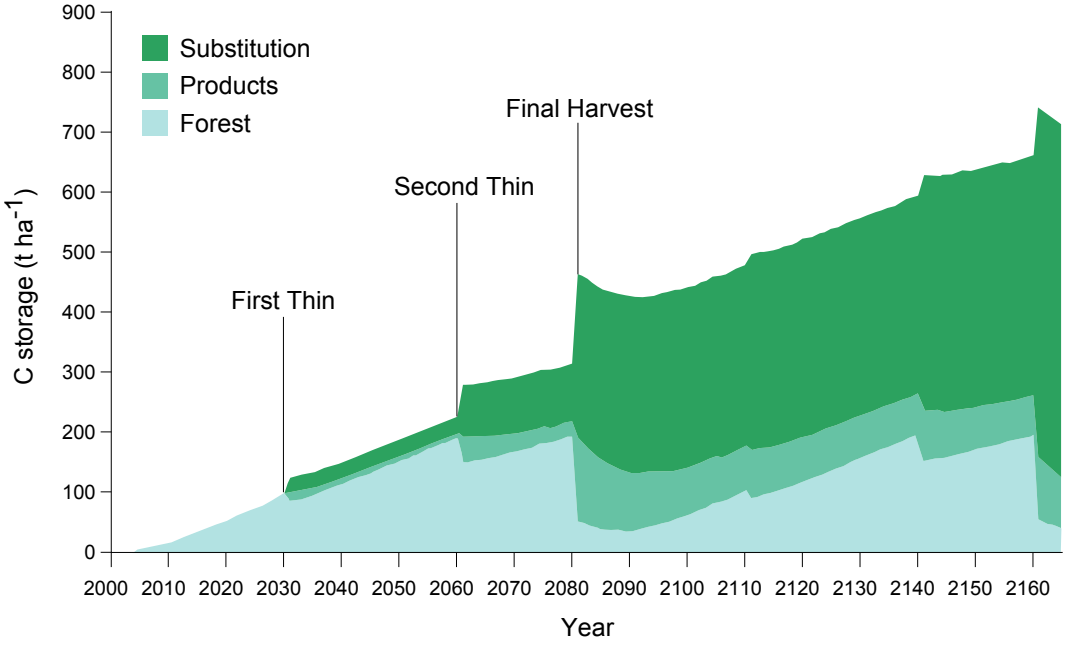

Figure 2.8: Carbon storage as a result of plantation growth, storage in products, and GHGs avoided by substitution for cement. Reproduced from Perez-Garcia et al. (2005).

Garcia et al. (2005) indicate that over 165 years, more C emissions can be prevented by using wood in place of cement than will be stored in the standing biomass and the products resulting from the first harvest combined (assuming an 80 year lifespan of woody products, Figure 2.8).

Novel ideas such as the use of pine killed by the mountain pine beetle (*Dendroctonus ponderosae*) in the construction of tall buildings as cross-laminated timber (Seattle, 2012) may provide an elegant solution to a problem itself likely to have been caused by climate change (Kurz et al., 2008).

2.2 AGROFORESTRY AND FARM WOODLANDS

This section gives a brief description of agroforestry and farm woodland systems, and a more in depth discussion of C storage in these systems and the manner in which it can be measured, providing a framing of the major research questions.

2.2.1 *Agroforestry*

Definitions and history Researchers have struggled to define agroforestry (Lundgren, 1982; Nair, 1993) due to the diversity of systems which the term encompasses, and probably also the fact that these practices existed long before the term itself was coined (King, 1987). As the name implies, agroforestry is a combination of agricultural practices with trees, and a general definition can be given as 'the practice of deliberately integrating woody vegetation (trees and shrubs) with crop and/or animal production systems to benefit from the resulting ecological and economic interactions' (AGFORWARD, 2014) . The nature of the agricultural prac-

tice, the trees, and the way in which these components are combined is incredibly diverse, and varies greatly with geography.

These systems may involve the growing of crops with trees (silvoarable agroforestry), or the raising of livestock with trees (silvopastoral agroforestry); the growth of trees for timber, fodder, non-timber forest products (NTFPs), or shelter; and these combinations may be spatial, temporal, or both (Figure 2.9).

(a) A 10 year-old poplar based silvoarable system at Silsoe, Bedfordshire. Photo credit: Paul Burgess.

(b) Portugese Montado with cattle, southeast Portugal. Photo credit: João HN Palma.

(c) Oak trees intercropped with lavender, South of France, Drôme. Photo credit: AGROOF.

(d) Ploughing between 14 year old walnut trees, Montpellier, France. Photo credit: Agforward project

Figure 2.9: Some examples of agroforestry systems. Images are presented under a generic Attribution - NonCommercial - ShareAlike 2.0 Generic license (CC BY-NC-SA 2.0): https://creativecommons.org/licenses/by-nc-sa/2.0/. Images have been cropped.

The most traditional agroforestry systems tend to be extensive subsistence farming (Sheldrick and Auclair, 2000), particularly in the tropics, where forest gardens are common. In areas of Central America, Asia, and Africa, small plots have tra-

ditionally been cultivated with a wide range of plant species filling different ecological niches. In these tropical regions, where forest historically had to be cleared for agricultural production by hand, making the most efficient use of space was an essential means of conserving energy (King, 1987).

In Britain, mention is made of agroforestry practices in Evelyn's seminal forestry text Sylva (Evelyn, 1729). Evelyn notes the use of oak forests for grazing of cattle and game:

> *And this upon consideration how slowly a full-grown oak mounts upwards, and how speedily they spread, and dilate themselves to all quarters, by dressing and due culture; so as above forty years advance is to be gain'd by this only industry: And, if thus his Majesties forests and chases were stor'd, with this spreading tree at handsom intervals, by which grazing might be improv'd for the feeding of deer and cattel under them...*

These silvopastoral, parkland systems, were widespread across Europe, and in places represented the dominant land use: for instance the Iberian peninsula. The Spanish *dehesa* and equivalent Portuguese *montado* (Figure 2.9) is the combination of (among others) holm oaks (*Quercus ilex*) or cork oaks (*Q. suber*) for acorn or cork production with the grazing of a range of livestock species (Joffre et al., 1999).

Evelyn later mentions silvoarable systems, and the beneficial combination of Walnut trees with wheat crops in southern France:

> *Thus Burgundy abounds with them, where they stand in the midst of goodly wheat-lands, at sixty, and an hundred foot distance; and it is so far from hurting the crop, that they look on them as a great preserver, by keeping the grounds warm; nor do the roots hinder the plow.*

Here Evelyn hits upon one of the central tenets of agroforestry: the combination of the two systems should be complementary. The form that this complementarity takes may be varied, but in general one can characterise the system with the equation (Cannell et al., 1996):

$$I = F - C \tag{2.1}$$

I = Increase in yield attributable to the presence of trees.
F = Fertility effect: increase in crop yield attributable to fertility effects of trees.
C = Competitive effect: decrease in yield caused by competition between crops and trees.

Cannell et al. (1996) explain this equation very much in terms of silvoarable yield, but it is also applicable to other systems if we think in more general terms, and consider 'benefit'. This also allows the equation to encompasses socio-economic benefits that may also result from agroforestry.

At the very least, for agroforestry systems to be considered viable, the product of this equation should be positive. When considering yield, this is often described in terms of Land Equivalent Ratio (LER) which takes into account the equivalent production of a sole crop on a similar area of land (Equation 2.2, (Mead and Willey, 1980)).

$$LER = \frac{Y_A}{S_A} + \frac{Y_B}{S_B} \tag{2.2}$$

Y_A, Y_B = yield of individual crops in an agroforestry system.
S_A, S_B = yield of individual crops grown separately on a similar area of land.

Hence a LER of > 1.0 indicates a positive interaction (in terms of yield) even though a crop or tree component in a silvoarable agroforestry system may perform less well than a sole crop or plantation grown individually under similar conditions.

Decline and recent resurgence Over the last few centuries, agriculture and forestry in Europe have increasingly come to be looked upon as the pursuit of farmers and foresters apart, with little exchange between the two. This is particularly so in the case of silvoarable agroforestry, for which there are several contributing factors.

The increasing mechanisation and intensification of agriculture has meant that trees have increasingly been seen as an unwelcome impediment to the efficient use of machinery (Eichhorn et al., 2006). Further, a co-concomitant reduction in the availability of agriculture labour has rendered certain labour intensive systems untenable (Eichhorn et al., 2006). Unfriendly subsidy regimes, in particular the Common Agricultural Policy (CAP) have favoured single-crop systems, and the separation of woody areas, whilst more stringent quality requirements have led to a need to standardise production, which is often unfriendly to agroforestry practices (Eichhorn et al., 2006).

In the tropics and sub-Saharan Africa, interest in agroforestry never waned, since the combination of trees with agriculture was more deeply ingrained within the culture of societies that practiced it (King, 1987). In addition, in more hostile growing environments, the interactions between trees, crops and animals may be essential, not merely beneficial and because the nature of the combinations provide additional benefits not available in temperate agroforestry (e.g. the planting of nitrogen fixing *Fabaceae* trees among crops).

Towards the end of the 20th century, there was renewed interest in temperate agroforestry, partly due to concerns over the unsustainability of intensive forms of agriculture. Agroforestry is seen as a means of providing a number of ecosystem services, whilst keeping land in agricultural production. Ecosystem services that may be provided by agroforestry systems include: improved biological diversity, pest control, erosion control, soil enrichment, and not least carbon sequestration (Jose, 2009; Klaa et al., 2005; Nair et al., 2009; Peng and Sutton, 1996; Williams-Guillen et al., 2008).

2.2.2 *Agroforestry for carbon sequestration*

The basic premise behind managing land for C sequestration is that the difference between C accumulated through photosynthesis, and C returned to the atmosphere by respiration, is positive (Montagnini and Nair, 2004). More specifically

in terms of agroforestry, it is hoped that the C accreted per hectare by the system (particularly the soil and tree components which are likely to be long-lived), is greater than the equivalent area of land given to pure agricultural or pure forestry systems.

Figure 2.10 shows a conceptualisation of the C cycle as it applies to agroforestry systems. Atmospheric CO_2 is captured through the process of photosynthesis and incorporated into the vegetative tissues of trees and crops. Vegetative carbon, in general, is considered to be a labile carbon stock; carbon in non-woody vegetation is likely to persist only for a few months before decomposition returns the bulk of the carbon to the atmospheric pool. Fahey and Arthur (1994) suggest that up to 63% of the dry matter of root biomass is lost within the first four years following harvesting of aboveground material. Woody material is likely to persist for years, perhaps centuries depending on tree management and longevity of the species (Janzen, 2005).

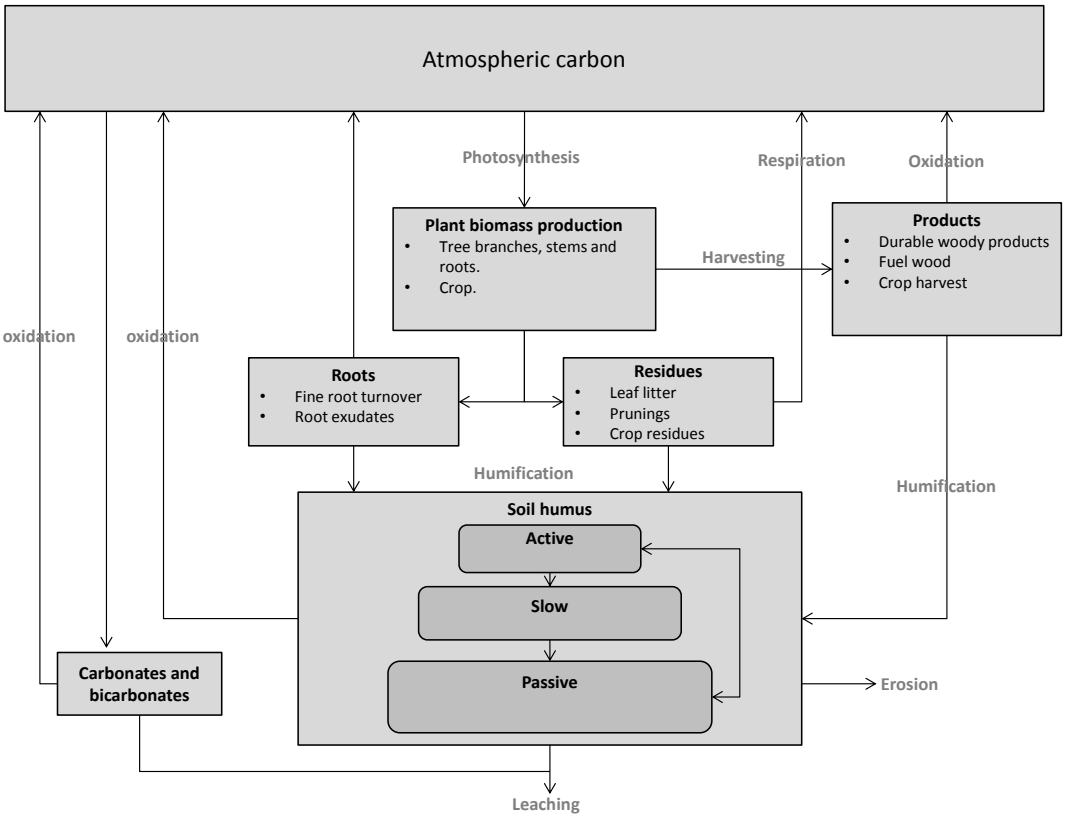

Figure 2.10: Conceptualisation of the carbon cycle in an agroforestry system. Adapted from Brady and Weil (2008).

On harvest most of the C captured in aboveground tissues is converted to food and other products. The longevity of this product pool is likely to be short – C stored in crop harvests will persist only until consumed or spoiled, whilst C in products derived from trees may be returned immediately to the atmopsheric pool if burnt, or more slowly if converted to a more durable product. C may be stabilised in paper, pulp and packing materials for only very short periods of time, whilst wood used in high quality furniture or the construction industry may remain a C sink for decades or even centuries (Perez-Garcia et al., 2005; Thomp-

son and Matthews, 1989). Note that over successive rotations, the aboveground biomass C pool will reach an average C storage which will not increase unless the retention time of C in woody products extends beyond the time of the next harvest (Dewar, 1990).

Fractions of both the plant biomass C (roots and residues) and product pools (waste) will be incorporated into the soil as soil organic matter (SOM). Soil organic matter is often conceptualised into a number of pools (Figure 2.10) with differing turnover times according to the complexity of the compounds within it, and its relationship to the soil (Szott, 1991). Broadly speaking there are three conceptual pools: active, slow and passive SOM (Brady and Weil, 2008). The active pool consists of easily decomposable materials with short half-lives, between a few days and a few years (Brady and Weil, 2008). The passive pool consists of very stable material and organo-mineral complexes. Intermediate between these groups is the slow organic matter. This fraction likely includes fine particulate organic matter (POM) that is chemically resistant to decomposition (Brady and Weil, 2008). At its most stable SOM may take from decades to millennia to release its C back into the atmospheric pool (Gaudinski et al., 2000; Rumpel et al., 2002; Schöning and Kögel-Knabner, 2006); conversely soluble carbon in the form of root exudates – the most active of soil C, may only be present in the soil for a matter of hours (Janzen, 2005).

Various estimates have been put forward for the average carbon storage by agroforestry systems. Partly because of the wide range of systems that this definition encompasses, and differing methodologies, there is a great deal of variation among estimates. Nair et al. (2009) presented net annual sequestration values from a variety of studies which ranged from 0.3 to 15.2 t C ha^{-1} $year^{-1}$ with values of 0.8 and 1.1 t C ha^{-1} $year^{-1}$ for the temperate region for vegetative C, and values of 30 to 300 t C ha^{-1} for up to 1 m of soil (Nair et al., 2010). Whilst there is a lot of variation in these estimates, they do highlight the relative contribution from the vegetative and soil components, and it is thought that agroforestry systems are capable of sequestering more C than crop and pasture lands, but less than managed forests (Kirby and Potvin, 2007; Pandey, 2002). It is worth note however that particularly in temperate systems, few studies consider agroforestry systems as the tree component reaches harvest; average vegetative C stock values derived from younger systems before trees have reached their maximum mean annual increment (MAI), are therefore likely to underestimate C sequestration rates.

2.2.3 *Biomass carbon*

The primary way in which an agroforestry system may sequester atmospheric carbon, is through the accumulation of carbon in the tissues of trees and its residues (Mosquera-losada et al., 2011). Calculation of aboveground C stocks is a straightforward, if labour intensive operation. Quick estimates of aboveground biomass C stocks can be made by reference to pre-existing yield tables which allow the calculation of tree volume from proxy measurements such as diameter at breast height (D_{bh}) or height. Volume can then be converted to mass using specific gravity measurements Williamson and Wiemann (2010), although yield tables often only include merchantable timber – i.e. not branches.

Yield-tables rely on the 'site-index hypothesis' which states that yield can be classified by height at a given age (Skovsgaard and Vanclay, 2008). Whilst classifying forest productivity by height is an almost universal practice, it is well established that high or low stem densities as a result of planting or thinning may influence stand height in relation to what are considered to be 'normal' planting densities (Skovsgaard and Vanclay, 2008, and references therein). This is particularly relevant to agroforestry systems, which almost certainly have lower stem densities than the scenarios envisaged by traditional forestry yield tables (e.g. Hamilton, 1996).

Hypothesis

6. Using traditional forestry yield tables to predict the growth of trees in agroforestry systems and farm woodlands (which are typically planted at much wider spacings) will over-estimate yield.

More accurate measurements can be made by determining the mass of a representative sample of trees by destructive harvest. This may include division of the tree into constituent parts (stem, branches, twigs) from which samples are then taken for moisture and C content analysis. From these measurements, total C in biomass can be calculated with a good degree of accuracy, and mathematical models (allometric equations) developed to predict C from similar trees based on a proxy measurement (Picard et al., 2012).

These biomass measurements can also be used for the parameterisation of more complicated process based models for example the Forestry Commission's CSORT (and BSORT) model (Morison et al., 2012), C-FLOW (Dewar, 1990, 1991; Dewar and Cannell, 1992), CO2FIX (Masera et al., 2003), and Yield-SAFE (Graves et al., 2007). Yield-SAFE

For this particular purpose, Yield-SAFE has two advantages. Firstly, Yield-SAFE operates on a daily timestep, thereby offering greater resolution than other models which typically have an annual timestep. Secondly, Yield-SAFE calculates biomass directly, without recourse to yield tables which may not be appropriate for agroforestry systems (Nair, 2011). This does therefore require additional work to parameterise the model, particularly for parameters such as the ratio of crown to total biomass Dewar and Cannell (1992) as trees grown at lower densities tend to have more branches than those growing in dense plantations (Picard et al., 2012).

Calculations of belowground biomass are substantially more challenging than studies of aboveground biomass particularly in mature trees, due to the difficulty of excavating large quantities of soil and biomass intact. Such studies have been completed for established agroforestry systems (e.g. Peichl et al. 2006) but are much more common for dense stands of younger trees where root mass and therefore labour requirements are smaller (e.g. Das and Chaturvedi 2005; Friend et al. 1991; Gielen et al. 2005; Lodhiyal et al. 1995*a*; Lodhiyal and Lodhiyal 1997; Pallardy et al. 2003; Puri et al. 1994). In a similar way to aboveground biomass, destructive studies can be used to establish allometric equations for root biomass, but compared to aboveground biomass relatively few exist however. Where such relationships are employed, it is often necessary to make compromises, for example in the absence of any better estimates Jenkins et al. (2011) recommend using an equa-

tion derived from oak trees to calculate root biomass of all broadleaved species. Standardising methods for measuring belowground biomass is thus highlighted by Nair (2011) as one of the areas in which C studies should be improved through further research. Future studies will benefit from the use of new technologies such as ground penetrating radar and electrical resistivity tomography, but at present the use of such techniques for root biomass quantification is in a stage of relative infancy (Borden, 2013; Fourcaud et al., 2002; Hirano et al., 2008; Wielopolski et al., 2000; Zenone et al., 2008).

2.2.4 *Soil carbon*

Soil carbon is the largest terrestrial C sink, containing ≈ 2225 Pg in the first metre, and accounting for roughly three times the C present in the atmosphere (≈ 750 Pg) (Batjes, 1996). Roughly a third of this ≈ 2225 Pg is contained in inorganic carbonates (Batjes, 1996). Whilst significant, this inorganic soil C pool is not directly contributed to by the action of trees, and for this reason, is not considered further in this review.

Soil organic carbon stocks can be several times greater than the stock of C stored in aboveground biomass, even at quite modest depths. Hence, it is possible for relatively minor changes in SOC stock to have major ramifications for carbon storage (Carney et al., 2007), which are of particular importance to verification standards such as the WCC.

Hypothesis

7. Small losses in SOC may offset a large proportion of gains of C in aboveground tree biomass.

Organic carbon enters the soil mainly through the incorporation of organic matter (of which it comprises around 50%) from plant and animal residues. The majority of SOM comes from the inclusion of fine roots and leaf litter into the soil (Jackson et al., 1997) and is essentially regulated by net primary productivity (NPP) and the rate at which organic compounds therein decompose (Batjes, 1996).

Leaf litter is a source of SOC, and has been demonstrated to make up a large percentage of carbon inputs as a result of reforestation (Harper et al., 2012), and may quickly exceed the levels of native forest (George et al., 2010). However leaf litter addition is considered to be much less important than root derived carbon (Kramer et al., 2010); indeed there is evidence from leaf litter addition experiments that leaf litter can actually be responsible for a decline in mineral SOC stocks (Sayer et al., 2011).

Root inputs (rhizodeposition) are recognised as playing a more important role in the stabilisation of SOM (Balesdent and Balabane, 1996). Rhizodeposition occurs in several ways at the root level, but includes attrition of individual cells (particularly root caps, but also root hairs and other cells), loss of C to bacterial and fungal symbionts, and loss of C in exudates, mucilage deposits at the root tip, and volatile organic C (Jones et al., 2009). Three main modes of stabilisation help to explain why root derived C appears to be more important to SOC stock than shoot derived C.

Firstly, root (particularly tree root) inputs have been found to contain higher quantities of recalcitrant compounds, particularly lignin and suberin, than shoot inputs from the same plants (Fernandez et al., 2003; Recous et al., 2008). The range of microorganisms that are able to decompose lignin in particular is limited, as it requires the use of strong oxidation agents, and may therefore be limited only to white rot fungi (Rasse et al., 2005).

Root derived C inputs also benefit from better stability relative to shoot derived C from the interaction with soil minerals. This is not only due to the proximity of root C inputs to the mineral phase; if it was one might expect ploughing to improve SOM stability, which it does not (Chan et al., 2002). Instead it is likely to do with modes of C deposition that are peculiar to roots, particularly the release of C at the root tip, thus making root elongation in particular the most important factor governing root C deposition to the soil (Farrar et al., 2003) and not fine root mass (Guo et al., 2005). Indeed this may in part be because roots are continually sloughing off root tip cells as they colonise the soil, distributing C over mineral surfaces (Rasse et al., 2005). In addition, roots exude a range of organic acids which, while generally considered to be very labile C sources, are readily sorbed to the mineral soil phase due to their negative charge (Rasse et al., 2005). Sorption to the mineral phase may happen more readily where the soil is not already saturated with C, as more sites are available for new SOM to bind to. This presents an opportunity for deep soil C to accumulate from tree root deposits deep into the soil, where it is likely to be less saturated with C.

Another mechanism by which root inputs might be better at stabilising SOM than shoot inputs is through the formation of soil aggregates. Fine roots and their associated root hairs and mycorrhizal hyphae (if present) form networks binding the soil together, and reducing the availability of SOC to microbial decomposition (Golchin et al., 1994). Fine root hairs may be < 10 µm diameter (Wulfsohn and Nyengaard, 1999), whilst mycorrhizal hyphae are typically around 5 µm diameter (Dodd and Boddington, 2000). This minute scale is important in that it may result in pore sizes too small for microbes to gain access to C locked up in aggregates or inhospitable anoxic conditions within these pores (Rasse et al., 2005).

Hypothesis

3. Tree related SOC is more stable than arable crop or grass related SOC.

Fine root C can be measured in a number of ways. Samples of fine roots can be taken using soil cores which are then washed and the fine root material recovered (Mulia and Dupraz, 2006). Fine root mass and carbon content can easily be determined from these samples, whilst fine root length can be measured using the intersection method, either employed by human operators or by computer (Newman, 1966). Other methods include the use of 'windows' into the soil environment or 'rhizotrons', and most recently 'mini-rhizotrons' within which data can be captured automatically using digital photography (e.g. Joslin et al., 2000). It is also possible to sample root growth using so-called 'in-growth' cores: fine mesh cylinders sunk into the soil into which fine roots are able to grow. This method is most suitable for estimating potential fine-root production between different sites,

whilst the more common soil core method is better for assessing variations over different sampling intervals (Makkonen and Helmisaari, 1999).

2.2.5 *The role of mycorrhizae*

Mycorrhizal fungi are obligate symbionts which form associations with around 80% of all plant species in almost every habitat on the planet, and it is thought that between 10–20% of net photosynthate is allocated to mycorrhiza (Jastrow et al., 2006; Treseder and Allen, 2000).

Mycorrhiza thus represent a significant input of C to the soil both through the beneficial impact on plant growth, and directly through the turnover of mycorrhizal fungi themselves (Jastrow et al., 2006). These direct C may be long-lived. For instance, the glycoprotein glomalin, which is exclusively produced by arbuscular mycorrhizae (AM) has been found to have a turnover time of years to decades (Rillig et al., 2001), much longer than the day–week timescale assumed for AM hyphae (Treseder and Allen, 2000). This is significant because glomalin can make up 30 to 60% of SOC in certain soils (Treseder and Allen, 2000),and has been correlated with aggregate stability (Wright and Upadhyaya, 1998). Further, the contribution of glomalin has been demonstrated to be substantially greater than the contribution to SOC by microbial biomass. Chitin, which may make up to 60% of fungal cell walls (Treseder and Allen, 2000) is also considered to be a recalcitrant compound (Zhu and Michael Miller, 2003).

Whilst this thesis does not consider the impact of mycorrhizal C inputs, it should be noted that Poplar trees in particular are an interesting case, as certain hybrids (e.g. *Populus* X *euramericana*) can form associations with ecto-, endo-, and ectendo mycorrhizae; a relatively unusual situation (Schultz et al., 1983).

2.2.6 *The importance of depth*

The distribution of SOC throughout the soil profile varies according to land use and vegetation type. Jobbágy et al. (2000) found that relative to the first metre, the top 20 cm of soil contained 33%, 42%, and 50% in shrublands, grasslands, and forests respectively. Jobbágy et al. (2000) also notes that an additional 77%, 43%, and 56% of the SOC was found relative to the first metre) in the next two metres. Despite this, it is quite normal for studies to report results from only the first few cm of soil (e.g. Bellamy et al., 2005). Even depths of three metres may not be deep enough: Harper and Tibbett (2013) consider 'deep' SOC to be that found beneath 5 m in depth, which is close to the mean maximum rooting value for shrubs given by Canadell et al. (1996) - but shallower than the mean for trees of close to 7 m. For poplar (*Populus spp.*) and ash (*Fraxinus spp.*) trees, which are the focus of this thesis, maximum rooting depths for trees within these genera have been recorded as 1–3 m and 2 m respectively (Canadell et al., 1996; Stone and Kalisz, 1991).

There are reasons why SOM incorporated into the soil at depth may be decomposed more slowly than at shallower depths, including a reduction in the activity of soil microorganisms, low nutrient concentrations, and higher proportions of particles in the clay size fraction (although this is likely to be site specific) (Job-

bágy et al., 2000; Rasse et al., 2005). In SOC studies related to trees, it is therefore important to sample as deeply as possible, especially since changes in SOC at relatively modest depths may offset a large proportion of the aboveground storage (Carney et al., 2007).

Hypothesis

2. The incorporation of trees into the arable environment will lead to increases in soil organic carbon (SOC) storage at depth.

2.2.7 *Measuring soil organic carbon stock*

2.2.7.1 *Soil bulk density*

Typically two measurements are required to determine SOC stock. The first, organic carbon content ($C_o\%$) is simply the percentage of C in a given mass of soil. To calculate the stock of C in a given volume of soil, $C_o\%$ must be combined with a measurement of soil bulk density (ρ_b). Measurements of ρ_b are usually taken by removing an undisturbed core of known volume, drying to constant weight, and then weighing (Klute, 1986). Typically, $C_o\%$ and ρ_b measurements are then multiplied along with a depth over which the product is generalised. In this way, a measurement of SOC stock in a complete soil profile can be built up using smaller depth increments which are assumed to be uniform.

It has been recognised however that simply multiplying ρ_b with $C_o\%$ – the 'fixed depth method' – does not take into account changes in volume that could result from differences between treatments (Ellert and Bettany, 1995). Figure 2.11 illustrates this point in relation to a treatment which increases ρ_b. Assuming no increase in $C_o\%$ in the pre- and post-treatment measurements (concentration remains at 5%), the post-treatment is found to have 20% more SOC stock than the pre-planting treatment purely because the volume of the top 0–10 cm has reduced by 20%.

This problem can be solved by applying the equivalent soil mass (ESM) method of SOC calculation (Ellert and Bettany, 1995). Using this method, a reference soil mass for each depth increment is assumed, and changes in soil bulk density normalised against this reference value. In the 'original' ESM method, this reference value would be the ρ_b observed prior to the treatment taking place – in the example given in Figure 2.11 this would be 1.0 $g\,cm^{-3}$. Applying the 'original' equivalent soil mass method to the example in Figure 2.11 results in the same SOC stock for pre- and post-planting. In retrospective experiments however, and those without pre-treatment measurements, it is not always clear which value to use for the reference mass, hence the minimum or maximum observed ρ_b can be used (Lee et al., 2009), or an arbitrary value can be selected Bambrick et al. (2010). These methods are an important part of the SOC stock calculation, and are increasingly being adopted (Shi et al., 2013).

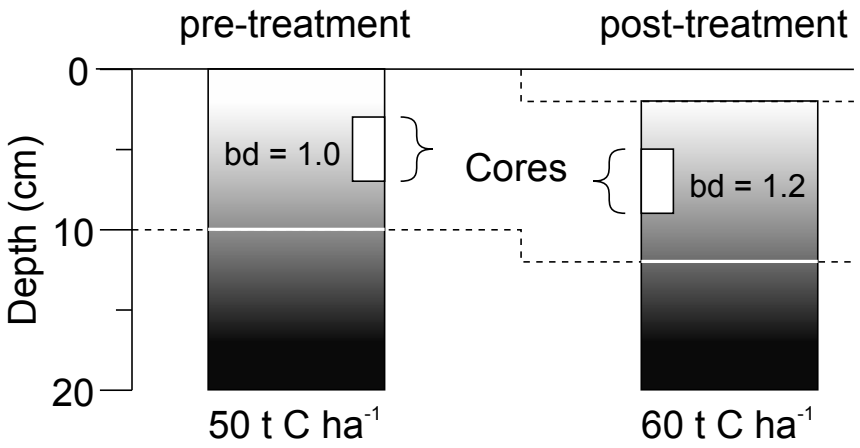

Figure 2.11: An illustration of the limitations of the 'fixed depth method' of soil organic carbon (SOC) calculation. This example assumes the implementation of a management treatment that increases ρ_b. Cores are removed from the middle point of the depth increment. An increase in soil bulk density (ρ_b) from 1.0 g cm^{-3} to 1.2 g cm^{-3} is enough to increase soil organic carbon (SOC) stock from 50 t C ha^{-1} to 60 t C ha^{-1}, assuming that no change in organic carbon content (C_o%) has occurred. Shading represents increasing ρ_b with depth.

2.2.7.2 *Measurements of organic carbon content*

Calculation of C_o% in soils is carried out combustion by wet or dry combustion of the organic C.

Wet combustion The most widely used wet combustion method involves digesting organic carbon with potassium dichromate ($K_2Cr_2O_7$). This method, proposed by Walkley and Black (1934), although now variously modified, involves heating exothermically with H_2SO_4. During this reaction (Equation 2.3) the $K_2Cr_2O_7$ oxidises organic C forming CO_2 and H_2O. Optionally, orthophosphoric acid (H_3PO_4) may be added to reduce interference by Fe^{3+} ions present in the soil.

$$2\,Cr_2O_7^{2-} + 3\,C^0 + 16\,H^+ \longrightarrow 4\,Cr^{3+} + 3\,CO_2 + 8\,H_2O \tag{2.3}$$

After reaction, unreacted $CR_2O_7^{2-}$ is back-titrated colourimetrically with $FeSO_4$ and N-phenylanthranilic acid indicator solution (British Standards Institute, 1990) giving a measurement of how much of the $CR_2O_7^{2-}$ was required, and by extension how much organic matter was present. This method can be improved upon by the use of automatic titrators which determine an end point potentiometrically rather than colourimetrically, removing some of the subjectivity related to determining a colour change. Measuring the evolved CO_2 from the wet oxidation reaction can also reduce errors related to the titrimetric procedure (Rosell et al., 2001). This method returns a measurement of organic matter content, not organic C, and a conversion factor is therefore applied, usually 58% although this can vary (Schumacher, 2002).

Whilst the Walkley-Black method has been the mainstay of assessments of SOC because of its low cost and scaleability (Rosell et al., 2001) there are concerns over operator and environmental exposure to $K_2Cr_2O_7$ which is acutely toxic and a known human carcinogen.

Dry combustion methods The simplest dry combustion method is the so called weight loss on ignition (LOI) method. This involves heating the sample to 430 °C for 24 hours (Rosell et al., 2001) to ignite any C in the soil, allowing changes in sample weight and therefore $C_o\%$ to be measured (Cambardella et al., 2000). Whilst this provides an inexpensive method of determining the carbon content of soils, the technique also has a serious methodological flaw in that there is an implicit assumption that all the SOC will be oxidised within a narrow temperature range. This assumption does not always hold, and some SOC may resist oxidation at temperatures in excess of 600°C. Furthermore, structural water stored within the lattice of clay minerals may not be lost during initial drying at 105°C, whilst hydrated salts and other volatile compounds may cause overestimations of SOC as they are ignited during heating (Rosell et al., 2001). Some authors have argued that careful preparation of samples (Cambardella et al., 2000), and differential heating to separate the organic from the inorganic carbon (Wang et al., 2012) can give accurate estimates of SOC, but in general this technique is not favoured where high accuracy is needed (Salehi et al., 2011).

Automated elemental analysis is a much more accurate method of SOC determination, offering a recover rate of carbon of $> 99.5\% \pm 0.1\%$ (Elementar Analysensysteme GmbH, 2002). This method relies on combustion of the sample at very high temperatures (> 900°C); the quantity of hydrogen, nitrogen, and carbon are then determined individually by a 'thermal conductivity detector'.

Automated gas analysers do not differentiate between organic and inorganic carbon, and hence carbonates must be reacted away prior to analysis by addition of dilute HCl, or must be accounted for by other methods, and the results corrected (Rosell et al., 2001).

Although the most accurate, elemental analysis is also the most expensive method. At time of writing, in the UK, this method can cost several pounds (GBP) per sample, which can be a considerable impediment to accurately determining SOC from a large quantity of samples.

2.2.7.3 *Statistical difficulties in measuring soil carbon*

Whilst the experimental procedure of measuring $C_o\%$ is relatively straightforward, the nature of $C_o\%$ measurements mean that it may not be a straightfoward procedure statistically (Hungate et al., 1995; Kravchenko and Robertson, 2011). Soils are extremely heterogeneous, especially when measurements are taken to great depth, whilst the quantities of C measured are typically very small, and tend to change at a very slow rate following changes in management – for example tree planting. Therefore measurements tend to have a high coefficient of variation (CV) which is difficult to overcome without much expensive sampling, especially when samples are taken at depth.

Hypothesis

8. Frequentist hypothesis testing is an appropriate tool to determine differences in SOC in newly planted woodlands.

2.2.7.4 *Fractionation of soil organic carbon*

Whilst measurements of bulk SOC are useful and standard, they are limited insofar as they only give a value for the total soil C at the time the measurement was taken; no information is given about the quality of the C or its likely turnover time. However, whilst it is easy to conceptualise pools of SOM, actually separating, and measuring the magnitude and longevity of these pools is much more complicated. Several methods for 'fractionating' SOM into its functional pools have been proposed, however most methods are not capable of extracting uniform SOM pools, and hence it has rarely been possible to discover clear relationships between particular mechanisms of stabilisation and soil carbon fractions (von Lützow et al., 2007). This disclarity has made it difficult to link measured SOM pools with conceptual pools, particularly those found in SOM turnover models.

Particle size fractionation is one of the most common methods employed, working on the assumption that particles composed of different minerals interact with SOM in different ways – quartz based sand particles do not bond well with SOM, whereas clay and silt particles with larger surface area and more reactive sites sorb SOM more readily (von Lützow et al., 2007). Hence, the assumption can be made that SOM in the sand fraction of a soil can be attributed to the conceptually active pool, whilst SOM in the silt and clay fractions are considered to be slow and passive respectively (von Lützow et al., 2007). However, this distinction is not clear-cut, and it has been found that the finest clay fraction (< 0.2 µm) can contain less C than coarser clay fractions, whilst C turnover times in silt have been found to be longer than in clay, suggesting that more than one mechanism of stabilising organic C is at play (von Lützow et al., 2007).

Fractionation can also be completed on the basis of density. A light fraction (LF) of SOM not associated with soil minerals, often referred to as 'uncomplexed' is separated from a heavier fraction using organic liquids or inorganic salts, for instance $Na_6(H_2W_{12}O_{40})$ - sodium polytungstate (von Lützow et al., 2007; Zimmermann et al., 2007). The lighter fraction is largely (though not exclusively) composed of particulate organic matter (POM) for instance: partly decomposed plant and animal residues, fungal hyphae, spores, faeces, skeletons, root fragments, seeds, and perhaps charcoal (Christensen, 2001). Gregorich et al. (2006) and von Lützow et al. (2007) differentiate LF from POM as that fraction which is isolated by density alone, whereas POM is fractionated either on the basis of size (< 53 µm) or a combination of size and density (<1.6–2.0 $g\,cm^{-3}$). Organic matter in this pool is generally considered to be labile, and would typically have a turnover time measurable in years (Janzen et al., 1992; von Lützow et al., 2007).

Chemical methods are also used for the fractionation of SOM, based on the extraction of SOM in aqueous solutions, organic solvents, water or acids, or the resistance of SOM to oxidation (von Lützow et al., 2007). Dissolvable organic matter (DOM) is considered to be one of the most labile fractions of SOM, since mechanisms of microbial decomposition require a water environment (Marschner and Kalbitz, 2003). Dissolvable organic matter may be extracted with cold or hot water, or solutions designed to mimic soil water in their ionic strength; in all cases DOM is defined as being able to pass through a 0.45 µm aperture in solution (von Lützow et al., 2007). Soil microbial biomass may also be determined through chemical

means, usually incorporating fumigation with chloroform; with turnover times of less than 5 years, microbial biomass is widely considered to be an active or labile C pool (von Lützow et al., 2007). Treatment with oxidation agents has been shown to remove younger, more reactive OM, leaving an older, more stable pool. Kleber et al. (2005), in a study of twelve soils from a variety of parent materials, found that treatment with NaOCL (sodium hypochlorite) increased the radiocarbon age of samples relative to the bulk soil in all cases.

Determining turnover rates (k) of isolated fractions can be done through a variety of methods. Decomposition studies of litter give reasonably accurate estimates of turnover of the active pool (von Lützow et al., 2007). Labeling with stable ^{13}C over a chronosequence of samples allows changes in soil carbon to be monitored and turnover times calculated, for instance charting a move from predominantly C3 plants to C4 plants (Oelbermann and Voroney, 2007). Archived samples can also be used to age soil carbon, utilising ^{14}C released from the testing of thermonuclear weapons in the 1950–1960s (Richter et al., 1999). Finally organic matter in soils provides a suitable substrate for the ^{14}C radiocarbon dating technique (Trumbore, 1993; Wang et al., 1995).

2.2.8 *Factors affecting soil organic carbon storage*

A number of factors which can impact the stability of SOC stock have been identified in several recent meta-analyses (Guo and Gifford, 2002; Laganiere et al., 2010; Paul and Polglase, 2002; Post and Kwon, 2000; Shi et al., 2013). The consensus that emerges from these studies is that previous land use is probably the most important factor, and that clearing forest for arable agricultural or forest plantation plantation is largely detrimental; for instance Guo and Gifford (2002) report SOC stock losses of 13% ($n = 30$) following changes from native forest to plantation, and 42% ($n = 37$) from native forest to crop. In one study SOC stock losses of 66% were recorded following the conversion of forest into arable land (Beheshti et al., 2012). Accordingly, planting trees on arable land (or other C depleted soils) tends to lead to increases in SOC stock (Post and Kwon, 2000).

Hypothesis

1. Establishing silvoarable agroforestry systems on arable land will increase soil organic carbon (SOC) stocks relative to a pure arable control.

Converting grassland or pasture to plantation, on the other hand, has been shown to lead to either much smaller increases, or even losses of SOC (Table 2.1). The exact reasons for these declines is not clear, however Post and Kwon (2000) postulate that perennial grasses are simply better at storing carbon in the soil than trees; hence afforestation and exclusion of grass beneath the trees leads to a decline in SOC inputs. The findings of Guo et al. (2005) support this view, and further show that the mass of dead fine root mass incorporated into the soil does not seem to be the critical factor in SOC stabilisation – rather it is is something peculiar to the action of live fine roots (and in particular grass roots) that is responsible for increasing SOC stocks in the soil.

Whilst the values in Table 2.1 are fairly uniform in showing declines in SOC stock following planting, there is some evidence that after sufficient time, pre-planting SOC stock will be recovered and possibly exceeded, although this recovery may be limited to the light SOC fraction, at least initially. This recovery has been recorded in a relatively modest time period of 5–10 years, or as long as 50 years (Huang et al., 2011; Poeplau et al., 2011) when the O horizon is included. When considering just the mineral soil, such a recovery is likely to take at least 140 years or longer to occur (Poeplau et al., 2011).

Hypotheses

4. Planting trees on grassland will lead to a decline in SOC stock.
5. Losses of SOC from tree planting on grassland are dependent on the density of the tree planting.
    - Less densely planted silvopastoral systems under which a grass understory can be maintained will have a smaller initial loss of SOC than more densely planted systems, but less potential to accumulate SOC in the long-term owing to a smaller input of SOM from trees.
    - Conversely, dense systems under which grass is excluded, will exhibit greater initial losses, but a faster recovery and greater maximum SOC.
    - Early SOC losses may thus be recovered over the long-term as SOM inputs from the trees increase beyond the inputs of a grass understory.

    This is conceptualised in Figure 2.12.

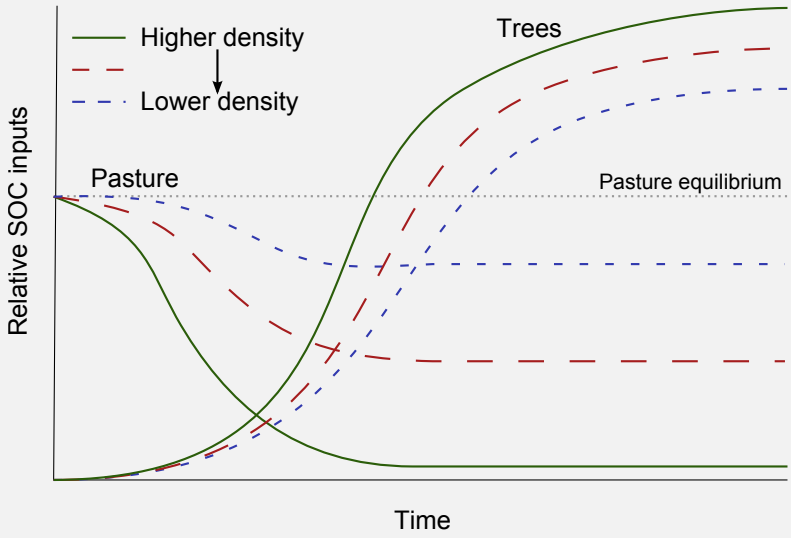

Figure 2.12: Conceptual diagram of how inputs of C to the soil might differ with different planting density in a silvopastoral system.

A number of other factors can also have an impact. Pre-planting soil preparation and the level of disturbance as a result of management also have an effect – sites with high levels of disturbance show lower SOC accumulation rates (Jandl et al., 2007; Laganiere et al., 2010). Sites afforested with broadleaf trees tend to have greater increases in SOC stock than sites afforested with coniferous species (Guo and Gifford, 2002; Laganiere et al., 2010; Paul and Polglase, 2002), whilst climatic zone has been shown to have varied effects (Laganiere et al., 2010; Paul and Polglase, 2002). Finally precipitation, particularly following the change from pasture to forest/plantation has (Guo and Gifford, 2002; Kirschbaum et al., 2008) has been shown to have negative effects on SOC stock.

Table 2.1: Summary of SOC stock change following tree planting on arable and pasture land from four recent meta-analyses. Depths, and number of studies on which estimates are based (n) are included where available.

Source	Depth (cm)	Units	Arable % Change	Arable n	Pasture % Change	Pasture n
Paul and Polglase 2002	< 10	% year^{-1}	1.55	_	−0.07	_
Paul and Polglase 2002	> 10	% year^{-1}	0.49	_	−0.13	_
Paul and Polglase 2002	< 30	% year^{-1}	1.51	_	−0.20	_
Shi et al. 2013	O[a]	t C ha^{-1} year^{-1}	0.42	_	0.43	_
Shi et al. 2013	0–20	t C ha^{-1} year^{-1}	0.58	_	−0.19	_
Shi et al. 2013	20–40	t C ha^{-1} year^{-1}	0.19	_	−0.09	_
Shi et al. 2013	40–60	t C ha^{-1} year^{-1}	0.07	_	−0.06	_
Shi et al. 2013	> 60	t C ha^{-1} year^{-1}	−0.03	_	−0.01	_
Guo and Gifford 2002	_	%	18.00	83	−10.00	29
Laganiere et al. 2010	34[b]	%	26.00	17	3.00	9
Poeplau et al. 2011	_	% 20 year^{-1}	16.00	_	−4.00	_
Poeplau et al. 2011	_	% 100 year^{-1}	83.40	17	−6.50	_

[a] O horizon is given rather than a fixed depth.

[b] Mean depth of all studies.

3 METHODOLOGY

Two main fields sites were used as part of the project. In this section a description of each field site is given in turn.

3.1 SILSOE SILVOARABLE TRIAL

3.1.1 *History*

In 1992 a network of experimental sites was set up as part of a Ministry of Agriculture, Fisheries and Food (MAFF) sponsored UK silvoarable trial. Experimental sites incorporating hybrid poplar with arable crops were established at Cirencester, Leeds, and Silsoe. The site was later managed as part of the Silvoarable Agroforestry for Europe (SAFE) project, a European project to investigate the uncertainties related to silvoarable systems.

Although the SAFE project came to an end in 2003 and management of the site ceased, the experiment remained an important resource for assessing how a silvoarable system has developed nearly two decades after establishment.

3.1.2 *Location*

The silvoarable experiment was set up in Olney field, on the Silsoe college site of Cranfield University (N52°0′8.06″, W0°25′46.80″)[1] in April 1992. The site is almost entirely flat, with a minor slope to the east of less than 1%. Historic mapping suggests that the site has been under agriculture since at least the 1880s.

3.1.3 *Climate*

A weather station was maintained at the Silsoe College site for many years, prior to its closure. Data collected at the site for the years during which the experiment was in place (1992-2006) are summarised here.

3.1.3.1 *Solar radiation*

Solar radiation recorded at the site ranged between values of 1.9 MJ d^{-1} in December and 19.4 MJ d^{-1} in July (Figure 3.1).

3.1.3.2 *Temperature*

The mean daily air temperature recorded at the site was 10.4°C. Median monthly values for the years 1992-2006 ranged from 4.7°C in December to 17.2°C in July (Figure 3.2). The extreme values were a minimum of −5°C, and maximum 27.7°C.

1 http://g.co/maps/5bnxx

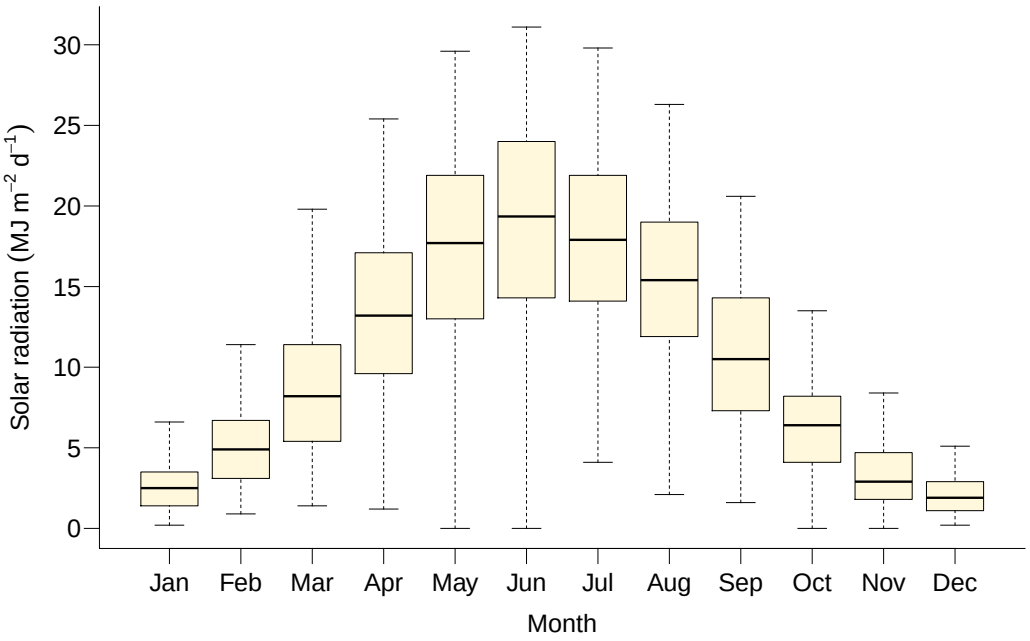

Figure 3.1: Daily solar radiation receipt (MJ d^{-1}) for each month for the years 1992-2006 as recorded at Silsoe College. The format of this boxplot (and all subsequent boxplots in this thesis) is to denote the median with the thick line at the centre of each box. The upper and lower limits of each box relate to the upper and lower quartiles ($q_{0.75}$ and $q_{0.25}$). The ends of the dashed lines (the whiskers) represent the upper and lower adjacent values. The adjacent values are calculated by adding or subtracting the 1.5 times the interquartile range ($q_{0.75} - q_{0.25}$) from the upper and lower quartiles. The highest or lowest values within these limits are regarded as being the upper and lower adjacent values. Any values which are beyond this limit are considered to be outliers, and are represented with dots.

3.1.3.3 *Precipitation*

Total monthly precipitation at Silsoe for the period 1992-2006 varied between 1.2 mm d^{-1} in March, and 2.3 mm d^{-1} in October (Figure 3.3). Mean yearly precipitation was 633 mm d^{-1}, and varied between 410 mm d^{-1} in 1996, and 867 mm d^{-1} in 2000.

3.1.4 *Soil*

The soil at Olney field has been classified as belonging predominantly to the Holdenby series (Verma and Bradley, 1988), a typical argilic pelosol, characterised as clay-loam with some flinty stones, overlying a similar mottled clay, passing to calcareous clay or mudstone with depth. Holdenby soils are recorded as being slowly permeable, often remaining waterlogged in winter (Verma and Bradley, 1988, p. 7a).

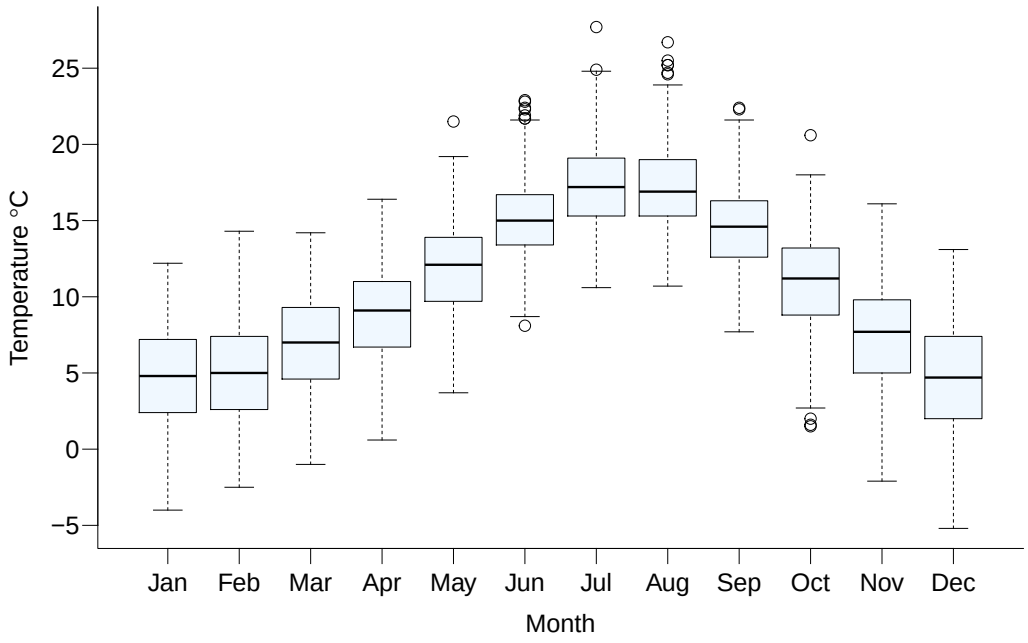

Figure 3.2: Mean daily air temperature (°C) for each month for the years 1992-2006 as recorded at Silsoe College.

An investigation of soil texture at the site was completed by Ashby (2001), using the pipette method for PSD. Over a depth of 1 m, Ashby found a clay (< 2 µm), silt (2-63 µm), and sand content (63-200 µm) of 53.2%, 26.8%, and 18.4% respectively[2].

Because of the clay mineralogy, and in particular high levels of montmorillonite, the soil shows a marked level of swelling and shrinkage in response to wetting and drying.

3.2 EXPERIMENTAL DESIGN

The agroforestry experiment at the Silsoe experimental farm formed part of a network of three silvoarable experiments (the other sites being Leeds and Cirencester) set up in April 1992. Prior to the establishment of the agroforestry experiment, the whole site had been used for arable cropping for at least 20 years.

The site consists of a 2.5 ha silvoarable block surrounded by approximately one hectare of conventionally cropped arable land. The silvoarable block was planted in April 1992, and comprised three replicated blocks, including each combination of four poplar hybrids and three agroforestry cropping treatments.

The poplars were planted at an interval of 6.4 m along rows, aligned in an approximate north-south direction; each poplar hybrid planted as a contiguous group of five trees, with a guard tree (buffer) at the end of each row (Figures 3.4 and 3.5). Rows were spaced 10 m apart, and comprised an uncultivated 2 m strip at the base of the trees and an 8 m wide strip that was ploughed each autumn. The poplars were planted as 1.5-2.0 m unrooted sets to a depth of 0.6 m, into a 1.5 m wide polythene-film mulch extending along the tree rows; the edges were

2 Rounding errors prevent the sum from equaling 100% – the complete data were not available.

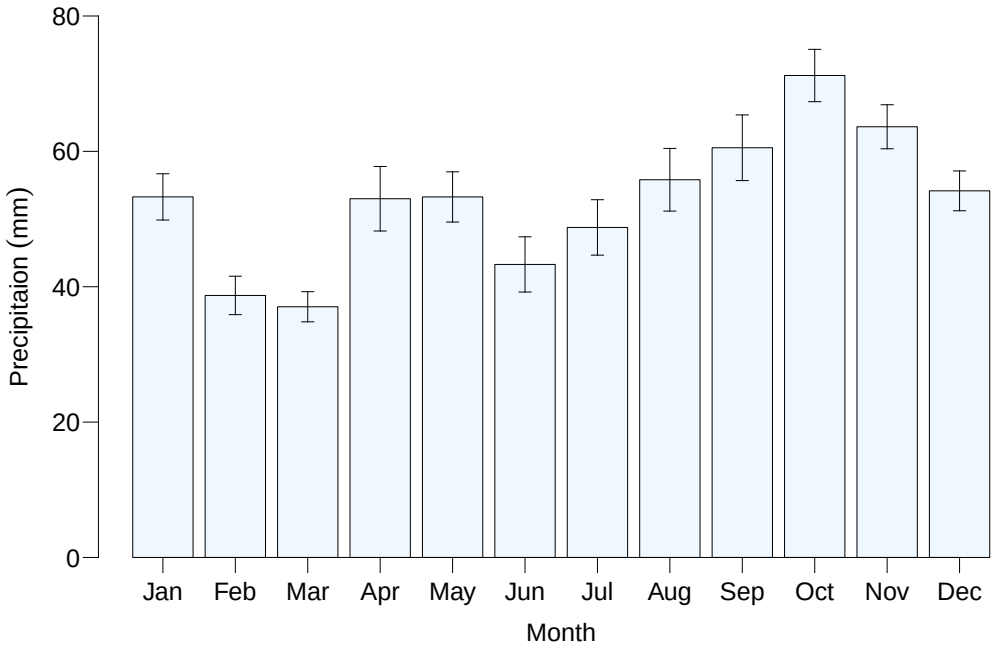

Figure 3.3: Mean daily precipitation (mm d^{-1}) for each month for the years 1992-2006 as recorded at Silsoe College. Error bars indicate standard errors of the mean.

mechanically buried under the soil to leave an exposed strip of plastic 1-m-wide. This was maintained until the end of 1999, when the polythene was removed and a grass-clover tree-strip was sown by hand.

Each replicate block included three pairs of alleys each with a central measurement tree row, including rows of 'guard' trees at the ends of the block. The alleys adjacent to these measurement rows were then allocated to one of three cropping treatments: cropped, fallow, and alternately cropped.

From 1992 to 2003, the control areas and each of the alleys were ploughed on an annual basis. An arable crop was then established in the control and cropped agroforestry treatment, with the exception of 2001, when waterlogging meant that all treatments were maintained as a bare-fallow (Table 3.1).

The alternately cropped treatment was changed in autumn 1999 so that a crop was grown on both sides of the tree row, effectively becoming continuously cropped. Active management of the site ended in 2003; since then a grass-sward has been allowed to emerge. Around the agroforestry block is a control area (roughly 1 ha) which was cropped with exactly the same regime as the cropped agroforestry treatment (Table 3.1).

The arable crops were conventionally managed and harvested receiving fertiliser and agrochemicals as appropriate. The last arable crop (spring beans) was planted and harvested in 2003. From 2004 to 2011 all of the agroforestry and control areas remained uncultivated and a grass sward was allowed to establish naturally.

The poplars were pruned during the autumns of 1993, 1995, 1997, 1998 and 2000; with the aim of achieving a clear bole to a height of about 8 m. Waste arising from pruning was removed from the experimental area. In June 2011, the Beaupré

poplars[3] had attained a mean diameter at breast height of 36.2 (±0.5 SE) cm and 38.0 (0.5 SE) cm in the cropped and fallow treatments respectively. Mean heights for these treatments were 24.6 (±0.2 SE) m and 25.4 (±0.3 SE) m respectively.

The four hybrid poplars chosen for the experiment were Beaupré (*Populus trichocarpa* × *deltoides*), Gibecq (*P. deltoides* × *nigra*), Robusta (*P. deltoides* × *nigra*) and Trichobel (*P. trichocarpa* × *trichocarpa*) (Burgess et al., 2003).

Table 3.1: Management of the cropped area in the fallow and cropped agroforestry, and arable control areas from 1992 to 2011. The cropped and fallow agroforestry treatments comprised a row of trees bordered on either side by a 10 m alley. A 2 m strip, centred on the tree row remained uncultivated during the course of the experiment. The remaining 8 m of each alley was cultivated as shown. From 1992 to 2003, each cultivated area was ploughed annually.

Year	Fallow	Cropped and Control
1992-2003	Bare-earth fallow	Winter wheat (92), linseed (93), spring wheat (94), winter wheat (95), winter wheat (96), winter wheat (97), winter beans (98), spring barley (99), winter wheat (0), bare fallow (1), winter barley (2), spring beans (3)
2004-2011	Uncultivated – natural regeneration of a grass sward	

Each of the measurement trees within the experiment can be identified with a code which describes its position within the experiment, for example 1CB4: block one, continuously cropped treatment, Beaupré hybrid, fourth tree. This system is depicted in Figure 3.4 and Figure 3.5.

3 In-depth information about the growth of all the trees at the site is included in Chapter 7. Soil carbon and root measurements were taken beneath the Beaupré hybrid only.

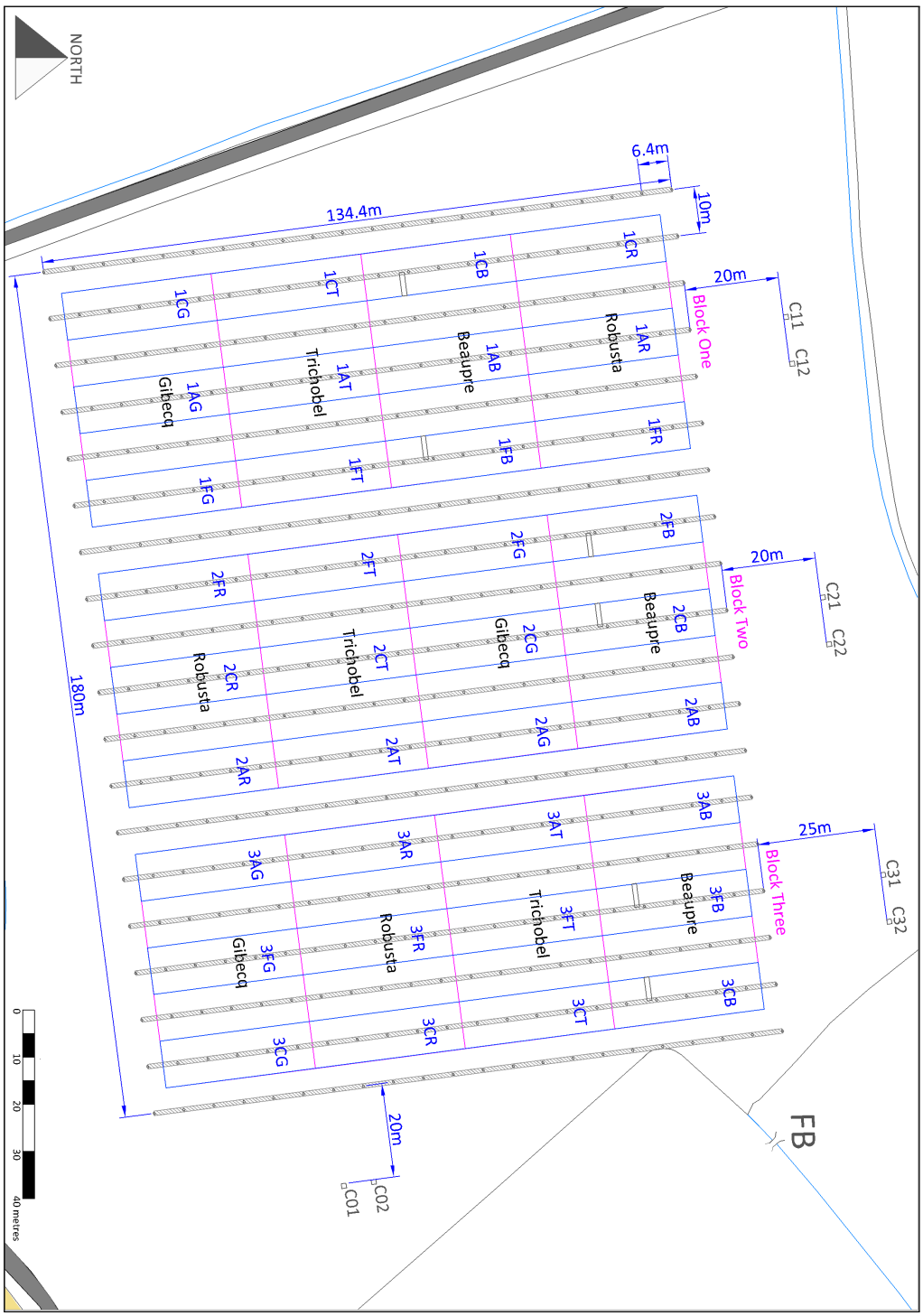

Figure 3.4: Plan view of the site. Note the location of control plots (designated C1-C32), and root trenches (denoted by grey rectangles in the inter-cropped alleys – see Figure 3.5).

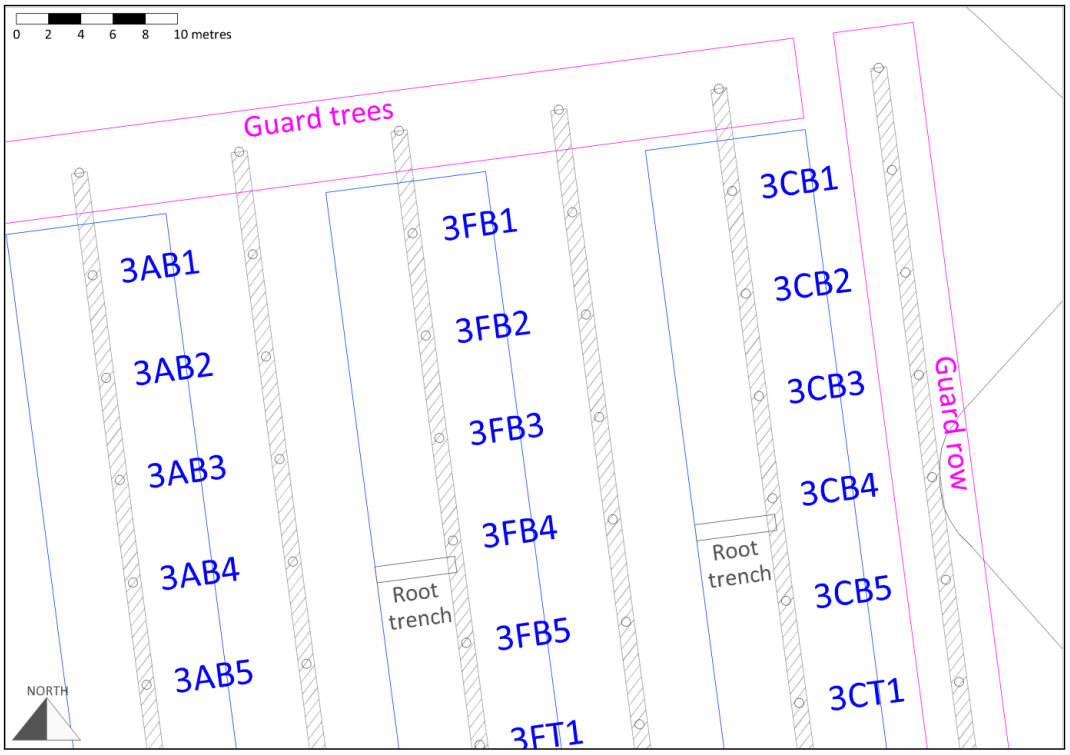

Figure 3.5: Close up of the north-eastern most corner of the agroforestry plot. Guard rows are indicated at the north and east end of the site. Note root trenches.

3.3 CLAPHAM PARK

3.3.1 *Location*

Experimental measurements were taken at a site (N52°9′36″, W0°28′27″)[4] in the village of Clapham, approximately 3 km north of the centre of Bedford. The site declines in height significantly from west to east (Figure 3.12), and covers a total area of about 15 ha.

3.3.2 *Climate*

Data from several MIDAS Land Surface Stations (UK Meteorological Office, 2013) were compiled to provide meteorological data for the site for the years 2003-2012. Temperature data were produced by averaging records from the Woburn MIDAS station (ID: 458, Lat: 52.01, Lon: −0.59, Elevation: 89 m) and the Bedford MIDAS station (ID: 461, Lat: 52.23, Lon: −0.46, Elevation: 85 m).

Precipitation data were obtained from the Wilstead MIDAS station (ID: 4363, Lat: 52.08, Lon: −0.43, Elevation: 37 m). It was not possible to obtain reliable values for solar radiation.

3.3.3 *Temperature*

Mean daily air temperature for the years 2003-2013 was 10.2°C, whilst monthly medians ranged from 16.6°C in July to 4.1°C in December. The extreme values over the ten year period were −12.7°C and 30°C.

3.3.4 *Precipitation*

Mean annual precipitation for the years 2002-2013 varied between 430 mm in 2005 and 921 mm in 2007 (mean: 652 mm). Mean monthly precipitation was greatest in August at 78 mm and least in March at 33 mm.

3.3.5 *Soil*

The soils at Clapham belong to the Evesham series, characterised as 'slowly permeable calcareous clay, and fine loamy over clayey soils' (NSRI, 2012). Soils in the Evesham series are considered to be 'Calcaric Stagnic Vertic Cambisols' in the World Reference Base for Soil Resources (WRB) classification (Cranfield University, 2014).

Soil texture was assessed using the pipette method for particle size determination (see Appendix B.4.1 for a complete description of this technique). The locations from which PSD samples were taken have been included in Figure 5.3.

Results from PSD suggested that the site could be predominantly classified as clay[5] (Figure 3.8). Of the 72 samples analysed, 51 were classified as clay. On av-

4 http://goo.gl/maps/PdEa1

5 Following the Natural England texture classification system (Natural_England, 2008).

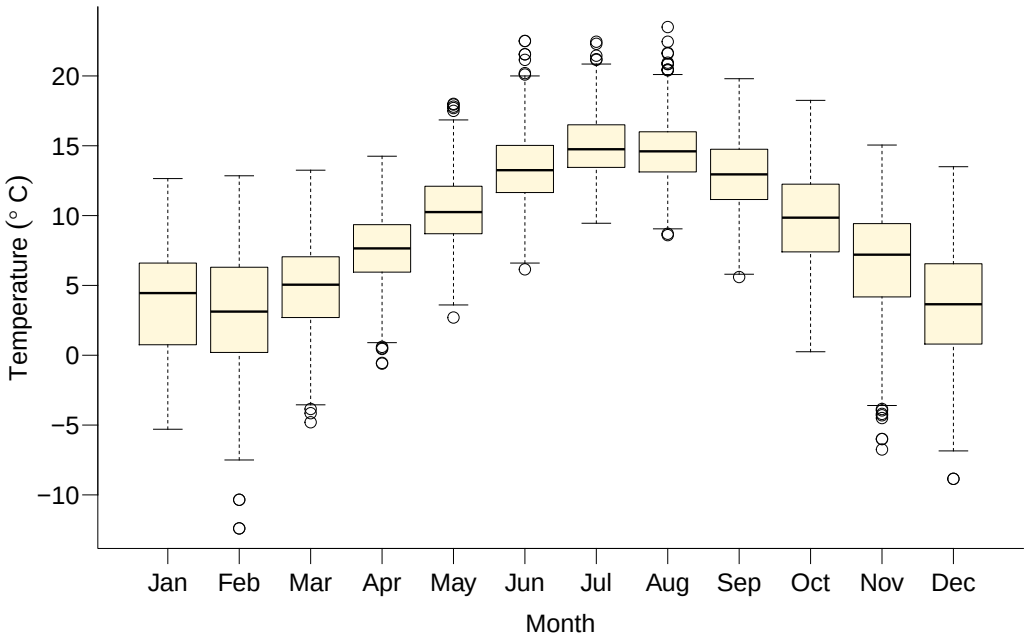

Figure 3.6: Mean daily air temperature for each month for the years 2002-2013 derived from MIDAS Land Surface Stations (UK Meteorological Office, 2013). See section 3.3.2 for details of the stations from which this data was derived.

erage, soil at the site was found to comprise $25.8 \pm 1.4\%$ sand ($0.063 - 2$ mm), $31.8 \pm 1.1\%$ silt ($0.002 - 0.063$ mm), and $42.4 \pm 1.3\%$ clay (< 0.002 mm). When analysed using analysis of variance (ANOVA), no significant depth effect was found (Table B.1)

3.3.6 *History*

The site formed part of the estate of Clapham Park, an Elizabethan manor house built in 1872 (Page, 1912). Historical mapping (Landmark Information Group, 2004) indicates that from at least the 1880s, the site was entirely parkland, with widely spaced individual trees, and a small number of tree groups. An avenue of trees lined the footpath (still present today - part of the John Bunyan trail) from Hawk drive, south towards Bedford (Figure 3.9).

Maps from the 1960s (Landmark Information Group, 2011*a*) and 1970s (Landmark Information Group, 2011*b*) indicate that substantial changes occurred to the local area at this time; several remaining woodland fragments in the site and adjacent fields were lost, leaving scattered trees and a lined avenue along the north - south footpath. In the present day, some few remnants hint at the historical presence of parkland trees. Contemporary field margins are marked by hedges of traditional hedgerow species including *Crataegus* spp., *Prunus spinosa*, *Acer campestre*.

In September 1996 the Commission of the European Communities, jointly with Bedfordshire County Council agreed to provide support for the 'Bedfordshire Farm Woodland Project'. The project was designed with the objective of diversifying the economic base of farms and improving the rural environment by 'demon-

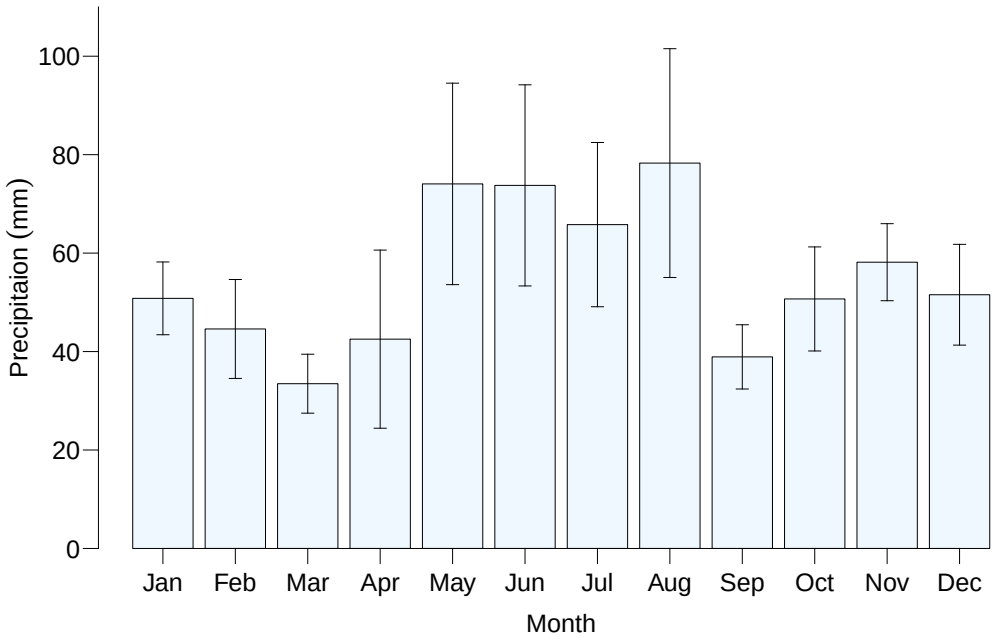

Figure 3.7: Mean monthly precipitation for each month for the years 2003-2012 as recorded at the Wilstead UKMO MIDAS station (4363). Error bars indicate standard errors of the mean.

strating the technical feasibility and the economic viability of incorporating improved farm-woodland and agroforestry within commercial farms' (Burgess et al., 2000).

The Clapham park site, by this time owned by Bedford Borough Council but leased to a tenant farmer, was selected as one of the field sites at which the trial would proceed. At this time the field was being used by the tenant farmer as pasture for a suckler-beef system (Burgess et al., 2000).

In 1998, the site was split into two discrete areas. The first, to the south was fenced and planted as community woodland comprising a mix of broadleaf species at 2.5 m spacing and a riparian system area to the east (not included in measurements). The remainder of the site was planted as a silvopastoral system comprising 34 discrete blocks of trees; 30 consisting of 16 trees, with 4 larger blocks of 75, and a number of hornbeam trees to replace those lost from the old avenue (Table 3.2).

Since then, the site has continued to be leased by the tenant farmer for grazing a suckler-beef herd. Cattle graze most of the season apart from a 3-4 week period before mowing for a hay/silage crop in June and September. The pasture is fertilised at a rate of 100 $\mathrm{l\,ha^{-1}}$ with an NPK compound, and treated with herbicide (MCPA) at a rate of 3 $\mathrm{l\,ha^{-1}}$ prior to mowing. In the community woodland, rides are mown to keep footpaths open.

A nearby woodland named 'Helen's Wood' (Figure 3.10 and 3.11) was also used in experimental measurements. In the 1880s, maps indicate that a mixed woodland stood upon the site (Landmark Information Group, 2004), but in the present day it is composed largely of mature ash (*Fraxinus excelsior*). This woodland is also grazed by the tenant farmer, and represents a mature silvopastoral system. The

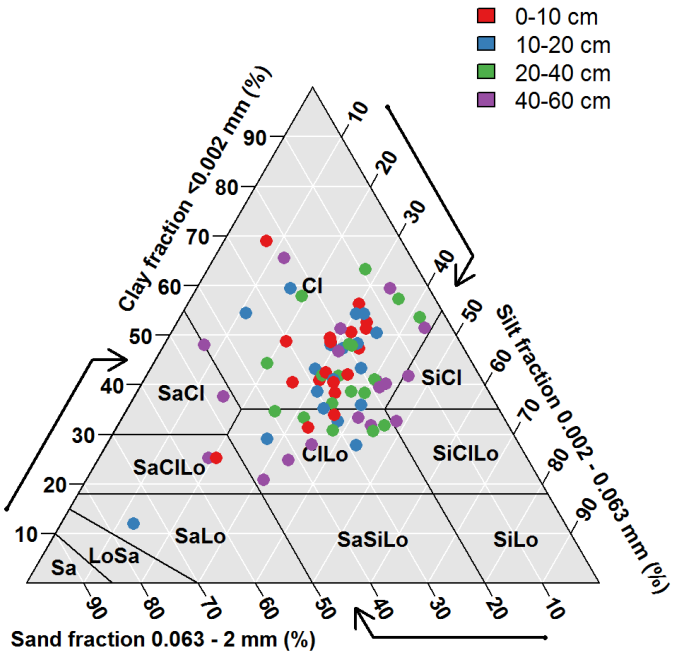

Figure 3.8: Soil texture by depth at Clapham Park, following the Natural England texture classification system (Natural_England, 2008).

wood has not seen active management for some years, there is little discernible regeneration, and would not therefore constitute a sustainable agroforesty system. Mature trees are widely spaced, and a grass understory persists throughout the year, even in the winter months (Figure 3.10).

Table 3.2: Description of planting at the Clapham site between 1998 and 2000, adapted from Burgess et al. (2000).

Area (ha)	Species composition	Arrangement
	Unit 1: Silvopastoral system	
7.98	Averaging 100 trees per hectare, in groups as follows: 40% oak, 30% ash 10% hornbeam 10% small-leaved lime 10% field maple.	4 groups of 75 trees 30 groups of 16 trees 6 half-standard hornbeam trees Within the groups, trees are spaced at 2 × 2 m. (The actual area covered by trees is approximately 0.45 ha).
	Unit 2: Community woodland	
6.11	Mixed-broadleaf: 30% ash, 10% oak, 10% wild cherry, 10% small-leaved lime, 20% 'shrub mixture' 20% open ground to form footpaths, rides and glades.	Fenced; principally 2.5 × 2.5 m spacing

(a) The Clapham Park site looking south in towards the farm woodland block in May 2004. Photo credit: Paul Burgess.

(b) The Clapham Park field side, looking North towards Hawk Drive in March 2014.

Figure 3.9: The Clapham Park field site in 2004 and 2014. Image a is presented under a generic Attribution - NonCommercial - ShareAlike 2.0 Generic license (CC BY-NC-SA 2.0): https://creativecommons.org/licenses/by-nc-sa/2.0/

Figure 3.10: Helen's wood mid-January 2014 facing southwest. Note the full grass understory.

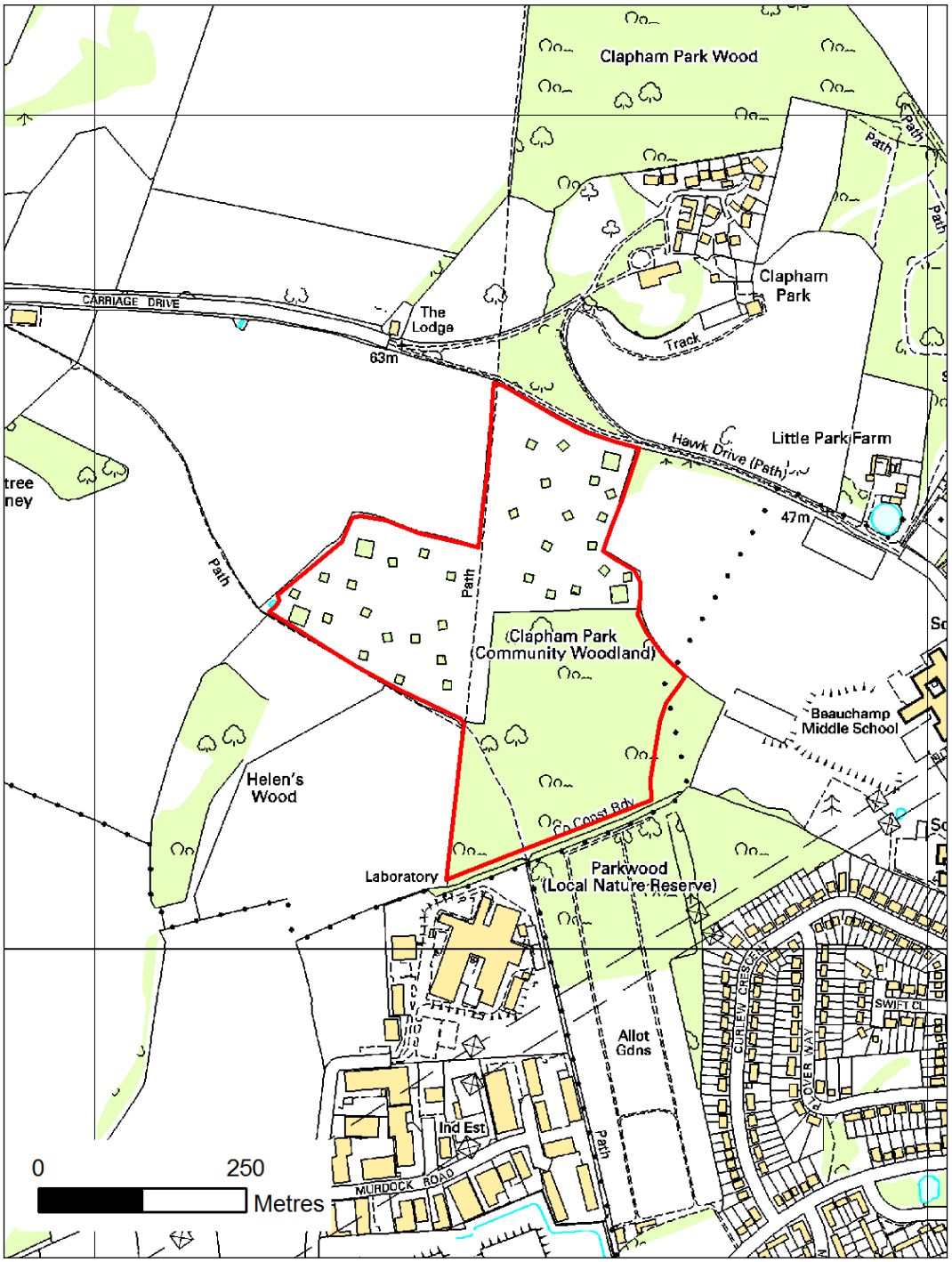

Figure 3.11: Map of the Clapham Park site (1:10 000). Red outline indicates site boundary (Ordnance Survey GB, 2011) © Crown Copyright/database right 2011. An Ordnance Survey/EDINA supplied service.

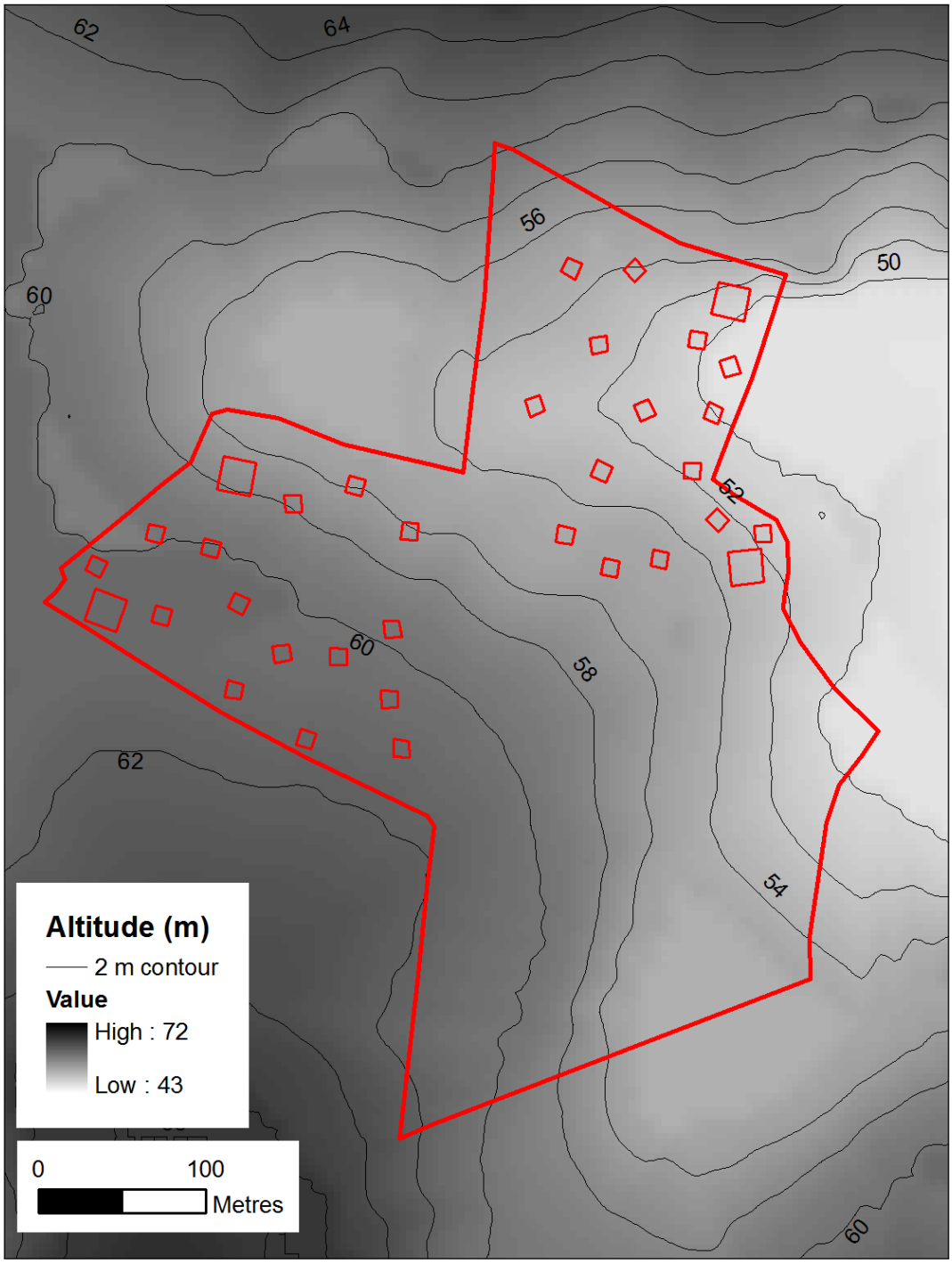

Figure 3.12: Altitude (m above sea level) map interpolated from OS data (Ordnance Survey GB, 2011) for the Clapham site.

Part II

SOIL ORGANIC CARBON

Soil organic matter is one of our most important national resources; its unwise exploitation has been devastating, and it must be given its proper rank in any conservation policy

— William A. Albrecht (1888 - 1974)

4

SOIL ORGANIC CARBON AND ROOT DISTRIBUTION IN A SILVOARABLE SYSTEM

This chapter is based on the paper Upson and Burgess (2013), with the addition of some tables and figures that were not included in the final paper. In addition, whilst in the published article soil organic carbon (SOC) was calculated using the 'fixed-depth' method, in the version presented here, calculations have been made using the equivalent soil mass (ESM) method, to allow better comparison to be made with results from Clapham Park (Chapter 5). This has resulted in minor changes in SOC stock reported in this chapter. Some other minor stylistic alterations have been made throughout to link better with the other chapters of the thesis[1].

In the context of this thesis, three hypotheses are tested in this chapter:

Hypotheses

1. Establishing silvoarable agroforestry systems on arable land will increase soil organic carbon (SOC) stocks relative to a pure arable control.
2. The incorporation of trees into the arable environment will lead to increases in soil organic carbon (SOC) storage at depth.
3. Tree related SOC is more stable than arable crop or grass related SOC.

1 Most notably, whilst in the paper the terms 'gravimetric' and 'volumetric soil' organic carbon were used, in this Chapter and the thesis in general, the terms organic carbon content (C_o%) and soil organic carbon (SOC) stock have been used instead.

ABSTRACT

Aim: To determine the effect of tree establishment and intercropping treatments, on the distribution of roots and soil organic carbon to a depth of 150 cm for arable land in a temperate area.

Methods: A poplar (*Populus* sp.) silvoarable agroforestry experiment, including arable controls, was established on arable land in lowland England in 1992. The trees were intercropped with an arable rotation or bare fallow for the first 11 years, thereafter grass was allowed to establish. Coarse and fine root distributions (to depths of up to 150 cm and up to 5 m distance from the trees) were measured in 1996, 2003, and 2011. In 2011 soil organic carbon stock was also calculated to a depth of 150 cm, and a subset fractionated to determine the type of carbon stored.

Results: Trees initially surrounded by arable crops, rather than fallow, had a deeper coarse root distribution with less lateral expansion. In 2011, the combined length of tree and understory vegetation roots was greater in the agroforestry treatments than the control at depths below 90 cm. Between 0 and 150 cm depth, the fine root carbon in the agroforestry treatment (2.56 t C ha^{-1}) was 79% greater than that in the control (1.43 t C ha^{-1}). Although the soil organic carbon in the top 0.6 m under the trees (161 t C ha^{-1}) was greater than in the control (142 t C ha^{-1}), a tendency for smaller soil carbon levels beneath the trees at lower depths, meant that there was no overall tree effect when the whole 1.5 m profile was considered. From a limited sample, there was no tree effect on the proportion of recalcitrant soil organic carbon.

Conclusions: The observed decline in soil carbon beneath the trees at soil depths greater than 60 cm, if observed elsewhere, has important implications for assessments of the role of afforestation and agroforestry in sequestering carbon.

4.1 INTRODUCTION

Society is facing the challenge of how to increase food production, in the context of a rising world population, whilst also reducing greenhouse gas emissions. By 2020, the United Nations Environment Program (2011) has calculated that annual global greenhouse gas emissions need to decline from an anticipated 56 $GtCO_2e$, under a business as usual scenario, to 44 $GtCO_2e$ to keep the mean global temperature increases beneath the target of 2°C. It has been estimated that between 2.4 and 8.5 $GtCO_2e$ of this reduction can be derived from changes in agricultural and forestry management. This includes 'enhancing carbon sequestration by undertaking afforestation and agroforestry projects' (UNEP, 2011).

Agroforestry systems are of particular interest because they combine the potential to increase carbon sequestration (Montagnini and Nair, 2004; Nair et al., 2009; Pandey, 2002) whilst maintaining agricultural production. Although biomass accumulation aboveground is an obvious result of introducing trees into agricultural systems, the carbon stored is relatively labile (Janzen, 2005), and dependent on the fate of the products derived from woody biomass. On the other hand, carbon accumulated in the soil can persist for millennia (Rumpel et al., 2002; Schöning and Kögel-Knabner, 2006) and forms the largest terrestrial carbon pool (Batjes, 1996).

The dominant pathway for carbon to enter the soil is through fine root turnover; this has been estimated to account for a third of global annual net primary productivity (Jackson et al., 1997). Agroforestry systems may be expected to increase soil carbon storage by increasing the depth to which roots are present in the system, by continually turning over fine roots throughout the year (albeit at a slower rate in the dormant season (Black et al., 1998)), and by the inclusion of recalcitrant compounds which slow the rate of mineralisation (Recous et al., 2008). Any consideration of changes in gravimetric soil organic carbon must also take into account changes in soil volume result of different management regimes (Bambrick et al., 2010; Ellert and Bettany, 1995).

Whilst there are several studies of temperate agroforestry systems, most consider soil carbon at depths of less than 50 cm (Bambrick et al., 2010; Gordon et al., 2006; Oelbermann and Voroney, 2007; Peichl et al., 2006; Sharrow and Ismail, 2004). In this study we attempt to quantify the impact of introducing trees into arable systems on the distribution of roots and soil organic carbon to a depth of 150 cm.

4.2 METHODS

The silvoarable site at Silsoe was planted in 1992. Full details of the site are included in Chapter 3.

4.2.1 *Coarse roots*

In 1996, 2003, and 2011, the distribution of coarse roots was investigated using the 'profile-trench' method detailed by Bohm (1979). The 1996 measurements were reported by Burgess et al. (1997), whilst the 2003 measurements were reported by Pasturel (2004)

In each case, a trench, 5 m long, 1.5 m deep and 1 m wide was excavated by mechanical digger alongside each of the six sample trees. The trench was orientated so that it ran to the centre of either a cropped or fallow alley, originating from the centre line of the tree row, one metre to the south of the stem (Figure 4.1a and 4.2). Different trees were sampled in 2003 and 2011, and a distance of 12 metres maintained between trees sampled in the two years.

(a) A completed root trench. The soil at the base of the trench was extremely dry.

(b) Quadrat positioned on trench wall. Note band of coarse sand visible to the right of the quadrat.

Figure 4.1: Completed root trench at the Silsoe silvoarable trial in May 2011.

In 2011, a one metre quadrat with divisions at every 20 cm was positioned on the north face of the completed trench wall and fixed to the clay (Figure 4.1b). The top of the quadrat was aligned with the soil level.

The presence of coarse roots ($>$ 2 mm diameter) within a 0.2 m $\times$ 0.2 m grid was recorded along the length of the trench to a depth of 150 cm. Roots were categorised into the following diameter classes: 2–5 mm (*i*), 5–10 mm (*ii*), 10–20 mm (*iii*) and $<$ 20 mm (*iv*). This provided a measurement of coarse root density 0.04 m^{-2}.

4.2.2 *Fine root length and mass density*

Measurements of fine roots were taken in 2003 and 2011. In July 2003, undisturbed soil cores (of volume 207 cm^3) were taken at distances of 0, 1, 2, 3, and 4 m from the base of six sample trees. At each distance, samples were taken at depths of 15, 45, 75, 105, and 135 cm. Samples were suspended in 3 l of water for 24 hours, then washed by hand and poured through a fine mesh sieve (710 µm). In June 2011, a second set of undisturbed soil cores (of volume 146 cm^3) were taken at the same distances and depths from six different sample trees, and at six control plots (with two at the same latitude of each block). The control plots were situated at least 20 m away from the nearest tree and field edge.

To release the fine roots, the core was separated into a plastic bottle (of 250 cm^3 volume), filled with de-ionised water and placed inside an end-over-end agitator

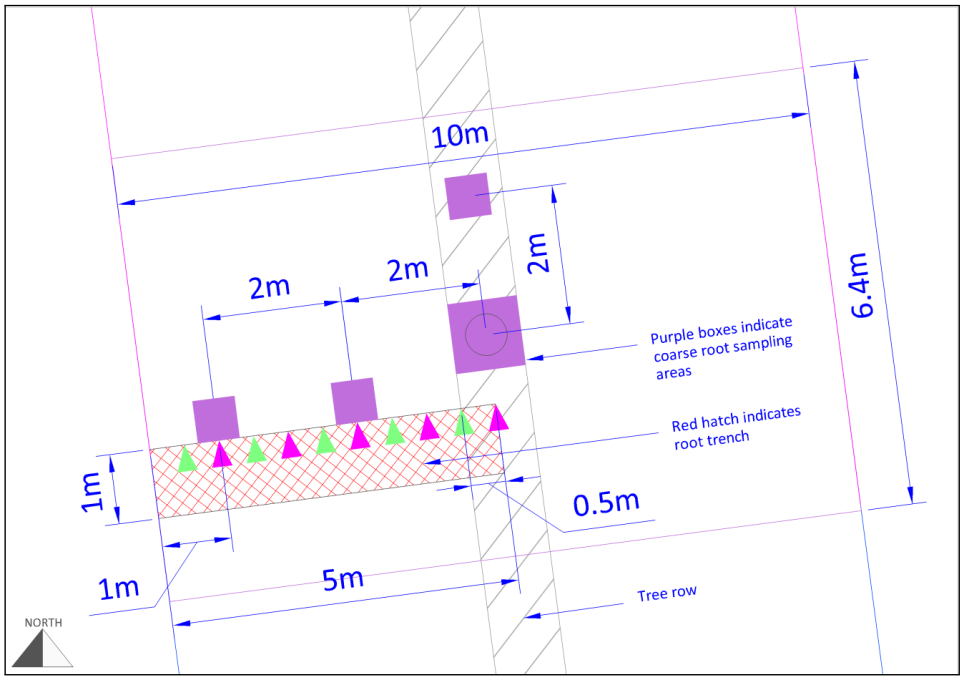

Figure 4.2: Schematic diagram showing the position of sampling points used in various parts of the study. Red hatch indicates root trench (1.5 m depth). Green and magenta triangles indicate the position of fine root, and SOM and ρ_b sampling respectively. Purple blocks indicate position of coarse root sampling.

for at least 12 hours. Samples were emptied onto a sieve with an aperture size of 710 µm and washed with water to remove the clay slurry.

In each year, roots were floated off from other debris, and the root length determined using the intersection method, devised by Newman (1966). It was not possible to separate tree roots from the roots of herbaceous plants in either year. After counting, the root samples were dried at 105°C to a constant weight, and reweighed. Fine root mass and length density were determined by dividing total length and mass by the volume of the sample giving units of $\mathrm{cm\,cm^{-3}}$ and $\mathrm{mg\,cm^{-3}}$.

4.2.3 *Soil organic carbon and bulk density*

Soil samples were taken at six depths which were assumed to be representative of depth increments totaling 150 cm (Table 4.1), and at five distances from each sampled tree (0.5, 1.5, 2.5, 3.5 and 4.5 m), perpendicular to the tree row. An associated ρ_b sample was taken at each sampling point, following the methods of Klute (1986). Corresponding samples were also taken at the same depths from the six control positions used for fine root length density (FRLD) measurements.

All 216 samples were analysed for organic carbon content (C_o%) using a modified Walkley-Black method (British Standards Institute, 1990). In addition, analysis of 27 samples (9 samples from each treatment) were repeated using a Vario EL III

Table 4.1: Summary of sampling depths and depth increments used in organic carbon content sampling.

Increment (cm)	Sample depth (cm)
0–10	5
10–20	16
20–40	30
40–60	50
60–105	83
105–150	128

Elemental Analyser[2]. Laboratory standard operating procedures (SOPs) for these methods are included in Appendix A.4 and A.5.

Volumetric SOC was calculated using the equivalent soil mass (ESM) method as described by Ellert and Bettany (1995), using the same modifications applied by Bambrick et al. (2010): namely that the equivalent soil mass was determined based on a reference value of 1 ($g\,cm^{-3}$) as measurements of the original soil mass – before tree planting – were not available.

The SOC stock was not measured at the time of tree establishment in 1992; however because the level field had been uniformly cultivated for the preceding 20 years, it was assumed that the soil carbon content across the field was uniform at the time of planting.

4.2.4 *Fractionation of soil organic carbon*

Eighteen soil samples (drawn from the 27 tested with the elemental analyser) were sent to Rothamsted Research in Hertfordshire, UK, for fractionation of SOC, using the procedure outlined by Zimmermann et al. (2007). Nine samples each were taken from the agricultural control and the cropped agroforestry treatment, from three depths (5, 30, 83 cm). All agroforestry samples were taken at a distance of 2.5 m from the sample tree.

The procedure outlined by Zimmermann uses a combination of particle size, density, and chemical fractionation to isolate five SOC fractions. Each sample was passed through a 2 mm sieve, then 30 g of soil was suspended in 150 ml of water and disrupted with $22\,J\,ml^{-1}$ to break up large aggregates. The sample was then passed through a series of filter papers; that portion < 65 µm was stirred with sodium polytungstate and centrifuged to separate a light ($< 1.8\ g\,cm^{-1}$) and a heavy fraction ($> 1.8\ g\,cm^{-3}$). These two fractions were considered to be POM and sand and stable aggregates (S+A) respectively.

A filtrate (< 0.45) of the portion < 63 µm, (suspended in water) was removed for the determination of dissolved SOC (DOC). The remaining 0.45 µm < fraction < 63 µm was taken to consist of silt and clay particles (s+c); of this, a chemically resistant fraction (rSOC) was determined by oxidation for 18 hours with sodium hypochlorite.

2 Elementar Analysensysteme GmbH, Donaustrasse 7, 63 452 Hanau, Germany.

Carbon and nitrogen for each solid fraction was determined by dry combustion with an elemental analyser. The dissolvable organic carbon fraction (DOC) was determined by thermal oxidation with a liquid analyser.

4.2.5 *Data presentation and statistical analyses*

Statistical analyses were completed using the statistical language R, version 2.13.0 (R Development Core Team, 2013).

4.2.6 *Analysis of variance*

Analysis of variance (ANOVA) was used to investigate the null hypothesis that no difference existed between groups. Non-significant third order (and above) interactions were removed from each model and the simplified model tested against the original using an F-test (Crawley, 2007; Johnson and Omland, 2004).

Organic carbon content (C_o%), soil bulk density (ρ_b), soil organic carbon (SOC), fine root length density (FRLD) and fine root mass density (FRMD) were tested by ANOVA using the 'aov' function (R Development Core Team, 2013). Treatment (control, cropped, fallow), distance, and depth were modelled as fixed effects, whilst block was included as a random effect. A further fixed effect (referred to as 'ctrltmt' in results tables) into which treatment and distance were nested, and which differentiated between the silvoarable and control was added to address the imbalance caused by the inclusion of distance into the model (since only one 'distance' was tested for each control plot).

Cumulative SOC stock was tested with fixed effects for treatment, crop and distance, and a random effect for block. This analysis was completed independently for each cumulative depth i.e. 0–10, 0–20, 0–40, 0–60, 0–105, and 0–150 cm. Model assumptions were checked using normality and residual plots, and where appropriate, transformations of the data were made. Multiple comparison tests were made using the least significance test function implemented in the package 'agricolae' (de Mendiburu, 2010) utilising the Benjamini & Hochberg procedure (Benjamini and Hochberg, 1995), with an α level of 0.05 throughout.

4.2.7 *Coarse root analysis*

In order to make comparisons with results recorded in previous years (Nkomaula, 1996; Pasturel, 2004), all size classes were pooled, and observations were limited to a depth of 1 m. Data from the three years were organised into similar depth increments and aggregated across distances from the tree into groups of one metre: 0–1, 1–2, 2–3, 3–4, 4–5 m. This reduced the zero counts and simplified the analysis. In 1996, sampling did not extend further than 4.8 m from the tree.

The diameter classes recorded in 2003 and 2011 were identical, but classes recorded in 1996 were adjusted to fit the current data. The two smallest size categories ($>$ 1 mm and 1–2 mm diameter) were discarded, whilst the largest class ($>$ 10 mm) was considered to be the same as the 10–20 mm size class recorded in 2003 and 2011.

Because the coarse root count data were highly skewed and did not satisfy the assumption of normality; the 'Kruskal-Wallis' test (Conover, 1971) implemented in the 'agricolae' package (de Mendiburu, 2010) was used to make pair-wise comparisons of root counts found at each depth and distance for each year and treatment. Depth and distance were analysed separately for simplicity, and independently for each year. Note that in 1996, the measurements of the coarse roots in a cropped and fallow treatment were taken on the same tree, and therefore are not independent of each other.

The vertical root distribution of each tree was also examined by fitting a logistic function to the cumulative root fraction (Yr) as a function of depth (D), (Silva and Rego, 2003). The model function is represented by Equation 4.1 where $MaxD$ is the maximum sample depth, and a and b are model parameters.

$$Yr = \frac{1}{1 + \frac{MaxD - D}{aD}^{\frac{1}{b}}} \tag{4.1}$$

Using the model, the depths which corresponded to the 50% and 90% of Yr were calculated using the following equations (Mulia and Dupraz, 2006):

$$d_{50} = \frac{MaxD}{1 + a} \tag{4.2}$$

$$d_{90} = \frac{MaxD}{1 + a(0.11)^{\frac{1}{b}}} \tag{4.3}$$

Model fit was assessed using Spearman's rank correlation coefficient. High d_{50} and d_{90} values are associated with deep rooting patterns: a d_{50} of 30 indicates that 50% of the roots were found above 30 cm in depth.

4.3 RESULTS

4.3.1 *Coarse root distribution*

The total of 1018 coarse roots, counted across the six trenches in 2011, was greater than the 858 roots counted in 2003, and the 268 counted in 1996. Effects ($p < 0.05$) of treatment, depth, distance and distance $\times$ depth interactions were found in each year.

4.3.1.1 *Cumulative root function*

Application of the cumulative root function (Table: 4.2) described in Equation 4.1 showed good fit to the data. As with Mulia and Dupraz (2006) and Silva and Rego (2003), model fits were very good; in all cases $R_s = 0.97$ or greater. In one instance in the cropped treatment in 1996, application of the function failed as all the roots were found in one depth increment.

Table 4.2: Cumulative coarse root fraction models developed using root count data. Mean $\pm$ standard error of the mean (cm) for d_{50} and d_{90} derived from the function described in Equation 4.1. The d_{50} and d_{90} give the depth above which 50% and 90% of the cumulative root fraction are found.

Year	Treatment	d_{50}	d_{90}	n
1996				
	Cropped	48 ± 4	69 ± 4	2
	Fallow	38 ± 6	78 ± 6	3
2003				
	Cropped	52 ± 4	87 ± 4	3
	Fallow	42 ± 6	76 ± 4	3
2011				
	Cropped	34 ± 2	74 ± 1	3
	Fallow	38 ± 2	77 ± 1	3

4.3.1.2 *Root distribution*

At each distance or depth increment, the root counts in the fallow silvoarable treatment were greater ($p < 0.05$) than or similar to those in the cropped silvoarable treatment (Table 4.3). In addition within the fallow treatment, in each of the three years, the coarse-root count at a distance of 1–2 m from the tree was statistically similar ($p > 0.05$) to that in the tree row (0–1 m). By contrast, within the cropped treatment, the coarse root count at a distance of 1–2 m was less ($p < 0.05$) than that in the tree row (0–1 m) in each of the three years.

Four years after planting the poplars, penetration of coarse roots into the continuously cropped alley was minimal, but they extended to the middle of the alley (5 m from the tree) in the fallow treatment. Consequently root counts at distances between 1 m and 4 m were found to be significantly greater ($p < 0.05$) in the

fallow treatment. With the exception of the most shallow (0–0.2 m) and the penultimate depth (0.6–0.8 m), the root counts in the fallow treatment were greater ($p < 0.05$) than in the continuously cropped treatment (Table 4.3). Similarly, the d_{90} was found to be less in the cropped than the fallow treatment. The d_{50} on the other hand was greater in the cropped treatment, indicating that the first 50% of roots were found at greater depths in the cropped than in the fallow treatment (Table 4.2).

In 2003, there were only significantly ($p < 0.05$) more coarse roots in the fallow treatment than the cropped treatment at a distance of 2–3 m (Table 4.3). The fallow silvoarable treatment also had more ($p < 0.05$) roots than the cropped silvoarable treatment at a depth of 0.2–0.4 m. This is reflected in the d_{50} which indicates that the first 50% of roots in the fallow treatment were found at a shallower depth (42 cm) than in the cropped treatment (52 cm).

In 2011, following the end of annual cultivation in 2003, the mean coarse root count in the fallow treatment was greater ($p < 0.05$) than that in the cropped treatment at distances of 1–2 m and 3–4 m. The fallow treatment also had more ($p < 0.05$) coarse roots than the cropped treatment at a depth of 0.6–0.8 m (Table 4.3). Eight years after the end of cropping and cultivation, the d_{50} in the cropped treatment (34 cm) was, for the first time, marginally less than in the fallow treatment (38 cm).

4.3.2 *Fine root length density*

Although the number of fine roots is expected to increase as the trees increase in size, the use of an agitator in 2011 to release roots trapped in the soil is thought to have increased the recovery of very fine roots. For this reason, and the fact that no arable control was sampled in 2003, fine root length data from these two years has been analysed independently.

In 2003, no difference ($p = 0.957$) was found between the FRLD of the fallow and cropped silvoarable treatments, however there were effects of distance ($p < 0.001$) and depth ($p < 0.001$) for the agroforestry treatments as a whole (note, root counts were not made in the arable control in this year (Table 4.4). The mean fine root length decreased ($p < 0.05$) from 1.22 $cm\,cm^{-3}$at a depth of 0-30 cm to 0.37 $cm\,cm^{-3}$at a depth of 150 cm. The FRLD to a depth of 150 cm declined ($p < 0.05$) from 0.93 $cm\,cm^{-3}$below the grass sward directly beneath the tree, to 0.31 $cm\,cm^{-3}$in the centre of the alley.

The data recorded in 2011 indicate significantly greater FRLD in the arable control ($p < 0.05$), an effect of depth ($p < 0.001$), and the control and silvoarable treatments showed different responses to depth ($p < 0.001$) (Table 4.4). The mean FRLD in the cropped and fallow silvoarable treatments were similar ($p = 0.45$). At the most shallow depth (0–30 cm) FRLD was greater ($p < 0.05$) in the arable control than the silvoarable treatments, but at the greatest depth increment (120–150 cm) the opposite was true, and greater FRLD was found in the silvoarable treatments (Figure 4.3).

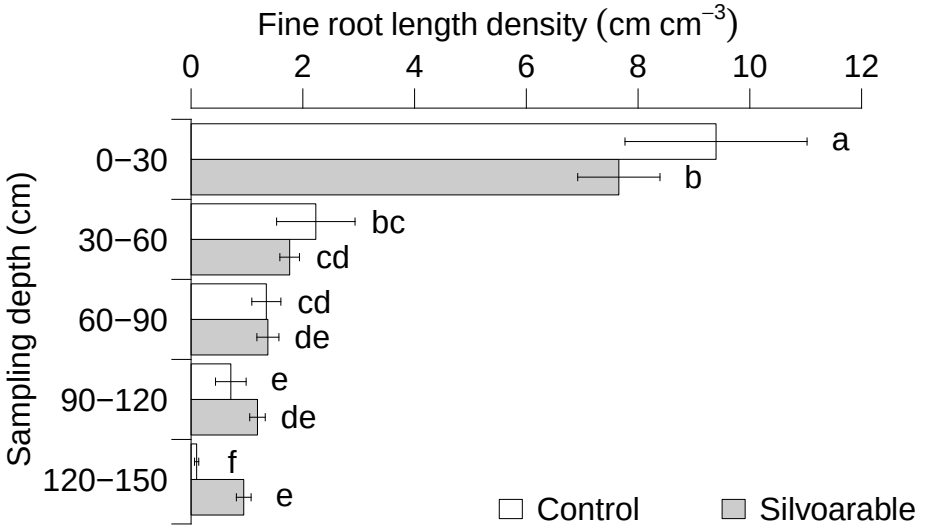

Figure 4.3: Mean fine root length density from the Silsoe silvoarable experiment, recorded in 2011. Bars with the same letter indicate a non-significant difference ($p > 0.05$). Error bars indicate standard error of the mean (control: $n = 6$, silvoarable: $n = 30$).

Table 4.3: Coarse root distribution measurements in 1996, 2003, and 2011: mean number of roots recorded across the three blocks (roots per 0.04 m^2). Data have been summed across distance in increments of 1 m, from five 0.2 m × 0.2 m square for each 1 m section. Values greater than 1 per 0.04 m^2 have been shaded. Only data recorded to a depth of 1 m were included in statistical analyses ($n = 3$). Results from Kruskal-Wallis tests have been included for each depth and distance. Note that each year was analysed independently, hence results from these tests are not comparable over successive years.

		Agroforestry treatment and distance (m)									
Depth (cm)		Agroforestry-fallow						Agroforestry-cropped			
		0–1	1–2	2–3	3–4	4–5		0–1	1–2	2–3	3–4	4–5
1996		a	abc	bc	c	d		ab	d	d	d	d
0–20	bc	3.7	0.6	0.1	0.0	0.0	bc	1.7	0.0	0.0	0.0	0.0
20–40	a	3.0	0.8	0.9	1.3	0.0	bc	1.7	0.1	0.0	0.0	0.0
40–60	a	1.9	1.3	0.3	0.3	0.1	bc	4.6	0.0	0.0	0.0	0.0
60–80	ab	1.4	0.7	1.0	0.6	0.0	bc	1.7	0.1	0.0	0.0	0.0
80–100	ab	0.2	0.2	1.2	0.2	0.0	c	0.1	0.0	0.0	0.0	0.0
2003		kl	kl	lm	mn	ne		k	lm	ne	ne	e
0–20	mn	2.2	2.2	1.1	0.4	0.2	n	3.2	0.7	0.4	0.2	0.1
20–40	k	3.5	4.7	2.9	1.5	1.3	lmn	3.3	1.8	1.2	0.5	0.3
40–60	kl	2.7	2.4	1.8	1.6	0.7	klm	3.5	2.1	0.8	0.9	0.7
60–80	lmn	1.9	2.5	1.1	1.1	0.3	lmn	3.2	1.5	0.7	0.5	0.3
80–100	mn	1.2	1.2	0.6	0.2	0.5	lmn	2.8	1.2	0.8	0.6	0.4
100–120		1.0	1.3	0.3	0.2	0.1		1.2	1.2	0.4	0.3	0.0
2011		v	vw	xy	wx	xy		v	xy	wx	y	y
0–20	wx	1.5	2.8	1.8	2.4	1.8	wx	2.4	2.2	2.8	1.3	1.1
20–40	v	3.2	4.5	3.0	3.2	2.1	vw	4.3	2.4	3.1	1.2	1.9
40–60	wx	4.2	2.4	1.4	1.4	0.4	wx	4.0	1.3	1.3	1.1	1.0
60–80	xy	3.1	1.6	1.1	0.8	0.5	z	2.3	0.4	0.8	0.1	0.2
80–100	yz	1.2	1.3	0.5	0.5	0.4	z	1.0	0.5	0.5	0.5	0.0
100–120		1.0	0.7	0.2	0.2	0.2		0.7	0.4	0.1	0.2	0.0
120–140		1.2	0.4	0.1	0.4	0.1		0.3	0.2	0.2	0.2	0.4
140–150		0.8	0.2	0.1	0.0	0.1		0.3	0.1	0.0	0.3	0.0

Table 4.4: Analysis of the effects of depth, agroforestry-cropping treatment, distance and interactions on the fine root length density (FRLD) ($cm\,cm^{-3}$) and fine root mass density (FRMD) ($mg\,cm^{-3}$) in a) 2003 and b) 2011. In 2011, the effects included a comparison of the control with the agroforestry treatments.

a) Effects in 2003	df	p-values	
		Fine root length density	Fine root mass density
Depth	4	< 0.001	< 0.001
Treatment	1	0.277	0.776
Distance	4	< 0.001	< 0.001
Treatment × distance	4	0.097	0.049
Treatment × depth	4	0.707	0.694
Distance × depth	16	0.786	0.984
Residual	114		

b) Effects in 2011	df	p-values	
		Fine root length density	Fine root mass density
Agroforestry v Control	1	0.119	< 0.001
Depth	4	< 0.001	< 0.001
Treatment	1	0.943	0.936
Distance	4	0.005	0.024
Agroforestry v Control × depth	4	< 0.001	0.421
Treatment × distance	4	0.547	0.209
Treatment × depth	4	0.719	0.214
Distance × depth	16	0.974	0.691
Residual	289		

Table 4.5: Effect of depth and distance on the fine root length density (FRLD) ($cm\,cm^{-1}$) and fine root mass density (FRMD) ($cm\,mg^{-1}$) in a) 2003 and b) 2011. The measurements in 2011 include the control area. Mean ± standard errors of the means, and number of replicates (n), with results from multiple comparison tests shown in superscript: means with the same letter are not significantly different. Note, test results are not comparable across year and distance/depth. Multiple comparison tests were not completed for fine root length and distance in 2011 as ANOVA did not find this relationship significant.

a) 2003		Fine root length density		Fine root mass density		n
Depth (cm)	0–30	1.22^{a}	±0.19	0.13^{a}	±0.02	30
	30–60	0.56^{b}	±0.09	0.04^{b}	±0.01	30
	60–90	0.41^{b}	±0.05	0.04^{b}	±0.01	30
	90–120	0.40^{b}	±0.05	0.04^{b}	±0.01	30
	120–150	0.37^{b}	±0.04	0.03^{b}	±0.01	30
Distance (m)	0–1	0.93^{a}	±0.17	0.09^{a}	±0.02	30
	1–2	0.82^{a}	±0.14	0.08^{ab}	±0.02	30
	2–3	0.49^{b}	±0.06	0.05^{bc}	±0.01	30
	3–4	0.42^{bc}	±0.06	0.05^{cd}	±0.01	30
	4–5	0.31^{c}	±0.03	0.03^{d}	±0.01	30
b) 2003		Fine root length density		Fine root mass density		n
Depth (cm)	0–30	7.95^{a}	±0.67	0.97^{a}	±0.06	36
	30–60	1.84^{b}	±0.18	0.31^{b}	±0.04	36
	60–90	1.37^{c}	±0.17	0.20^{c}	±0.03	36
	90–120	1.11^{c}	±0.13	0.20^{c}	±0.04	36
	120–150	0.80^{d}	±0.12	0.11^{d}	±0.02	36
Distance (m)	0–1	2.37	±0.38	0.45^{a}	±0.08	30
	1–2	2.95	±0.62	0.43^{a}	±0.07	30
	2–3	1.98	±0.42	0.38^{a}	±0.07	30
	3–4	2.56	±0.67	0.27^{b}	±0.05	30
	4–5	3.06	±0.76	0.39^{a}	±0.08	30
	Control	2.76	±0.71	0.45^{a}	±0.08	30

4.3.3 *Fine root mass density and carbon*

Although fine root length density (FRLD) is often the focus of studies of water and nutrient uptake, fine root mass density (FRMD) is of interest in studies of carbon sequestration.

In 2003, FRMD showed similar trends to FRLD, with significant effects of depth ($p < 0.001$) and distance ($p < 0.001$) (Table 4.4). Fine root mass was significantly greater ($p < 0.05$) in the first 30 cm than all subsequent depths whilst FRMD in the tree row (0–1 m) was greater ($p < 0.05$) than that at distances between 2 m and 5 m within the arable alley (Table 4.5).

In 2011, the fine root mass also declined significantly ($p < 0.001$) with depth, ranging from 0.97 mg cm^{-3} in the top 30 cm of soil, to 0.11 mg cm^{-3} at a depth of 120–150 cm (Tables 4.4 and 4.5). The mass of fine roots at a distance of 3–4 m was less than for other distances (0.38–0.45 mg cm^{-3}, Table 4.5).

The quantity of carbon contained in the fine roots in each depth increment to 150 cm was calculated by multiplying the mean fine root mass for each treatment by the depth of the sampling increments and the carbon content. This showed that the cumulative carbon associated with fine roots, to a depth of 1.5 , in the silvoarable treatments (2.56–2.58 t C ha^{-1}) was 80% greater ($p < 0.05$) than in the control (1.43 t C ha^{-1}, Figure 4.4).

The specific root length was determined by dividing the fine root length by the corresponding fine root mass. The specific root length in the cropped (69 m g^{-1}) and agroforestry-fallow (60 m g^{-1}) treatments were less ($p < 0.05$) than that (175 m g^{-1}) in the control, probably due to the presence of heavier lignified tree roots.

4.3.4 *Soil bulk density*

Table 4.6: Analysis of the effects of the control, depth, agroforestry-cropping treatment, distance and interactions on the soil bulk density (ρ_b), and the organic carbon content (C_o%) and soil organic carbon (SOC) in 2011.

Effect	df	ρ_b	C_o%	SOC
Agroforestry v Control	1	< 0.001	0.541	0.051
Depth	5	< 0.001	< 0.001	< 0.001
Treatment	1	0.187	0.436	0.193
Distance	4	0.344	0.013	0.175
Agroforestry v Control × depth	5	0.003	0.040	0.002
Treatment × distance	4	0.914	0.044	0.271
Treatment × depth	5	0.224	0.094	0.431
Distance × depth	20	0.256	0.541	0.760
Residuals	168			

In 2011, ρ_b was greater ($p < 0.001$) in the silvoarable plots than the control, but this effect varied with depth ($p < 0.001$, Table 4.6). At a depth of 0–40 cm ρ_b in the control (1.22 g cm^{-3}) and silvoarable treatments (1.28 g cm^{-3}) were similar (Figure 4.6). At depths of 40–60, 60–105, and 105–150 cm, the ρ_b in the control (1.32, 1.30

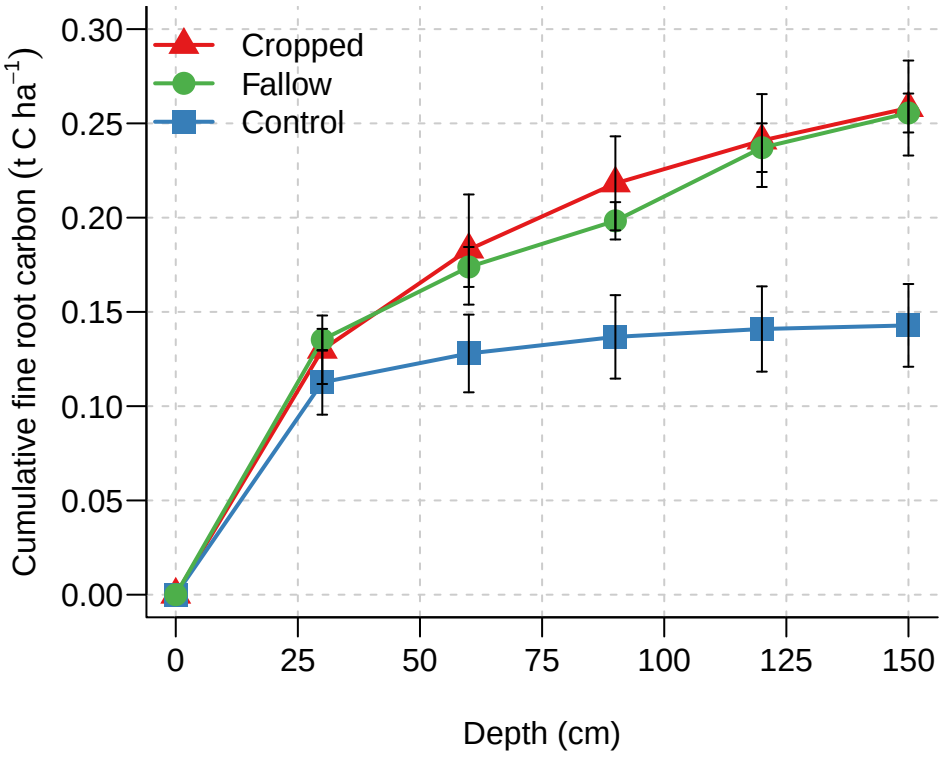

Figure 4.4: Cumulative C content present in fine roots, calculated by taking the mean fine root mass density (FRMD) for each treatment at each depth and multiplying it by the assumed increment depth of 30 cm. This was in turn multiplied by the known relative carbon content of fine roots (44.47%). Error bars indicate standard error of the mean (fallow: $n = 15$, cropped: $n = 15$, control: $n = 6$).

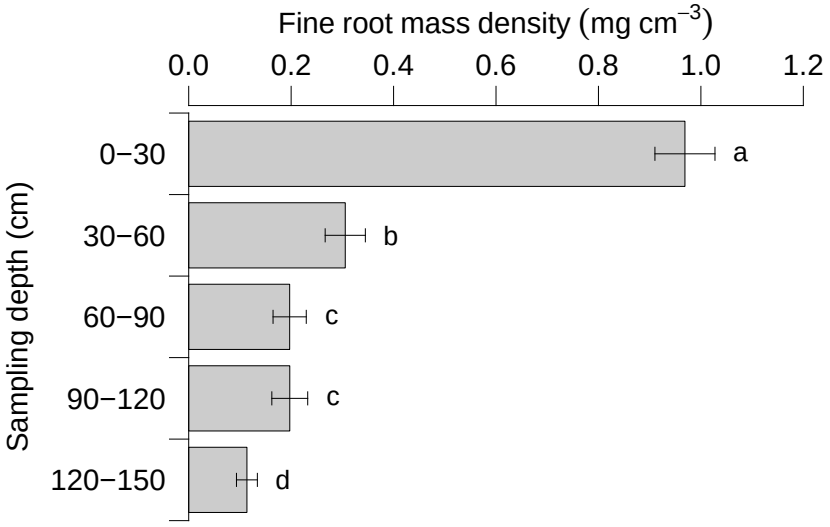

Figure 4.5: Mean fine root mass density (FRMD) from the Silsoe silvoarable experiment, recorded in 2011. Bars with the same letter indicate a non-significant difference ($p > 0.05$). Error bars indicate standard error of the mean (control: $n = 6$, silvoarable: $n = 30$).

and 1.15 g cm^{-3}) were less than those in the silvoarable (1.44, 1.45 and 1.42 g cm^{-3}). There was no difference ($p = 0.18$) in the ρ_b of the fallow and cropped silvoarable treatments.

When considered to a depth of 150 cm, there was no effect ($p = 0.34$) of distance from tree on the mean bulk density in the agroforestry plots. However there was a distance effect for the top 40 cm ($p < 0.01$). Here, ρ_b increased ($p < 0.01$) towards the centre of the alley, and was greater ($p < 0.05$) at 2–5 m (1.30–1.33 g cm^{-3}) than the tree row (1.23 g cm^{-3}) and the arable control (1.22 g cm^{-3}).

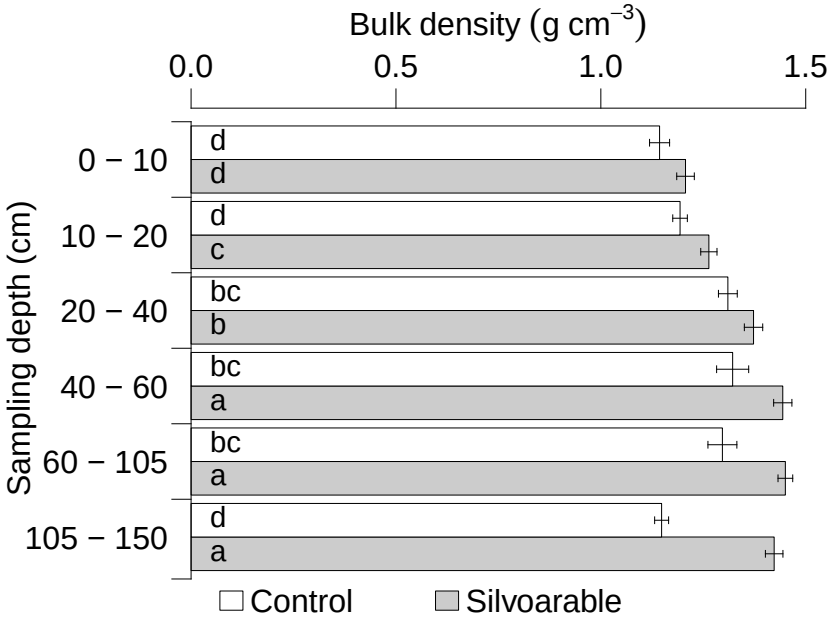

Figure 4.6: Mean soil bulk density (ρ_b) for the agroforestry plot and the arable control. Bars with the same letter indicate no significant difference ($\alpha = 0.95$). Error bars indicate standard error of the mean (control: $n = 6$, silvoarable: $n = 30$).

Table 4.7: Results of multiple comparison tests on the effect of distance on soil bulk density (ρ_b) (g cm^{-3}) in the top 40 cm, and organic carbon content (C_o%) (g 100 g^1) over the whole depth profile (0–150 cm) in 2011: mean, standard error of the mean and replication (n). Means with the same letter indicate no significant difference

	ρ_b (g cm^{-3})			C_o% (g 100 g^{-1})		
Distance (m)	Mean	SE	n	Mean	SE	n
Agroforestry						
0–1	1.23^{c}	0.04	18	1.96^{a}	0.2	36
1–2	1.25^{bc}	0.03	18	1.72^{b}	0.2	36
2–3	1.30^{ab}	0.03	18	1.71^{b}	0.2	36
3–4	1.30^{ab}	0.03	18	1.75^{b}	0.2	36
4–5	1.33^{a}	0.03	18	1.64^{b}	0.2	36
Control	1.22^{c}	0.02	18	1.71^{b}	0.2	36

4.3.5 *Organic carbon content*

In 2011 $C_o\%$ varied with depth (< 0.001) and this relationship differed ($p < 0.05$) between the arable and the agroforestry plots (Table 4.6). Distance from the tree also had an effect ($p < 0.05$), which varied with silvoarable cropping treatment ($p < 0.05$). Although the $C_o\%$ was similar in the arable control and the silvoarable treatments at a depth of 0–20 cm (Figure 4.7); at 20–40 cm $C_o\%$ was greater in the silvoarable treatments (1.95 g 100 g^{-1}) than in the control (1.47 g 100 g^{-1}). Below 40 cm, no difference was found between treatments.

Mean $C_o\%$ was found to be greater ($p < 0.05$) under the tree row (1.96 g 100 g^{-1}) in the agroforestry treatment than in the cropped alleys (1.64–1.75 g 100 g^{-1}), or the arable control (1.71 g 100 g^{-1}, Table 4.7). This difference was associated with particularly high $C_o\%$ in the tree row in the cropped treatment (2.10 g 100 g^{-1}).

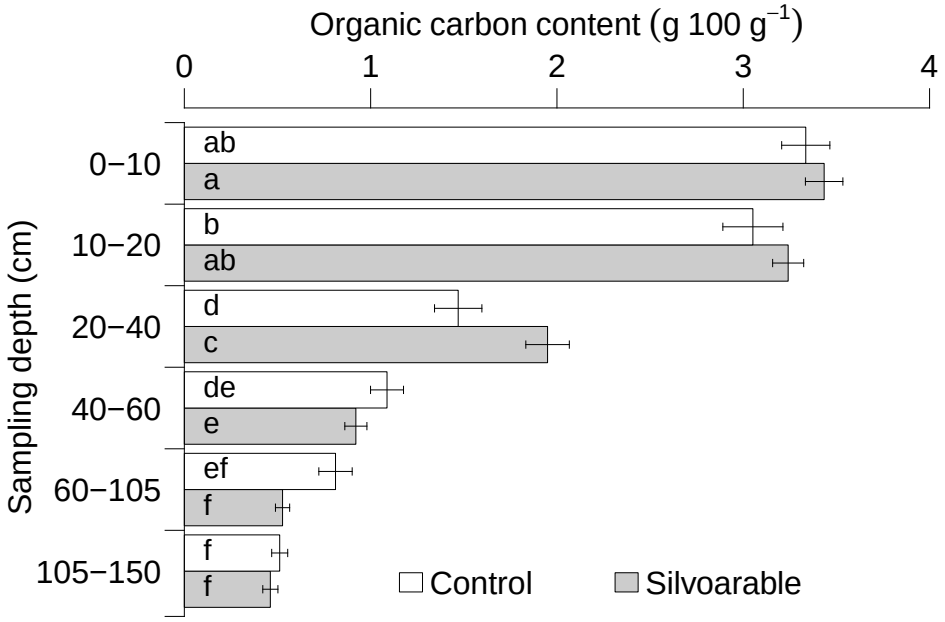

Figure 4.7: Organic carbon content ($C_o\%$) by sampling depth for the silvoarable treatments and the arable control. Error bars indicate standard errors of the means. Bars with the same letters indicate no significant difference (Silvoarable: $n = 30$, Control: $n = 6$).

4.3.6 *Changes in organic carbon content since 2001*

Organic carbon content at 16 cm was not found to have changed since 2001, based on the samples collected by (Donkin, 2001)[3]. However, the concentration of carbon at a depth of 30 cm was found to have increased between 2001 and 2011 in the silvoarable plot ($p < 0.05$, Table 4.8).

3 An explanation of how the data were prepared for this analysis is included in Appendix A.3

Table 4.8: Mean organic carbon content (C_o%) (g 100 g^{-1}) for the agroforestry plot and the arable control in 2001 and 2011. Data were compiled from the present study and Donkin (2001).

		Organic carbon content (C_o%)		
Year	Depth (cm)	Mean	SE	*n*
2001	16	3.16	0.09	36
	30	1.52	0.11	36
2011	16	3.16	0.09	18
	30	2.04	0.15	18

4.3.7 *Fractionation*

Fractionation indicated that across the whole site, 96% of the organic C was associated with the silt and clay fraction (s+c) and sand and stable aggregates (S+A) fractions; less than 1% was found to be dissolvable organic carbon fraction (DOC) and just over 2% was particulate organic matter (POM). Whilst, on average, 44% of the sample mass was found to be contained within the fraction used to determine chemically resistant soil organic carbon (rSOC), this fraction accounted for just 11% of the organic C (Figure 4.8). Conversely, 46% of the C_o% of the sample was found to be contained in the silt and clay fraction which was not chemically resistant (s+c − rSOC), but by mass, this fraction accounted for just 5%.

Table 4.9: Summary of results (p-values) from statistical analyses of organic carbon content (C_o%) found in the isolated fractions. Complete results from analysis of fractionation results are included in Appendix: A

Term/Interaction	DOC	POM	rSOC	S+A	s+c
Treatment	0.296	0.667	0.360	0.009	0.657
Depth	0.021	< 0.001	0.472	0.082	0.052
Treatment × Depth	0.808	0.257	0.457	0.020	0.998

Fractionation data were analysed with ANOVA for each fraction, taking into account treatment and depth, and including a random effect for block (Appendix A). With the exception of the rSOC fraction, C_o% was found to decline with depth ($p < 0.001$, Table 4.9). The only difference between treatments was found in the S+A fraction, which was found to be slightly higher in the arable control. This relationship was entirely driven by differences at the 83 cm depth (Table 4.9 and 4.10), and is likely the result of textural differences.

Table 4.10: Comparison of organic carbon content (C_o%) g 100 g^{-1} found for each soil fraction in the cropped silvoarable and arable control treatments. Mean and standard error of the mean, $n = 3$. One outlier has been removed from the cropped treatment at 83 cm for each fraction ($n = 2$).

		Organic carbon content (g 100 g^{-1})			
		Control		Silvoarable	
Fraction	Depth (cm)	Mean	SE	Mean	SE
DOC					
	5	0.76	0.11	0.98	0.17
	30	1.00	0.04	1.05	0.11
	83	0.54	0.04	0.63	0.21
POM					
	5	7.18	1.29	5.52	0.52
	30	1.92	0.30	2.04	0.78
	83	1.73	0.26	2.50	0.31
rSOC					
	5	12.18	0.79	10.83	1.17
	30	10.03	0.09	12.25	3.35
	83	10.87	2.87	38.57	30.19
S+A					
	5	40.29	2.45	40.08	3.71
	30	32.83	3.05	26.61	1.81
	83	56.00	0.50	24.71	9.71
s+c − rSOC					
	5	39.59	2.39	42.59	2.39
	30	54.22	2.78	58.05	4.00
	83	30.87	3.08	33.60	21.23

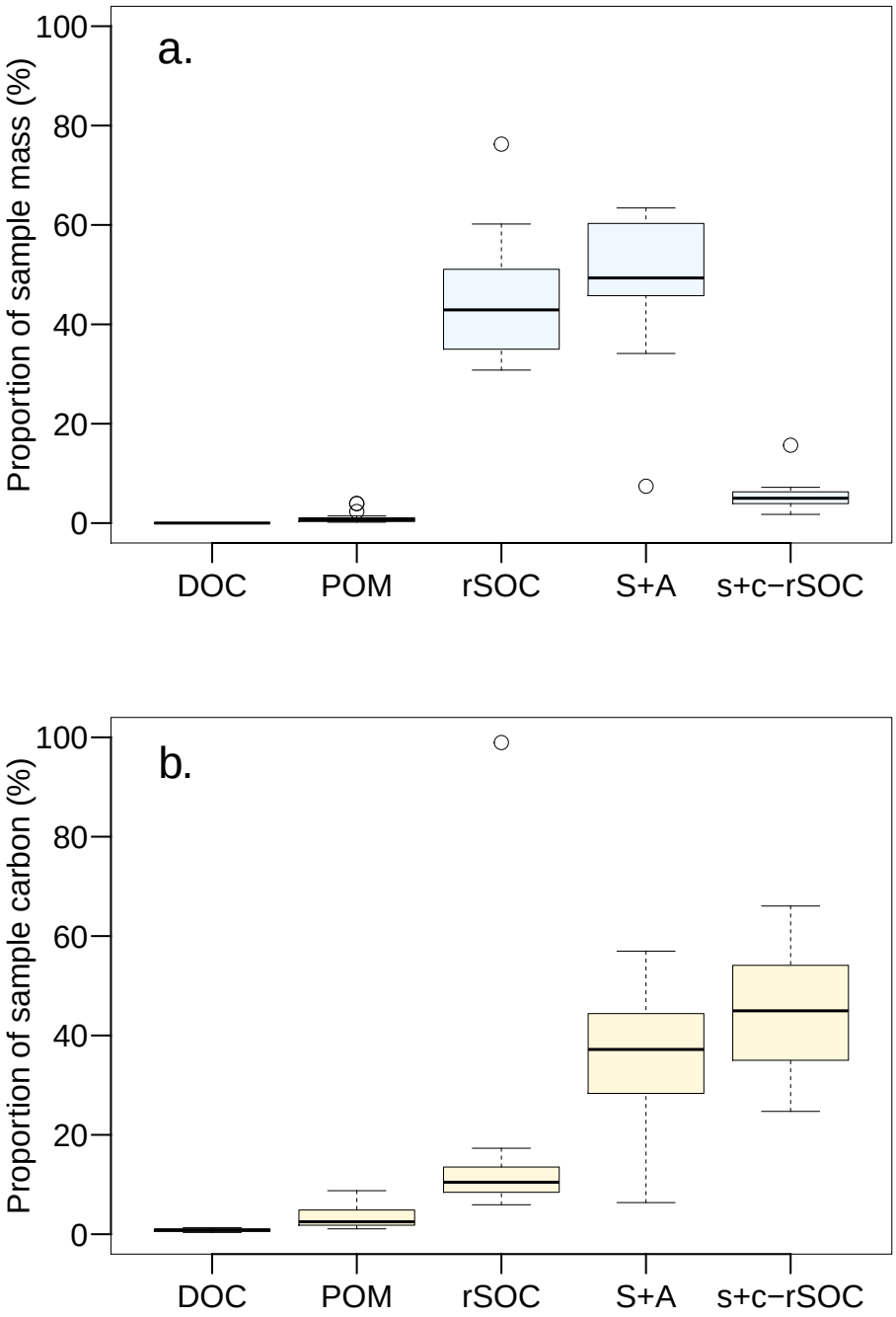

Figure 4.8: Percentage of total mass (a.) and C (b.) that each fraction contained. Dissolvable organic carbon (DOC), particulate organic matter (POM), sand and stable aggregates (S+A). Note chemically resistant soil organic carbon (rSOC) is entirely contained within the silt and clay fraction (s+c), hence s+c − rSOC is the remainder of the s+c, once rSOC has been deducted. A full explanation of the fractionation technique is included in the methods, based on Zimmermann et al. (2007).

4.3.8 *Soil organic carbon stock*

The interpretation of the data and statistical significance between treatments when considered as individual depth increments (Table 4.12) and as cumulative depths (Table 4.13) did not change with the application of the ESM method: greater SOC stock was found beneath the trees at 20–40 cm, but (as noted) less was found at 60–105 cm.

When SOC stock was considered cumulatively, significant differences were only found between the control and the agroforestry treatments at 0–40 cm ($p < 0.05$, Table 4.13). To a depth of 1.5 m, cumulative SOC was not different ($p > 0.05$) between the agroforestry (169 t C ha^{-1}) and the control (175 t C ha^{-1}) (Table 4.13, Figure 4.9).

Calculation of SOC stock using the ESM method resulted in reductions at every depth increment relative to 'fixed-depth' values presented by Upson and Burgess (2013) however. Overall, 41 and 55.7 t C ha^{-1} were found following the recalculation in the arable control and silvoarable treatments respectively, when the whole depth profile was considered (Table 4.11). Although not statistically significant, this means that at a depth of 0–105 cm or the full depth profile of 0–150 cm the establishment of trees had a negative impact on SOC stock ($p > 0.05$, Table 4.13). These changes are driven largely by losses of C (which was statistically significant, $p < 0.05$) at the 60–105 cm depth increment (Table 4.12).

Table 4.11: Difference in cumulative soil organic carbon (SOC) stock (t C ha^{-1}) based on two different methods of SOC calculation: the fixed-depth method (Upson and Burgess, 2013), and the equivalent soil mass (ESM) method (following Ellert and Bettany (1995) and Bambrick et al. (2010)).

	Soil organic carbon stock (t C ha^{-1})		
	Arable control		
Depth (cm)	Fixed-depth	ESM	Difference
0–10	38.2	33.4	−4.8
0–20	74.7	63.9	−10.8
0–40	113.2	93.3	−19.9
0–60	141.9	115.0	−26.9
0–105	189.2	151.5	−37.7
0–150	215.6	174.6	−41.0
	Silvoarable treatments		
Depth (cm)	Fixed-depth	ESM	Difference
0–10	41.2	34.3	−6.9
0–20	82.0	66.7	−15.3
0–40	135.1	105.7	−29.4
0–60	161.2	124.1	−37.1
0–105	195.2	147.9	−47.3
0–150	224.3	168.6	−55.7

Whilst significant differences were indicated by ANOVA between distances from tree at the cumulative depth increments of 0–40 cm no obvious patterns emerged during multiple comparison testing.

Table 4.12: Soil organic carbon (t C ha^{-1}) calculated using the equivalent soil mass (ESM) method for the agroforestry treatments and the arable control in 2011: mean, standard error of the mean, and replication (n). Means with the same letter indicate no significant difference. Note that comparisons should only be made across treatments at the same depth increment, as the size of these increments varies.

	Soil organic carbon stock (t C ha^{-1})					
	Agroforestry			Control		
Depth (cm)	Mean	SE	n	Mean	SE	n
0-10	34.3^{b}	1.0	30	33.4^{b}	1.3	6
10-20	32.4^{b}	0.8	30	30.5^{bc}	1.6	6
20-40	39.0^{a}	2.3	30	29.4^{bc}	2.5	6
40-60	18.4^{e}	1.2	30	21.8^{cde}	1.8	6
60-105	23.7^{cd}	1.7	30	36.5^{ab}	4.0	6
105-150	20.8^{de}	1.8	30	23.0^{cde}	1.9	6

Table 4.13: Summary of F-values and significance for ANOVA of SOC stock for cumulative depth increments. Each column of F-values is derived from a separate ANOVA. AGF = agroforestry. Statistical significance (p-values) are denoted by stars: $p <= 0.001$ (***), $p <= 0.01$ (**), $p <= 0.05$ (*), not significant (^{ns}).

		Cumulative depth (cm)					
Term		0–10	0–20	0–40	0–60	0–105	0–150
Block	2						
AGF vs Control	1	0.20^{ns}	0.95^{ns}	4.44*	1.68^{ns}	0.17^{ns}	0.37^{ns}
Distance	4	2.34^{ns}	2.45^{ns}	2.94*	1.85^{ns}	1.85^{ns}	1.40^{ns}
Treatment	1	$< 0.01^{ns}$	0.56^{ns}	0.18^{ns}	0.44^{ns}	0.44^{ns}	1.48^{ns}
Distance × Treatment	4	1.46^{ns}	2.46^{ns}	2.65^{ns}	2.11^{ns}	2.11^{ns}	1.14^{ns}
Residual	4						

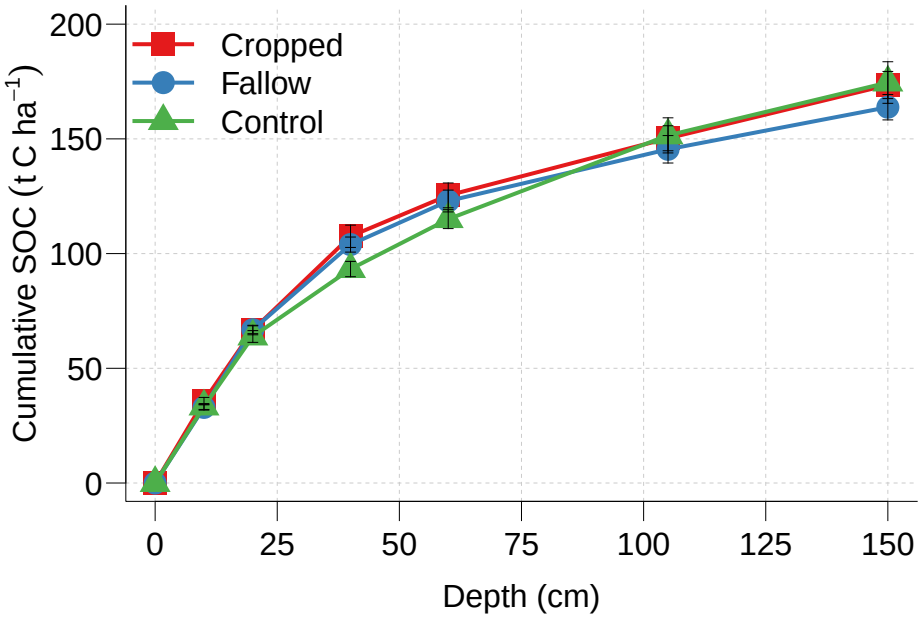

Figure 4.9: Cumulative soil organic carbon (SOC) for each treatment, calculated by multiplying each SOC measurement by the depth of each assumed sampling increment (t C ha^{-1}) to the appropriate depth). Error bars indicate standard error of the mean (fallow: $n = 15$, cropped: $n = 15$, control: $n = 6$).

4.4 DISCUSSION

4.4.1 *Coarse roots*

Our results indicate that during the first four years after tree establishment, competition from arable crops and cultivation of the soil altered the distribution of the tree roots (Table 4.7). Measurements of soil water content, reported by Burgess et al. (1997, 1996), suggest that the primary reason for the poor colonisation of tree roots in the cropped alleys was water competition. Generally the arable crop, established in the preceding autumn, was able to develop an extensive root system to extract substantial quantities of water before the leaves of the deciduous poplar had reached maximum area (Burgess et al., 2006). This competition from the arable crop restricted lateral extension in the first few years after establishment, and confined a large part of tree root development to the tree row.

By eleven years (2003), the cumulative growth of the tree meant that it had become more competitive, however the roots of trees surrounded by the cropped alleys continued to show a more restricted distribution than those previously surrounded by fallow. Mulia and Dupraz (2006) found a similar distribution of fine tree roots with depth within a 7–9 year old poplar agroforestry experiment in southern France.

The coarse root data suggest that competition from arable crops and cultivation of the soil had an important role in shaping the tree root systems. Competition with the arable crop restricted lateral and vertical extension in the first few years after establishment, and confined a large part of root development to the tree row.

Measurements of soil water content suggest that the primary reason for the poor colonisation of tree roots in the cropped alleys was due to water competition. Generally the arable crop, established in the preceding autumn was able to develop an extensive root system to extract substantial quantities of water before the leaves of the deciduous poplar had reached maximum photosynthetic potential (Burgess et al., 2004).

Nineteen years after planting (2011), and following the development of a naturally regenerating grass sward from 2003, the cessation of annual cultivation meant that the tree roots could colonise the surface layers. However, at least in the fallow treatment, the greatest concentration of roots continued to occur at a depth of 20–40 cm, perhaps as a result of competition from the perennial grass crop.

4.4.2 *Fine roots*

Unfortunately, unlike other studies (Mulia and Dupraz, 2006), we were unable to distinguish between the fine roots of the grass understory and the poplars. Between 2003, when a grass understory was allowed to establish in each treatment, and 2011, the mean fine root length density in the top 30 cm of soil increased from 1.2 $cm\,cm^{-3}$ to 7–8 $cm\,cm^{-1}$. The lack of a difference between the agroforestry and the control at this depth indicates a high presence of grass roots. The fine root density of 7–8 $cm\,cm^{-3}$ lies between relatively low values of 2 $cm\,cm^{-3}$for grassland within a Dehesa agroforestry system of oak and grass in Spain (Moreno

et al., 2005), and 10–15 $cm\,cm^{-3}$for ryegrass in Norway (Pietola and Alakukku, 2005).

Between a soil depth of 90 cm and the deepest sample at 150 cm, the fine root length density in the agroforestry treatments was greater than in the control (Figure 4.3), suggesting a high proportion of fine tree roots. The presence of fine tree roots is certainly indicated by the presence of coarse tree roots at this depth.

The specific root length for trees can be a magnitude lower than that for grass. Guo et al. (2007) reported in Australia, that specific root length ranged from 8.5 $m\,g^{-1}$ for a pine plantation to 56 $m\,g^{-1}$ for grassland. Data presented by Pietola and Alakukku (2005) suggest a fine root length of ryegrass of 269 $m\,g^{-1}$. The values in the current study (59–161 $m\,g^{-1}$) are within the above range of values for a mix of tree and herbaceous roots.

Although the total length of tree fine roots may be relatively small compared to grass roots, the mass of tree fine roots can be important when considering fine root C. In fact, there was a greater total mass of fine roots under the trees, particularly when measurements were taken below a depth of 30 cm, as about half of the fine root C mass in the agroforestry treatments occurred below this depth (Figure 4.4). Overall, measured fine root C was found to contribute just 1.1–1.2 and 0.7% of the total SOC stock in the agroforestry treatments and the non-tree control respectively.

4.4.3 *Soil bulk density*

The soil bulk density was generally greater in the agroforestry plots than the arable control. A more detailed analysis of the top 40 cm of soil demonstrates that greater bulk density in the agroforestry plot tended to occur in the centre of the cultivated part of the alleys (Table 4.7). This contrasts with other studies (Messing et al., 1997; Seobi et al., 2005) which suggest that bulk density under afforested land and agroforestry systems tend to be lower than arable systems. The high bulk density in the agroforestry-fallow could have been caused by compaction during the regular mechanical cultivation. Data collected by Aves (2002) also identified compaction under the tramlines in the cropped alleys which, unlike the control area, remained in the same place each year[4]. In addition there was some additional machinery use associated with tree pruning and yield measurements.

Bukhari (1998) found, in a cracking clay in central Sudan, that soil bulk density was greater under a forestry treatment than an abandoned farm. They attribute increased bulk density beneath trees to be the result of both compression of the soil exerted by root growth, and lower soil moisture content caused by increased water uptake by trees.

A similar effect may have occurred at this site, where the soil is also a cracking clay. Based on some simple calculations (Appendix G.1), it is highly unlikely that tree root growth could cause a significant increase in soil bulk density. However in the 2011 study, the soil was visually observed to be drier under the trees than in the arable control during sampling, and a strong relationship between bulk density

4 Aves did not come to this conclusion, but had not completed any statistical analysis of the data. An ANOVA of this data has been included in Appendix A.3.1.

and soil moisture content was observed in a heavy clay soil at the Clapham Park field site (Figure 5.5).

4.4.4 *Soil depth and soil organic carbon*

Although this experiment did not measure fine root turnover, it was assumed that increased fine root turnover due to the presence of the trees would increase soil organic matter. The measurement of the different soil fractions in both the agroforestry-cropped and the control treatments certainly indicates that the proportion of labile C was greatest at shallow depths (5 and 30 cm), coinciding with the greatest levels of fine roots in both treatments and coarse roots in the agroforestry treatment.

Within the top 20 cm, there was no significant effect of the trees on C_o%. This could partly be explained by the ploughing that occurred to this approximate depth for each of the first 11 years of the experiment, and the associated disaggregation and mineralisation of organo-mineral complexes. By contrast, between 20 and 40 cm, C_o% under the trees (1.95 g 100 g^{-1}) was 33% greater than that (1.47 g 100 g^{-1}) in the arable control. This corresponds to the depth with the greatest quantity of coarse roots. Had the coarse roots been included in the soil C measurement, the total C content (soil + plant) within the soil at this depth increment would be even higher.

Similar results have been found with another 19 year old poplar based agroforestry experiment in Canada. Gordon et al. (2006) report that within the top 5 cm C_o% (2.3 g 100 g^{-1}) in an agroforestry system with 111 trees ha^{-1} was similar to that (2.2 g 100 g^{-1}) in the arable control. However a study at the same site to a greater depth of 20 cm indicated a greater ($p < 0.05$) organic C in the agroforestry system (3.0 g 100 g^{-1}) than a barley monoculture (2.4 g 100 g^{-1}) (Peichl et al., 2006).

Below 90 cm, the fine root length density in the agroforestry plot was greater ($p < 0.05$) than the arable control; however, there was not an increase in C_o%. In fact, there was lower SOC stock in the agroforestry treatment at a depth of 60–105 cm ($p < 0.05$, Table 4.12). These differences imply that sampling to a depth of 20 cm would indicate no effect of the trees, sampling to 40 cm would indicate a benefit from trees, and sampling to 150 cm would again suggest no effect. This observation raises questions about whether the experiment was completed with sufficient experimental power; this question is considered in more detail in Chapter 6.

One initial explanation of why the SOC stock was smaller under the trees at a depth of 60–105 cm is the effect on bulk density of the trees drying the soil. However, this can be discounted because the higher bulk densities observed in the agroforestry treatments (Figure 4.6) would tend to lead to greater rather than lower SOC stock, whilst the equivalent soil mass method should correct sufficiently for changes in soil volume.

It is also possible that the difference is due to pre-experimental soil heterogeneity; perhaps the soil at this particular depth in the agroforestry plot has always had a lower SOC stock. Unfortunately we do not have data to indicate if this was or was not the case. However it is worth noting that other studies have also demon-

strated that establishing trees on arable land can lead to declines in SOC stock at depth. Vesterdal and Ritter (2002) report that in a 30 year study of afforestation of former arable land in Denmark, SOC stock increased at 0–5 cm, whilst there was a decrease at 15–25 cm. Jug et al. (1999) in a study of short-rotation poplar plantations on arable land in Germany, also showed that the cessation of ploughing led to a tendency for soil C to decline at 30 cm. These two results may be explained by the cessation of ploughing which had formerly incorporated surface organic matter at depth. However in a 40 year study of forest re-establishment on former agricultural land in South Carolina in the USA, Richter et al. (1999) found that there was a significant increase in SOC stock in the top 7.5 cm of soil, but a significant decline between depths of 35 and 60 cm. Richter et al. (1999) proposed that the decline may be caused by the slow oxidation of previous organic matter associated with crops. It is also possible that increased water use by the trees could have resulted in greater soil aeration at depth and consequently greater respiration rates (Moore and Knowles, 1989). Certainly the soil in the control plots was visually wetter than the soil under the trees.

An alternative explanation is the 'priming effect'; where inputs of readily accessible C from root exudates and root deposition leads to a change in the composition of microbial and fungal communities towards those which favour decomposition of older, recalcitrant forms of soil C (Fontaine et al., 2007, 2011). Observing this effect, Carney et al. (2007), found in a free air C enrichment experiment, that 52% of aboveground gains in C storage were offset by 'priming effect' induced C losses in the top 0–10 cm of soil, in scrub oak in Florida.

In the present study, there was insufficient replication of soil fractionation measurements to demonstrate whether the proportion of recalcitrant soil C (rSOC) at a depth of 83 cm under the trees (8.4%) was significantly lower than that under the control (10.9%). In fact, statistical analysis showed no treatment or depth effect on the proportion of chemically resistant soil organic carbon (rSOC), 19 years after tree establishment.

4.4.5 *Rates of change in soil organic carbon*

Assuming that SOC stock over a depth of 1.5 m was similar in 1992, the non-significant difference in the SOC stock between the agroforestry and control treatments of -5.92 t C ha^{-1} after 19 years (Figure 4.9), would be equivalent to an annual change of -0.31 t C ha^{-1}. However this non-significant loss masks significant gains at individual depths. For example the annual rate would be equivalent to a gain of 0.50 t C ha^{-1} at 20–40 cm, and a loss of -0.67 t C ha^{-1} at 60–105 cm. Post and Kwon (2000) cite average annual changes of soil C from eight studies, following a change from agriculture to forestry in cool temperate regions, that range from a loss of 0.04 t C ha^{-1} to a gain of 0.66 t C ha^{-1}. For a 21 year old poplar silvoarable system (111 trees ha^{-1}) in Ontario, Canada, the mean annual SOC sequestration rate in the top 30 cm of a sandy loam soil was 0.30 t C ha^{-1} year^{-1} (Bambrick et al., 2010). The greater change in the surface layer at the Silsoe site may be due to the higher tree density (156 rather than 111 trees ha^{-1}). In addition, the clay at the Silsoe site may be better suited to the accumulation of organic matter than the sandy-loam found at the Canadian site (Veen and Ladd, 1985).

4.5 CONCLUSIONS

This study affirms many of the methodological issues recently leveled against studies of C sequestration in agroforestry systems (Nair, 2011). Chief among these is the question of depth: our results demonstrate that to get an accurate picture of the C sequestration potential of temperate agroforestry systems, soil sampling needs to be conducted to a greater depth than is routinely practiced. In this study, 80% and 61% of the SOC stock detected was found below 0 and 40 cm respectively (relative to 1.5 m). This literal lack of depth in research is peculiar to temperate systems; Nair et al. (2009) cites seven studies of soil C in tropical agroforestry systems that conducted sampling to a depth of a metre or more – one at 2 m.

Whilst temperate agroforestry systems undoubtedly store more C aboveground compared to conventional agricultural systems, the impact of tree planting on SOC stock at depth is important. Whilst this study indicates that poplar based agroforestry systems may accumulate soil C rapidly at shallow depths; they may also be responsible for a rapid loss of soil C deeper in the soil profile. Possible reasons for this are soil drying leading to oxidation, and the priming effect of new accessible C. Further study is needed to establish if this is a general effect which can be generalised over a range of sites.

4.6 POSTSCRIPT

As indicated, this chapter has been presented as a paper based on Upson and Burgess (2013). Some changes were made to bring the chapter into line with the rest of the thesis, most notably the recalculation of SOC stock using the equivalent soil mass (ESM) method, rather than the 'fixed-depth' method.

The effect this change has on SOC stock is shown in Table 4.11, but in general terms whilst the absolute SOC stock was reduced, relative to each treatment and in terms of statistical significance, the calculation made only limited difference.

Hypotheses

In the context of this thesis, three hypotheses were tested in this Chapter, which are addressed here in turn:

Hypothesis

1. Establishing silvoarable agroforestry systems on arable land will increase soil organic carbon (SOC) stocks relative to a pure arable control.

Incorporating trees into the arable environment as a silvoarable system did increase SOC stock, however this occured only at one depth (20–40 cm) and corresponded to the depth at which most coarse roots were found. When the whole depth profile was considered, this increase was not found.

Hypothesis

2. The incorporation of trees into the arable environment will lead to increases in soil organic carbon (SOC) storage at depth.

Tree planting did not result in a detectable increase in SOC stocks at depth. In fact, at a depth of 60–105 cm, SOC stocks declined in relation to tree planting.

Hypothesis

3. Tree related SOC is more stable than arable crop or grass related SOC.

It was not possible to falsify the hypothesis that tree planting would lead to an increase in stable SOC. The fractionation procedure did not indicate differences between treatments, although it is likely that there was too little replication for a definitive answer to be given here.

5

SOIL ORGANIC CARBON IN SILVOPASTURE AND FARM WOODLANDS

This chapter presents measurements of soil C take at the Clapham Park field site, as described in Chapter 3, and is presented in a paper format. The aim is that this chapter be submitted for peer review before September 2014, with the inclusion of results from fractionation work which was completed between May and July 2014.

5.1 OBJECTIVES

This chapter attempts to falisfy two hypotheses:

Hypotheses

4. Planting trees on grassland will lead to a decline in SOC stock.
5. Losses of SOC from tree planting on grassland are dependent on the density of the tree planting.

5.2 INTRODUCTION

Agroforestry is widely cited as having great potential for the sequestration of atmospheric carbon (IPCC, 2000*b*; Montagnini and Nair, 2004; Mosquera-losada et al., 2011; UNEP, 2011). It is thought that combining woody perennials with forage crops (silvopasture) may offer great carbon sequestration benefits, whilst also potentially improving animal welfare, diversifying incomes, and providing other ecosystem services. Whilst planting trees in pastoral environments will undoubtedly lead to an accumulation of carbon in the form of biomass, the effect on soil carbon is less clear.

Existing literature that afforestation of pasture, at least in the short term, can lead to declines in soil organic carbon (SOC) (Guo and Gifford, 2002; Laganiere et al., 2010; Paul and Polglase, 2002; Post and Kwon, 2000; Shi et al., 2013). These losses tend to be exacerbated in areas of high rainfall (Guo and Gifford, 2002; Kirschbaum et al., 2008), but may be restricted to the most labile 'light fraction' or particulate organic matter (POM), and may be recovered over a long enough timespan (Hoogmoed et al., 2012; Huang et al., 2011; Paul et al., 2003).

Very few studies however consider the impact of establishing silvopastoral systems on existing pastures, particularly in the temperate environment. An important difference being that the tree stocking densities of silvopastoral systems tend to be much lower than pure forestry systems, and hence ground vegetation may be maintained after the trees have reached maturity.

Since root turnover is an important pathway by which carbon enters the soil, and root carbon is known to be more recalcitrant than shoot carbon (Jackson et al., 1997; Rasse et al., 2005); hence in a silvopastoral system where a combination of tree and grass roots are maintained, inputs of carbon into the soil may be greater than monoculture pasture or forest systems. Indeed there is also evidence that increased species diversity may increase soil C stocks (Stockmann et al., 2013).

A resurgence of interest towards the end of the twentieth century led to the creation of a number of new silvopastoral systems, for research and demonstration purposes (Burgess et al., 2000; Sibbald et al., 2001). As these examples and case studies are now 12 or more years old, they offer the potential to investigate soil C changes over long enough periods to be able to detect a change. The intervening years have also seen the introduction of the UK Woodland Carbon Code (WCC): a voluntary scheme to encourage woodland creation for C sequestration benefits (Forestry Commission, 2013). The WCC allows for carbon accumulated in biomass, litter and deadwood, non-tree biomass, and the soil to be quantified, and used to calculate a net benefit in terms of sequestered carbon. Soil carbon changes are included in the WCC, either by a laboratory based soil carbon assessment, or by calculations determined from 'baseline' figures derived from Bradley et al. (2005). Because it has been observed that afforestation of pasture can result in soil carbon losses, the WCC currently assumes no change in SOC stores following afforestation in the case of permanent pasture/grassland (West, 2011). Most of the approx. 200 projects (total of 15 000 ha) projects registered under the WCC so far have been to create native woodlands, typically with mixed broadleaved species, planted at spacings of 2.5-3.0 m, with a mean area of 19 ha (Morison,J., personal communication, 14 February 2014).

This study aims to address some of the uncertainties of measuring SOC stocks at a lowland site in Bedfordshire, E. England, which is typical of WCC projects. As we have demonstrated for a poplar based silvoarable system (Upson and Burgess, 2013), sampling depth is of critical importance in soil carbon studies; failing to sample deeply enough could allow the wrong conclusions about the magnitude of SOC changes to be drawn. Shi et al. (2013) note for instance that studies should look to at least 60 cm in depth to capture changes effected by afforestation. However, the additional variability captured by sampling more deeply can make detecting statistically significant differences in SOC stocks between treatments difficult. Therefore, building on power analyses completed following a previous experiment (Upson and Burgess, 2013), we collected a large number of samples to attempt to accurately assess the impact of tree planting on deep SOC stocks.

5.3 METHODS

The Clapham Park field site is described in detail in Chapter 3.

To assess the impact of the different kinds of tree planting on soil organic carbon, the Clapham Park field site was split into three treatments: the *community (farm) woodland*, the *silvopastoral blocks*, and the *pastoral control*. These treatments are hereafter referred to as FW, SP, and PA.

Based on soil carbon analyses completed at the Silsoe field in 2011 (Chapter 4), power analyses were completed in order to address the question of how many samples would be required to detect any changes that might exist between treatments (Chapter 6). This analysis indicated that a substantial sampling effort would be required to detect the magnitude of SOC changes that have been indicated in the literature (< 1 t C ha^{-1} year^{-1}). Hence within the time constraints of the project it was decided to maximise the number of samples that were analysed to give the best possible chance of detecting any effect. Eighty sampling points were thus identified, 40 in the pastoral control, and 20 each in the silvopastoral and woodland treatments.

GIS software (Polmear, 2010) was used to stratify the sampling points over a 30 m $\times$ 30 m grid in the pastoral area (8.0 ha), and 50 m $\times$ 50 m in the woodland (6.1 ha). Samples taken in the silvopastoral blocks were located at the centre of each tree block; 20 being chosen at random from the possible 34. In order to minimise the impact of tree roots on samples taken from the pastoral control, a 10 m buffer was introduced around the silvopastoral blocks, all surrounding hedgerows and individual trees; and no samples taken within these areas. In order to find the sampling points in the field, a combination of GPS measurements and triangulation with a compass and a fine scale aerial photo were used.

It is recognised that by using a stratified system of sampling, the assumption of independence would normally be violated. In the current case however, given that so many samples are being taken over so small an area, it is likely that a random sampling system would result in samples being taken closer than the 30 or 50 m generated by the stratified sampling system, and therefore even less independent than in the present case. On balance, it was decided that a stratified system would enable a more accurate picture of the site to be established, whilst also allowing the possibility of using geostatistics to investigate any spatial trends in the data.

An additional three points were sampled within a nearby mature ash woodland (Helen's Wood) following the same protocols used in the other treatments.

5.3.1 *Soil bulk density*

Twelve bulk density samples of known volume were taken, centred upon each sampling point: three replicates at each depth of 5, 15, 30 and 50 cm. This equated to a total of 960 soil bulk density (ρ_b) samples. The three replicates were arranged in a triangular pattern around the location of the organic carbon content (C_o%) sample at 30 cm distance.

Samples were extracted vertically with a hand corer of internal diameter 4.51 cm, and the resulting core cut to a length of 5–10 cm (dependent on the intactness of the core), which multiplied by the internal cross section of the auger, was used

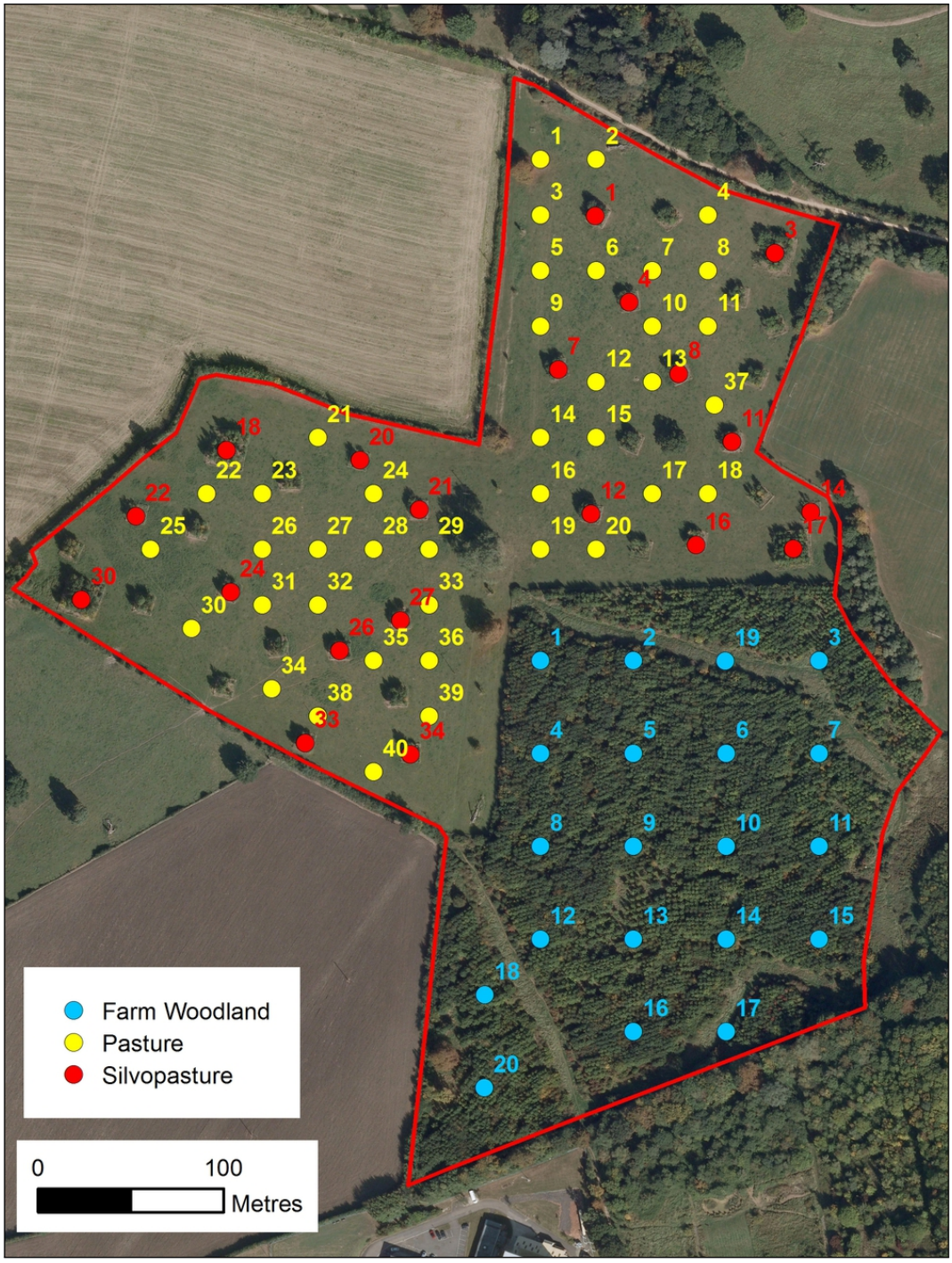

Figure 5.1: Aerial image of the site (2009–2010) showing the location of the 80 soil sampling points.

to calculate the sample volume (typically giving a core of 37 ± 7 SD cm^3). Between each sampling depth small increments were removed sequentially between each sampling depth to minimize the impact of compression caused by driving the auger into the ground. Samples were not taken at depth below 50 cm due to labour constraints, instead bulk density for > 50 cm was assumed to remain unchanged. Samples were dried to a constant mass and bulk density ($g\,cm^{-3}$) calculated by dividing sample mass by core volume (Equation 5.1).

$$\rho_b = \frac{d}{v} \tag{5.1}$$

d = weight of sample in grams after drying in an oven at 105°C (g).
v = volume of the extracted soil core (cm^3).

This vertical coring method was chosen in preference to the more traditional ring method of Klute (1986) which requires access to a horizontal soil profile, as it was prohibitively expensive in terms of time and labour to hand dig 80 soil pits to a depth of at least 50 cm in heavy clay soil. It was recognised however that the efficacy of extracting cores with an auger needed to be evaluated against the more traditional ring method, hence a pilot study was conducted prior to the commencing sampling across the site.

Results from this study (Appendix B.5) did not indicate increased compaction as a result of extraction using an auger, on average ρ_b from samples extracted with an auger were found to be 13% lower than for samples extracted using the ring method. No differences between methods were found at individual depths, meaning that this potential underestimation of ρ_b is not an impediment to comparisons between treatments, although it may result in lower values compared to other studies. Values presented in this chapter are the 'uncorrected' values obtained from the auger method. The pilot study also indicated increased variability of the auger method, hence the decision to complete three replicates at each sampling point.

5.3.2 *Soil moisture content*

Two type of soil moisture content measurement were taken at Clapham Park. The first: gravimetric soil water content (θ_g) was calculated for the same samples that were used for determining soil bulk density. To determine θ_g, each sample was weighed, dried at 105°C to a constant weight, then reweighed. Moisture content was calculated using Equation 7.6.

$$\theta_g = \frac{(w - d)}{d} \tag{5.2}$$

w = field wet weight of sample (g).
d = weight of sample after drying in an oven at 105°C (g).

These samples were collected between September and December 2012, and hence were subject to a variety of weather conditions. For this reason, these data cannot be used for comparing between treatments.

A second set of soil moisture measurements were recorded in the winter of 2013 and spring of 2004 using a 'Diviner 2000'[1] capacitance probe, at a series of 9 access tubes (SP1, SP2, SP3, FW1, FW2, FW3, PA1, PA2, PA3) installed by hand auger in October 2013 (Figure 5.3). Access tubes were sunk to a maximum depth of 1.5 m, however the maximum reach of the capacitance probe was 1.25 m. Readings were taken at 15, 25, 35, 45, 55, 65, 75, 85, 95, 105, 115 and 125 cm. It was necessary to cut two access tubes short due to the presence of chalk which could not be drilled through by hand (Figure 5.2). Hence tube FW3 had a maximum depth of 95 cm, whilst access tube SP3 was to just 85 cm in depth.

On 31 January 2014, tube SP2 was found to be full of water. Since the top of this tube remained sealed since the last measurement, it was assumed that there is a leak in the seal at the bottom of the access tube, only visible now that the soil water level has reached a new high. This tube was replaced on 19 March 2014, and measurements continued. Tube PA1 was also found to contain water on 19 March, but it appeared that this water had entered the tube through a poorly fitting cap rather than a leak at the base. Since the water remained beneath 1.2 m, the cap was changed and measurements continued.

(a) Augering a hole with a dutch auger into which an access tube will be installed in the farm woodland treatment. Note the dryness of the clay spoil.

(b) Completed access tube installed, sitting flush with the soil surface.

Figure 5.2: Installation of access tubes for use with the 'Diviner 2000' for volumetric soil moisture content measurements. Both photos were taken in September 2013.

Readings from these tubes were taken on a weekly basis beginning 23 October 2013, and ending 19 March 2014. Before each set of readings, the capacitance probe was setup with a new air and water reading. Volumetric moisture content (θ_v) was calculated using the calibration equation (Equation 5.3) given for a clay soil at Silsoe given by Burgess et al. (2006).

$$\theta_v = 0.475 SF^{0.418} \tag{5.3}$$

SF = scaled frequency recorded by the diviner 2000 capacitance probe.

1 Sentek Sensor Technologies, Stepney SA 5069, Australia. www.sentek.com.au.

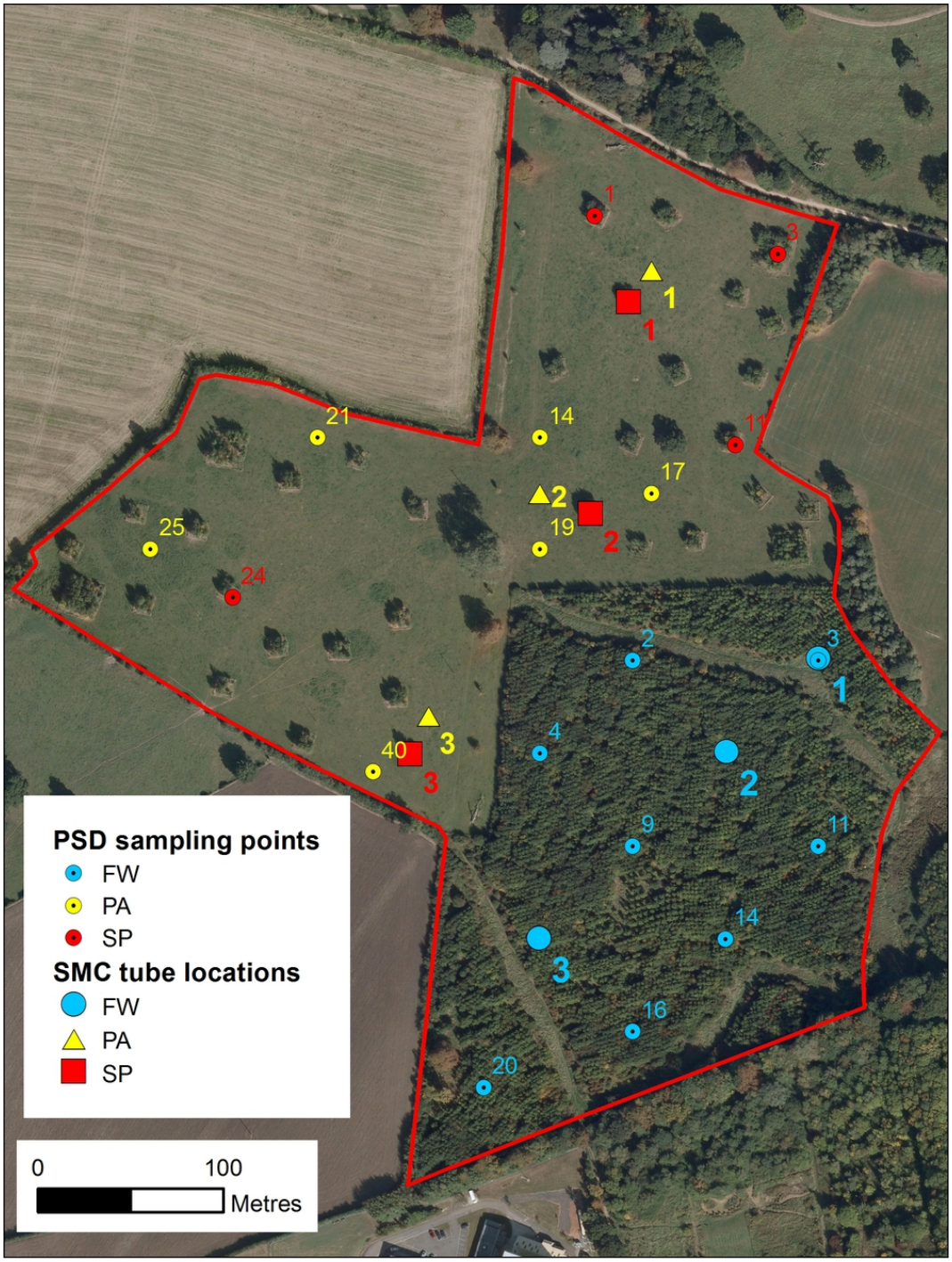

Figure 5.3: Aerial image of the site showing the location of particle size determination and soil moisture content sampling locations.

5.3.3 *Fine root mass*

Fine root mass density (FRMD) measurements were taken by releasing fine roots from within soil cores collected from bulk density measurements. To release the fine roots, the core was inserted into a plastic bottle (of 250 cm^3 volume), filled with deionised water and placed inside an end-over-end agitator for at least 12 hours.

Root material was floated off from the bottle, and caught on a sieve with an aperture size of 710 µm. The clay and silt slurry was washed away, and root material dried at 105 °C) and weighed to a precision of a milligram. The fine root mass density (FRMD, $mg\,cm^{-3}$) of fine roots was then calculated with Equation 5.4.

$$FRMD = \frac{m}{v} \tag{5.4}$$

m = mass of roots (g).
v = volume of core ($g\,cm^{-3}$).

Fine root carbon (C_{root}, t C ha^{-1}) for each depth increment was calculated using Equation 5.5.

$$C_{root} = \frac{m}{v} \times\ d \times\ TOC_{root} \times 10^{-6}\ t\,g^{-1} \times 10^{8}\ cm^2\,ha^{-1} \tag{5.5}$$

C_{root} = carbon content of roots in a particular soil layer (t C ha^{-1}).
m = mass of roots (g).
v = volume of core (cm^3).
d = depth of sampling increment (cm).
TOC_{root} = Proportion of total organic carbon of fine roots, determined by elemental analysis.

5.3.4 *Soil organic carbon*

At each sampling point, six samples were taken for soil organic carbon analysis, at depths of 5, 15, 30, 50, 83 and 120 cm, and assumed to be representative of 0–10, 10–20, 20–40, 40–60, 60–105, and 105–105 cm.

Samples were analysed by dry combustion using a Vario EL III Elemental Analyser[2]. A laboratory standard operating procedure (SOP) for this method is included in Appendix A.4.

Because of small volume changes which occurred as a result of changes in the bulk density within different treatments, we analysed SOC on an equivalent soil mass (ESM) basis (Ellert and Bettany, 1995). This method is increasingly used by researchers to analyse changes in SOC following changes in management as the heretofore common 'fixed-depth' method has been shown to be imprecise because variations in soil mass are ignored (Lee et al., 2009; Shi et al., 2013).

First, a reference value for the mass of soil in the depth layer of interest is calculated using a pre-determined soil bulk density (ρ_b). In this thesis, the method of Bambrick et al. (2010) is followed, and a reference ρ_b of 1.0 $g\,cm^{-3}$ used. However,

2 Elementar Analysensysteme GmbH, http://uk.elementar.de

in other studies, the minimum or maximum observed ρ_b, or the ρ_b derived from a pre-treatment measurement might be used (Lee et al., 2009). This reference or 'equivalent mass' (M_{equiv}) and the actual measured mass (M_{act}) are calculated in Equations 5.6 and 5.6 – these essentially follow the 'fixed-depth' method of SOC calculation

$$M_{equiv} = \rho_{bref} \times d \tag{5.6}$$

M_{equiv} = equivalent soil mass (g cm^2)
ρ_{bref} = reference bulk density (g cm^{-3}).
d = depth of sampling increment (cm).

The actual soil mass (M_{act}) is calculated in a similar way, using the measured bulk density (Equation 5.7).

$$M_{act} = \rho_{bmeas} \times d \tag{5.7}$$

M_{act} = actual soil mass (g cm^2)
ρ_{bmeas} = measured bulk density (g cm^{-3}).

An adjusted soil thickness (T_c; cm) is then calculated using M_{act} and M_{equiv} giving the depth adjustment required to reach the equivalent soil mass (Equation 5.8).

$$T_c = \frac{M_{equiv.} - M_{meas.}}{\rho_{b\ meas.}} \tag{5.8}$$

T_c = depth adjustment required to reach equivalent soil mass (cm)

The SOC stock in the adjusted soil thickness (T_c) is calculated by multiplication with the C content and measured ρ_b for that layer (Equation 5.9)

$$SOC_{adj} = C \times \rho_{meas} \times T_c \tag{5.9}$$

SOC_{adj} = soil organic carbon stock in the adjustment layer (g cm^3).
C = proportional carbon content for the appropriate depth.

Finally, SOC stock in the adjustment layer, and the actual measured SOC stock are combined for each depth increment and converted to units of t C ha^{-1} (Equation 5.10).

$$SOC = ((M_{act} \times C) + SOC_{adj}) \times\ 10^{-6}\ \text{t g}^{-1} \times 10^{8}\ \text{cm}^2\ \text{ha}^{-1} \tag{5.10}$$

SOC = soil organic carbon stock in the depth layer (t C ha^{-1}).

5.3.5 *Data presentation and statistical analyses*

Statistical analyses were completed using the statistical development environment: R, version 3.0 (R Development Core Team, 2013). Analysis of variance was used to test for differences between groups, and model assumptions were checked using normality plots, histograms of the residuals and plots of residuals versus fitted values, created using commands in the basic R package. A random effect was included in the statistical models to take account of the proximity of the PA and SP sampling points.

A random effect for date was included into the analysis of variance (ANOVA) of θ_v to account for the temporal pseudoreplication, as these measurements were taken concurrently, at approximately weekly intervals.

Transformations of the data were made where appropriate. Multiple comparisons between group means were made using the least significant test function, implemented in the package 'agricolae' (**?**), utilising the Benjamini & Hochberg correction to control the family-wise error rate (Benjamini and Hochberg, 1995).

5.3.5.1 *Bulk density data*

Because substantial variability was detected in bulk density measurements, some outliers were removed from the data. Those values which lay beyond 1.5 times the interquartile range beyond the $q_{0.25}$ or $q_{0.75}$ of their respective groupings (i.e. treatment $\times$ depth) were removed as outliers. This equated to 16 out of a total of 960 samples.

To solve the problem of spatial pseudoreplication (Hurlbert, 1984) caused by the replication of measurements ρ_b measurements were averaged at each depth to give a single value to accompany each $C_o\%$ measurement[3].

For calculation of equivalent soil mass (ESM), those bulk density values which were removed as outliers were substituted by the means of their respective treatment $\times$ depth grouping.

3 'Averaging away' the pseudoreplication is a simplification that results in a loss of explainable variance, however this simpler method fitted best with the other analyses conducted in this chapter. However analysis of the complete data including the appropriate error term for the nested measurements resulted in exactly the same results.

5.4 RESULTS

5.4.1 *Soil bulk density*

Highly significant variations in bulk density were detected between the three treatments ($p < 0.001$, Table 5.1), and as a result of depth ($p < 0.001$), but not the interaction between depth and treatment ($p > 0.05$).

Depth was found to be the most important predictor of bulk density ($p < 0.001$); each depth was found to have a significantly greater bulk density than the increment above.

Overall, significant differences ($p < 0.05$) were found between the silvopasture (SP) ($NA \pm NA$ g cm^{-3})[4] and the pasture (PA) treatment (1.30 ± 0.016 g cm^{-3}), whilst the farm woodland (FW) treatment (1.29 ± 0.017 g cm^{-3}) was similar to both ($p > 0.05$).

Table 5.1: Results from analysis of variance (ANOVA) of soil bulk density (ρ_b), organic carbon content (C_o%), fine root mass density (FRMD), and soil organic carbon (SOC) stock on an equivalent soil mass (ESM) basis for Clapham Park in 2012. Degrees of freedom and F-values are given with significance denoted by stars: $p <= 0.001$ (***), $p <= 0.01$ (**), $p <= 0.05$ (*). Note that it was necessary to transform FRMD by a power of 0.2 in order to meet the normality assumptions of a linear model.

Term/Interaction	Bulk density		Organic carbon content	
	df	F-value	df	F-value
Block	1		1	
Treatment	1	14.12***	1	2.55^{ns}
Depth	3	400.03***	5	924.86***
Treatment×Depth	6	1.52^{ns}	10	6.86***
Residuals	308		462	
Term/Interaction	**Fine root mass density**		**Soil organic carbon**	
	df	F-value	df	F-value
Block	1		1	
Treatment	1	30.88***	1	0.25^{ns}
Depth	3	220.68***	5	118.61***
Treatment×Depth	6	1.85^{ns}	10	2.16*
Residuals	308		462	

4 Means are given with standard errors of the mean.

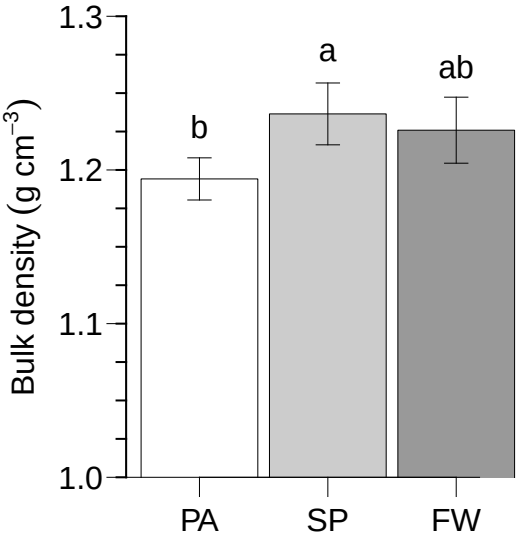

Figure 5.4: Soil bulk density (ρ_b) for each treatment (PA = Pasture, SP = Silvopasture, FW = Farm Woodland) at Clapham Park. Bars represent unweighted means of all depth increments: 0–10 cm, 10–20 cm, 20–40 cm, and 40–60 cm. Error bars indicate standard errors of the mean, PA $n = 160$, FW and SP $n = 80$. Note that the y-axis has been limited to 1.0 g cm^{-3} for clarity.

5.4.2 *Soil moisture content*

5.4.2.1 *Laboratory analysis*

Soil moisture content is heavily influenced by precipitation, and hence should be considered with some caution when sampling has taken place over a prolonged period. In the present study, sampling took place over a period of nine weeks, and hence has been confounded by rainfall over that period.

It is possible to relate soil bulk density to the gravimetric moisture content (θ_g) of each individual sample. Regression analysis showed a highly significant correlation ($p < 0.001, df = 330, t = -27.32, \bar{R}^2 = 0.69$) between the two variables (Figure 5.5).

Table 5.2: Results from ANOVA of volumetric water content (θ_v) for each depth, and treatment (and the interaction thereof) at Clapham Park, Winter 2013. Degrees of freedom and F-values are given with significance denoted by stars: $p <= 0.001$ (***), $p <= 0.01$ (**), $p <= 0.05$ (*), $p > 0.05$ (ns).

Term/Interaction	θ_v	
	df	F-value
Date	1	
Date × Block	1	
Treatment	2	108.46***
Depth	11	8.32***
Treatment×Depth	22	3.37***
Residuals	859	

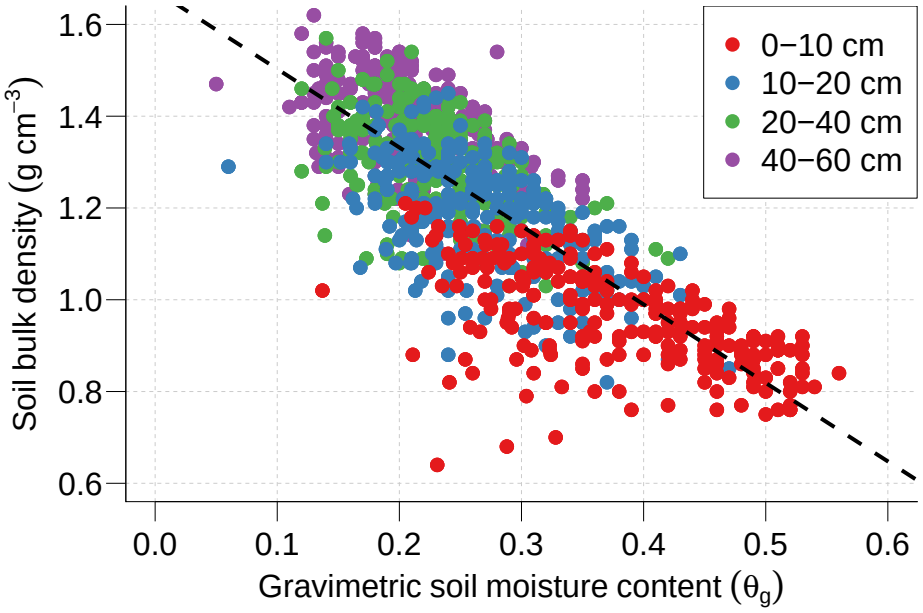

Figure 5.5: The effect of gravimetric moisture content (θ_g) on soil bulk density for all samples collected in 2012 at Clapham Park. Points have been coloured by depth increment. Dashed line follows the equation $y = 1.674 - 1.71x$, $R^2 = 0.69$, $n = 332$.

5.4.2.2 *Field measurements*

As noted, in the absence of site-specific calibration data, the calibration equation determined by Burgess et al. (2006) was used to convert 'scaled frequency' to volumetric soil moisture content (θ_v). It was observed however that this equation may overestimate θ_v for the Clapham Park site. When θ_v is calculated from θ_g, determined from samples collected in 2012, the mean θ_v of all samples was 0.27 $cm^3\,cm^{-3}$ for depths 0–50 cm, whilst the mean of θ_v from diviner readings for 0–55 cm is 0.56 $cm^3\,cm^{-3}$. These were taken in October 2012 and 2013, however the magnitude of the difference may suggest that there is more than annual variation at play.

ANOVA of these data over the whole sampling period indicated statistically significant differences between treatments ($p < 0.001$), and highly significant differences between depths ($p < 0.001$) and the interaction between the two (Table 5.2, Figure 5.6).

Significant differences were found between all treatments ($p < 0.05$). Mean θ_v (0.593 ± 0.003) in the pastoral treatment was greatest, followed by the farm woodland (0.565 ± 0.003), and the silvopastoral treatment (0.540 ± 0.003).

Data from the whole season are presented in Figure 5.7, along with cumulative rainfall collected from a nearby weather station. Note that due to the need to replace one of the access tubes in the SP on 31 January 2014, this data point has been removed from Figure 5.7.

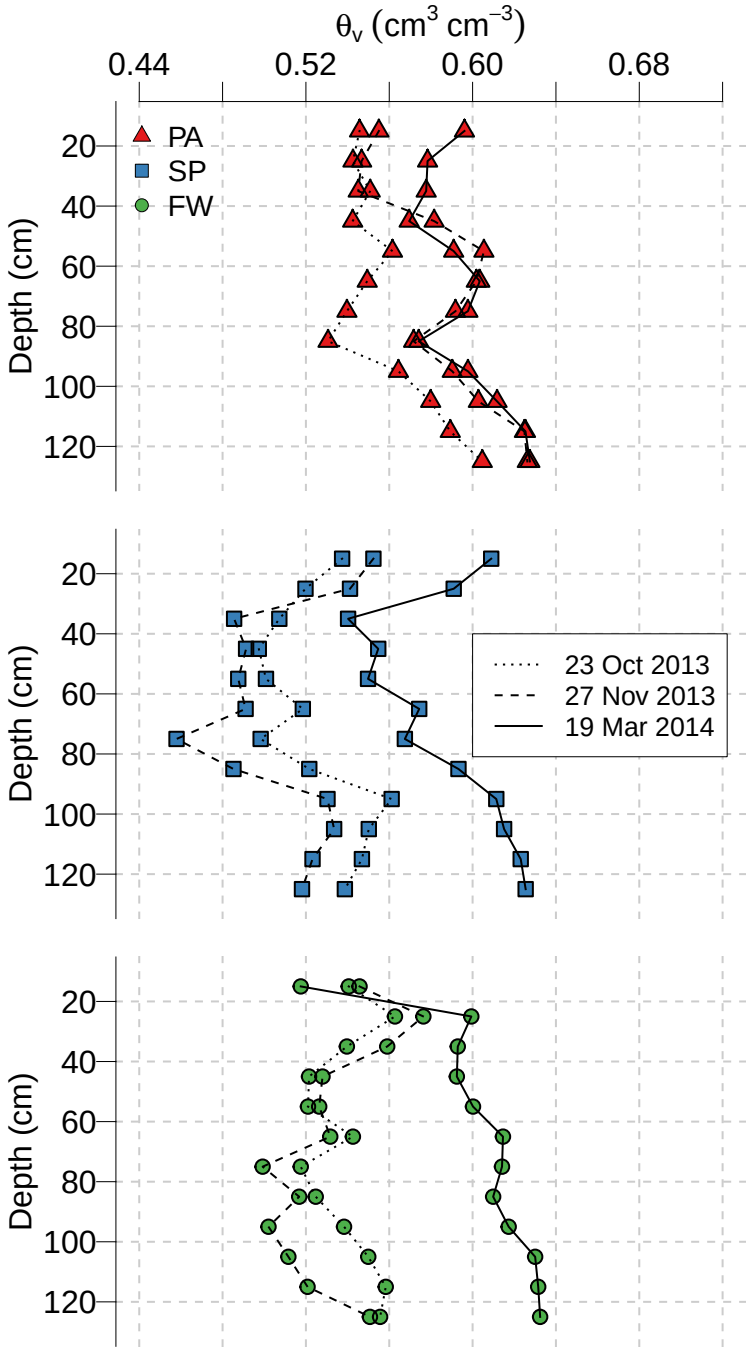

Figure 5.6: Volumetric soil moisture content (θ_v), as measured by the 'Diviner 2000' capacitance probe for the complete depth profile (down to 125 cm), on the first, middle, and last sampling date. On each individual date, three replicates of each treatment were sampled except for SP beneath 85 cm and FW beneath 95 cm. In these two cases, $n = 2$.

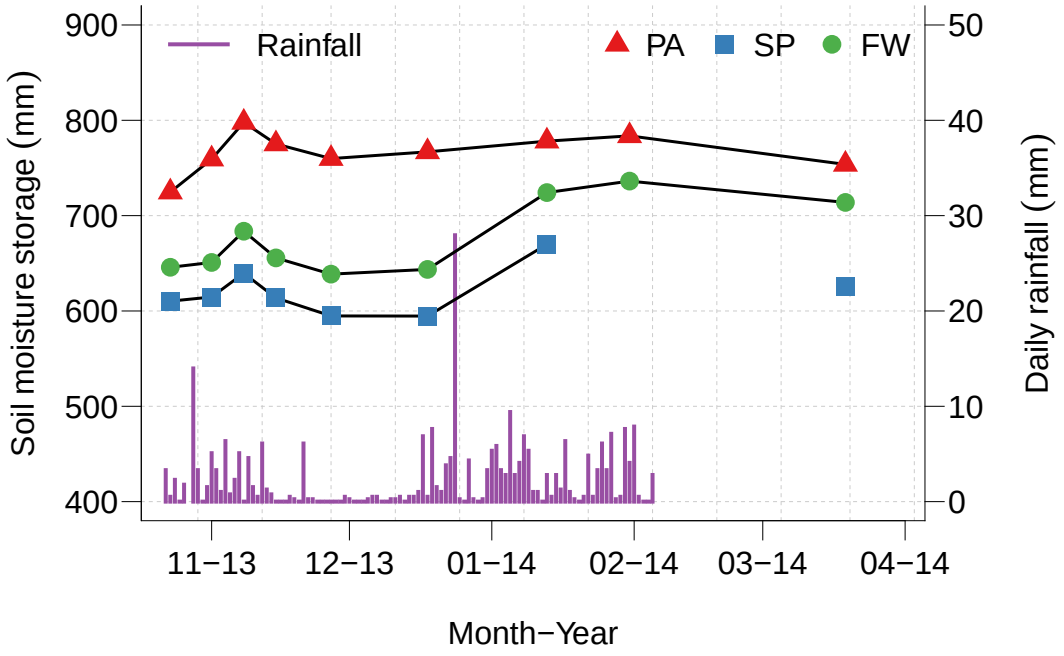

Figure 5.7: Mean soil water storage (mm depth 0 to 130 cm), as measured by the 'Diviner 2000' capacitance probe. Sum of water storage ($\theta_v \times$ measurement increment depth: 10 cm) of all measurement depths ($n = 3$). The data point for 31 January 2014 has been removed since one of the tubes had filled with water, but was corrected before the next measurement was completed.Daily rainfall (mm) has been included on the right-hand y-axis. Rainfall data were taken from the Bedford weather station (Lat: 52.23, Lon: -0.46, Elevation: 85 m) and were accessed via global summary of the day (GSOD) data provided by the US National Climatic Data Centre (http://www7.ncdc.noaa.gov/CDO/country).

5.4.3 *Fine root mass density*

Depth was found to be the best predictor of fine root mass density (FRMD)[5]; significant differences were found between each depth increment (Table 5.1). At the most shallow depth increment (0-10 cm), mean FRMD was found to be 1.28 ± 0.15 mg cm^{-3}, falling to 0.76 ± 0.15 mg cm^{-3} at the deepest depth increment (40–60 cm).

Significant differences in the mass of fine roots recovered were also found between all three treatments (Figure 5.8). Fine root mass density was similar in the silvopastoral blocks (1.85 ± 0.24 mg cm^{-3}) and farm woodland (1.72 ± 0.26 mg cm^{-3}), but lower in the pasture (1.22 ± 0.14 mg cm^{-3}).

No significant interactions between depth and treatment were found (Table 5.1).

As in the 2011 study of FRMD (Upson and Burgess, 2013), cumulative fine root carbon was calculated by multiplying FRMD with the assumed carbon content (0.5) and assumed depth of each sampling increment. Results are presented in Figure 5.9.

Significant differences ($p < 0.05$) were detected at each cumulative depth (Figure 5.9) between all three treatments, except when considering only 0–10 cm: in this instance no differences were detected between the FW and SP treatments ($p > 0.05$), although both tree treatments showed greater cumulative fine root carbon than the pasture ($p < 0.05$).

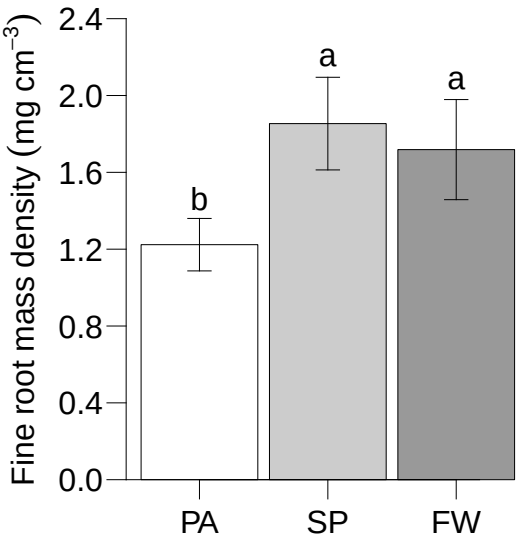

Figure 5.8: Fine root mass density (FRMD) for each treatment (PA = Pasture, SP = Silvopasture, FW = Farm Woodland). Bars represent mean of all depth increments: 0–10 cm, 10–20 cm, 20–40 cm, and 40–60 cm. Error bars indicate standard errors of the mean, PA $n = 160$, FW and SP $n = 80$.

5 Note that FRMD was transformed by a power of 0.2 in order to meet the normality assumptions of a linear model.

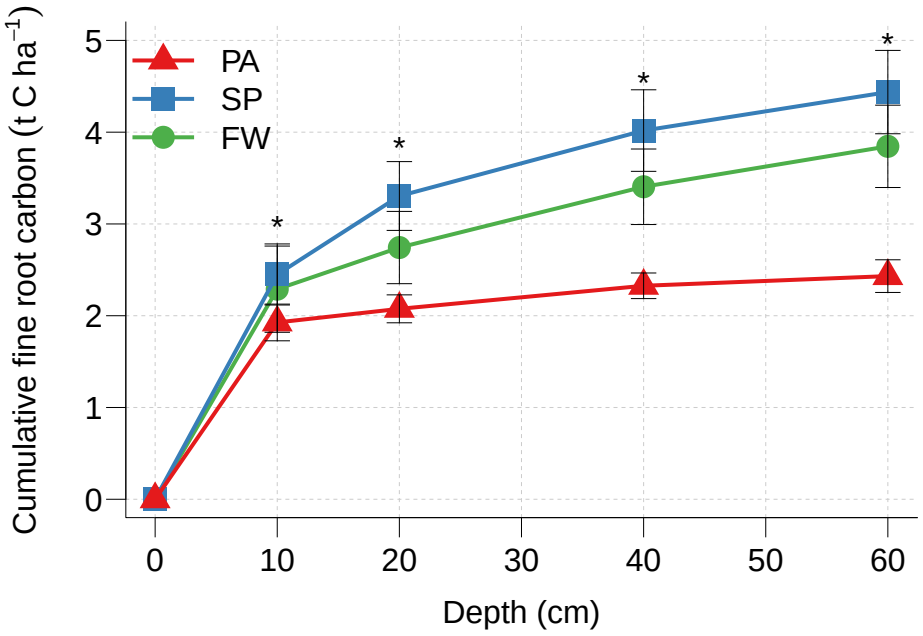

Figure 5.9: Cumulative carbon content present in fine roots, calculated by taking the mean fine root mass for each treatment at each depth and multiplying it by the assumed increment depths (0–10, 10–20, 20–40, 40–60 cm). This was in turn multiplied by the assumed carbon content of fine roots (50%). Error bars indicate standard error of the mean (PA: $n = 40$, SP: $n = 20$, FW: $n = 20$).

5.4.4 *Organic carbon content*

No overall difference in $C_o\%$ was found between treatments ($p = 0.111$), Table 5.1), however depth ($p < 0.001$) and the interaction between depth and treatment were found to have strong effects ($p < 0.001$).

At the most shallow depth increment, significant differences were found between all three treatments ($p < 0.05$, Figure 5.10). The farm woodland was found to have the lowest $C_o\%$ (4.6 ± 0.2 g 100 g^{-1}), with the silvopastoral blocks intermediate (5.3 ± 0.2) and greatest $C_o\%$ in the pasture (6.0 ± 0.2).

At the 10–20 cm depth increment, significantly less organic carbon ($p < 0.05$, Figure 5.10) was found in the farm woodland treatment (2.8 ± 0.1 g 100 g^{-1}) than either the pasture (3.2 ± 0.1 g 100 g^{-1}) or the silvopasture (3.2 ± 0.1 g 100 g^{-1}). Below 20 cm, no significant differences ($p > 0.05$) were identified between treatments at individual depth increments.

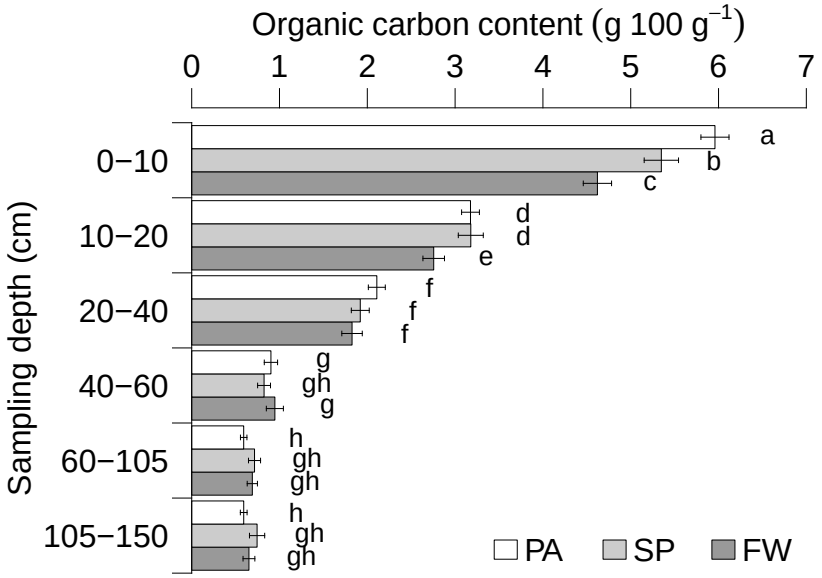

Figure 5.10: Organic carbon content in each of the three treatments recorded at Clapham Park in 2012. FW = Farm woodland ($n = 20$), SP = Silvopasture ($n = 20$), PA = Pasture control ($n = 40$). Error bars indicate standard errors of the means.

5.4.4.1 *Soil organic carbon stock*

Soil organic carbon (SOC) stock was considered on an ESM basis (Ellert and Bettany, 1995), thereby taking into account changes in the mass of soil beneath each treatment. A full explanation is given in the methods (p.100). These data are summed to give cumulative SOC in Figure 5.11.

Since bulk density data was not collected for below 50 cm, it was assumed that bulk density remains unchanged below this depth. This is an assumption that is partly supported by results from similar work completed in 2011 although at a

different site (Upson and Burgess, 2013). No difference in bulk density was found beneath 20 cm in the silvoarable plots (Figure 4.6).

Analysis of individual depth increments indicated a significant effect of depth ($p < 0.001$) and an interaction between depth and treatment ($p < 0.001$, Table 5.3). The presence of significant differences as a result of depth is not surprising given that the depth increments vary from 10 cm to 45 cm. Multiple comparison tests indicated that differences between treatments were only significant in the 0–10 cm layer: the FW treatment was found to have less ($p < 0.05$) SOC stock than the PA control, but neither differed from the SP blocks (Table 5.3).

Table 5.3: Mean (±SE) SOC stock (t C ha^{-1})by layer for each treatment (FW = Farm woodland, SP = Silvopasture, PA = Pasture control) calculated using the equivalent soil mass (ESM) method. Note that comparison of different depths should only be made between layers of a similar size.

Depth (cm)	PA		SP		FW	
0-10	59.6^{a}	±1.6	53.5^{ab}	±2.0	46.2^{bc}	±1.6
10-20	31.7^{efg}	±1.0	31.8^{efg}	±1.4	27.6^{ghi}	±1.2
20-40	42.2^{cd}	±1.9	38.4^{de}	±2.0	36.5^{def}	±2.3
40-60	18.0^{j}	±1.5	16.5^{j}	±1.5	18.9^{j}	±1.9
60-105	26.6^{hi}	±1.7	32.2^{fgh}	±3.1	31.1^{fghi}	±2.6
105-150	26.7^{i}	±1.7	33.5^{fgh}	±3.9	29.3^{ghi}	±3.0

Analysis of each cumulative depth (i.e. 0–10, 0–20, 0–40 cm, to 0–150) highlighted significant differences between treatments only when the most shallow (0–10 cm) depth increment was considered (Table 5.4).

At the most shallow depth (0-10 cm) significant ($p < 0.05$) differences were found between all three treatments. As with the analysis completed in Table 5.1, most carbon was found in the pasture (59.59 ± 1.60 t C ha^{-1}), followed by the silvopasture (53.48 ± 1.95) and farm woodland (46.20 ± 1.61).

Note that these data were log transformed for ANOVA due to a strong negative skew present when data from all individual depth profiles were included, hence they differ somewhat from analysis of individual layers presented in Figure 5.11 and Table 5.4.

Table 5.4: Summary of F-values and significance (denoted by stars). for ANOVA of SOC stock for cumulative depth increments. Each F-value is derived from a separate ANOVA.

		Cumulative depth (cm)					
Term	df	0–10	0–20	0–40	0–60	0–105	0–150
Block	1						
Treatment	1	5.96*	2.45^{ns}	2.79^{ns}	2.41^{ns}	0.46^{ns}	$<0.01^{ns}$
Residual	77						

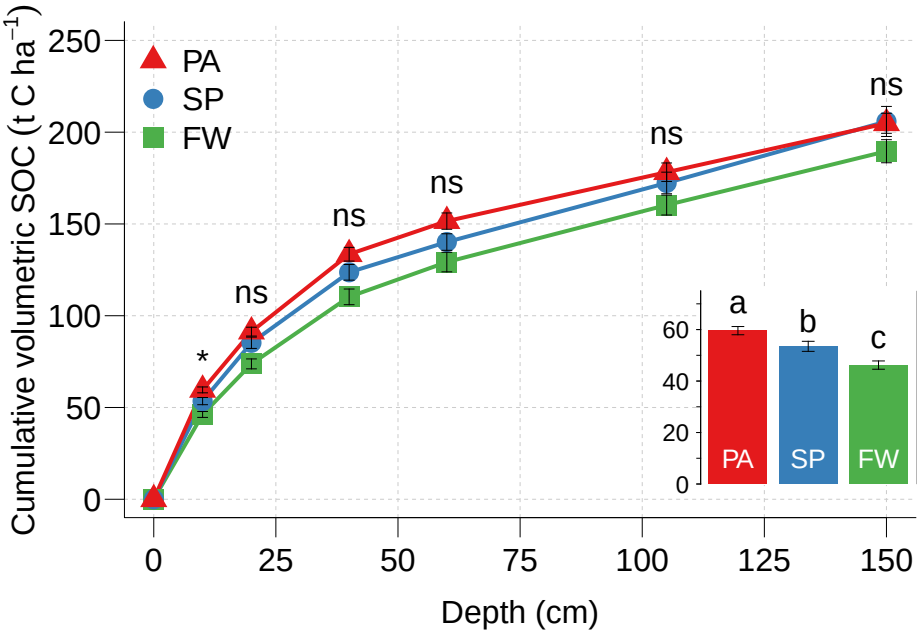

Figure 5.11: Cumulative soil organic carbon (SOC) in each of the three treatments recorded at Clapham Park in 2012. FW = Farm woodland ($n = 20$), SP = Silvopasture ($n = 20$), PA = Pasture control ($n = 40$). Error bars indicate standard errors of the means. Inset boxplot shows data for just the 0–10 cm increment. SOC was calculated on an equivalent soil mass (ESM) basis (Ellert and Bettany, 1995).

5.4.4.2 *Mature grazed ash woodland*

Too little replication was completed to include measurements from the mature grazed woodland, in the statistical analyses along with the other treatments[6]. The limited sample suggests that $C_o\%$ tended to be higher in Helen's Wood that the other treatments (Table 5.5); to a depth of 150 cm SOC stock was 217 $\pm$ 8.5 SE t C ha^{-1}.

Without seeking to read too much from a very small sample size: confidence intervals applied to SOC values from Helen's Wood (referred to as MW – mature woodland, Figure 5.12) suggest that with further sampling significant differences between both the SP and FW treatments and the mature woodland would probably be found in at least the two most shallow cumulative depths.

Table 5.5: Mean and SE ρ_b (g cm^{-1}), $C_o\%$ (%), and SOC (t C ha^{-1}) for each depth layer sampled at Helen's Wood. A summary of bulk density data from Helen's Wood is included in Appendix B.2.

	ρ_b		$C_o\%$		SOC	
Depth (cm)	Mean	SE	Mean	SE	Mean	SE
0-10	0.91	0.01	7.48	0.04	74.79	0.37
10-20	1.12	0.03	3.87	0.10	38.65	1.04
20-40	1.37	0.02	1.76	0.06	35.11	1.17
40-60	1.62	0.03	0.64	0.01	12.72	0.27
60-105	1.62	0.03	0.62	0.01	27.97	0.48
105-150	1.62	0.03	0.62	0.02	27.92	0.68

6 The topic of replication and statistical power is dealt with in detail in Chapter 6.

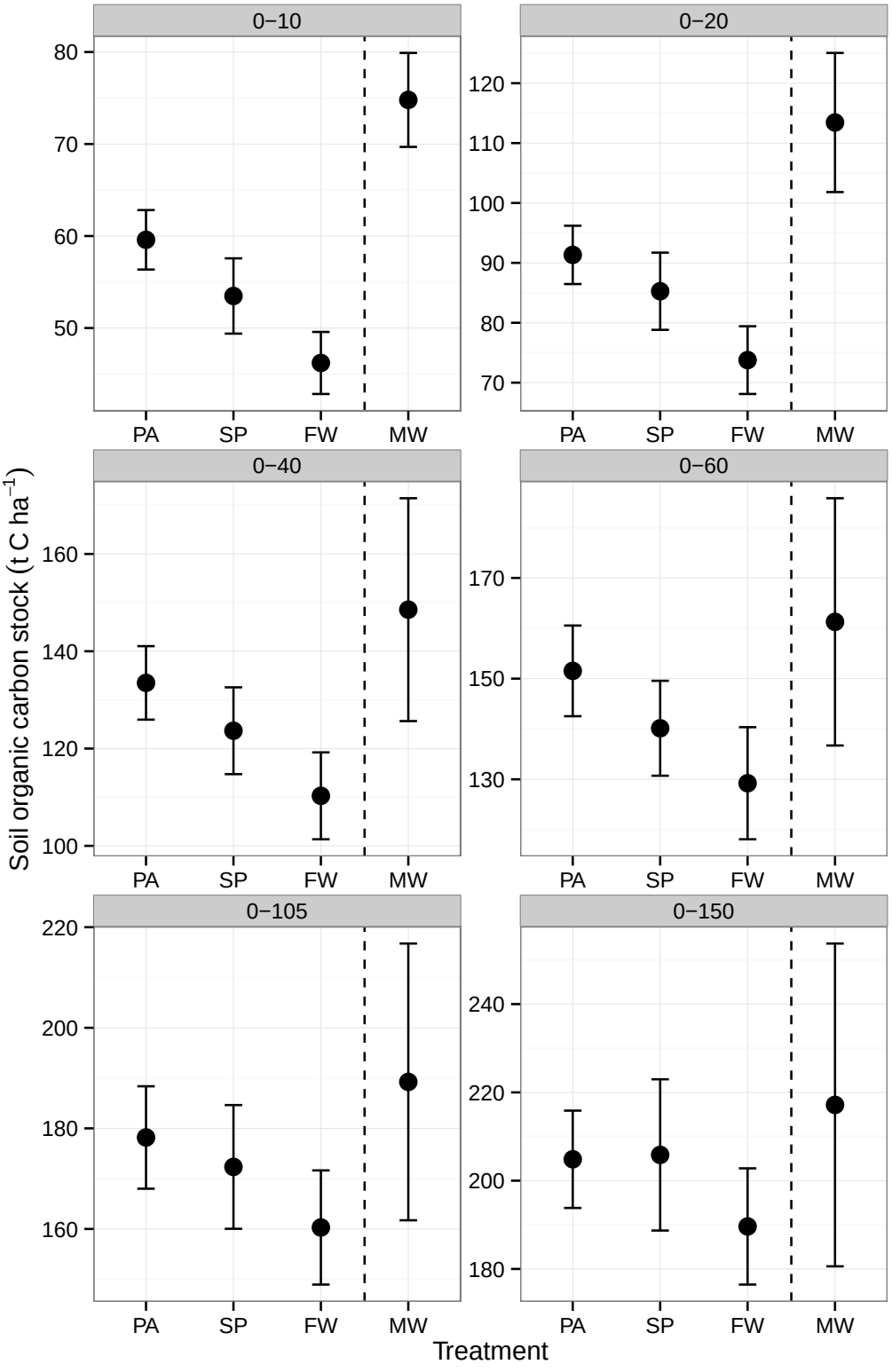

Figure 5.12: Comparison of whole profile soil organic carbon (SOC) stock measurements (t C ha^{-1}) for six depth increments (0–10 to 0–150 cm) taken in the pasture (PA) control, silvopasture (SP) and farm woodland (FW) treatments with measurements taken in a nearby mature grazed woodland, Helen's Wood (MW). Error bars show 95% confidence intervals.

5.5 DISCUSSION

5.5.1 *Soil bulk density*

It was not possible to excavate sample pits in which to take horizontal samples into the soil profile, hence vertical sampling was used. A comparison with the more common ring method described by Klute (1986), taken horizontally into a soil wall, indicated that overall the vertical method underestimated ρ_b by an average 13%. No differences between methods at individual depths were found however; hence this potential underestimation is not an impediment to comparisons between treatments. Furthermore, because the equivalent soil mass (ESM) method used to calculate SOC stock normalises against a reference ρ_b (in this case 1.0 g cm^{-3} following Bambrick et al. 2010), recalculating SOC values to include an additional 13% ρ_b did not alter SOC stock by more than 0.01%. In addition, investigation of the influence of core volume, did not indicate that there was a systematic bias due to the use of unequal sized cores. However there was an effect of core volume, but this was probably mostly due to deeper cores containing fewer sand particles thereby reducing the ρ_b (Appendix B.3).

Comprehensive measurements undertaken at Clapham Park present a mixed picture of the effect of tree planting on soil bulk density. The silvopastoral blocks were found to have a greater density than the pasture control. It is likely that this effect is mostly due to compaction by livestock, which tend to take shelter beneath the trees as the farm woodland treatment, which has remained fully fenced since establishment, showed a similar bulk density to the pasture despite also being afforested.

A lower moisture content in the SP blocks probably plays a part too as there is a strong negative relationship between bulk density and gravimetric moisture content at the site's soils. Due to the high clay content, heavy clay soils will tend to to shrink with drying, increasing the effective bulk density, and it is clear from moisture measurements that the two afforested treatments are drier overall than the pastoral treatment (Figure 5.6 and Figure 5.7).

This is consistent with the observation that, despite trampling by livestock, the silvopastoral blocks maintained a grass understory. Whilst Figure 5.13 shows a reasonably consistent ground cover in the farm woodland in April 2012, this sward was variable, and in places almost entirely composed of cleavers (*Galium aparine*). Such cover disappeared as the season progressed, with the exception of in canopy gaps and at open edges of the woodland.

The present results are also consistent with our earlier observations of bulk density made beneath a poplar silvoarable system (Upson and Burgess, 2013). In that study, also a heavy clay soil, bulk density was found to be significantly greater beneath the afforested treatments overall, and without exception at depths of 40–150 cm. Whilst no soil moisture content measurements were taken at this time, there is some evidence from earlier work (Pasturel, 2004, p.81) that water use by afforested treatments was greater than the arable crop control.

(a) April 2012: Note the effect of livestock on grass cover beneath the trees, in comparison to the pastoral area beyond.

(b) November 2013: Despite some bare areas, the field layer is relatively intact.

(c) April 2012: In this photo, taken near to sampling point FW1 (facing South), vegetation was almost exclusively composed of cleavers (*Galium aparine*).

(d) November 2013: The field layer was almost totally devoid of vegetation, with the exception of occasional tufts of grass, herb robert (*Geranium robertanium*), and tree seedlings.

Figure 5.13: Contrasting images from the silvopastoral system (a and b) and farm woodland (c and d) in April 2012 and November 2013.

5.5.2 *Fine root mass density*

Fine root mass density FRMD in the FW and SP (1.72–1.85 $\mathrm{mg\,cm^{-3}}$) was 40–52% greater than in the pastoral area (1.22 $\mathrm{mg\,cm^{-3}}$). Despite the high level of replication no treatment $\times$ depth interactions were found at either site.

Measurements of FRMD at Clapham Park are greater than measurements take at the Silsoe site (Chapter 4) – by as much as four times in the most shallow depth increments. The magnitude of this differences is largely due to the fact that different depth increments were measured at the two study sites; the present study looked more closely at FRMD close to the soil surface where most fine roots are likely to be found.

In fact, the most shallow depth increment sampled at Silsoe was 0–30 cm with a sample taken at 15 cm. It is therefore equivalent to measurements taken in the present study for the 10–20 cm depth increment (also taken at 15 cm). When these two measurements are compared, they are broadly similar: 0.97 ± 0.06 $\mathrm{mg\,cm^{-3}}$ at Silsoe, compared to 1.18 ± 0.11 $\mathrm{mg\,cm^{-3}}$ at Clapham Park.

Calculation of cumulative fine root carbon indicates that, to a depth of 60 cm (the limit of FRMD observations), fine roots make up 4.4% and 3.8% in the SP and FW treatments respectively, and just 2.4% of total cumulative SOC stock in the PA treatment.

Guo et al. (2007) conducted a similar experiment in a native pasture and adjacent 16 year old pine plantation in Kowen Forest, Australia. The magnitude[7] of the values found by Guo et al. are similar to those presented here, but interestingly Guo et al. found that C in fine roots was greater in the pasture (2.2 t C ha^{-1}) than the plantation treatment (1.9 t C ha^{-1}) – the opposite of the observation in this study. Fine root C was found by Guo et al. (2007) to make up a similar percentage of SOC stock as was found at Clapham Park: 3.1% in the pasture, and 3.3% in the plantation.

5.5.3 *Organic carbon content*

Measurements of C_o% at depth were challenging. As the depth of samples increased, the proportion of carbon found declined to levels which came close to the detection limits of the elemental analyser, and there was the potential for these very small amounts of organic C to be confounded by high levels of carbonates found in the soil at these depths. An explanation of the methodology adopted in order to overcome these issues is included in Appendix B.4.2.

Taking the pastoral treatment as a control, it is possible to assess the impact of introducing trees. In the top 10 cm of the soil, we found a 22% decline in C_o% following the establishment of the farm woodland (4.62 g 100 g^{-1}) compared to the pasture (5.96 g 100 g^{-1}), double the value suggested by Guo and Gifford (2002) following conversion of pasture to plantation. A 10% decline was found in the silvopasture treatment (5.35 g 100 g^{-1}).

At 10–20 cm the farm woodland was found to have 13% less C_o% than the pasture, whilst no differences were found between the pasture and silvopasture. Beneath these depths, no differences were found except between the silvopasture and pasture at the greatest depth increment.

Laganiere et al. (2010), in a comprehensive meta-analysis, notes that high levels of pre-planting disturbance can result in slower gains (and perhaps even losses) of soil carbon. This is unlikely in the present case, as planting was conducted by hand using cell grown or bare rooting stock (Burgess et al., 2000), and prior to this the entire site had seen undisturbed use as parkland or pasture since at least the 1880s.

There were small differences in the planting density of trees within the silvopastoral and farm woodland treatments - Burgess et al. (2000) records a nominal spacing of 2 m × 2 m for trees within the silvopasture, and 2.5 m × 2.5 m or trees in the woodland. This difference is unlikely to have a significant impact of C_o%. Laganiere et al. (2010) found no relationship between planting density and C_o%, and in fact, the woodland planting density was found to be quite variable, and in places was <2 m.

7 Note that Guo et al. (2007) sample from 0–100 cm, which may account for the lower values than at Clapham Park. Guo et al. (2007) observed that there were fewer roots beneath 60 cm, which would have reduced the overall mean.

What seems a more likely explanation is the presence or absence of understory vegetation, and consequently the incorporation into the soil of above and below-ground biomass. Whilst the density of tree planting was not very different between the two afforested treatments, the silvopastoral blocks were much smaller, and lacked the native shrub mixture at the edges of the woodland, hence more light was able to reach the understory in the SP treatment. Consequently, understory vegetation was much more variable beneath the farm woodland, and despite almost complete cover early in the season, had largely disappeared by the August–September (Figure 5.13), with the exception of canopy gaps and open woodland edges. Contrast this with the silvopastoral blocks, where although some loss did occur due to trampling by livestock, it tended to be focused on a few of the tree blocks, and did not result in a complete denuding of vegetation either across the treatment as a whole, or in any particular block (Figure 5.13).

Interestingly, we did not find a similar response in FRMD – more roots were found overall in the afforested treatments than the pasture. This suggests either that fine root mass is not the major factor driving the loss of soil carbon in afforested treatments, or that a qualitative difference in fine roots resulting from the afforestation had resulted in losses of C_o%.

Our measurements are only a snapshot of FRMD captured across a two month sampling period, and do not represent turnover rates, which might have a greater bearing on C_o%. It is conceivable, that whilst a greater mass of roots was detected in the afforested treatments, these roots turnover more slowly, and hence lead to a slower incorporation of organic matter into the soil. This is consistent with observations whilst extracting roots – those recovered in the afforested treatments, were larger, secondary thickened roots, likely to have a longer lifespan than the sub mm diameter grass roots predominantly recovered in the pasture (Guo and Gifford, 2002). This echoes the findings of Guo et al. (2005) that increases in SOC has more to do with the actions of live roots than the decomposition of fine root mass.

5.5.4 *Volumetric soil organic carbon*

Our findings agree with those of Shi et al. (2013), who in a recent meta-analysis found that the response ratio (defined as the change in SOC stock divided by the SOC stock of the control at each depth, normalised to one) in studies of afforestation of grasslands tended to be negative, but in general close to 1. In this study the response ratio for the silvopastoral treatment varied between 0.90 and 1.26, whilst the woodland treatment varied between 0.77 and 1.16, values close to or within the 95% confidence intervals reported by Shi et al. (2013).

In the 0–10 cm layer, the rate of change of SOC stock relative to the PA control was -0.96 t C ha^{-1} $year^{-1}$ and -0.44 t C ha^{-1} $year^{-1}$ respectively for the FW and SP treatment. These rates of change far outstrip the mean values for 0–20 cm quoted by Shi et al. (2013) of -0.19 t C ha^{-1} $year^{-1}$, although if the top two layers (0-10 cm and 10–20 cm) in the present study are averaged, lower values of -0.22 t C ha^{-1} $year^{-1}$ and -0.63 t C ha^{-1} $year^{-1}$ are obtained.

This rate of SOC change is very high, and although we cannot preclude the possibility that site factors are at play, if these changes are a result of tree planting,

preliminary measurements of total tree biomass carbon (above and belowground) indicate that SOC losses at the 0–10 cm layer would be responsible for offsetting 8% and 31% of the total biomass carbon stored over 14 years in the SP and FW treatments.

Results from the adjacent mature grazed woodland (Helen's Wood) suggest that these observed differences may not be maintained into the future. If the preliminary results found at Helen's Wood can be replicated with a greater sample size, and the effect of site accounted for, it appears a reasonable conclusion to draw that SOC stock in the SP blocks and FW treatment will eventually recover any initial losses and eventual sequester more carbon than the PA control. This effect is noted by Huang et al. (2011) for *Eucalyptus nitens* following afforestation of a pasture in New Zealand within ten years of planting. How long this may take in the present case is impossible to assess from this experiment as Helen's Wood has been under continuous woodland for at least 200 years (and probably longer), and grazed for an indeterminate time. Results from Helen's Wood can be regarded as having attained 'climax' SOC storage for a silvopastoral system in this locality, that said given the degraded nature of the woodland, SOC storage is probably in decline: the current intensity of grazing at present is unsustainable and has prevented natural regeneration; once the current cohort of trees die (perhaps as a result of the pathogen *Hymenoscyphus pseudoalbidus*) the wood will be in desperate need of restocking lest it revert entirely to pasture. Interestingly, in a modelling study based on 100 observations from 16 papers, Poeplau et al. (2011) did not find a recovery in SOC as much as 140 years after afforestation of grassland, how this fits with observations from Helen's Wood is difficult to assess, but a future round of measurements at Clapham Park would certainly be instructive.

Considering the whole depth profile (0–150 cm), the differences between the grassland control and the silvopasture and woodland treatment equate to 0.07 t C ha^{-1} $year^{-1}$ and -1.09 t C ha^{-1} $year^{-1}$ respectively, although due to increased variability, no significant difference was found at these cumulative depth.

Our findings agree with those of Shi et al. (2013) in that deep SOC stock did not show a significant response associated with tree planting. However, 30% of the total SOC detected in the 0–150 cm profile was found at depths greater than 60 cm, meaning that deep sampling remains important in quantifying SOC stocks. By comparison, more than a quarter (26%) of the total measured SOC was found in the top 10 cm of soil, whilst between 10–20 cm, 20–40 cm, and 40–60 cm, 16%, 19%, and 9% of the total measured SOC stock was found.

Compared to national values presented by Vanguelova et al. (2013) for UK forests on Cambisols, our data are very consistent when the same depth increments were measured. For instance, Vanguelova et al. (2013) found average values over 74 plots of 25.0 ± 1.0 t C ha^{-1} and 37.0 ± 2.4 t C ha^{-1} at 10–20 cm and 20–40 cm respectively; in the present study, we found 27.6 ± 1.2 t C ha^{-1} and 36.5 ± 2.3 t C ha^{-1} in the woodland treatment for the same layers. However, for 0–10 cm, perhaps in part because we did not stratify our sampling into two layers, we found 46.2 ± 1.6 t C ha^{-1} compared to a national value of 39 ± 1.7 t C ha^{-1} (0–5 cm and 5–10 cm summed). Comparing values for the cumulative layer 0–105 cm, data is somewhat greater than the national values for 0–100 cm, we found 178, 172, and

160 t C ha^{-1} in the grassland, silvopasture and farm woodland treatments respectively, compared to 152 t C ha^{-1} under woodland nationally.

Our findings at Clapham Park are similar to the Silsoe experiment where differences were indicated at more shallow depth increments, but not when the entire profile was considered. One should however be a little cautious in studies where a cumulative SOC has been calculated. This is because with greater cumulative depth, variance inevitably increases, yet the effect size increases only marginally (as the majority of changes occur at the most shallow depth increments). Hence, since the number of samples remains the same, the statistical power of these tests declines with increased depth, and with it the ability to reject a false null hypothesis (Crawley, 2007).

Although the sampling strategy at Clapham Park was informed by power analyses conducted based on data collected at the Silsoe experiment, differences between the two experiments meant that the original assessment was too optimistic, and that 40 paired sampling was probably too few samples to provide sufficient experimental power under the usual assumptions ($\alpha = 0.05, \beta = 0.2$) for some depths. Power analyses based on this study indicate that more than 100 paired sampling points would be required to ensure a power of 0.8 over the complete depth profile, and hence in the present study the probability of making a Type II error may be unacceptably high. However, we can be reasonably sure based on these power analyses (Chapter 6) that if the experiment were repeated (and we encountered the same variance and effect sizes) that we would only incorrectly fail to reject the null hypothesis 20% of the time for cumulative depth increments up to 0–20 cm (Chapter 6). Below this cumulative depth, the Type II error rate would be larger, quite how much larger is difficult to calculate, without falling into the 'observed power' fallacy (Hoenig and Heisey, 2001).

5.6 CONCLUSIONS

In line with the literature consensus, afforestation of pasture was found to be associated with a loss of carbon in the surface layers. This trend did not continue at subsequent depths however, and no overall difference in soil carbon was found between treatments 14 years after planting when depths greater than 0–10 cm were considered.

The hypothesis which arises from this work is that carbon losses detected at the shallowest increment are related to the loss of understory vegetation following canopy closure; hence in the silvopastoral treatment, where light was still able to penetrate beneath the trees, losses in soil carbon were less great.

It did not seem to be the case that declines in soil carbon were directly related to differences in root mass; rather, it is inferred that a qualitative difference between tree roots and grass roots, caused the decline.

Based on power analyses (Chapter 6), it is concluded that the measurements of cumulative depths of 0–40 cm and greater, have a higher than acceptable chance of failing to reject the null hypothesis, and should therefore be considered with caution.

That so much soil carbon was detected across the complete depth profile highlights the importance of sampling as deeply as possible. However, in general, stud-

ies are not likely to sample such a small study site so intensively and hence the difficulties in determining statistical differences between treatments at depth could be more acute. Studies of deep soil organic carbon stocks should therefore complete both pre- and post-experimental power analyses.

5.7 SUMMARY OF FINDINGS

In the context of this thesis, two hypotheses were tested in this Chapter, which are addressed here in turn:

Hypothesis

4. Planting trees on grassland will lead to a decline in SOC stock.

In line with the literature consensus, planting trees into a grassland caused a decline in SOC stocks at depths of 0–10 cm and 10–20 cm over 14 years. This effect was not found when the whole 0–150 cm depth profile was considered.

Hypothesis

5. Losses of SOC from tree planting on grassland are dependent on the density of the tree planting.

At 0–10 cm SOC losses were greater in the farm woodland treatment than the silvopastoral blocks. This seems to confirm the hypothesis that a loss of ground vegetation productivity is related to SOC stock losses. Once the canopy had come into leaf in the woodland treatment, ground vegetation was shaded out, leaving the woodland floor bare for much of the year. Conversely, in the silvopastoral blocks, where there was not a continuous canopy and light was able to reach the ground throughout the year, a grass layer was maintained.

Measurements of SOC stock taken at an adjacent mature grazed woodland (Helen's Wood) suggest that losses in SOC stock may recover over an undefined timescale. Greater SOC stock in this woodland may be the result of the legacy of many previous decades of tree cover (the site has been under continuous woodland cover since at least the 1880s), carbon inputs from the grass understorey (as the woodland is sparse enough to allow a grass understorey to be maintained throughout the year), or or a combination of the two. This latter possibility would fit with the conceptual framework outlined in Figure 2.12.

6

SAMPLING SOIL ORGANIC CARBON IN AGROFORESTRY AND FARM WOODLAND SYSTEMS

In this chapter the results presented in Chapters 4 and 5 are used to conduct power analyses and a resampling study to calculate the minimum number of samples required to determine soil organic carbon (SOC) stock, with a view to informing the carbon accounting schemes such as the Woodland Carbon Code.

6.1 HYPOTHESES

In this chapter the following hypothesis is tested:

Hypothesis

8. Frequentist hypothesis testing is an appropriate tool to determine differences in SOC in newly planted woodlands.

6.2 INTRODUCTION

6.2.1 *Soil carbon in the Woodland Carbon Code*

At present, the Woodland Carbon Code suggests two methodologies by which a project can account for changes in SOC stock (West, 2011):

1. The use of look-up tables to make estimations of soil carbon changes.
2. By conducting a soil carbon assessment prior to tree planting with repeat assessments as the project progresses.

In the case of look-up tables, the approach is as follows (West, 2011):

1. If necessary, the site is stratified according to pre-planting preparation and soil depth.
2. A soil C baseline is established based on Bradley et al. (2005) in the absence of any site-specific values.
3. A proportion of topsoil C stock is removed to account for the losses caused by planting preparation.
4. Changes in SOC are calculated according to the method of woodland management. For woodlands managed with thinning and clear-felling operations, currently no values are available for estimating changes in SOC, but a

future release is anticipated. For woodlands managed by minimum intervention[1] the approach differs according to previous land use.

- For woodlands planted on former arable or permanent pasture, a rate of SOC accumulation of 0.15 t C ha^{-1} is assumed for the first 50 years of the project; thereafter a rate of 0.1 t C ha^{-1} is assumed (based on rates reported by (McKay, 2011).
- For projects established on former permanent pasture or grassland, it is recognised that there is an initial drop in SOC stock, but that this may later be recover in subsequent years. For this reason, no change in the baseline SOC stock is assumed.

The results presented in Chapters 4 and 4 cannot be used to evaluate the look-up table approach because the Woodland Carbon Code (WCC) has been designed for forest plantings, not the establishment of agroforestry systems such as the Silsoe silvoarable trial. Equally, results from Clapham Park cannot be used, since it is a minimum intervention woodland, and the assumption is that there will be no change from the baseline values, although results presented in Chapter 5 show an initial loss of SOC stock on planting, and the possibility of recovery in time (Helen's Wood).

For the SOC assessment approach, one of the key questions that needs careful consideration is the number of samples required to give a robust assessment. This is important since relatively minor changes in SOC stock can have major ramifications for the total amount of carbon sequestered.

In this chapter, two approaches are considered for answering the question of how much sampling is required to give a sufficiently robust answer to this question.

6.2.2 *Power analysis*

In classical Neyman-Pearson statistics, hypothesis testing (which is based on assumptions of normality, amongst other things) depends on α: the probability of rejecting the null hypothesis when it is true (H_0) – a Type I error, and β: the probability of failing to reject H_0 when it is false – a Type II error. These possible outcomes are summarised in Table 6.1.

Table 6.1: Possible outcomes from a hypothesis test, where H_0 is the null hypothesis and H_a is the alternative hypothesis, and α is the probability of a Type I error, and β the probability of a Type II error.

	H_0 True	H_a True
Reject H_a	No error	Type II error$^{\beta}$
Reject H_0	Type I error$^{\alpha}$	No error

Whilst researchers are usually explicit about their assumptions for α, it is much less common to see reference to β in the methods sections of published articles,

1 Minimum intervention woodlands typically are planted at a lower density than traditional thin/clear-fell woodlands, and are thinned less frequently, if at all.

despite the fact that Type II errors make up one of the four possible outcomes of a hypothesis test.

As Crawley (2007) puts it: "In an ideal world, we would obviously make β as small as possible. But there is a snag. The smaller we make the probability of committing a Type II error, the greater we make the probability of committing a Type I error, and rejecting the null hypothesis when, in fact, it is correct". This relationship can be seen in Figure 6.1 which illustrates the relationship between α and β, and $1 - \beta$ or the 'power' of a test.

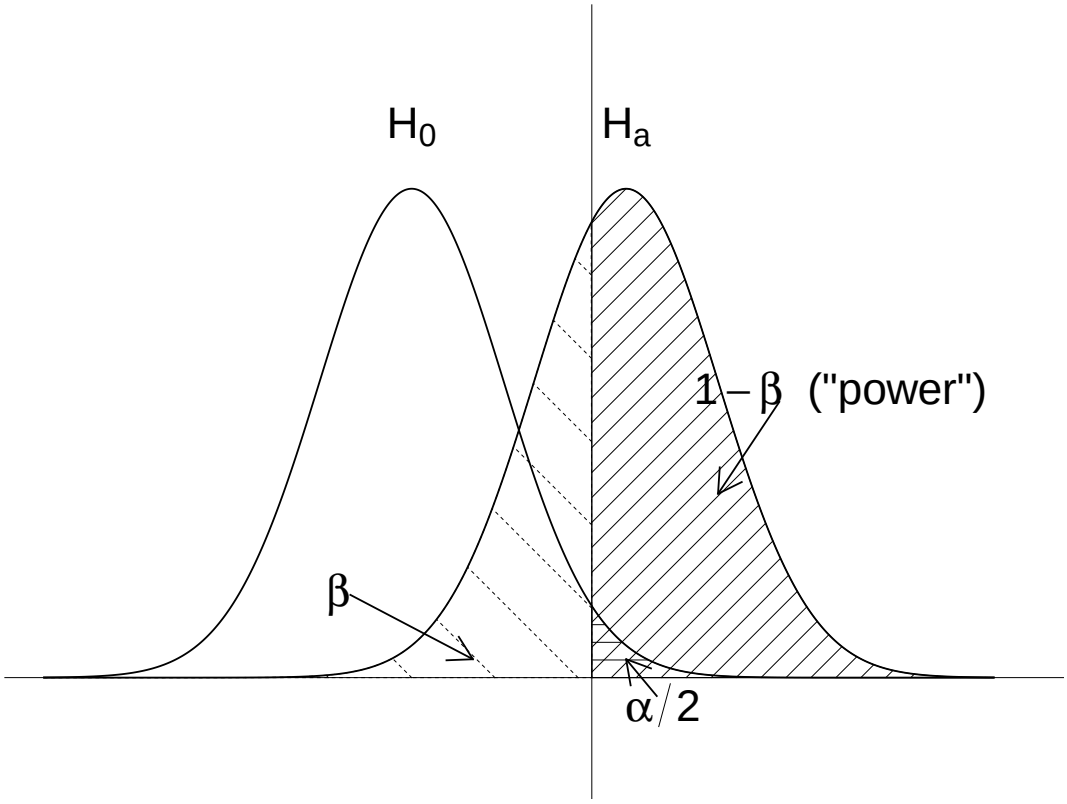

Figure 6.1: Classical textbook representation of the relationship between α, β, H_0, and H_a. The R code used to produce this plot was taken from Magnusson (2013), and is licensed under a Creative Commons Attribution 4.0 International License.

In this figure, the left hand curve represents the theoretical distribution of the sample mean if H_0 is true, and the right hand curve represents the theoretical distribution of the sample mean if H_a is true. In the context of this chapter H_0 can be stated as there being no difference in SOC stock between the pre-planting and tree treatment, whilst H_a indicates that there is a difference (Equation 6.1).

$$\begin{cases} \mathrm{H}_0 : \overline{x}_{control} = \overline{x}_{tree} \\ \mathrm{H}_a : \overline{x}_{control} \neq \overline{x}_{tree} \end{cases} \tag{6.1}$$

$\overline{x}_{control}$ = mean SOC in agricultural control.
$\overline{x}_{tree}$ = mean SOC in tree planted treatment.

The area $\alpha/2$ indicates the 'rejection area' where H_0 will be rejected if $\overline{x}_{tree}$ is found in this area[2], i.e. if a value more extreme than this threshold value is found, it is deemed very unlikely to have occurred by chance alone ($\leq 0.025\%$), and thus comes from a different distribution: H_a where $\overline{x}_{tree}$ is the true mean. It is possible that a value less extreme than this may be found for $\overline{x}_{tree}$ but still be part of the distribution of H_a, in which case this value will occur in the area β. Hence the power of the test is the area $1-\beta$, as if $\overline{x}_{tree}$ is found to occur within the area $1-\beta$, H_0 will be rejected.

In simple terms, and to restate Crawley (2007), reducing α innevitably increases β – the two are inextricably linked, and hence it is impossible to obtain a lower Type II error rate without generating a greater Type I error rate. Since a Type I error rate is usually considered to be less desirable, it is common that a compromise of $\alpha = 0.05$ and $\beta = 0.2$ is used (Crawley, 2007).

Power is dependent on three things: the effect size (signified by the the horizontal position of the curves H_0 and H_a in Figure 6.1), the variability of the two distributions (indicated by the width of the curves), and the number of samples used (this has an impact on the normalisation into t or z-distributions required for hypothesis testing). Given the interaction between these three factors, it is possible to calculate power in advance of conducting an experiment. By completing 'power analyses' researchers can better understand the circumstances which lead to a failure to reject a null hypothesis (H_0), allowing inferences to be made about whether or not a failure to reject H_0 occurred simply because there was insufficient power, or because $\overline{x}_{control} \neq \overline{x}_{tree}$. Alternatively power analyses can be conducted after the experiment to ask the question in a different way: given an assumed variability and effect size (determined by field measurements) what is the minimum number of samples required to ensure a specified level of power (Figure 6.2).

Note that an incorrect usage of retrospective power analysis is to attempt to determine the power of a test which has already failed to reject H_0. Despite this method being available in many popular statistical packages, calculating 'observed power' from the observed p-value (in place of α) can never be informative because there is a 1:1 relationship between the two (Hoenig and Heisey, 2001; Thomas, 1997; Thomas and Krebs, 1997).

Working under the common assumption of $\alpha = 0.05$, $\beta = 0.2$, it is possible to graphically represent the relationship between sample size, effect size, and sample standard deviation. This relationship can be used to determine the number of samples needed to detect an effect of specified size, with the probability of making a Type II error of 20% and a Type I error of 5% (Figure 6.2).

Power analysis is nothing new, and was first proposed by Cohen in 1962 in the field of behavioural psychology; however some 52 years later, power analyses continue to be neglected by researchers as an aid to correctly interpreting results from hypothesis testing. As early as 1992, thirty years after publishing his first article on the topic, Cohen decried the lack of uptake of the test, despite there being no methodological controversy and the fact that the test is routinely published in statistical textbooks, and is available in many statistical computer programs (Cohen, 1992; Erdfelder et al., 1996; Thomas and Krebs, 1997).

2 This rejection area is mirrored on the left hand side of the distribution, but not shown in this plot.

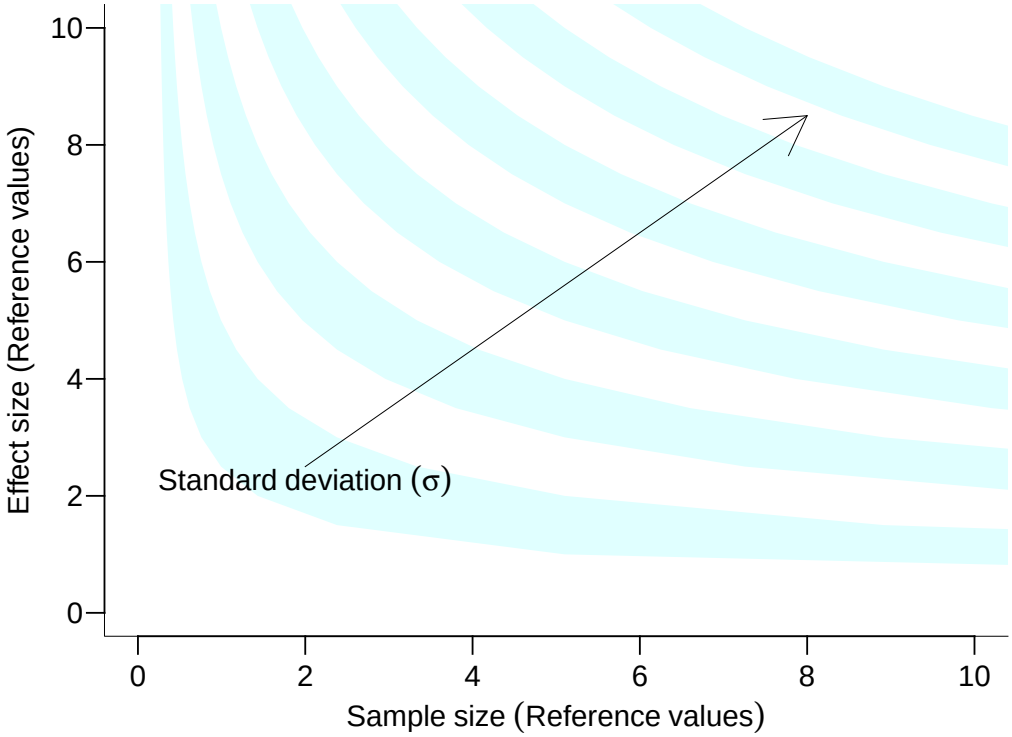

Figure 6.2: Demonstration of the relationship between sample size, effect size and sample standard deviation. Blue bands show increasing standard deviations. As effect size increases (at a given standard deviation), the number of samples required to detect that effect, decreases. Increased variability in the data increases the sample size required to detect an effect of a specific size.

6.2.2.1 *Power analysis in soil carbon studies*

Power analyses are particularly important in studies of SOC for two reasons. Firstly, correctly judging whether a particular land use or management practice is beneficial for improving SOC stocks is essential for our understanding of greenhouse gas (GHG) balances, given that soil is the largest terrestrial carbon sink. Second, power analyses are important because the rate of change of SOC is very small relative to the total stock, whilst the variation between sampling points, sites, and soils can be very great. Hence, especially when considering changes over large depth increments, it is likely that we will fail to reject false null hypotheses, but it is only by correctly completing the required power analyses that we can make an informed judgement about whether there really is no difference between the treatments in question, or because of the inherent difficulties in sampling SOC, we just simply did not conduct enough replication.

In this chapter, a pre-specified power (0.8) is used to determine a 'detectable' effect size for a given sample size, based on the observed variance from Silsoe and Clapham Park; so-called 'reverse power analysis' (Thomas, 1997). We are then able to infer roughly how many samples would have been required in these two studies to achieve an acceptable level of power.

6.2.3 *Resampling simulations*

An alternative method for calculating the number of samples required to correctly characterise a population, is to compare experiments with different levels of replication and compare confidence intervals about the mean. Since we sampled intensively at the Clapham Park we are able to simulate this procedure by resampling within the observed values at different sampling intensities. With this kind of resampling, the variation among sub-sets with different sampling intensities is likely to be asymptotic, allowing a sample size to be determined at which the bulk of the variation has been captured. The strength of this method lies in the fact that it does not rely on the distribution of the second treatment in order to determine a necessary sample size, but considers the question of 'how much sampling is required to characterise the observed distribution' directly.

This resampling procedure was conducted by Vanguelova et al. (2013) in a recent paper reassessing SOC stocks in the UK for each of the major soil types, and is replicated in this chapter with two key differences. Firstly, Vanguelova et al. (2013) define coefficient of variation (CV) as in Equation 6.2: the sample standard error divided by the population mean; this differs from the classical definition of CV, which is more normally defined as the sample standard deviation divided by the sample mean (Equation 6.3).

$$CV_v = \frac{\frac{s}{\sqrt{n}}}{\mu} \qquad (6.2) \qquad\qquad CV = \frac{s}{\overline{x}} \qquad (6.3)$$

n = sample size.
μ = population mean.
$\overline{x}$ = sample mean.
s = sample standard deviation.

Whilst use of the population mean is probably valid[3] and differs little from the sample means, use of standard error instead of the standard deviation changes the shape of the curve from asymptotic to exponentially declining, because sample size is taken into account with standard error but not standard deviation. Whilst this is a legitimate approach in terms of demonstrating the effect of sample size, referring to this descriptive statistic as CV could be misleading. Furthermore it is easier to visually determine a point at which the bulk of variation has been captured by using standard deviation rather than standard error.

Vanguelova et al. (2013) re-sampled the whole data on the basis of the order collected, and then sorted the data to smooth the bumps in the resulting curve. Whilst this method is correct in principle, in that this is *one possible* outcome had smaller non-repeating samples been taken, it neglects all the other possible outcomes from resampling within the existing data, and consequently is unable to provide confidence intervals for them.

These non-repeating sub-samples taken from a larger population are called partial-permutations (Charalambides, 2002, p.42). The total number of partial permutations for a population can be denoted as ${}^{n}P_{k}$ where n is the 'population' size,

3 in this instance population mean is used to denote the mean of *all* samples that have been collected from the field and analysed – in this case 80.

and k the number of samples taken from it (Charalambides, 2002, p.42), and is calculated according to Equation 6.4.

$$^{n}P_{k} = \frac{n!}{k!(n-k)!} \tag{6.4}$$

n = population size.
k = sub-sample size.

Given Equation 6.4, for the case of $^{80}P_{40}$, i.e. 40 samples chosen from within a 'population' of 80 (the scenario likely to offer the most combinations: Figure 6.3), Vanguelova et al. (2013) present one partial-permutation from a possible 1.0751×10^{23}.

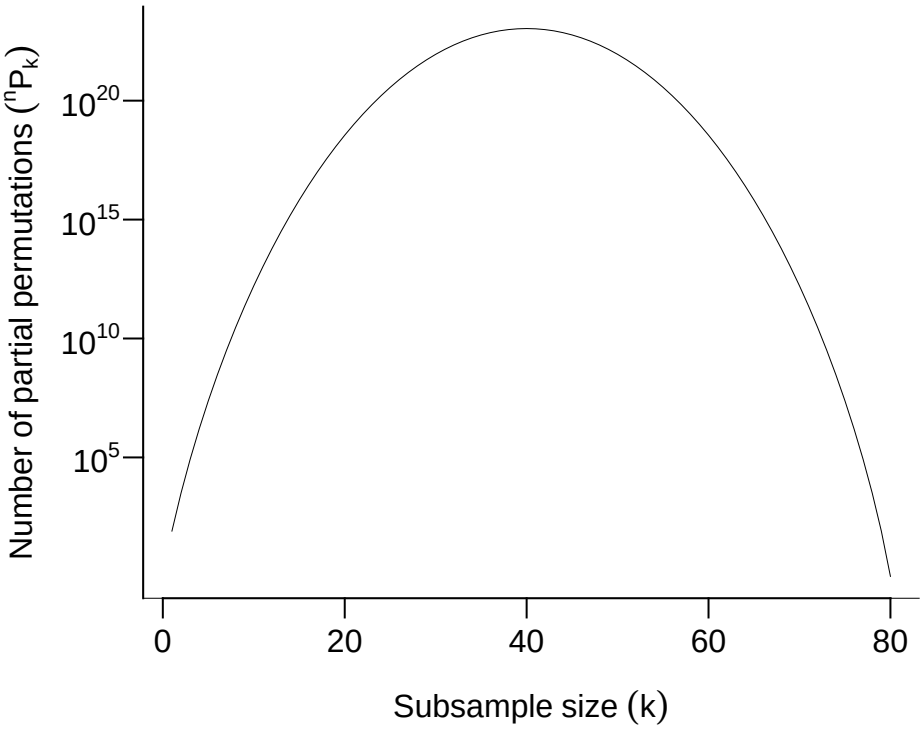

Figure 6.3: Number of possible partial-permutations of size 1:80 from a population of 80 samples ($^{80}P_{1:80}$). $^{n}P_{k}$ has been shown on a $\log_{10}$ y-axis for clarity. Untransformed, the distribution is more recogniseably normal.

With such a large number of potential sub-samples it would be computationally expensive to compute all the possibilities, and largely unnecessary. Sampling a large number of possibilities (usually $> 10\,000$) allows a normal distribution to develop, from which traditional descriptive statistics can be used to calculate confidence intervals. Note that $^{n}P_{k}$ will also follow a normal distribution (Figure 6.3), hence care must be taken that the descriptive statistics are not affected by the varying number of possible sub-samples.

The second way in which the approach taken in this chapter differs from Vanguelova et al. (2013) is by attempting to characterise the population of possible sub-sets of the original data by running a large number of resampling simulations.

6.3 METHODS

6.3.1 *Power analyses*

Power analyses were conducted based on SOC data from the Silsoe and Clapham Park study sites. The `power.t.test()` function within the `base` package of the statistical environment `R` (R Development Core Team, 2013) was used. Following Crawley (2007), α was set at 0.05, and β at 0.2. Tests were run for each cumulative depth increment, i.e.: 0-10, 0-20, 0-40, 0-60, 0-105, and 0-150 cm. Power tests were conducted on the difference between the cropped-silvoarable treatment and the traditional arable control, and the farm woodland treatment and the pasture control at the Silsoe and Clapham Park respectively.

Both the experiments were imbalanced, so a compromise was sought when conducting power analyses. To conduct a power analysis, the differences between two treatments and the standard deviation of those differences are required. This poses a problem when there are unequal numbers of samples taken between treatments. If one averages the samples to provide a more accurate estimate of the mean variation is inevitably reduced, hence it is necessary to reduce the sample size to that of the smallest treatment. In the case of the Silsoe silvoarable trial, this meant selecting just one sampling plot from each block for the cropped-silvoarable treatment[4], whilst at the Clapham Park, twenty out of the possible forty samples in the pasture (PA) treatment were randomly selected[5].

In the context of the experiments conducted at Silsoe and Clapham Park, a sampling plot refers to one point at which up to six samples at depths of 0-10, 10-20, 20-40, 40-60, 60-105, and 105-150 cm were taken. Hence 'paired' sampling plots means a minimum of two samples (in the case of 0-10 cm), from two treatments, at one depth, or a maximum of twelve samples (for 0-150 cm) from two treatments at six depths.

6.3.2 *Resampling simulations*

Resampling simulations were conducted only on the whole profile SOC stock from each sampling plot at the PA and farm woodland (FW) treatments from Clapham Park.

Custom software was written in the `R` statistical environment (R Development Core Team, 2013) to firstly generate a large number of possible partial-permutations[6], and then use these partial-permutations to subset the actual data collected at Clapham Park for all the possible sample sizes up to the maximum, and generate descriptive statistics on each sub-sample. This procedure was conducted for the PA and FW treatments.

4 Samples at a distance of 4.5 m were selected; i.e. close to middle of the cropped alleys.

5 In `R` parlance, `set.seed()` was set to 1337, and `sample()` used to select 20 values from 1:40, giving: 1, 3, 5, 6, 8, 10, 12, 14, 17, 22, 23, 24, 26, 27, 28, 29, 30, 32, 33, and 40.

6 The code for this software is available in a github repository: https://github.com/ivyleavedtoadflax.

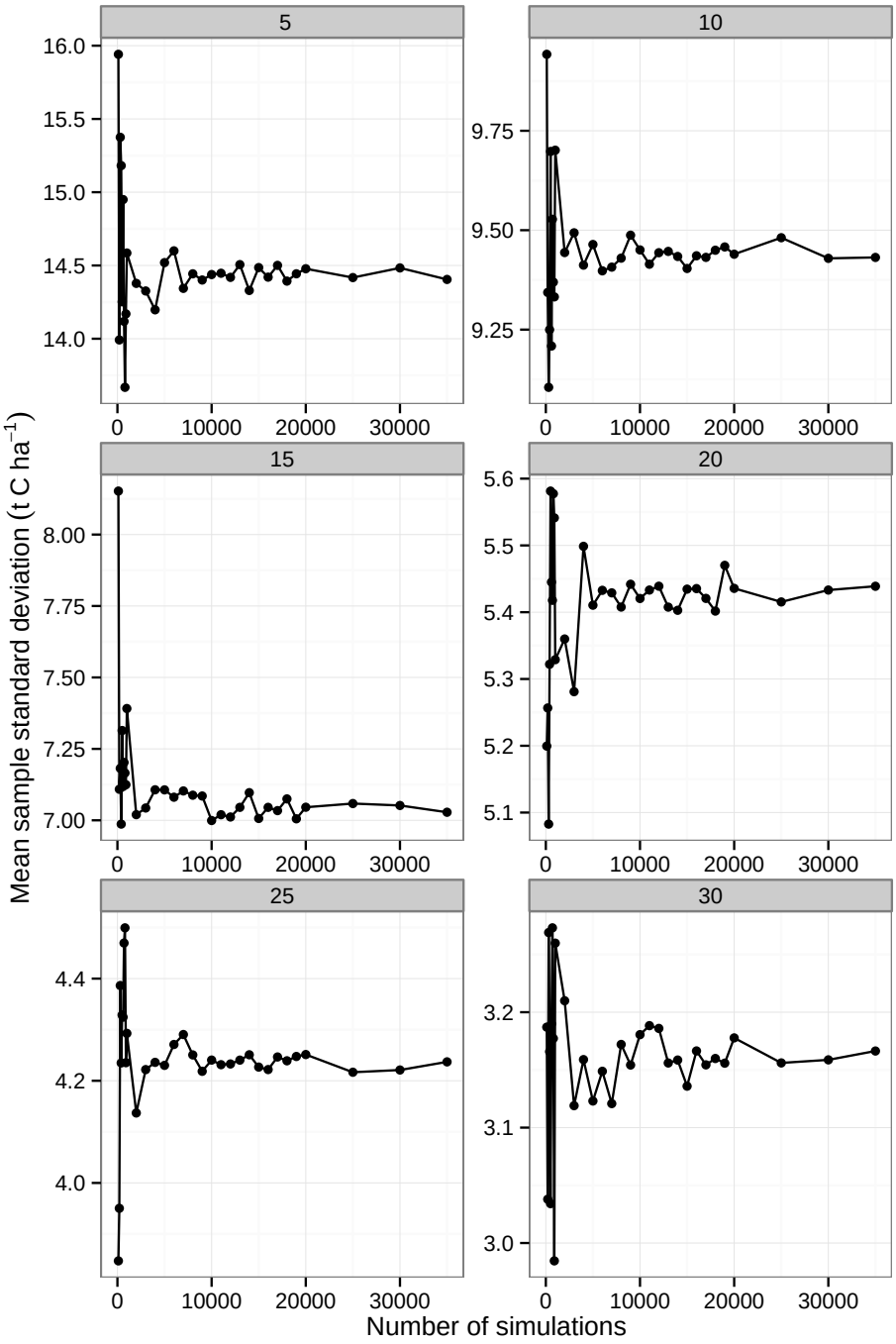

Figure 6.4: Variation in standard deviations of mean SOC (t C ha^{-1}) as a function of the number of Monte-carlo simulations run for subsets of 5, 10, 15, 20, 15, and 30 samples.

To determine whether a large enough number of simulations had been run, the software was executed multiple times with a varying number of iterations, and the effect on the mean sample standard deviation observed. Figure 6.4 indicates that upwards of a few thousand simulation runs, the majority of the amplitude of the fluctuations in mean standard deviations have settled, 20 000 simulations was established as a reasonable number of simulations to run.

6.4 RESULTS

6.4.1 *Power Analysis*

Power analyses based on cumulative depth increments for each site are presented in Figures 6.5 and 6.6. The values on which these plots were derived are included in Tables 6.2, in which 'Effect size' refers to the difference between mean carbon storage in the arable control and the cropped agroforestry treatment at Silsoe and the PA treatment and the FW treatment at Clapham Park.

Note that Figures 6.5 and 6.6 should be used with caution when attempting to make inferences about the experiments described in Chapters 4 and 5 as it was necessary to balance the sample sizes across treatments for the power analysis[7].

Power analyses indicate that to the maximum depth (150 cm), a larger number of samples would be required to detect even relatively modest changes in SOC following afforestation of pasture land. To detect a rate of change of 1 t C ha^{-1} $year^{-1}$ to 150 cm, which is considered to be a rapid rate of accumulation (Richter et al., 1999), would require greater than 100 paired samples based on analysis from Clapham Park, but around 20 paired samples based on the analysis from Silsoe (Figure 6.7). This is despite the fact that the magnitude of the effect detected was almost double at Clapham Park that of the Silsoe trial (Table 6.2).

This difference is a result of greater variation in the differences between the PA and FW treatment at the Clapham Park site. Note that because of the different sample size used in the power analyses, it is difficult to know whether the lower variation found at Silsoe is a true reflection of the actual variation, or an artifact of the sample size. However it is almost certain that the larger sample size at Clapham Park results in a more robust power analysis.

Results from power analysis at Silsoe for 0-40 cm are somewhat skewed by the 20-40 cm increment, where there were large differences of low variability between treatments (Figure 6.5).

7 This is explained in more detail in Section 6.3.1

Table 6.2: Differences between the cropped silvoarable treatment and the arable control for cumulative depths for the Silsoe silvoarable trial and the farm woodland (FW) treatment and the pasture (PA) control for Clapham Park. Values are expressed as actual difference (effect size) calculated on cumulative depth increments and standard deviation of the differences. Rate of SOC change is also given by dividing the effect size by the years since establishment (19 and 14 for Silsoe and Clapham Park respectively). At Silsoe differences are derived from just three paired sampling points: the control pits associated with each block, and one sampling point at the centre of the cropped silvoarable alleys for each block. At Clapham Park differences are derived from twenty paired sampling points: all the measurements from the FW treatment, and twenty chosen at random from the PA treatment.

Depth (cm)	Effect size (t C ha^{-1})	Std.Dev (t C ha^{-1})	Rate (t C ha^{-1} $year^{-1}$)
Arable minus silvoarable ($n = 3$)			
0-10	1.1	4.5	0.06
0-20	−0.6	8.9	−0.03
0-40	15.8	0.9	0.83
0-60	9.8	10.3	0.52
0-105	−3.2	23.6	−0.17
0-150	−6.6	30.1	−0.35
Pasture minus farm woodland ($n = 20$)			
0-10	−14.7	13.6	−1.05
0-20	−18.9	23.4	−1.35
0-40	−23.7	34.8	−1.69
0-60	−22.7	44.1	−1.62
0-105	−17.9	48.0	−1.28
0-150	−13.9	53.8	−0.99

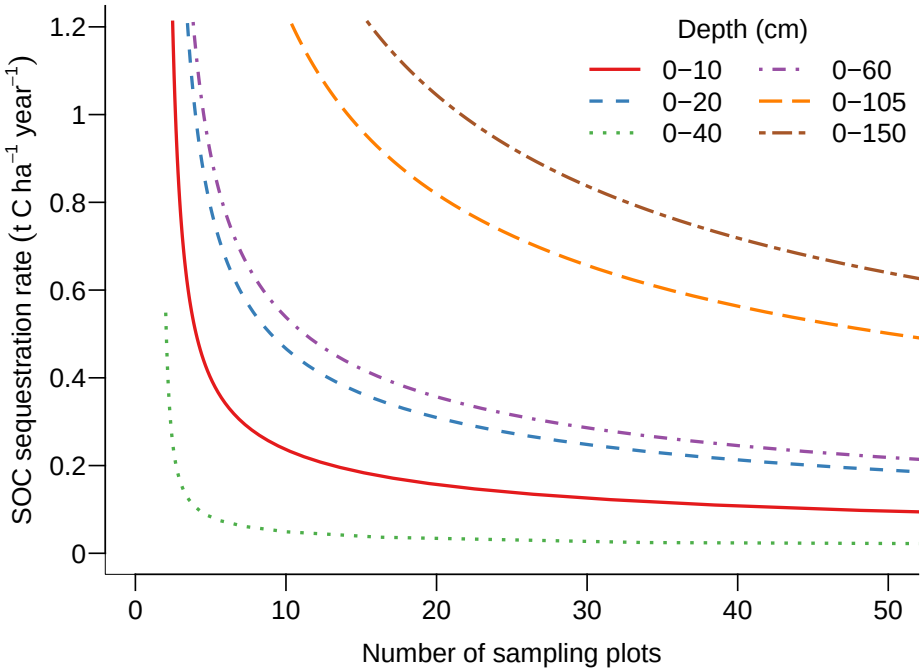

Figure 6.5: Number of paired sampling plots ($n = 12$ samples) required to detect a given rate of soil organic carbon (SOC) change (t C ha^{-1} year^{-1}) over cumulative depth increments after 19 years whilst maintaining a Type I error rate (α) of 0.05, and a Type II error rate of 0.2 (β). Curves based on data from the arable control and cropped silvoarable treatment from the Silsoe silvoarable trial. Based on 3 paired plots – see methods.

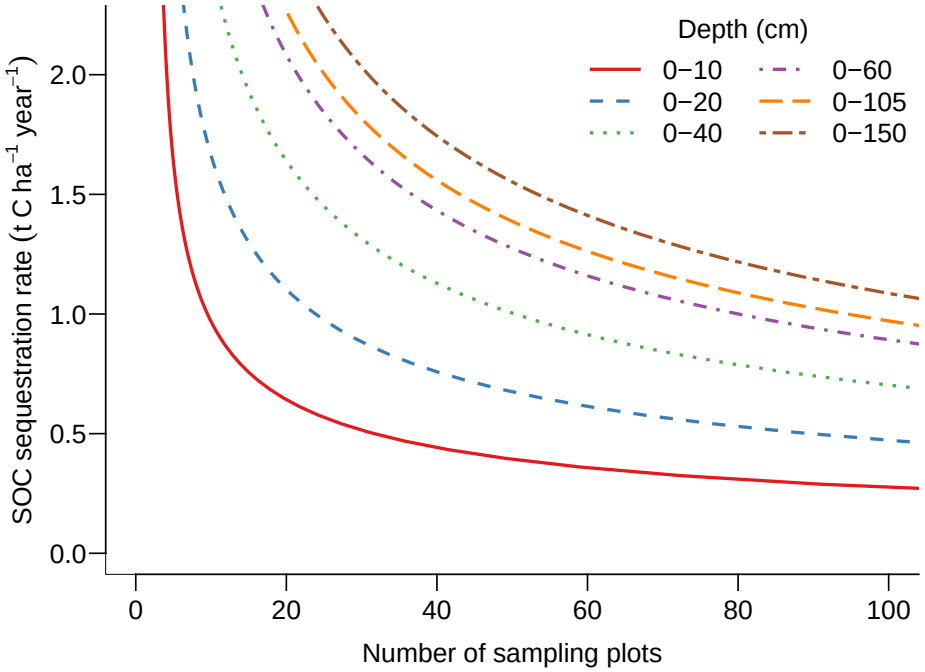

Figure 6.6: Number of paired sampling plots ($n = 12$ samples) required to detect a given rate of soil organic carbon (SOC) change (t C ha^{-1} year^{-1}) over cumulative depth (α) increments after 14 years maintaining a Type I error rate of 0.05 and a Type II error rate (β) of 0.2, based on the experimental data from the pasture (PA) and farm woodland (FW) treatments at Clapham Park. Based on 20 paired plots – see methods.

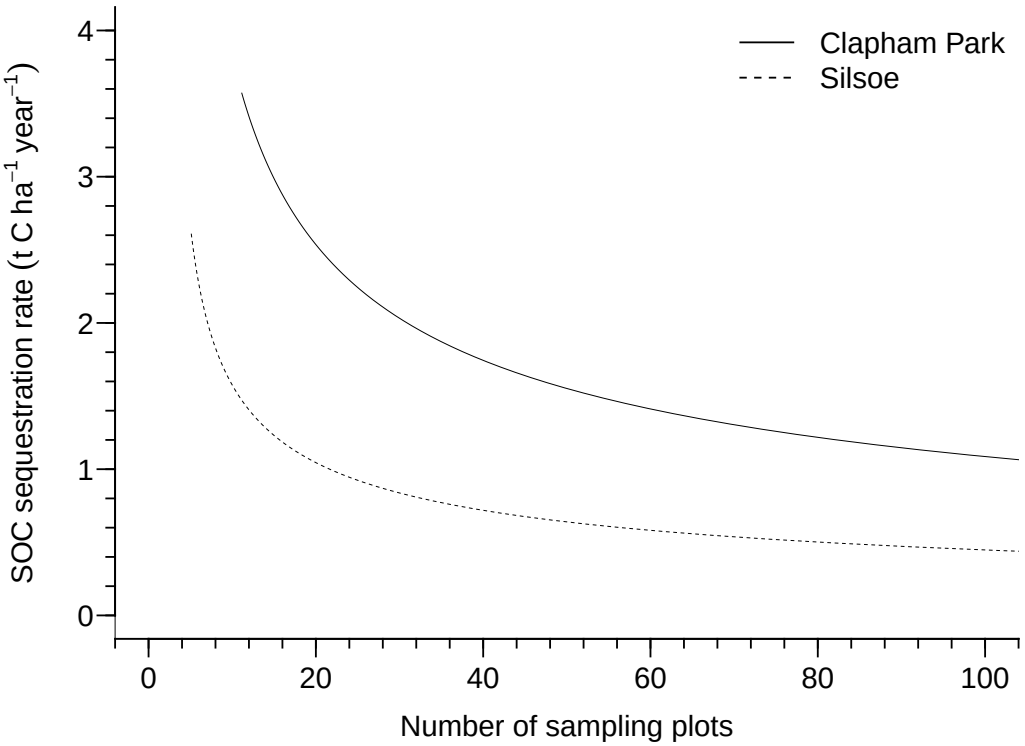

Figure 6.7: Number of paired sampling plots ($n = 12$ samples) required to detect a given SOC change (t C ha^{-1} year^{-1}) for 0-150 cm. The Clapham Park curve is based on 14 years of growth, while the Silsoe curve is based on 19 years.

6.4.2 *Resampling simulations*

6.4.2.1 *Sample size*

Outputs from the resampling simulations are displayed in Figure 6.8 and 6.9. These plots have been limited to between 4 and 36 sampling plots, and to between 4 and 13 ensure that 20 000 simulations are presented for each sample size. Clearly, the range of mean SOC values determined by simulations were much closer to the final mean as the number of plots sampled increased.

In the PA treatment with just just four sampling plots the 99% and 95% confidence intervals were 115-295 and 156-254 t C ha^{-1}. When the maximum number of sampling plots were used (36), the 99% and 95% confidence intervals dropped to 189-220 and 193-216 t C ha^{-1} (Figure 6.11).

In the FW treatment with just four sampling points, the 95% and 99% confidence intervals were 135-244 and 157-223 t C ha^{-1}. When the maximum amount of samples were taken into account (13), the 99% and 95% confidence intervals dropped to 166-213 and 173-206 t C ha^{-1} respectively.

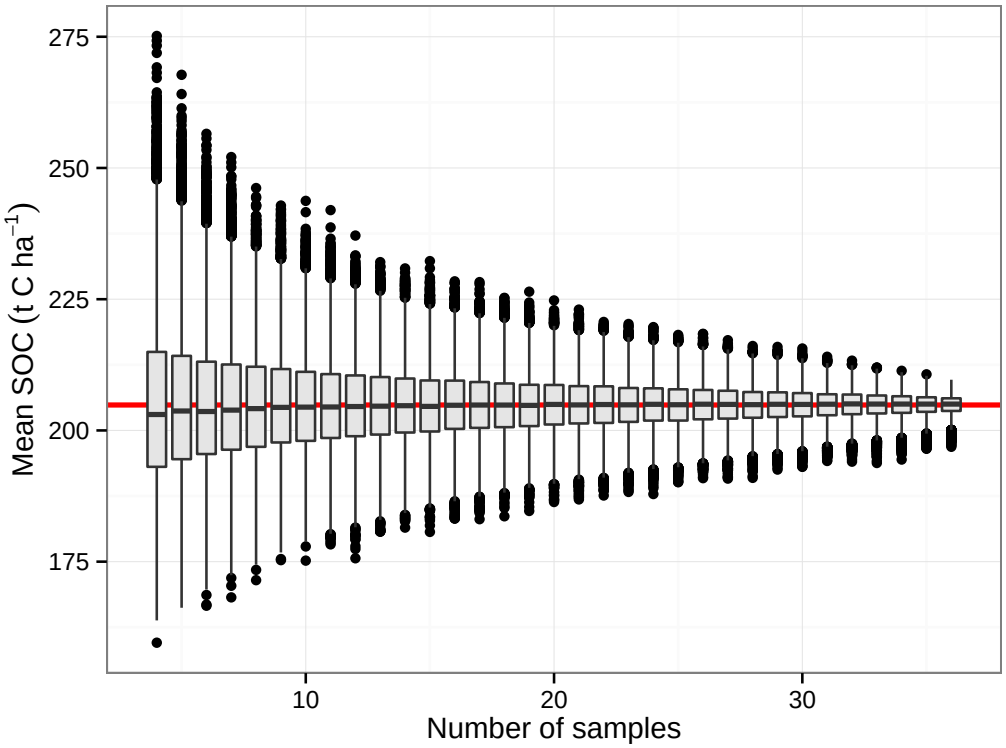

Figure 6.8: Results from 20 000 resampling simulations from 4 to 36 samples in the PA treatment. Each boxplot is based on the means from 20 000 simulations, with each mean being the result of a different subset of the original data. Red line shows the actual mean of all 40 samples (205 t C ha^{-1}, which is the best estimator of the final population mean.

Following Vanguelova et al. (2013) the CV was also plotted as a function of sample size (Figure 6.11). If the CV is calculated in the classical way as defined in Equation 6.3, CV in the PA treatment increases asymptotically with sample size,

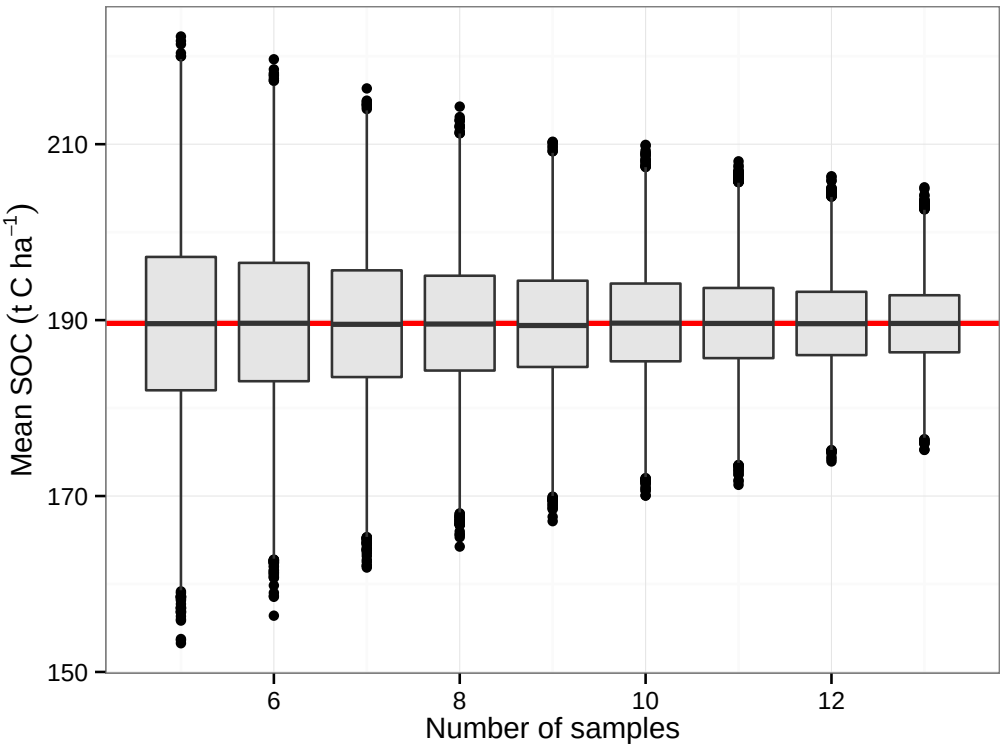

Figure 6.9: Results from 20 000 resampling simulations for the farm woodland (FW) treatment. Each boxplot is based on the mean from 20 000 simulations, with each mean being the result of a different subset of the original data. Red line shows the actual mean of all 20 samples (190 t C ha^{-1}, which is the best estimator of the final population mean.

beginning to plateau at around 15 samples, and a mean CV of about 0.16. For the FW treatment, CV has plateaued at about 10 samples, with a CV of about 0.14.

Using the same resampling methodology (Figure 6.12), it was possible to analyse the data for brown earths used by Vanguelova et al. (2013). This plot shows that the CV_v calculated from the data presented by Vanguelova et al. (2013) falls within one standard deviation of the mean of simulated values, but tends to over-estimate CV_v at lower sampling densities, and underestimate it at higher sampling densities. Notably Figure 6.12b indicates that the true CV stabilises at about 0.4 (40%), much higher than Vanguelova et al. (2013) indicate. Interestingly, Figure 6.12b also indicates that after about thirty samples, CV has stabilised, the same conclusions reached by Vanguelova et al. (2013), however the plateau is much easier to discern in Figure 6.12b than Figure 6.12a.

Figure 6.10: Mean SOC (t C ha^{-1}) as a function of number of sampling points for the pasture (PA) control and farm woodland (FW) treatment derived from 20 000 Monte-carlo simulations. Plots have been limited to those values for which 20 000 partial permutations were available. To smooth the mean line, a regression model were fit to the data derived from simulations, and the confidence intervals from the actual data added to the modelled means.

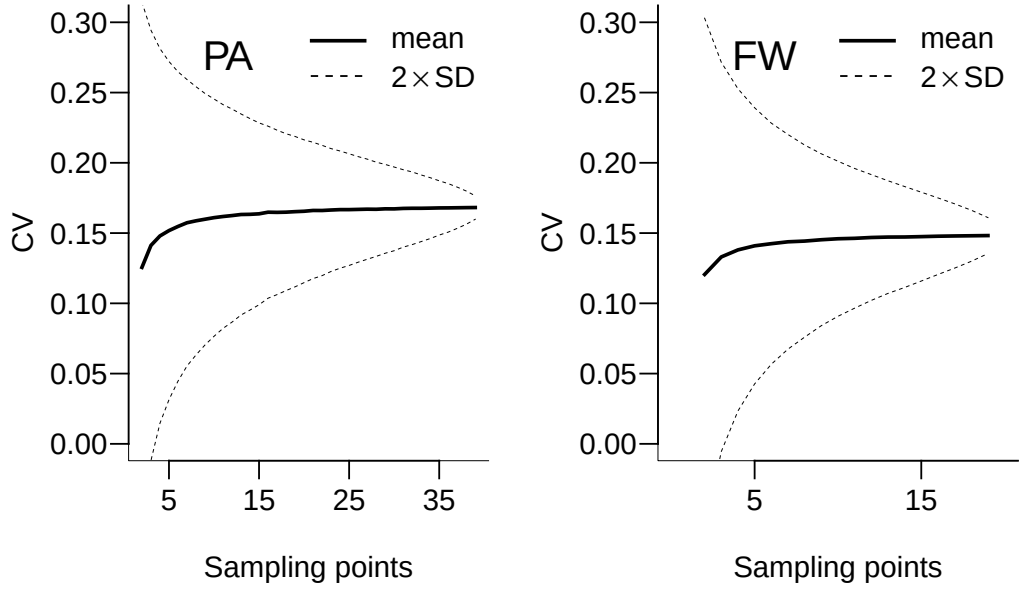

Figure 6.11: Mean coefficient of variation (CV) for the pasture (PA) control and farm woodland (FW) treatment at Clapham Park, based on 20 000 resampling simulations. Only sample sizes for which 20 000 partial permutations were possible have been included. Dashed lines show the means ±2 standard deviations.

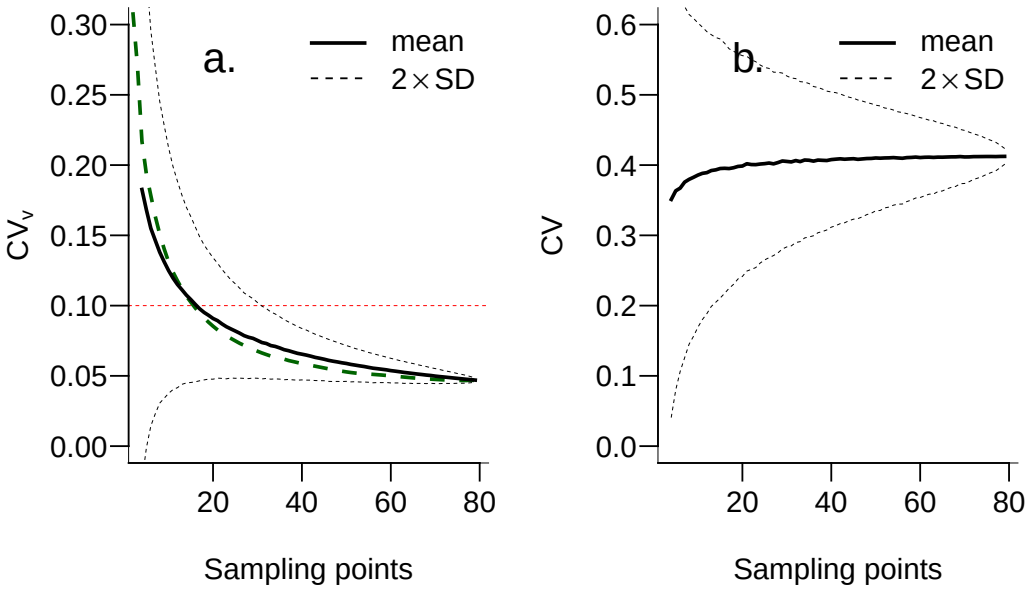

Figure 6.12: Repeat of Figure 2a from Vanguelova et al. (2013) using the brown earth data, based on 10 000 resampling simulations (a.). The actual curve estimated by Vanguelova et al. (2013) has been included as the dashed dark green line. The same data has been used (right) to show actual coefficient of variation (CV) as a function of sampling density. Red dashed line shows a coefficient of variation (as defined by Vanguelova) of 0.1 (10%).

6.5 DISCUSSION

6.5.0.2 *Power analysis*

If the results presented here can be generalised to other sites, power analysis indicates that large numbers of paired sampling plots are required in order to determine the differences between treatments where tree planting has taken place and unplanted controls.

The design of the sampling strategy conducted at the Clapham Park site was informed by power analyses completed from the results obtained at the Silsoe silvoarable site. On this basis, 40 paired plots (of 6 vs. 6 samples each plot) appeared to have been a sufficiently large sample size in order to detect significant differences between tree planting and the pasture control for the complete depth profile if it existed (Figure 6.5). The analysis suggests that an effect size of 1 t C ha^{-1} $year^{-1}$ should have been been detectable.

In actual fact, an effect size of 1.09 t C ha^{-1} $year^{-1}$ was detected over the whole depth profile between the FW treatment and the PA control[8]. Hence if the variation of the difference follows that assumed in the initial power analysis, then one can conclude that this analysis is robust, and conducted with a good level of power. However, the assumption of homogeneous variances between the two experiments does not hold particularly well, and in fact the standard deviation of the difference was somewhat greater at Clapham Park (45.5 t C ha^{-1} than had been predicted from the Silsoe data (30.1 t C ha^{-1}).

In addition, although 40 plots were sampled in the PA treatment, a matching 40 were taken across the two tree planted treatments: FW and silvopasture (SP). When the rate of change is averaged across these two treatments, the actual rate of change was 0.51 t C ha^{-1} $year^{-1}$, but the variation similar (45.7 t C ha^{-1}), indicating that 324 paired plots would be required to ensure an experimental power of 0.8 $(1 - \beta)$. This is an interesting observation, given that the rate of change of SOC detected was so high, in fact double that suggested by Morison et al. (2012), despite the fact that the sampling depth is greater than many studies report. In terms of percentage change however, the values determined at the Clapham Park study fall within the 95% confidence intervals reported by Guo and Gifford (2002) for afforestation studies sampling $>$ 100 cm in depth.

Whilst variation in the level of SOC at Silsoe may have been homogenised by ploughing over many years (the site has been under arable agriculture since the 1880s), it is also evident that a larger sampling effort at Clapham Park resulted in more variation being captured, but little change in the mean. As with CV, standard deviation (SD) initially increases with continued sampling until it reaches a plateau (Figure 6.11), which is a contributing factor in why the power analysis at Clapham Park in particular indicates that so much sampling is required: greater sampling effort at least initially increases the SD, but has almost no impact on the effect size.

8 Note that this is not the same value that is quoted in Table 6.2 because it is based on the difference between all 40 plots taken from the PA treatment, and 20 from the FW, whereas values quoted in the table are based on just 20 from each treatment. This was a necessary step in order to accurately calculate the variance of the difference between the two treatments, which is required for the power analysis.

6.5.0.3 *Resampling simulations*

Results from the resampling analysis at Clapham Park indicate that after about 15 and 10 sampling plots, the confidence intervals are relatively settled for the PA control and the FW treatment respectively (Figure 6.10). This observation is echoed in the plots of CV (Figure 6.11) which indicate that by approximately 10-15 samples no major changes are detected in the mean CV. For the plots of the brown earth data, reproduced from Vanguelova et al. (2013), around 30 plots is sufficient to capture the bulk of the variation, however true CV stabilises at about 40%, and does not drop below 10% as Vanguelova et al. (2013) suggest.

It is notable that at Clapham Park the PA control is more variable than the FW treatment from the start, independent of sample size. The reasons for this are not clear, but may have to do with a more varied deposition of grass root litter. Future geospatial analysis may elucidate this observation further.

Note that these resampling simulations only give a sense of how many sampling plots would be required in order to adequately capture the bulk of the variation at a site. They are not a replacement for proper power analysis when comparing two treatments or a chronosequence of measurements from a single site, since they do not of themselves reveal anything about β.

6.5.0.4 *Recommendations for sampling*

Taking the example of afforestation on a former pasture, as at Clapham Park, power analyses indicate that to test for changes in the SOC stock to a depth of 150 cm with confidence, 118 paired sampling points would be required assuming a rate of change of SOC of at least 1 t C ha^{-1} $year^{-1}$ (over 14 years). This equates to 1416 individual samples for organic carbon content (C_o%) analysis, equating to about £5000 just for the materials relating to C_o% quantification by dry combustion. This does not include the cost of technician labour, nor the time and wages required for the collection of samples. As a point of comparison, it took over 8 weeks for one worker to collect all the C_o% and soil bulk density required for the Clapham Park analysis (40 paired sampling plots). Hence, it would be a considerable investment of time, labour, and money to quantify SOC changes to a satisfactory level of statistical robustness.

However, it is extremely important that some assessment of SOC is made when one considers that at Clapham Park as much as 30% of the aboveground carbon stored in the FW treatment may have been lost as a result of changes in SOC stock in the top 10 cm alone – and although analysis of the full depth profile indicates no change, power analysis conducted in this chapter indicate that there was probably not sufficient experimental power to adequately conclude that there was no effect.

The resampling study conducted in this chapter indicates that to calculate a robust baseline of SOC in a pasture before afforestation, would require around 15 sampling plots (of 6 individual samples each) to ensure that the bulk of the variation had been adequately captured. This would still require a significant investment of time and non-trivial cost, with no guarantee that once compared to a later SOC measurement (after afforestation) that the analysis would be sufficiently powerful to be statistically robust. Sampling 10-15 plots can however be consid-

ered an absolute minimum, failing to do this many samples will almost certainly mean that variation at the site is being underestimated.

The challenge of insufficient statistical power in studies of soil carbon has been noted before by Hungate et al. (1995) and Kravchenko and Robertson (2011). Hungate et al. (1995) conclude that it is a significant methodological issue when quantifying SOC stocks, and that more powerful techniques, or longer experiments in which a greater effect size can develop, are necessary if we are to adequately quantify SOC.

Kravchenko and Robertson (2011) conclude that researchers should complete (*a-priori*) power analyses and quote the related power, and probably should not rely on conducting hypothesis testing on carbon stocks over the whole depth profile. Instead researchers should conduct hypothesis tests on individual depth increments, and quote the change over the whole profile based only on those depth increments at which statistically significant differences had been detected. By adopting this methodology, a smaller total number of samples could be analysed, because the test will not rely on a very small power likely to result from high variances across a whole depth profile, and instead will rely on smaller variances across individual depth profiles. Of course, the required number of samples would still need to be determined in advance by power analysis. Sample sizes thus may vary according to the effect sizes, variability, and depth of the chosen increments, and would ideally therefore be informed by a suitable pilot study.

Using Kravchenko and Robertson's suggestions for data collected at Clapham Park would mean that only differences in the top 0-10 cm layer would contribute to the whole profile change in SOC between the PA and the FW treatments; this would equate to a loss of 13.4 t C ha^{-1}(Chapter 5, Table 5.3).

6.6 CONCLUSIONS

Quantifying SOC changes in recently afforested woodlands, is a significant challenge. The slowness and expense of current methods is a major bottleneck in the measuring of SOC for accounting schemes like the Woodland Carbon Code. If a chronosequence of sampling is planned (one sampling being conducted before afforestation, and further sampling after afforestation) it would be advisable to wait as long as possible before attempting to conduct a second round of sampling, so that the effect size may be sufficiently large as to be detectable with an acceptable level of experimental power, thereby reducing the likelihood of Type II errors.

At the very least, when establishing a baseline, sufficient sampling should be completed to capture the bulk of the variation. Failing to do so risks an increased chance of committing Type I errors, and erroneously rejecting the null hypothesis.

Cheaper solutions, which allow much more sampling to be conducted at a lower cost, for example updated weight loss on ignition (LOI) methods (Cambardella et al., 2000; Wang et al., 2012), may provide a solution, if reports of efficacy can be substantiated and replicated. Even so, it is likely that LOI methods, whilst cheaper and quicker, will not have the accuracy of dry combustion; and given that considerable uncertainty can remain even when using this more accurate method, LOI may not be solution.

Aside from the $C_o\%$ analysis itself, the extraction of samples from deep horizons with associated undisturbed cores for soil bulk density (ρ_b) analysis, was one of the most time consuming, and physically laborious aspects of all the fieldwork reported in this thesis, and hence is also likely to be a considerable expense. Since ρ_b measurements are essential to calculating SOC stock, finding a cost effective solution to this problem should also be a priority. That said, the equivalent soil mass methodology (Ellert and Bettany, 1995) significantly reduces the impact of errors in ρ_b measurements. Work at Clapham Park (Chapter 5) indicated that using an auger to extract ρ_b measurements under-estimated the true values by on average 13%, however, when SOC stock was calculated on an equivalent soil mass basis, increasing ρ_b values by 13% made no appreciable difference to SOC stock.

Finally, the recommendations of Kravchenko and Robertson (2011) of focusing on the differences between incremental depth only should be evaluated as a possible method for minimising the problems associated with low experimental power in SOC studies.

6.7 SUMMARY OF FINDINGS

In the context of this thesis, this chapter attempts ot falsify the following thesis.

Hypothesis

8. Frequentist hypothesis testing is an appropriate tool to determine differences in SOC in newly planted woodlands.

Given the evidence presented in this chapter, traditional hypothesis testing does not emerge as an appropriate tool for assesing differences in SOC between newly planted and unplanted treatments.

Full profile sampling of soil organic carbon stock is complicated by the inherent variability of soil. Although sampling more deeply, and more intensively in a given area both increase variability, the mean soil organic carbon stock changes much more slowly, leading to an increased coefficient of variation. Without first quantifying the power of a hypothesis test which subsequently results in a non-significant result, it is difficult to judge whether there truly was no effect, or there simply was not enough replication.

Power analyses based on results obtained at Silsoe and Clapham Park indicate that for an expected rate of soil organic carbon stock change of 1.0 t C ha^{-1} (over 19 and 14 years respectively), which would be considered a very rapid rate of accumulation for the complete 1.5 m depth profile, 20 and 130 paired plots (6 vs. 6 samples for each plot) would be required to meet the statistical assumptions of $\alpha = 0.05$ and $\beta = 0.20$. Therefore, the experiments conducted in Chapter 4 and 5 most likely did not have sufficient power to satisfactorily conclude that there was truly no effect across the whole depth profile: not enough replication was completed.

For Clapham Park, which best represents the situation encountered in the Woodland Carbon Code – mixed broadleaf woodland planted at 2.5 m spacing on former agricultural land – obtaining an acceptable experimental power may be prohibitively expensive using these methods.

Based on resampling methods, around 15 sampling plots (comprising 6 samples at each plot) were required to adequately capture the variation within a 14 ha grassland site prior to planting. Around 10 plots were required to adequately characterise a farm woodland planted at the same site. These values should be considered the absolute minimum sample size.

Part III

BIOMASS MEASUREMENTS

A nation that destroys its soils destroys itself.
Forests are the lungs of our land, purifying the air
and giving fresh strength to our people.

— Franklin D. Roosevelt (1882 - 1945)

7

POPLAR GROWTH PATTERN

In this chapter new and historical measurements from the Silsoe silvoarable experiment are presented in comparison to Forestry Commission yield tables. Biomass and C content of above and belowground biomass is determined by destructive harvest.

7.1 OBJECTIVES

This chapter aims to address the following hypothesis:

Hypothesis

6. Using traditional forestry yield tables to predict the growth of trees in agroforestry systems and farm woodlands (which are typically planted at much wider spacings) will over-estimate yield.

7.2 INTRODUCTION

Introducing trees into agricultural landscapes is recognised as one method of enhancing the C density of agricultural land (IPCC, 2000*a*; Montagnini and Nair, 2004). The accumulation of C in above and belowground woody biomass is one of the ways in which trees can enhance C sequestration. Quantifying the size of this biomass C pool is therefore important to understanding the contribution agroforestry can make to mitigating anthropogenic greenhouse gas emissions.

In traditional forestry plantations trees tend to be planted at high density with the expectation that a proportion of the trees will be harvested (thinned) on several occasions before the final density is reached (Savill et al., 1997). It is conceivable therefore that trees may be planted at an initial density of 10 000 trees ha^{-1} but less than 5% of that number survive to maturity. This can be considered the extreme end of a spectrum, the opposite of which is open grown trees with no competition from neighbouring trees.

In agroforestry systems where the growth of an arable crop or pasture beneath the trees is as important as the growth of the trees (if not more so), trees are planted at or closer to the final densities and are therefore much closer to the open grown end of the spectrum. Agroforestry systems may have initial planting densities as low as 100–400 trees ha^{-1} (Burgess et al., 2004; Sibbald et al., 2001). This is largely to reduce the impact of competition between trees and the other components of the system, be they arable or pastoral. Furthermore, intensive forestry systems have high labour requirements that may not be appropriate for trees planted on farms.

In order to predict the final yield of trees from earlier measurements, foresters often use 'yield tables' and allometric relationships constructed from forestry models (Hamilton, 1996). Yield tables typically classify trees into a number of 'yield classes' relating to the maximum expected rate of volume accretion measured in $m^3\ ha^{-1}\ year^{-1}$. Allometric equations on the other hand allow proxy measurements (usually diameter and height) to be taken and used to predict other measurements like volume or biomass. Since these models are typically established for traditional forestry plantations, there is some uncertainty over whether such models are be appropriate for agroforestry systems in which trees are planted at much lower densities (Hein and Spiecker, 2008), and often subject to other management interventions like annual cultivation.

The Silsoe silvoarable trial was set up as part of a Ministry of Agriculture, Fisheries and Food (MAFF) sponsored trial in 1992, and incorporates annual cropping with hybrid poplar (see Chapter 3). The trial, which has been measured on a nearly annual basis since establishment presents a rare opportunity to assess the growth of mature trees in a silvoarable system. In this chapter, new and historical measurements from the silvoarable trial are combined and used to assess the quality of fit to Forestry Commission yield tables, and growth predictions made earlier in the life of the trees. A subset of the trees were destructively sampled in order to quantify the amount of C contained in biomass above and belowground. Results from these analyses are included here, and are later used to parameterise the Yield-SAFE model (Chapter 8).

7.3 METHODS

The silvoarable site at Silsoe is described in Chapter 3. In addition to the measurements made in 2011, measurements were available from between 1992 to 2006

7.3.1 *Tree mensuration*

7.3.1.1 *Diameter at breast height*

Measurements of diameter were made using a standard diameter at breast height (D_{bh}) tape in late May 2011. A stick was cut at a length of 1.3 m which was then used to quickly determine the correct height for measurement. Where an accurate measurement was complicated by epicormic or a significant stem deformity, two measurements were made, one above and one below the deformation. These were later averaged to give an approximate diameter. Measurements were taken to the nearest millimetre.

7.3.1.2 *Height measurements*

Measurements of tree height were taken with a Carl Leiss hypsometer[1]. Two measurements were taken for each tree to the nearest cm, from a variable distance (at least 25 m) depending on visibility.

1 Carl Leiss GmbH, Berlin, Germany

7.3.1.3 *Volume of standing timber*

In addition to destructive sampling, the volume of standing timber was calculating following conventional forestry practices, outlined by Hamilton (1996). Stand basal area (BA; $m^2\,ha^{-1}$) was calculated using Equation 7.1.

where D_{bh} = stand mean diameter at breast height (cm), and n = tree density (n ha^{-1}).

$$BA = (\frac{D_{bh}}{2})^2 \pi n \times \ 0.01 m^2\,cm^{-2} \tag{7.1}$$

D_{bh} =stand mean diameter at breast height (cm).
n =tree density (trees ha^{-1}).

Stand volume is the product of stand basal area and form height (height adjusted to take account of stem taper). Form height (FH; m) is usually derived from species specific data as in Hamilton (1996). To improve the accuracy of form height measurements (which would usually be derived from a table and therefore subject to minor inaccuracies), a non-linear polynomial function was fitted to the data presented by Hamilton (Figure 7.1), allowing form height to be calculated with the equation derived from the fit. Stand volume can thus be derived from Equations 7.2 and 7.3.

$$FH = -\alpha h^2 + \beta h - \gamma \tag{7.2}$$

h = height (m).
α = 0.0053.
β = 0.5494.
γ = 1.4589 m.

$$V = BA \cdot FH) \tag{7.3}$$

BA = stand mean basal area (ha^{-1}).

7.3.2 *Aboveground fresh mass*

7.3.2.1 *Trees*

Six sample trees were felled on 4 July 2011. Stems were sectioned into six lengths and branches were trimmed flush with the stem and grouped into bundles.

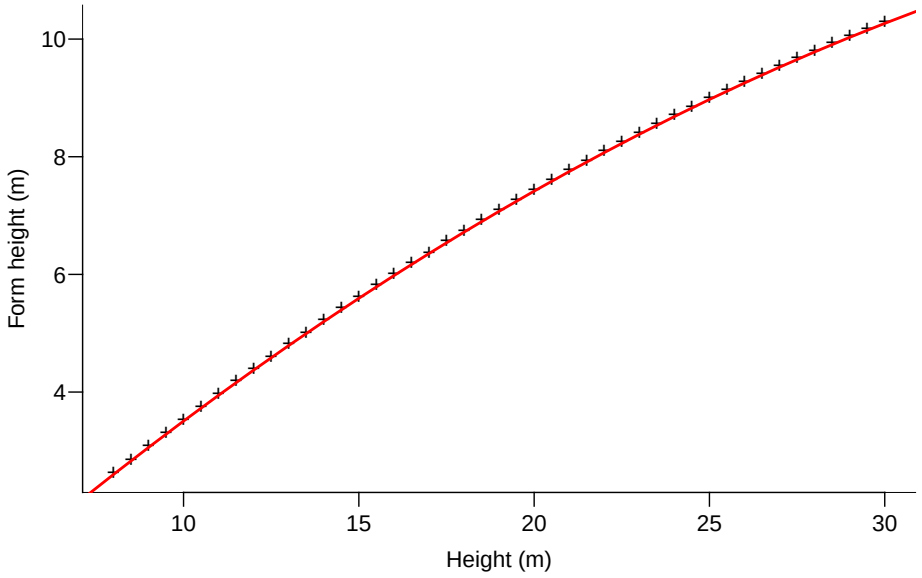

Figure 7.1: Relationship between poplar form height and height, extrapolated from tables in Hamilton (1996). Line follows the equation $-\alpha h^2 + \beta h - \gamma$, where α, β, and γ are constants, and h = top height, $R_s = 1$

Figure 7.2: Weighing a stem section with the telescopic loader. Inset shows a close-up of the load cell.

Each section of stem and branch bundle was weighed (to the nearest kg) with a calibrated load cell suspended from a telescopic loader (Figure 7.2) to obtain fresh mass (M). Weighing was completed within two hours of felling.

All the leaves from one of the sample trees were removed and weighed on a large electronic balance to the nearest 0.1 kg. Estimates of leaf mass were calculated for the other trees by multiplying branch mass by the proportion of branch mass to leaf mass found in the complete leaf sample (0.1198). This mass was then subtracted from the branch mass values.

7.3.3 *Understory vegetation*

In order to quantify the mass of vegetation beneath the canopy and in the arable control, 16 square metre samples of vegetation were taken in July 2011. From each sample tree, two samples were taken, one at 3.2 m to the north along the tree row, and one at 5 m into the adjacent alley. One further sample was taken within 2 m of each control plot.

7.3.4 *Rootball mass*

A one metre cube monolith was created around each of the rootballs, which was then removed by mechanical digger. The bulk of soil attached to the rootball was removed with the mechanical digger, and the remainder cleaned by hand. Rootballs were trimmed to a depth of 45 cm and to a radius of 50 cm around the stem before weighing to the nearest kg (Figure 7.3).

(a) A mechanical digger was used to excavate root monoliths.

(b) Excavated rootballs were cleaned of soil, and trimmed to a cylinder of 0.45 m depth with a radius of 0.5 m.

Figure 7.3: Photos taken during the removal of the rootball of tree 3CB4, Silsoe agroforestry trial, July 2011.

Due to time constraints, it was not possible to get accurate measurements from rootballs in block 1. Rootball weight for trees in block 1 were thus calculated using the average proportion of total aboveground mass to rootball mass (0.1) calculated from the four other trees.

Because it was some time between the extraction of the root balls and the final weighing, a correction was applied to account for moisture loss. This was calculated by reweighing the stem sections of one of the sample trees, and calculating the moisture lost over the same period (4%).

It was not possible to weigh the mass of the rootball between depths of 45–90 and 90–135 cm. Coarse root mass densities recorded in the tree row at 2 m during coarse root mass sampling were used to estimate the mass of roots beneath the rootball.

7.3.5 *Coarse and fine root mass*

7.3.5.1 *Coarse root sampling*

Coarse root sampling was completed according to the schematic in Figure 7.4. The digger back-actor bucket was used to take nine samples from each of the sample trees. Samples were taken at 2 and 4 m into the alley adjacent to the root trench, and at 2 m along the tree row to the north. At each sampling point, soil was removed at depths 0–45 cm, 45–90 cm and 90–135 cm.

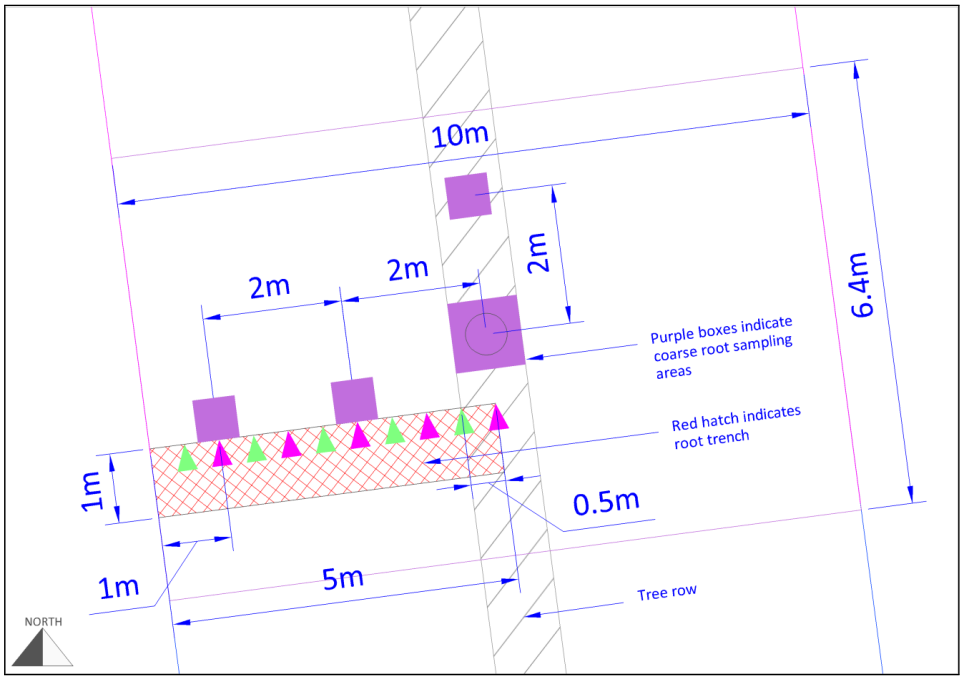

Figure 7.4: Schematic diagram showing the position of sampling points used in various parts of the study. Purple blocks indicate position from which coarse root samples were taken at depths of 0–45 cm, 45–90 cm, and 90–135 cm.

Each sample of 0.4 m^3 was then sub-sampled with a large plastic ring of volume 0.04 m^3. Each sample was then sorted by hand, and all coarse roots (< 2 mm diameter) within the subsample removed. These samples were then washed of soil and dried at 105°C for 18 hours. Samples were then weighed to the nearest 0.01 g.

Within each treatment, the mean coarse root mass density (MD) from the tree row was used to estimate the rootball mass at the appropriate depths.

7.3.5.2 *Coarse root model*

To extrapolate total coarse root mass from the coarse root mass data, a simple model was devised based on three assumptions.

- The roots of a tree within the agroforestry block can be determined by measuring the roots within a 6.4 × 10 m area centred upon the tree; it was assumed that roots which extended further than this area, were likely to be countered by root growth into this area by surrounding trees - tessellation.
- The rooting density of the tree declines with increased distance from the tree, and this decline can be modelled with an exponential function.
- The decline in root mass with increased distance from the tree varies with depth.

A full description of the model is included in Appendix C.1.

7.3.6 *Dry mass*

Stem, branch, leaf, root and bark samples from each of the sample trees were removed to the laboratory, weighed and dried in an oven at 105°C for 18 hours. Samples were then reweighed to determine moisture content (mc) on a fresh weight basis using Equation 7.4.

$$mc = \frac{(M_f - M_o)}{M_f} \tag{7.4}$$

M_f = fresh mass of sample in grams.
M_o = mass of sample in grams after drying in an oven at 105°C.

Moisture content values for each biomass component were then averaged and used to determine dry mass (M_e) of the corresponding component at the tree level, using Equation 7.5.

$$M_e = (1 - mc) \times M_f \tag{7.5}$$

M_e = the estimated oven dry sample mass.
M_f = fresh mass of sample in grams.
mc = ash wood moisture content, calculated using Equation 7.4.

For understorey vegetation, the complete sample was dried at 105°C before weighing.

7.3.6.1 *Bark mass*

The proportion of bark in each of the components of the tree biomass was estimated by regressing the bark mass against the total mass of each of the samples taken for dry mass measurements. Using the formulae derived from these regressions (Equation 7.6), the mass of bark for each tree component could be calculated and subtracted from the total (Equation 7.7).

$$M_b = \alpha + \beta \cdot M_t \tag{7.6}$$

M_b = estimated bark fresh mass.
M_t = total measured fresh mass.

$$M_w = M_t - M_b \tag{7.7}$$

M_w = fresh (under bark) wood mass.

This calculation was completed on M prior to conversion to M_e; M_e and C content of the bark of each component was thus calculated separately.

7.3.7 *Total organic carbon*

The proportional carbon content (C%) within each tree component and of understorey vegetation was determined using a Vario EL III Elemental Analyser. The dried samples were ground to a particle size <0.5 mm with a flail grinder. A small amount of this sample was then weighed and packed inside a small foil envelope before oxidation at very high temperature in the elemental analyser. Laboratory standard operating procedures (Appendix: A.5) were followed throughout.

7.3.8 *Final carbon content*

Final C content for stems, branches, leaves and rootballs were calculated by multiplication of M_e of each component with the appropriate C% as determined by elemental analysis. This value was then multiplied by the tree density to provide values of C content per hectare.

Measurements of crop yield from 1993 to 2003 were also used to calculate how much C had been removed from the site in those years. A C content of 50% was assumed for the crop.

7.4 RESULTS

7.4.1 *Tree mensuration*

7.4.1.1 *Diameter at breast height*

Analysis of variance indicated that there were highly significant variations in D_{bh} in 2011 across the four hybrids ($p < 0.001$) and the three cropping treatments ($p < 0.001$); no significant interactions were found (Table 7.1).

Table 7.1: Results from ANOVA of diameter at breast height (D_{bh}), height and volume for poplar tree measurements taken in 2006 and 2011 at the Silsoe agroforestry trial. Degrees of freedom and F-values are given with significance denoted by stars: $p <= 0.001$ (***), $p <= 0.01$ (**), $p <= 0.05$ (*).

Term/Interaction	DBH		Height		Volume	
2006	df	F-value	df	F-value	df	F-value
Block	2		2		2	
Crop	2	44.30***	2	12.68***	2	37.75***
Hybrid	3	110.71***	3	173.80***	3	167.78***
Row	4	0.32^{ns}	4	1.46^{ns}	4	0.48^{ns}
Crop × Hybrid	6	0.63^{ns}	6	0.41^{ns}	6	0.66^{ns}
Crop × Row	8	1.51^{ns}	8	1.00^{ns}	8	1.79^{ns}
Hybrid × Row	12	0.93^{ns}	12	0.62^{ns}	12	0.62^{ns}
Residuals	142		142		142	
2011	df	F-value	df	F-value	df	F-value
Block	2		2		2	
Crop	2	11.41***	2	11.76***	2	11.84***
Hybrid	3	107.16***	3	109.90***	3	144.02***
Row	4	0.42^{ns}	4	2.69*	4	1.06^{ns}
Crop × Hybrid	6	0.64^{ns}	6	1.70^{ns}	6	0.72^{ns}
Crop × Row	8	1.65^{ns}	8	0.69^{ns}	8	1.43^{ns}
Hybrid × Row	12	0.99^{ns}	12	0.61^{ns}	12	0.71^{ns}
Residuals	142		142		142	

Post-hoc analysis indicated that in 2011 there were significant differences between each hybrid. In both 2006 (the last year D_{bh} measurements were made) and in 2011, the Beaupré hybrid showed significantly greater D_{bh} than all the other hybrids (Figure 7.5).

In both 2006 and 2011, the fallow treatment showed the greatest mean D_{bh}, which was significantly greater than either the alternately cropped or the continuously cropped treatment. Although the difference in D_{bh} in the alternate and continuously cropped treatment had narrowed in 2011 since 2006, there continued to be significant differences in D_{bh} between all three treatments, as in 2006 (Figure 7.6).

Table 7.2: Multiple comparison test results for poplar diameter at breast height (D_{bh}), height, and volume for 2006 (Means ± SE). Different superscript letters indicated significant differences.

Term	Group	DBH (cm)	Height (m)	Volume ($m^3\,ha^{-1}$)
Crop ($n = 60$)				
	Fallow	$29.2^a \pm 3.1$	$19.4^a \pm 2.2$	$77.3^a \pm 23.9$
	Alternate	$27.7^b \pm 2.7$	$19.1^a \pm 2.1$	$68.3^b \pm 20.3$
	Continuous	$26.3^c \pm 3.0$	$18.4^b \pm 2.5$	$60.1^c \pm 20.8$
Hybrid ($n = 45$)				
	Beaupré	$31.5^a \pm 2.3$	$21.9^a \pm 1.0$	$98.3^a \pm 16.3$
	Trichobel	$27.4^b \pm 2.6$	$18.6^b \pm 1.7$	$65.1^b \pm 16.5$
	Robusta	$26.8^b \pm 1.9$	$18.7^b \pm 0.8$	$62.0^b \pm 10.4$
	Gibecq	$25.2^c \pm 2.0$	$16.6^c \pm 1.5$	$48.9^c \pm 10.5$

Table 7.3: Multiple comparison test results for poplar diameter at breast height (D_{bh}), height, and volume for 2011 (Means ± SE). Different superscript letters indicated significant differences.

Term	Group	DBH (cm)	Height (m)	Volume ($m^3\,ha^{-1}$)
Crop ($n = 60$)				
	Fallow	$34.2^a \pm 3.4$	$22.5^a \pm 2.6$	$120.4^a \pm 33.6$
	Alternate	$33.3^b \pm 3.1$	$23.0^a \pm 2.6$	$115.4^a \pm 30.3$
	Continuous	$32.5^c \pm 3.4$	$21.6^b \pm 3.0$	$105.5^b \pm 32.2$
Hybrid ($n = 45$)				
	Beaupré	$36.9^a \pm 2.2$	$25.1^a \pm 1.0$	$150.7^a \pm 19.6$
	Trichobel	$34.3^b \pm 2.6$	$23.2^b \pm 2.4$	$123.1^b \pm 25.5$
	Robusta	$32.1^c \pm 1.8$	$22.0^c \pm 1.2$	$102.1^c \pm 13.1$
	Gibecq	$30.0^d \pm 1.8$	$19.2^d \pm 2.2$	$79.1^d \pm 15.3$

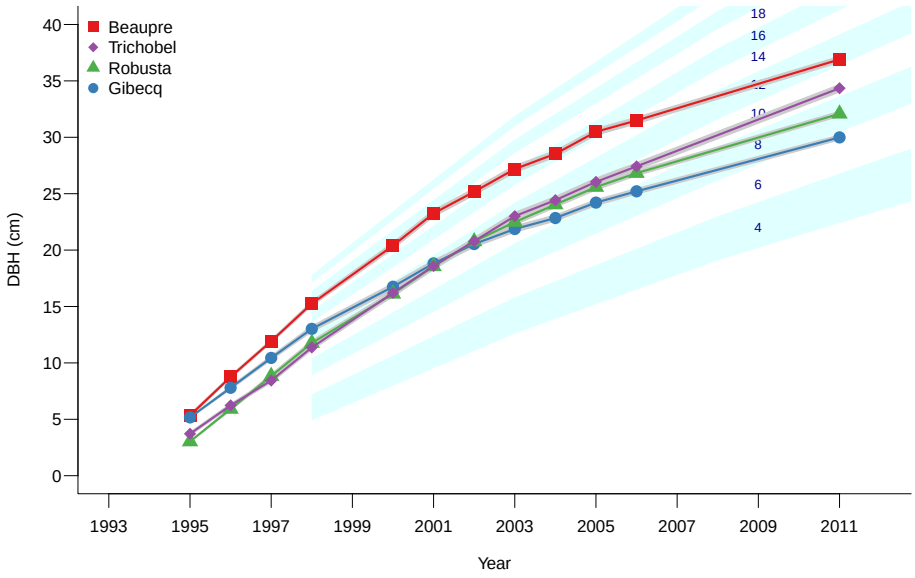

Figure 7.5: Mean diameter at breast height (D_{bh}) for each hybrid in each measurement year. Shading indicates SE ($n = 45$). Blue shading indicates poplar yield classes (Christie, 1994).

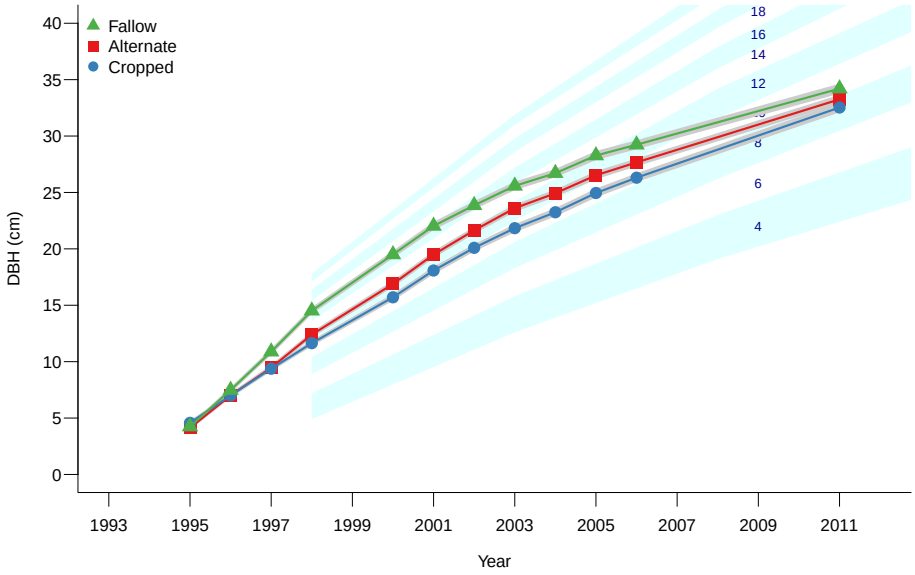

Figure 7.6: Mean diameter at breast height (D_{bh}) for each cropping treatment in each measurement year. Shading indicates SE ($n = 60$). Blue shading indicates poplar yield classes (Christie, 1994).

7.4.1.2 *Height*

As with D_{bh}, significant variations in height were found as a result of hybrid and cropping treatment (Table 7.1).

Post-hoc analysis indicates that there were significant variations in height across all four hybrids ($p < 0.05$, Figure 7.7). This differs from the results recorded in 2006, the last year of measurement, where no significant difference was found between the Robusta and Trichobel hybrids.

In both 2006 and 2011, tree height in the continuously cropped treatment was significantly less than in the fallow and alternately cropped treatment; no difference between the latter two treatments was found ($p < 0.05$, Figure 7.8).

No clear relationship could be found despite the significance of Row in the ANOVA.

Note, some errors in recording were noticed in the 2006 data. On many occasions, the height of trees was found to be less in 2006 than in 2005. Where this was the case, the erroneous 2006 figure was substituted for the greater 2005 value. However this is only a partial solution and it is likely that any values quoted for stand height in 2006 are likely to be underestimates.

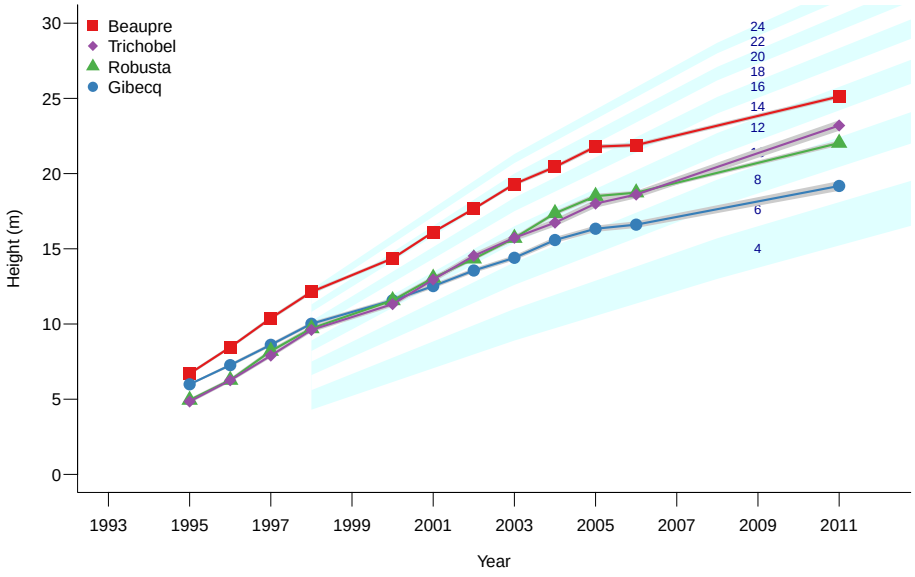

Figure 7.7: Mean height (m) for each hybrid in each measurement year. Shading indicates SE ($n = 45$). Blue shading indicates poplar yield classes (Christie, 1994).

7.4.1.3 *Volume*

Significant variations in tree volume were found between cropping treatments and hybrids, but no interactions were found between groups (Table 7.1). Post-hoc analysis indicates that there were differences between all four hybrids ($p < 0.05$), a departure from measurements in 2006 which suggest that the Beaupré hybrid had the greatest volume, and Gibecq the least, but no difference between the Trichobel and Robusta hybrids ($p < 0.05$, Figure 7.9 and Table 7.3).

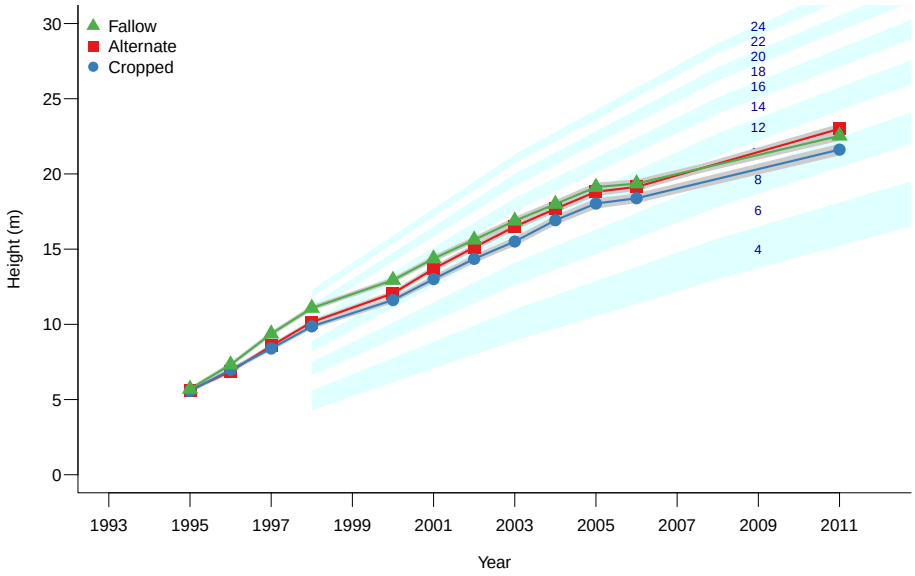

Figure 7.8: Mean height (m) for each cropping treatment in each measurement year. Shading indicates SE ($n = 60$). Blue shading indicates poplar yield classes (Christie, 1994).

In 2011, no difference in tree volume was found between the fallow and the alternatively cropped treatment, but trees in the continuously cropped treatment were found to have a smaller volume ($p < 0.05$). This was a change from 2006, where differences were found between all three treatments ($p < 0.05$, Figure 7.10).

Mean and current annual volume increment are displayed in Figure 7.11 for each hybrid, and Figure 7.12 for each cropping treatment.

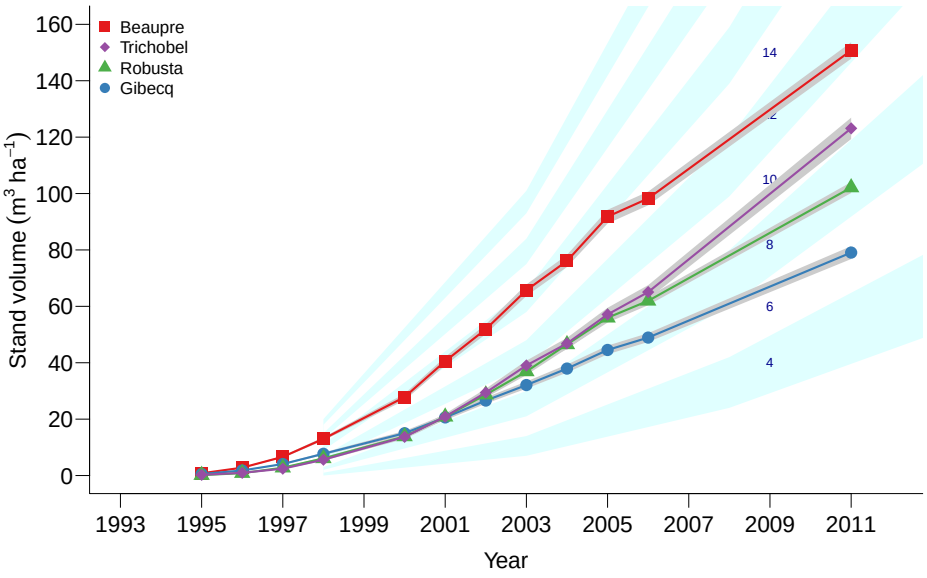

Figure 7.9: Mean stand volume ($m^3\,ha^{-1}$) for each hybrid in each measurement year. Shading indicates SE ($n = 45$). Blue shading indicates poplar yield classes (Christie, 1994).

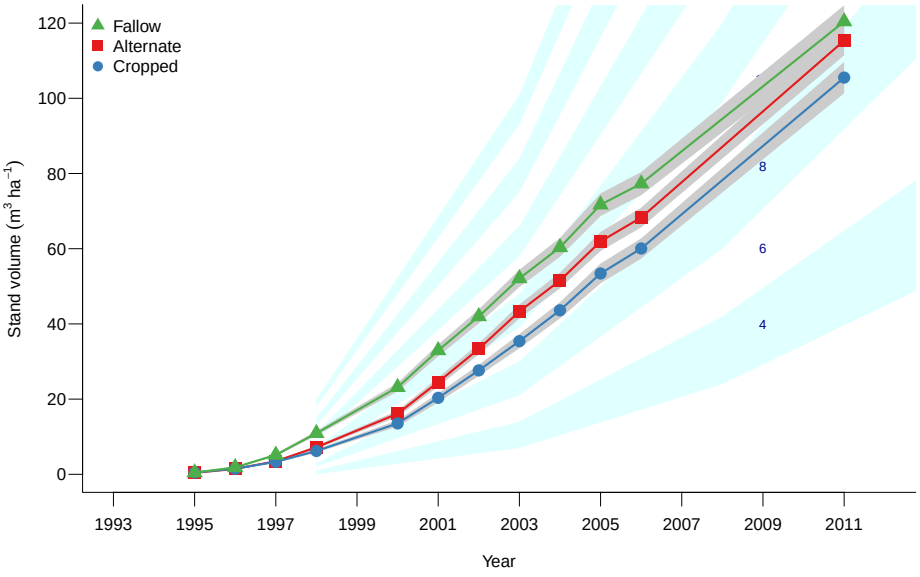

Figure 7.10: Mean stand volume ($m^3\,ha^{-1}$) for each cropping treatment in each measurement year. Shading indicates SE ($n = 60$). Blue shading indicates poplar yield classes (Christie, 1994).

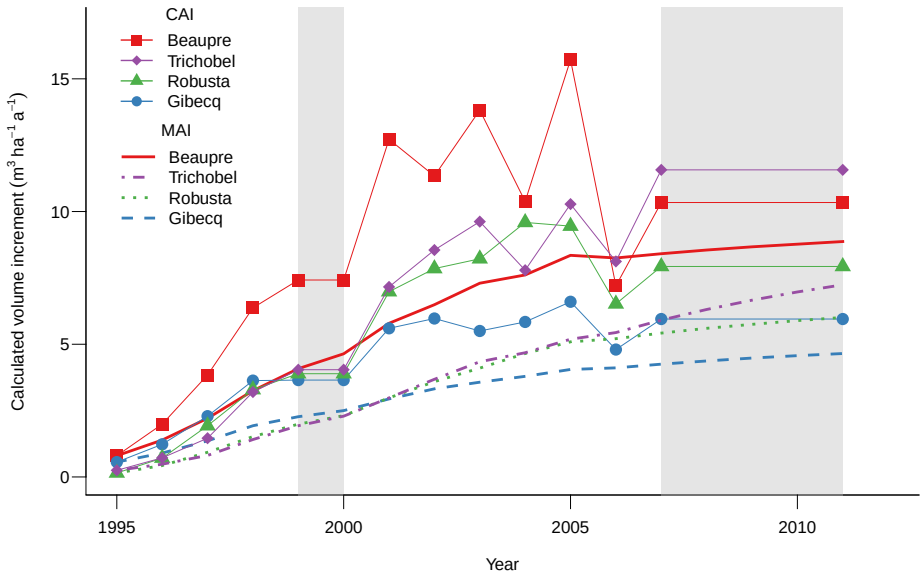

Figure 7.11: Current annual increment (CAI) and mean annual increment (MAI) for volume for the four hybrids. Note, no data was available for 1999 and between 2007 and 2011, an average growth rate has been assumed for these dates (shading).

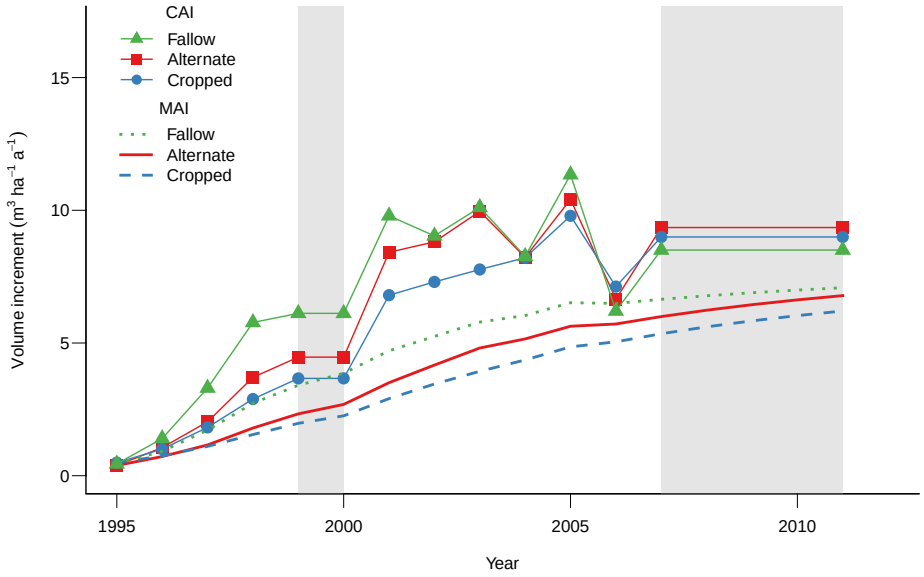

Figure 7.12: Current annual increment (CAI) and mean annual increment (MAI) for volume for each cropping treatment. Note, no data was available for 1999 and between 2007 and 2011, an average growth rate has been assumed for these dates (shading).

7.4.2 *Biomass*

7.4.2.1 *Moisture and carbon content*

Moisture contents ranged between 0.29 in the case of branch wood, and 0.66 in the case of leaves. The full moisture content data has been included in appendix: B.3. A summary has been included in Table 7.4.

Table 7.4: Mean ± SE moisture content (fresh weight basis) for wood, bark and leaf samples taken from different components in 2011.

	Moisture content		
Tissue	Mean	SE	n
leaf	0.638	0.004	21
branch bark	0.492	0.021	6
branch wood	0.321	0.016	6
stem bark	0.560	0.004	6
stem wood	0.434	0.006	6
root bark	0.632	0.007	6
root wood	0.471	0.029	6

Results from the elemental analyser were broadly similar, but varied between 41.4 and 49.5 for the proportional (%) C content of understorey vegetation and branch and root wood respectively. A summary of the data is included in Table 7.5.

Table 7.5: Mean ± SE of the proportion of C (%) present in each tree component and understorey vegetation.

	Carbon content (%)		
Tissue	Mean	SE	n
leaf	44.55	0.05	4
branch bark	47.28	0.40	4
branch wood	49.26	0.07	4
stem bark	47.40	0.07	4
stem wood	48.06	0.16	4
root wood	48.73	0.19	4
stem bark	47.40	0.07	4
understorey	43.53	0.72	4

7.4.2.2 *Fresh and dry mass*

The fresh and oven-dried mass for each measured tree components is given in Table 7.7. Note that due time constraints, it was not possible to get accurate measurements of the rootballs of trees within block 1. For this reason the rootball mass has been estimated based on the relationship of root mass to total aboveground mass (0.094) derived from trees in blocks 2 and 3.

Leaf mass was sampled only on tree 2CB4 immediately after felling, and the relationship of leaf to branch mass (0.1198) assumed to be the same for the five remaining trees.

Understory vegetation mass is presented in Table 7.6. The entire understorey mass sample was dried, hence no values of fresh mass are given.

Table 7.6: Understory vegetation mass ($g\,m^{-2}$) recorded from quadrat samples in each treatment of the silvoarable plot (July 2011).

Treatment	Mean	SE	n
Dry mass			
Cropped	122.2	5.0	6
Fallow	96.2	27.8	6
Control	167.3	37.7	4
Carbon content			
Cropped	53.2	2.2	6
Fallow	41.9	12.1	6
Control	72.8	16.4	4

Table 7.7: Fresh and oven-dried biomass (kg) from field measurements for the six sample trees felled in June 2011. Dry mass was calculated by applying Equation 7.5 to fresh mass data, using *mc* values listed in Table 7.4. Italicised values were derived using assumptions described in the text.

Tree	1*CB*4	1*FB*4	2*CB*4	2*FB*4	3*CB*4	3*CB*4
Fresh mass (kg)						
Leaves	*34*	*46*	30	*31*	*38*	*52*
Branches	284	387	247	255	319	433
Stem	750	940	683	695	914	988
Rootball	*100*	*129*	98	84	110	150
Total	1168	1502	1058	1065	1381	1623
Dry mass (kg)						
Leaves	*12*	*17*	11	*11*	*14*	*19*
Branches	185	253	160	166	208	283
Stem	413	519	376	382	504	545
Rootball	*49*	*64*	48	41	54	74
Total	659	853	595	600	780	921

7.4.2.3 *Coarse root mass*

Analysis of the data indicate significant variations in the mass density of coarse roots recovered as a result of cropping treatment, distance and depth (Table 7.8). A summary of coarse root mass data is included in Figure 7.13.

The mean mass density of roots recovered from the fallow treatment was significantly greater than in the cropped treatment ($p < 0.01$, Table 7.8). Across both treatments, coarse root mass density declined with increased depth from 1.05 $kg\,m^{-3}$ at 45 cm to 0.99 and 0.71 $kg\,m^{-3}$ at 90 and 135 cm respectively. The difference between the top two increments and the deepest, was statistically significant ($p < 0.05$).

In both treatments, coarse root mass density declined significantly with increased distance from the tree ($p < 0.05$, Table 7.9). In the cropped treatment, samples from the tree row were found to have significantly greater coarse root mass density than the cropped alley ($p < 0.05$, 7.9). This difference was not observed in the cropped treatment.

Table 7.8: Results from ANOVA of coarse root mass. Degrees of freedom (df), F-statistic and p value(denoted by stars): $p <= 0.001$ (***), $p <= 0.01$ (**), $p <= 0.05$ (*). Block was included as a random effect.

Term/Interaction	df	F-value
Block	1	
Treatment	1	9.04**
Distance	1	30.63***
Depth	2	15.21***
Type	1	1.55^{ns}
Treat × Distance	1	5.65*
Treat × Depth	2	0.57^{ns}
Distance × Depth	2	1.34^{ns}
Treatment × Type	1	5.35*
Depth × Type	2	0.57^{ns}
Residuals	39	

7.4.2.4 *Coarse root model*

Results from the coarse root model[2] suggest that trees in the cropped treatment had 19% less coarse root dry mass than trees in the fallow treatment. The distribution of mass by depth differs between treatments (Table 7.10). The model suggests that the greatest dry mass in the cropped treatment is to be found in the deepest depth increment.

7.4.2.5 *Bark proportion*

A log-linear relationship was found between total mass and bark mass for stem and branch samples ($p < 0.001$, $df = 16$, $F = 768.4$, Figure 7.14). This relationship was used to estimate the proportion of total tree mass which was composed of bark.

Because it was necessary to calculate the mass of coarse roots as dry rather than fresh mass, the proportion of bark present in coarse root dry mass was also

2 A thorough explanation of the model used to estimate coarse root mass is included in appendix C.1.

Table 7.9: Results from multiple comparison tests of coarse root mass density ($kg\,m^{-3}$) for the Distance × Treatment and Treatment × Type interactions (mean of all three depths). Different superscript letters indicate significant differences within an individual table.

Distance × treatment		
Treatment	Distance	Mean±SE
Cropped		
	2 m	$0.98^{ab} \pm 0.06$
	4 m	$0.54^{c} \pm 0.10$
Fallow		
	2 m	$1.05^{a} \pm 0.06$
	4 m	$0.88^{b} \pm 0.09$

Treatment × Type		
Treatment	Type	Mean±SE
Cropped		
	Alley	$0.70^{b} \pm 0.07$
	Tree row	$1.10^{a} \pm 0.07$
Fallow		
	Alley	$0.98^{a} \pm 0.07$
	Tree row	$1.02^{a} \pm 0.07$

calculated. Coarse root bark mass for each sample was regressed against the total mass for each sample (Figure 7.14).

7.4.2.6 *Total tree carbon*

The mean total carbon (excluding fine roots) stored by a tree in the fallow treatment (487 kg) was 17{ greater than in the cropped agroforestry treatment (415 kg). The proportion of C stored in particular components (e.g. leaves, branches) was relatively consistent between treatments.

Table 7.10: Modeled dry mass of coarse roots (kg) for a tree in the cropped and fallow treatment at each depth increment. Proportion of the total dry root mass for each treatment (%) are given in parentheses.

	Dry mass of coarse roots (kg)	
Depth (cm)	Cropped	Fallow
0–45	28.2(32)	49.8(48)
45–90	19.6(22)	44.8(43)
90–135	40.0(46)	9.8(9)
Total	87.8	104.4

It was possible to establish a significant correlation between D_{bh} and C content ($p < 0.01$, Figure 7.15) using a log-log regression, then back transforming the results.

Table 7.11: Mean, SE, and relative proportion (%) C content for each biomass component under each cropped treatment ($n = 3$). All values in kg C. Coarse root wood and bark values are based on model outputs, hence $n = 1$, and $SE = 0$.

	Cropped			Fallow		
Component	Mean	SE	%	Mean	SE	%
Leaves	5.5	0.4	1	6.9	1.0	1
Branch Wood	78.9	6.1	19	101.3	15.8	21
Branch Bark	11.4	0.6	3	13.4	1.4	3
Stem Wood	186.4	17.0	45	209.5	22.6	43
Stem Bark	20.3	1.2	5	21.9	1.6	4
Rootball Wood	40.7	0.8	10	49.0	4.4	10
Rootball Bark	5.9	0.1	1	6.6	0.4	1
Root Wood	36.0	0.0	9	43.2	0.0	9
Root Bark	6.0	0.0	1	6.8	0.0	1
Total	415	27	100	487	52	100

7.4.2.7 *Root carbon by allometric relationship*

A second measurement of total root dry mass was calculated using an allometric equation (Equation 7.8) provided for oak trees (and recommended for other broadleaved species) in the Forestry Commission Woodland Carbon Code (Jenkins et al., 2011). These data are presented in Table 7.12.

On average the root mass values derived from allometry were 19 % larger than those produced using the coarse root model.

$$M = 0.000149 DBH^{2.12} \tag{7.8}$$

Table 7.12: Summary of total root dry mass (kg) from sampling and coarse root model and derived from the allometric relationship.

Tree ID	D_{bh} (cm)	Measurement	FC model
1CB4	36.4	233	304
1FB4	39.5	288	361
2CB4	32.7	231	242
2FB4	34.4	242	270
3CB4	36.9	243	313
3FB4	38.9	309	350

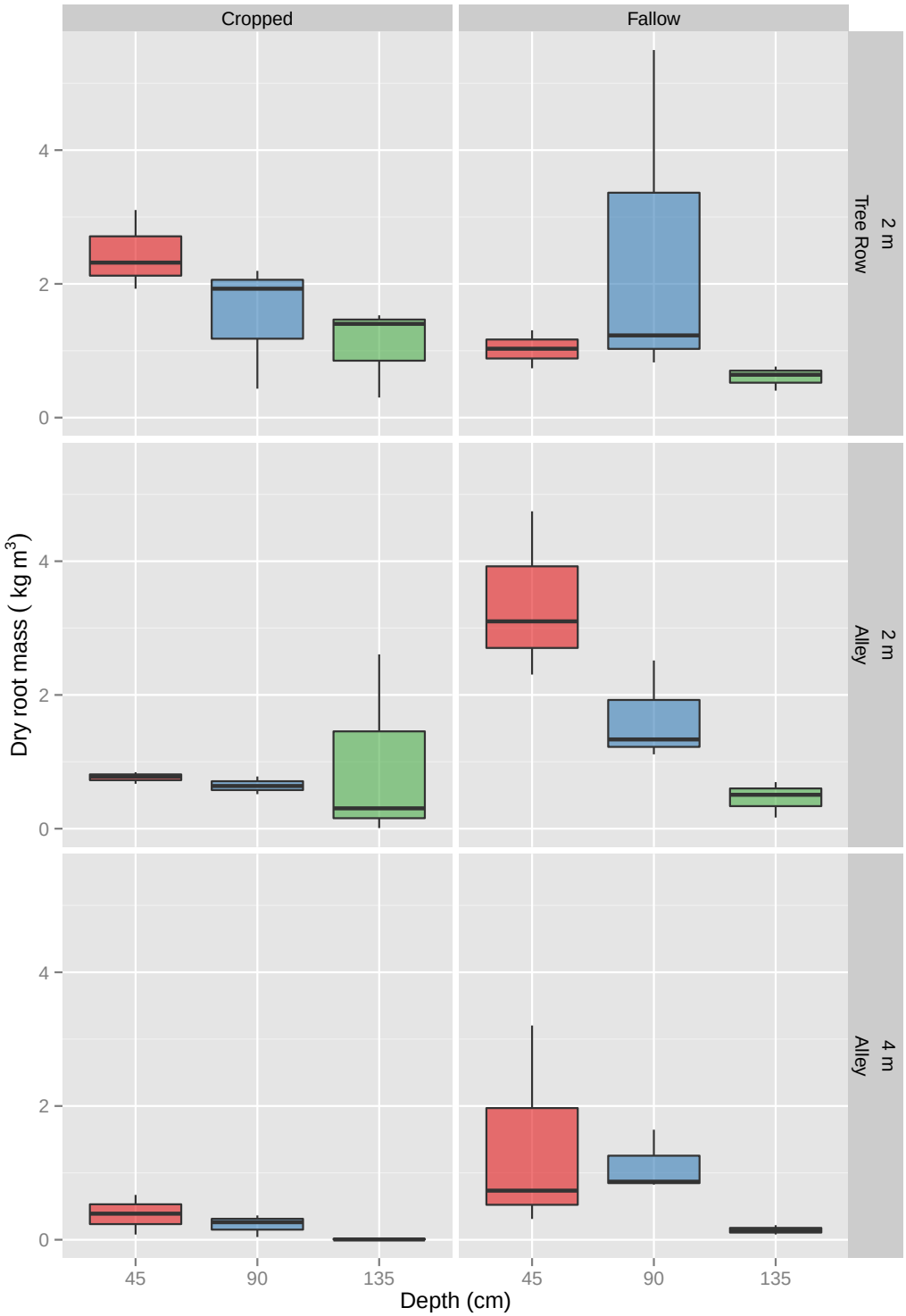

Figure 7.13: Coarse root dry mass ($\mathrm{kg\,m^{-3}}$) in the Cropped and Fallow treatments, in the tree row (2 m) and the cropped alley (2 m and 4 m) at three depths. The dark line in boxplots indicate the median; top and bottom of boxes, the upper and lower quartile respectively; whiskers show the highest value that lies within the upper and lower adjacent values (1.5 times the interquartile range above or below the upper and lower quartile.). In each case, $n = 3$.

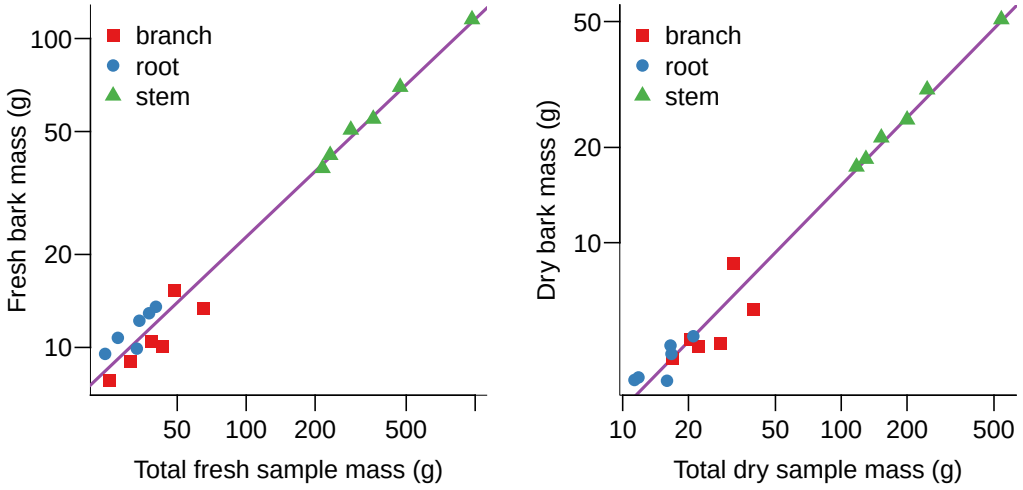

Figure 7.14: Relationship between $\log_{10}$ bark fresh (left) and dry (right) mass plotted against $\log_{10}$ total fresh and dry mass for each sample. Regression lines follow the equations $\log 10(y) = -0.233 + 0.707 \log 10(x)$, $R^2 = 0.98$ (left) and $\log 10(y) = -0.053 + 0.705 \log 10(x)$, $R^2 = 0.98$.

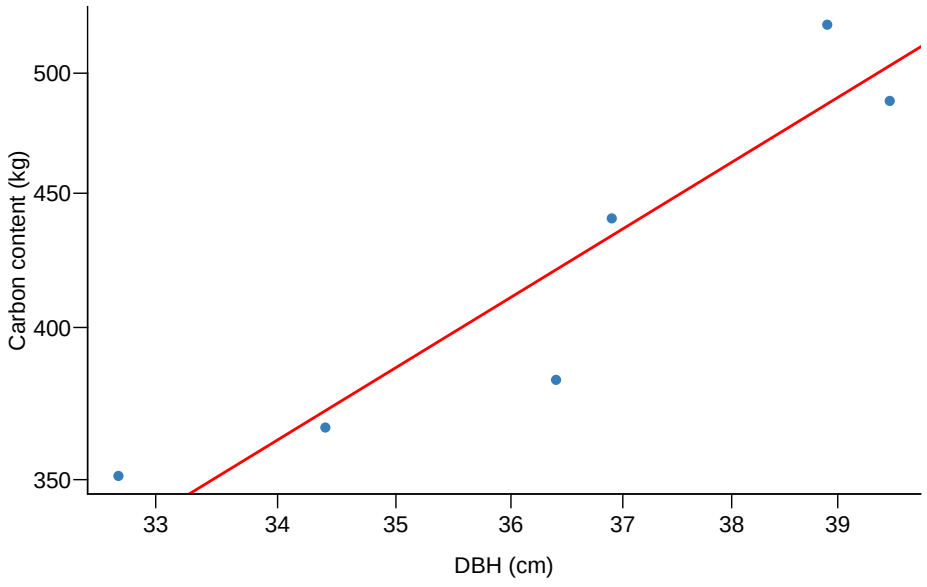

Figure 7.15: The allometric relationship between diameter at breast height (cm) and total above and belowground C content (kg) derived from the six sampled trees. The modeled line follows the curve described by the equation: $y = -0.16x^{2.19}$, $R_s = 0.94$.

7.5 DISCUSSION

7.5.1 *Tree Mensuration*

Results from measurements indicate quite clearly, that the Beaupré hybrid was the most successful in terms of achieving the greatest D_{bh}, top height, and volume. Compared to the poorest performing hybrid (Gibecq), the Beaupré hybrid produced 23% greater girth, and 31% greater height, and 90% more timber volume.

7.5.1.1 *Yield class*

A summary of yield classes, derived from plots, for each hybrid and cropping treatment, is given in Table 7.13. On average, the site produced trees of yield class 10, whilst Beaupré hybrids were found to most closely match yield class 12.

Various estimates of the productivity of the Beaupré hybrid have been published in the literature. Christie (1994) in his provisional yield tables, suggested that on good agricultural land, the Beaupré hybrid is expected to produce a yield class of 22, i.e. a maximum MAI of 22 $m^3\,ha^{-1}$. Three years after the trees were planted at Silsoe, Newman et al. (1995) was predicting a yield class of 26 from Beaupré hybrids based on measurements made at a sheltered site in Old Wolverton, Milton Keynes. This was literally 'off the scale' – beyond the scope of yield tables produced by Christie (1994). Based on measurements taken at the Silsoe site up until 1998 Burgess et al. (2004) expected the same trees measured in this study to achieve a yield class of 22, although this estimate was later downgraded to 14 following further measurements up until 2002 (Burgess et al., 2003).

Yields at the Silsoe site were therefore well below early expectation. At time of measurement in May 2011, the Beaupré trees had a maximum MAI of 8.87 $m^3\,ha^{-1}$ (Table 7.14), and according to yield tables were likely to attain yield class 14 (Figure 7.9). However, the trajectory of height, D_{bh} and volume curves from field measurements do not match the trajectory of the curves suggested by yield tables (Christie, 1994). Both D_{bh} and height curves seem to reach an asymptote earlier than predicted by yield tables; this divergence seems to begin between 2001 and 2003 in the case of D_{bh} (Figure 7.5 and Figure 7.6), and as early as 2000 for height (Figure 7.7 and Figure 7.8). In the case of the Beaupré hybrid, divergence from volume tables occurs as late as 2005–2006, but increases rapidly thereafter (Figure 7.9 and Figure 7.10).

Hence, the summary provided in Table 7.13 is probably not representative of the final yield classes after a thirty year rotation, and are likely to be overestimates. After nineteen years, maximum mean annual volume increments (Table 7.14, Figure 7.11 and Figure 7.12) are well below those predicted by yield tables, and presented in Table 7.13. This has important implications for financial analyses of poplar woodland and agroforestry systems, for example Graves et al. (2007).

7.5.2 *Growth limitation*

Despite early promise, growth of the poplar hybrids at Silsoe was disappointing. The reasons why there was such disparity from the maximum potential yields and

Table 7.13: Summary of yield class derived from Christie (1994), for each hybrid and cropping treatment.

Hybrid	D_{bh}	Height	Volume
Beaupré	12	12	14
Gibecq	8	6	6
Robusta	10	8	8
Trichobel	10	10	10
Crop	**DBH**	**Height**	**Volume**
Continuous	8	8	10
Alternate	8	10	10
Fallow	10	10	10

Table 7.14: Summary of maximum mean annual increment (MAI) (m^3 ha^{-1} $year^{-1}$) for each hybrid and cropping treatment in 2011.

Hybrid	Volume
Beaupré	8.87
Trichobel	7.24
Robusta	6.01
Gibecq	4.65
Treatment	**Volume**
Continuous	6.21
Alternate	6.79
Fallow	7.08

the actual yields, is not clear. It does not seem that this disparity was caused by competition with the arable crop - the curves for alternate, continuously cropped and continuously fallow, follow the same trajectory.

One explanation is that tree growth was limited by water availability. Total annual rainfall for the period 1992 to 2011 varied between 379 and 867 mm $year^{-1}$, with an average of 608 mm $year^{-1}$. This may have been sufficient in the early years of growth, but as the trees continued to increase in size, and their water requirements became greater, water availability may limited growth.

Certainly the linear nature of stand volume accretion (Figure 7.9 and Figure 7.10) hint at a limitation on growth, as do the current annual increment (CAI) and MAI (Figures 7.11 and 7.12) curves . Compared to the more usual relationships observed between CAI and MAI (e.g. Figure 7.16), there is relatively little difference between the two curves.

In a study of the response of poplar clones to drought, Souch and Stephens (1998) found that biomass production by Beaupré hybrids was reduced by 65% in one year, whilst the Trichobel hybrid fared even worse, with a 75% reduction in the same year. This may in part explain the better growth of the Beaupré hybrid compared to the other clones, although notably, at Cirencester and Leeds where this

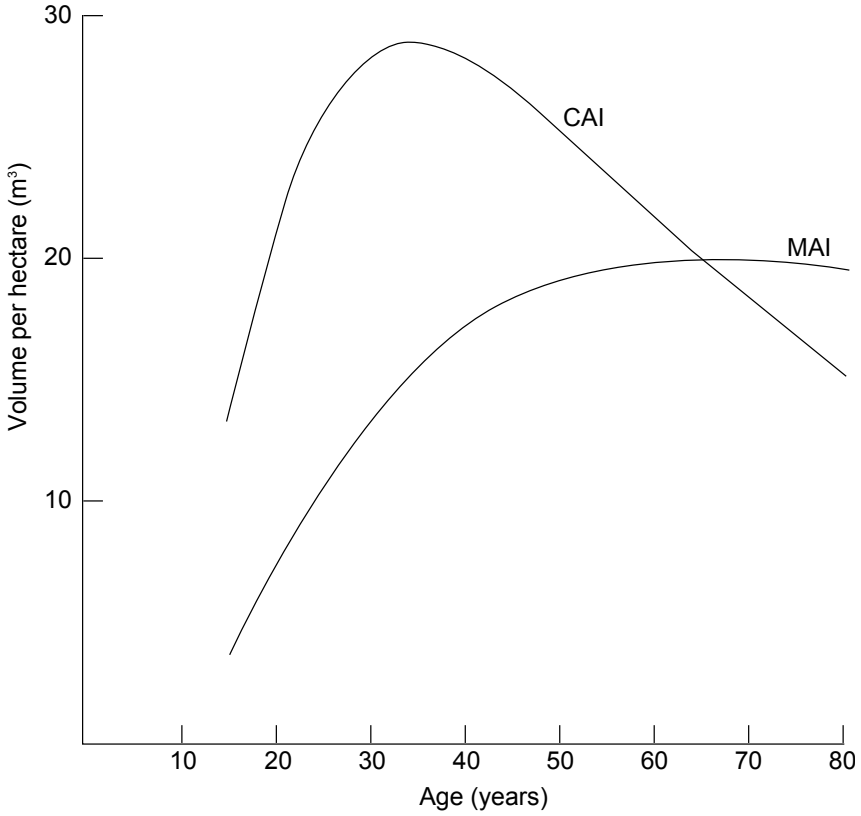

Figure 7.16: Relationship between age, MAI and CAI for yield class 20 Norway Spruce (*Picea abies*) adapted from Savill et al. (1997).

experiment was replicated, the Beaupré hybrid was also found to be most productive; although at least between 1992 and 2002, mean annual rainfall at Cirencester (875 mm) and Leeds (674 mm) was not radically different from Silsoe (875 mm).

It is also possible that provisional yield tables devised by Christie (1994) present an over-optimistic estimation of poplar growth in the UK. It is recognised by UK Forest Research that these yield tables do tend to over-estimate production (Jenkins, T., personal communication, 25 May 2012) but in the present case it seems unlikely that this can be the complete explanation. This observation is difficult to evaluate however, as to our knowledge, this is the first study to re-evaluate the question of clonal poplar yields close to the final rotation age.

7.5.3 *Allometric equation*

An allometric equation was developed for the relationship between D_{bh} and total (above and belowground) C content (Figure 7.15). Whilst in theory this relationship could be used to predict the C content of other Beaupré hybrids, in practice the relationship was developed over far too narrow a range of diameters and should not be used to make predictions beyond the range of the original data.

7.5.4 *Coarse root mass*

The impact of annual cultivation and growing of an arable crop adjacent to trees was detected in coarse root mass data. In the cropped agroforestry treatment greater coarse root mass was found in the uncultivated tree rows between alleys of arable crops (Table 7.9). Across the cultivated alleys, the presence of an annual crop also reduced coarse root mass at 4 m from the tree, relative to the uncropped fallow treatment, although at 2 m from the tree coarse root mass was unaffected. This mirrors findings from root distribution work reported in Chapter 4 in which root distribution determined by root counts indicated similar restrictions to root growth as a result of competition with the arable crop.

Calculating C content for coarse roots was challenging. Whilst it was possible to get an accurate value for the rootball (0.5 m radius, 0.45 m depth), estimations of root mass beyond and below these limits are difficult to extrapolate from sampling. The assumptions made in the creation of the coarse root model have a sound basis however, despite the discrepancy with values produced with allometric relationships.

The assumption that the trees' roots are contained within a 10 m $\times$ 6.4 m rectangle (tessellation), whilst undoubtedly false for a single 19 year old tree, is a necessary and acceptable simplification when considering trees spaced at 10 m $\times$ 6.4 m. Edge effects are minimised by the inclusion of rows of guard trees surrounding the experimental plot.

The assumption of an exponential decline over distance has been used in the HyPar (Mobbs et al., 1999) and WaNuLCAS biophysical models (van Noordwijk et al., 2004). Furthermore, exponential functions show a good fit to coarse root count over distance (Figure 7.17), which undoubtedly bears a close relationship to coarse root mass. Equally, results from coarse root mass sampling, and root distribution (Upson and Burgess, 2013) work show that the lateral distribution of roots differ markedly with depth.

The coarse root mass results results suggest that existing allometric relationships are far from ideal; firstly the allometric relationships quoted by Jenkins et al. (2011) derived largely from McKay et al. (2003) are not specific to hybrid poplar but are based on oak trees (presumably indigenous UK oaks - but this is not clear). Whilst different species have different rooting characteristics, and therefore are likely to differ in their root:shoot ratio, oaks are also known to be a great deal more dense than poplars. *Quercus robur* is recorded as having a wood density of between 560 and 705 $\mathrm{kg\,m^{-3}}$, and *Populus deltoides* a density of between 370 and 494 $\mathrm{kg\,m^{-3}}$ (Chave et al., 2009; World Agroforestry Centre, n.d.; Zanne et al., 2009), hence for a given dbh, estimates of root mass derived from an allometric relationship for oak will always overestimate poplar root mass.

7.5.4.1 *Other studies*

As a result of the difficulty of working within the rhizosphere, few studies examining the root mass of poplar trees exist in the literature. There are some data with which comparison can be drawn however (Table 7.15), though notably only

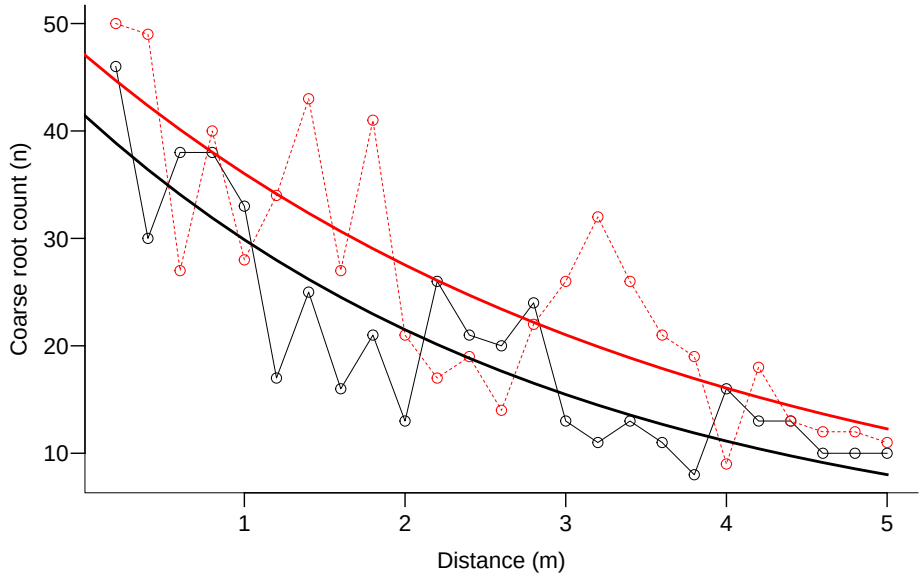

Figure 7.17: Coarse root count over distance from the tree (within 10 m × 6.4 m spacing), from data presented in Upson and Burgess (2013) for 2011. Model fits are derived from the exponential functions $y = 47.16e^{-0.27x}$ (fallow = red) and $y = 41.52e^{-0.33x}$ (cropped = black), with $R_s = 0.82$ and $R_s = 0.87$ respectively.

two studies are concerned with agroforestry systems (Das and Chaturvedi, 2005; Peichl et al., 2006), and neither of these systems are planted to the same density.

Table 7.15: Studies quantifying belowground biomass in *Populus* spp. and hybrids. Density is given in trees ha^{-1}.

Age	Density	Reference	Species (*Populus* spp.)
1–2	10 000	Pallardy et al. (2003)	*deltoides* × *nigra*
1–4	666	Lodhiyal and Lodhiyal (1997)	*deltoides*
2	10 000	Gielen et al. (2005)	*alba*, *nigra*, × *euramericana*
2	10 000	Friend et al. (1991)	*deltoides* × *trichocarpa*
3, 9	500	Das and Chaturvedi (2005)	*deltoides*
5–8	400	Lodhiyal et al. (1995*a*)	*deltoides*
9	208	Puri et al. (1994)	*deltoides*
13	111	Peichl et al. (2006)	*deltoides* × *nigra*
19	156	Current study	*deltoides* × *trichocarpa*

Comparing the root:shoot ratio (excluding fine roots) suggest some patterns. Firstly, the root:shoot ratio of trees planted at a spacing of 1 m × 1 m declines from planting to the age of three years. Second, data collected by Lodhiyal et al. (1995*a*) and Lodhiyal and Lodhiyal (1997) suggest that root:shoot mass as a function of age can be described with an asymptotic function (Figure 7.18). This effect is clear in the first four years of growth at a high stand density (666 trees ha^{-1}), but following thinning, the trajectory of this function shifts, suggesting that with

less competition, the relative mass of roots increases. Of course, it is difficult to disentangle these effects from the effect of increasing age.

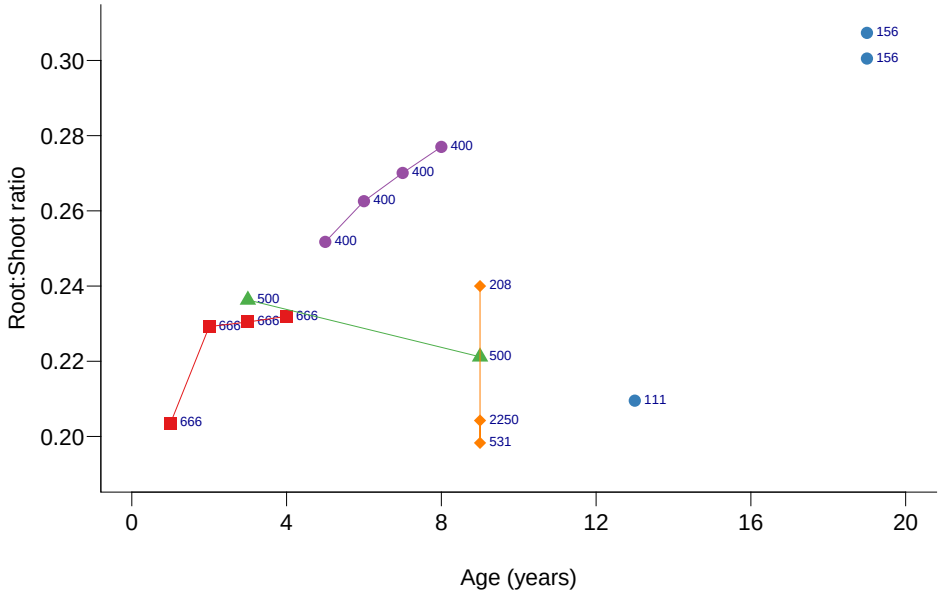

Figure 7.18: Root:Shoot ratio as a function of age from studies referred to in Table 31. Data labels indicate stand density (trees ha^{-1}). Joined data points indicate that data belong to a continuous series of measurements. Note red squares (Lodhiyal and Lodhiyal, 1997) and purple dots (Lodhiyal et al., 1995*b*) are a continuous system, the site was thinned between years four and five. Orange diamonds (Puri et al., 1994) are from three stocking densities at the same site.

Data collected by Das and Chaturvedi (2005) do not agree with these trends, and it is difficult to draw conclusions from these few data about the validity of estimates made with the coarse root model in the present study. In this study, we excavated trees that were 19 years old, substantially older than in all the other studies and the root:shoot ratio was about 0.30[3]. The closest comparable study was a 13 year old agroforestry system in Canada (Peichl et al., 2006), for which a root:shoot ratio of 0.21 was obtained. Using the coarse root model, we were able to obtain root:shoot values of 0.30 for both treatments. This value is beyond the range of values found in the literature, however from work by Lodhiyal et al. (1995*b*) at least suggests that the root:shoot ratio increases with age; 0.30 may not therefore be an unrealistically high value[4]. It is notable however that the system closest in age and management is a silvoarable system from Canada presented by Peichl et al. (2006). This system has one of the lowest root shoot ratios (0.21) presented, and yet is also the oldest system sampled. For this reason, it may be prudent to use the median of all values reported in the literature (0.23) – this value is used in Chapter 8.

3 If trees planted at a density of 10 000 trees ha^{-1} are included, the mean root:shoot ratio is 0.31
4 Note that the poplars at Silsoe were side pruned and hence the canopy size may have been slightly smaller than if left unpruned.

Hypothesis

6. Using traditional forestry yield tables to predict the growth of trees in agroforestry systems and farm woodlands (which are typically planted at much wider spacings) will over-estimate yield.

The results from this chapter affirm the hypothesis that Forestry Commission yield tables are not appropriate for agroforestry situations. This is despite the fact that the Christie (1994) yield tables are designed for trees planted at an equivalent spacing. The exact reasons why there is such a disparity between the modelled and observed is not clear, but it is possible that the disruption of root growth by the annual cultivation of the arable alleys may have played a part. It is also possible that the Christie (1994) yield tables over-estimate yield for all cases, not merely agroforestry situations.

8

PARAMETERISATION OF YIELD-SAFE FOR POPLAR GROWTH.

In this chapter the process of parameterising the Yield-SAFE model is described. Data from the mensuration and destructive harvest of poplar trees at the Silsoe silvoarable trial described in Chapter 7. The newly parameterised model is then validated against data from a site in Leeds which formed part of the network of three silvoarable sites, to which the Silsoe trial belonged. The results from the validated model are presented with additional outputs to allow accounting for carbon storage.

8.1 HYPOTHESIS

This aims of this chapter are to:

- Develop parameters for the Yield-SAFE biophysical model, based on field data collected at the Silsoe silvoarable experiment.
- Compare outputs from the model using the new parameters to actual data from the experiment, and optimise the parameters to achieve a good fit between the actual and predicted data.
- Modify Yield-SAFE to include outputs pertaining to carbon sequestration.
- Validate modifications and parameterisation of the model by comparing model predictions to actual data from the Leeds silvoarable network site.
- Consider carbon stored at the Silsoe site after a complete (30 year) rotation.

In addition, modelling outputs are used to attempt to falsify the following hypothesis:

Hypothesis

6. Using traditional forestry yield tables to predict the growth of trees in agroforestry systems and farm woodlands (which are typically planted at much wider spacings) will over-estimate yield.

8.2 INTRODUCTION

8.2.1 *Carbon sequestration in temperate agroforestry systems*

Few studies of carbon sequestration have been completed on mature, temperate, agroforestry systems, and hence the subject is poorly understood. Quantifying

carbon storage potential, particularly in trees reaching the end of their biological rotation can be prohibitively expensive in terms of time and resources.

Utilising existing data to parameterise carbon sequestration models allows predictions to be made (albeit within an error range) throughout the life of the trees, without the need for destructive harvesting of large, and in some cases, valuable trees.

8.2.2 *The Yield-SAFE model*

8.2.2.1 *Description*

Yield-SAFE, or 'YIeld Estimator for Long term Design of Silvoarable AgroForestry in Europe' (van der Werf et al., 2007) is a biophysical model arising from the SAFE (Silvoarable AgroForestry for Europe) project (2001–2005), designed to offer ecophysiologically based simulations for tree and crop growth based on a limited number of parameters (Graves et al., 2010). This 'parameter-sparse' approach was adopted in part because of the lack of quantitative data from agroforestry systems with which to parameterise a more complicated model (van der Werf et al., 2007).

Matthews (2002) classified crop models into three broad groups: (*i*) those used as tools by researchers, (*ii*) those used as tools by decision-makers, and (*iii*) those used as tools by those involved in education, training and technology transfer. Of these, Yield-SAFE can be said to be predominantly a tool used by researchers, but also to some degree: for education. It's ultimate goal as stated by van der Werf et al. (2007) is to 'predict dynamically site-specific long-term tree and crop yields under competitive conditions on the basis of historical or generated weather data...and relevant soil physical characteristics'.

The model is process-based, and is based on seven state variables: crop leaf area, tree leaf area, crop biomass, tree biomass, number of tree shoots, soil water and temperature sum (Graves et al., 2010; van der Werf et al., 2007). The model operates on a daily timestep. Crop development is primarily determined by a designated planting date and the accumulation of thermal time. As the season progresses, leaf area and light interception increases, governing potential biomass accumulation. Actual biomass accretion is limited by the availability of water, which is driven by soil properties, rainfall, evaporation, and removal of water by the crop and trees. Biomass is partitioned to different aboveground tissues, thus driving the increase in leaf area from season to season. This simple approach restricts the uncertainty in model predictions over more complex, highly parameterised agroforestry models such as WaNulCAS and HyPAR (Palma et al., 2007*b*).

8.2.2.2 *The Yield-SAFE equations*

An explanation of the main equations behind the Yield-SAFE model is given here, based heavily on van der Werf et al. (2007), which should be consulted for a more thorough explanation.

In the following equations t refers to time (days), whilst $_t$, $_c$, $_s$ are used to denote parameters which relate to the tree, crop, and soil components respectively.

Tree growth Potential tree growth per day (Equation 8.1) is derived from the proportion (f_t) of solar radiation (I) intercepted by the tree, and the radiation use efficiency (ϵ_t). This is divided by stand density ρ. The relationship between the proportion of light intercepted and leaf area index is given in Equation 8.2 and Figure 8.1.

$$\frac{dB_t}{dt} = \frac{If_t\epsilon_t}{\rho} \tag{8.1}$$

B_t = aboveground woody biomass (g dry matter) per tree.
I = solar radiation (MJ m^{-2} day^{-1}).
f_t = proportion of radiation intercepted by the tree, see Equation 8.2.
ϵ_t = aboveground biomass produced per unit of intercepted radiation (g MJ^{-1}).
ρ = stand density (trees m^{-2}).

$$f_t = 1 - e^{-k_t L_t} \tag{8.2}$$

L_t = leaf area index (m^2 m^{-2}).
k_t = light extinction coefficient, which has the effect demonstrated in Figure 8.1.

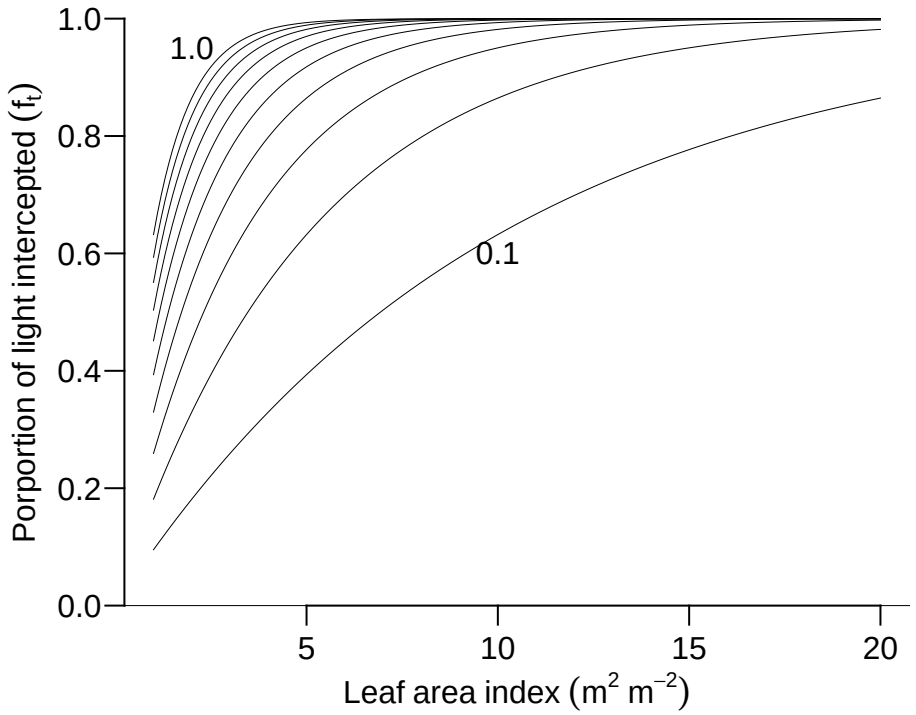

Figure 8.1: Proportion of radiation intercepted for a range of light extinction coefficients (k_t).

To account for the impact of tree biomass loss due to maintenance respiration, an additional function is subtracted from Equation 8.1 to give Equation 8.3. Here a adjusts daily biomass (B_t) for a maintenance respiration loss and loss through other attrition.

$$\frac{dB_t}{dt} = \frac{If_t\epsilon_t w_t}{\rho} - aB_t \tag{8.3}$$

a = proportion of biomass lost per day to maintenance respiration.

Tree leaf area The rate at which tree leaf area (L_t) increases is governed by τ, a constant intended to mimic the rate of spring carbohydrate mobilisation from roots to shoots (van der Werf et al., 2007). Stand density (ρ) is multiplied by N, the number of shoots per tree, which is multiplied by the difference between maximum leaf area per shoot (A_m) in m^2 and the current leaf area per shoot (A), also in m^2 (Equation 8.4).

$$\frac{dL_t}{dt} = \rho N \frac{A_m - A}{\tau} \tag{8.4}$$

N = number of shoots per tree.
A_m = maximum leaf area per shoot (m^2).
A = current leaf area per shoot (m^2).
τ = constant governing the rate of leaf area increase.

Number of shoots N is a difficult value to estimate from from field, so the equation for leaf area is formulated as:

$$\frac{dN}{dt} = \frac{dB_t}{dt}\frac{N}{B_t}(1 - \frac{N}{N_m}) \tag{8.5}$$

N_m = maximum possible number of shoots per tree.

In this way, the number of shoots for 1g of dry biomass is multiplied by total current biomass, and the proportional difference between the maximum possible number of shoots, and the current number of shoots.

If pruning is specified with a rotation, biomass and shoot number are reduced by multiplication with factors π_B and π_N. Tree density can also be modified with to simulate thinning.

Crop growth Potential crop growth is similar to Equation 8.1, with specific crop coefficients, and without a parameter to account for density (Equation 8.6).

$$\frac{dB_c}{dt} = I_c f_c \epsilon_c \tag{8.6}$$

B_c = crop biomass (g dry matter m^{-2}).
I_c = radiation available to the crop (MJ m^{-2} day^{-1}).
f_c = proportion of available radiation intercepted by the crop.
ϵ_c = aboveground crop biomass produced per unit of radiation ($g\,MJ^{-1}$).

Light available to be intercepted by the crop is given by the remainder of radiation that was not intercepted by the trees (Equation 8.7).

$$I_c = (1 - f_t)I \tag{8.7}$$

Of the radiation available to the crop (I_c), the proportion actually intercepted is given by a similar asymptotic function to Equation 8.2 (Equation 8.8), where L_c is the leaf area index of the crop ($m^2\,m^{-2}$) per total area and k_c is an extinction coefficient.

$$f_c = 1 - e^{-k_c L_c} \tag{8.8}$$

The proportion of radiation not intercepted by the trees or crop and which falls on the soil (F_s) is given in Equation **??**

$$f_s = (1 - C)(1 - f_t) + C(1 - f_t)(1 - f_c) \tag{8.9}$$

f_s = proportion of available radiation falling on the soil (MJ m^{-2} day^{-1}).
C = proportion of total area that is cropped.

Partitioning of biomass by the crop The change in the leaf area of the crop is given by Equation 8.10 where σ is the specific leaf area of the crop ($m^2\,g^{-1}$) and P the proportion of assimilate partitioned to leaves.

$$\frac{dL_c}{dt} = \sigma P \frac{dB_c}{dt} \tag{8.10}$$

P declines linearly as the crop continues to develop (van der Werf et al., 2007) after S reaches a threshold value of S_1, and becomes zero after a second threshold value S_2 (Figure 8.2).

Water limitation The effect of water-limited conditions on tree growth, are taken into account in Equation 8.3 with w_t, which governs the limiting impact of soil water potential (ψ). This is incorporated into the model as pF which is negative ψ expressed in cm and logged. A critical value for pF is set as a threshold (pF_c): the maximum pF under which no reduction in biomass accumulation occurs. When pF is above critical value pF_c, but less than the permanent wilting point (pF_{PWP}) then the reduction is proportional to the difference between pF and pF_{PWP}. If pF is greater than pF_{PWP}, a 100% reduction occurs, see van der Werf et al. (2007).

A coefficient governing transpiration (γ_t) in units of $m^3\,g^{-1}$ dry mass is multiplied by tree density (ρ) and tree biomass, to give the water use by the trees (W_t, m^3 m^{-2} day^{-1}, Figure 8.3).

$$W_t = \gamma_t \rho \frac{dB_t}{dt} \tag{8.11}$$

γ_t = transpiration coefficient ($m^3\,g^{-1}$).

The water limitation to crop growth follows an equivalent process to that shown in Figure 8.3. rop water use is calculated using a transpiration coefficient ($m^3\,g^{-1}$) for each crop (γ_c):

$$W_c = \gamma_c \frac{dB_c}{dt} \tag{8.12}$$

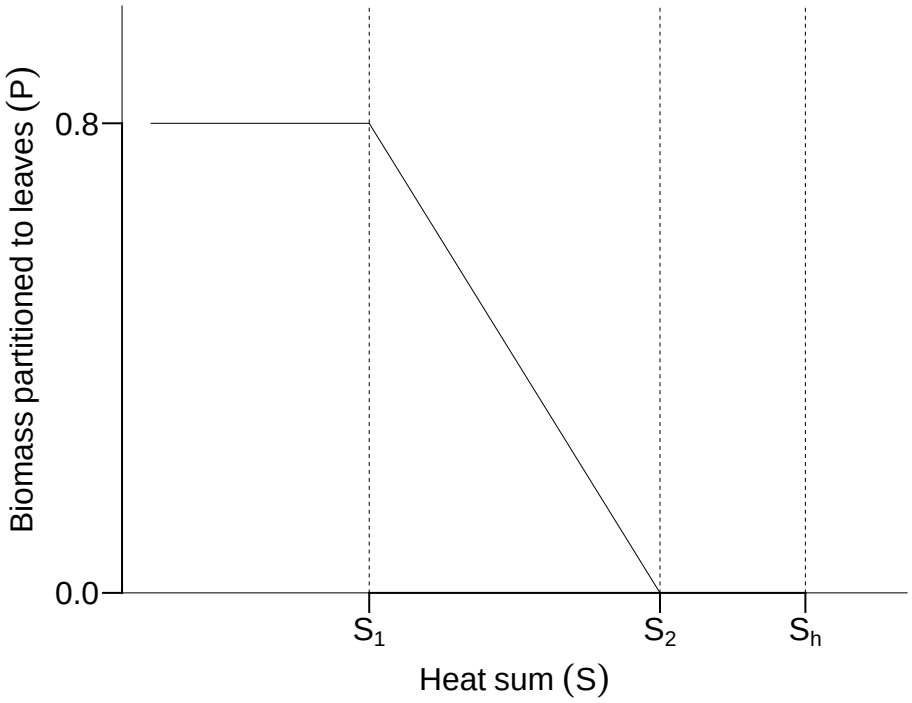

Figure 8.2: Illustration of the function governing partitioning of biomass to leaves. When heat sum (S) reaches the threshold value S_1, the partitioning of growth to leaf area (P) declines linearly until S_2 when leaf development ceases entirely.

Soil water content From Equation 8.11, it can be seen that the variable w_t limits tree biomass accretion according to the relationship demonstrated in Figure 8.3. The variable w_t itself is governed by soil water tension (pF) and two parameters: the critical value of soil water tension (pF_c), after which productivity begins to decline, and the permanent wilting point (pF_{PWP}), after which production completely stops.

As noted, pF is defined as $\log_{10}\psi$ where ψ is the total soil water potential. YieldSAFE defines soil water content (θ) simply as precipitation (R) plus water from irrigation (W_{irr}) minus the any drainage of water below the maximum rooting zone (F_{gw}), water removed by the crop (W_c, Equation 8.12) and trees (W_t, Equation 8.11), and water lost by evaporation from the soil surface (E_{act}). Each is measured in units of $m^3\ m^{-2}\ day^{-1}$:

$$\frac{d\theta}{dt} = \frac{1}{D}(R + W_{irr} - F_{gw} - W_c - W_t - E_{act}) \tag{8.13}$$

θ = soil water content ($m\,m^{-1}$).
D = soil depth (m).
R = precipitation (m).
W_{irr} = water input by irrigation (m).
F_{gw} = flow to groundwater (m).
E_{act} = evaporation from the soil (m).

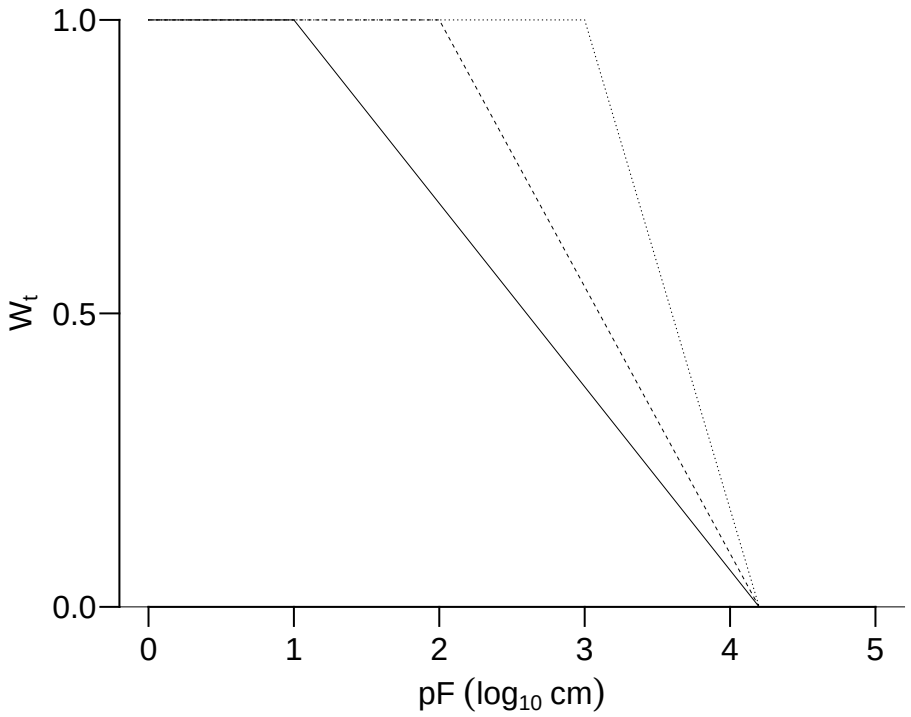

Figure 8.3: Relationship between the ratio limiting tree growth due to limited water (w_t), and the pF ($\log 10\psi$) for a given permanent wilting point of 4.2 (pF_{PWP}), and a critical value (pF_c) of 1 to 3. Adapted from van der Werf et al. (2007).

There is therefore a need to translate soil water content (θ) into a soil water potential (ψ) in order to calculate the variable w_t. This calculation is handled by a closed-form equation proposed by van Genuchten (1980), and reformulated by van der Werf et al. (2007) as:

$$\theta = \theta_{PWP} + (\theta_S - \theta_{PWP}) \left[\frac{1}{1 + (\alpha\psi)^n} \right]^m \tag{8.14}$$

θ_S = soil moisture content at saturation point ($\mathrm{m\,m^{-1}}$).
θ_{PWP} = soil moisture content at permanent wilting point (van Genuchten's θ_r, ($\mathrm{m\,m^{-1}}$).
α, m, n = soil specific parameters.

In the Excel implementation of Yield-SAFE, this formula is rearranged to give Equation 8.15: where θ_2 is a term included to take account of surface run off. The coefficient θ_2 is applied according to Equation 8.16: if the volumetric moisture content (θ) is greater than the saturated volumetric water content(θ_S), then θ_2 is fixed at θ_S, otherwise $\theta_2 = \theta$. The parameters θ_{PWP}, θ_S, α, n, and m are derived from Wösten et al. (1999).

$$\psi = \frac{1}{\alpha} \left(\frac{\theta_2 - \theta_{PWP}}{\theta_S - \theta_{PWP}}^{-(\frac{1}{m}-1)} \right)^{\frac{1}{n}} \tag{8.15}$$

$$\begin{cases} \theta \leq \theta_S : \theta_2 = \theta \\ \theta > \theta_S : \theta_2 = \theta_S \end{cases} \tag{8.16}$$

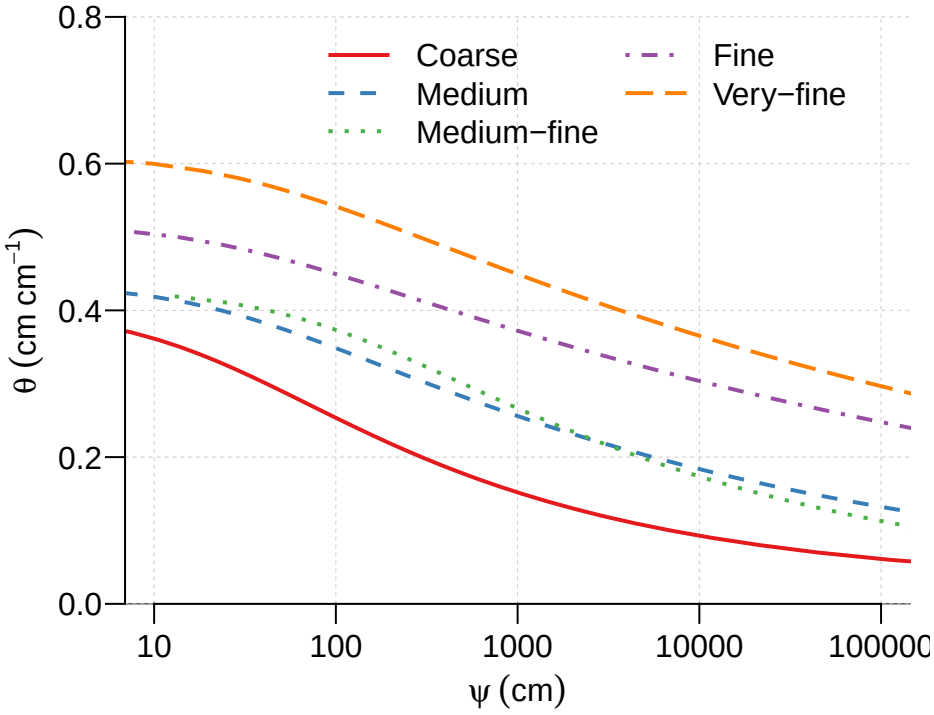

Figure 8.4: Soil moisture content θ as a function of soil water potential ψ, utilising Equation 8.15 for five soil textures as described by Wösten et al. (1999).

Yield-SAFE assumes a uniform depth of soil (D) in m; drainage of water beneath the soil rooting zone is determined by the value pF_{FC} - the soil water tension at field capacity. If water tension (pF) is below pF_{FC}, flow to groundwater (F_{gw}) is equal to δK_S, otherwise $F_{gw} = 0$. K_S is soil hydraulic conductivity at saturation, and is given by Wösten et al. (1999). Calculation of the factor δ is explained by van der Werf et al. (2007).

Evaporation Evaporation from the surface of the soil (E_{act}, Equation 8.17) is the product of the enathalpy of vaporisation for water (a constant: v in units of $m^3\,MJ^{-1}$), the radiation falling on the soil (I_s), and w_s - a factor which reduces evaporation from the soil as the soil becomes dry, and operates in the same way as w_t (Equation 8.3, Figure 8.1).

$$E_{act} = v I_s w_s \tag{8.17}$$

E_{act} = evaporation from soil ($m^3\ m^{-2}$).
v = enthalpy of vaporisation ($m^3\,MJ^{-1}$).
w_s = parameter governing the reduction of soil evaporation was the soil dries.

8.2.3 *Implementations of Yield-SAFE*

Having been implemented in a Microsoft Excel, Yield-SAFE can easily be adapted for a variety of purposes. To date, versions of Yield-SAFE have been used for a variety of applications, including: bio-economic modelling (Graves et al., 2007), modelling environmental benefits of agroforestry systems (Palma et al., 2007*a*,*b*), 'land equivalent ratios' in agroforestry systems (Graves et al., 2010), and intercropping in cider orchards (Vylupek, 2010).

8.2.4 *Yield-SAFE for studies of carbon sequestration and storage*

One of the great strengths of Yield-SAFE for carbon studies is that it directly predicts biomass, which has a linear relationship to carbon content. Other models, for instance the CEH C-FLOW model, and the Forest Research CARBINE, CSORT and BSORT models, refer to Forestry Commission yield tables (Jenkins et al., 2011) which predict height first, then convert using form and density parameters, into biomass. This backward approach may propagate errors, whilst also limiting these models to management regimes covered in existing yield tables (Edwards and Christie, 1981).

Indeed, as has been demonstrated in Chapter 9, diameter at breast height (D_{bh}) can be better predictor of total carbon aboveground carbon, than height.

8.3 METHODS

8.3.1 *Modifications to Yield-SAFE*

An initial parameterisation of the Yield-SAFE model highlighted a difficulty, in that the sensitivity of the trees to drought was assumed to be constant, irrespective of the tree size. Hence, it was was difficult to model the drought sensitivity of recently established trees.

Whilst changes in tree leaf area (L_t) have been incorporated in Yield-SAFE from an early stage, no attempt has been made to incorporate a similar parameter to account for increasing root length. Given our findings in Upson and Burgess (2013), modifying Yield-SAFE to take account of increasing colonisation of the soil by tree roots was a logical step.

It was also hoped that incorporating a function to limit water uptake as the tree developed would improve the fit of the tree component to observed data while the trees were young – prior to this, it had been observed that Yield-SAFE tended to over-estimate tree growth in the early stages.

In the version of Yield-SAFE used in this chapter, root length has been dealt with in the following way. Three new parameters have been included to the tree parameters page: the ratio of structural roots to aboveground biomass (π_{SR}), the length of fine root per gram of structrual root (r), and an extinction coefficient determining the interception of water per unit of root length (k_r).

These new parameters interact to give ϕ, a value between 0 and 1 (Equation: 8.18), which determines the ability of roots to intercept water, following an asymptotic relationship (Figure 8.5). A similar relationship was used in a wheat model by King et al. (2003). This was considered to be the most parsimonious method of calculating root water update, and directly mirrors the approach adopted in Yield-SAFE for light interception.

The current method differs from the approach taken by Ritchie (1998), which assumes a maximum daily water uptake by roots of 0.03 $cm^3\,cm^{-1}$. This value, which sets the upper-bound of root water uptake[1] is then moderated by other factors like soil and root resistance. Ritchie's approach also differs from the present case by stratifying the soil into a number of layers. This approach allows heterogeneity of the soil profile to be accounted for, but is not in the spirit of the parameter-sparse approach adopted by the Yield-SAFE model: Ritchie recommends the use of 7 to 10 layers to characterise the entire root-zone, each of which would require individual parameterisation.

$$\phi = 1 - e^{(B_t \pi_{SR} r k_r)} \tag{8.18}$$

k_r = extinction coefficient governing the absorption of water per unit of root length.
r = length of fine root per gram of structural root ($m\,g^{-1}$).
π_{SR} = ratio of structural root mass to aboveground biomass.

Equation 8.3 can then be adjusted to incorporate the term ϕ (Equation 8.19).

1 Ritchie notes that this value was determined by trial and error.

$$\frac{dB_t}{dt} = \frac{I f_t \epsilon_t w_t \phi}{\rho} - a B_t \tag{8.19}$$

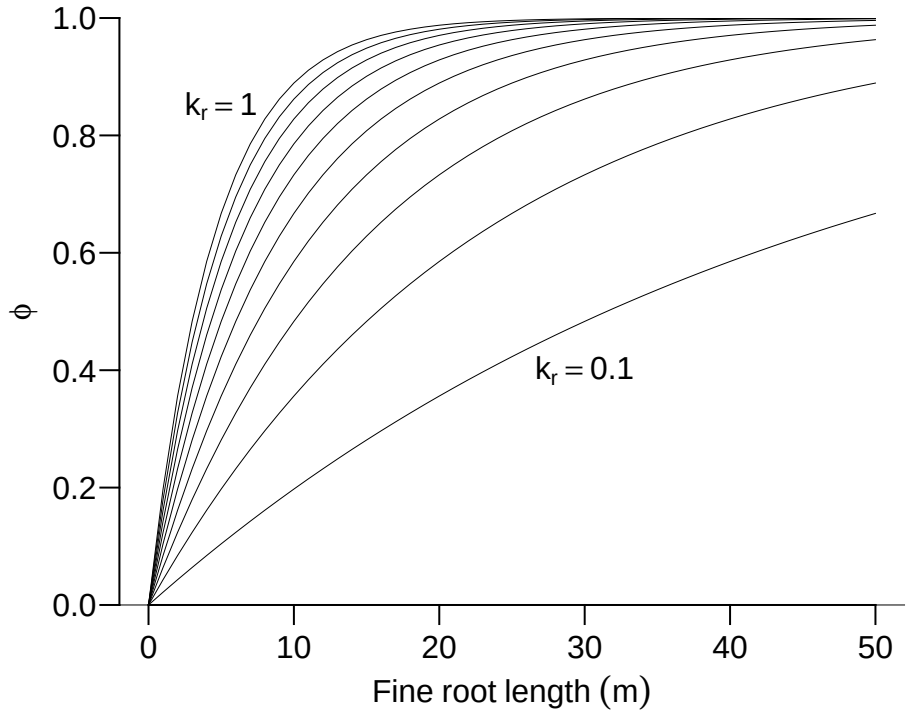

Figure 8.5: The capacity of tree roots to capture the available water (ϕ) is assumed to be related to fine root length (r) and a water capture extinction coefficient (k_r).

8.3.2 *Parameterisation of the model*

Initially, the model was parameterised using values specified by Graves et al. (2010) which had been used for the Silsoe site previously. These parameters are listed in Tables 8.3 and 8.4. Where it was possible to use field collected data to update these initial parameters, this was done so first. Data from field measurements was restricted just to the Beaupré hybrid. An explanation of how these parameter estimates were made follows.

8.3.2.1 *Maximum bole height*

Maximum bole height (H_{bole}) was adjusted from 8 m to 8.68 m based on the median of canopy break measurements taken in 2011 on felled trees. This showed good agreement with pruning data for the Beaupré hybrid, which suggested a maximum pruning height of 8.64 m (Table 8.1).

8.3.2.2 *Ratio of canopy width to canopy depth*

The value of 0.6 was changed to 0.53. This figure was arrived at from the data displayed in Table 8.1. Mean canopy depth was determined by subtracting mean

Table 8.1: Tree and canopy measurements taken from Beaupré trees in cropped and fallow treatments in 2011. N, E, S, W refer to cardinal points, CB = crown break, h_a = actual (measured height), h_e = height estimated from trigonometric methods, D_{bh} = diameter at breast height

id	Canopy extents (m)				CB (m)	h_a (m)	h_e (m)	D_{bh} (cm)
	N	E	S	W				
Cropped treatment								
1CB4	4.9	4.5	4.5	3.5	8.7	24.5	24.2	36.4
2CB4	4.4	4.8	2.2	4.4	8.3	25.0	25.4	32.7
3CB4	3.7	4.1	3.8	3.5	10.3	25.9	25.3	36.9
Fallow treatment								
1FB4	4.4	5.3	5.4	5.5	8.7	24.0	24.4	39.5
2FB4	3.9	4.8	4.1	4.1	7.4	26.1	24.6	34.4
3FB4	4.6	5.3	4.7	3.8	8.8	24.5	26.5	38.9
Mean	4.3	4.8	4.1	4.1	8.7	25.0	25.1	36.5

crown break from mean top height. Mean canopy width was obtained by averaging all canopy extent measurements, then multiplying by two. The ratio was arrived at by dividing mean canopy width by mean canopy depth.

8.3.2.3 *Maximum leaf area*

Measurements of leaf mass and area suggest that the value of maximum leaf area of 500 m^2 is an overestimate. In 2011, total leaf weight for tree 2CB4 was 33.6 kg, and the weighted mean of leaf weight was 1.03 g. From this an estimate of the total number of leaves can be drawn – in this case, tree 2CB4 was found to have around 32,563 leaves. Multiplying this by the average leaf area (43.45 cm^2), gives an estimated leaf area of 129.35 m^2 for a 19 year old tree. Given that, without thinning, the canopies of the trees are unlikely to increase greatly in size, this value was revised initially to 223.40 m^2 by assuming a linear relationship between tree age and leaf area up to 30 years. This is of course a gross simplification, but serves as a starting point for optimising the parameter.

8.3.2.4 *Ratio of branches to total (aboveground) biomass*

Based on the median of measurements taken in 2011, this value was changed from 0.15 to 0.31. Consequently, the ratio of biomass allocated to the stem was changed to 0.69. A summary of individual branch tree biomass measurements is included in Table 8.2.

8.3.2.5 *New root parameters*

As noted, the version of Yield-SAFE used in this chapter incorporated a new function to take account for an increasing root length as the tree increases in size. This was to account for the changing sensitivity of growing trees to drought.

Three new parameters were added: the proportion of aboveground biomass allocated to structural roots (π_{SR}), the length of fine roots per unit of structural root mass (r), and an extinction coefficient describing the interception of water per unit of root length (k_r).

The ratio of aboveground biomass to structural roots was set at 0.23, the median of literature values (Chapter 7). Based on measurements presented in Chapter 4 and Upson and Burgess (2013), r could be calculated (Equation **??**) from fine root mass and specific root length measurements. Measurements were used from the fallow agroforestry treatment, to exclude the influence of grass roots, as it was not possible to separate tree fine roots from grass fine roots. This yielded a value of 30.6 $\mathrm{m\,g^{-1}}$. Before parameterisation, the extinction coefficient k_r was set at 0.005.

Table 8.2: Poplar mass (kg) data collected from destructive harvests at the Silsoe silvoarable field site.

ID	Branch	Stem	Roots	Total	π_{branch}	π_{SR}
1CB4	185	412	138	735	0.310	0.231
1FB4	253	518	192	963	0.328	0.249
2CB4	161	376	145	682	0.299	0.272
2FB4	166	382	152	700	0.302	0.277
3CB4	208	503	153	864	0.292	0.215
3FB4	283	544	186	1013	0.342	0.225
Mean	209	456	161	826	0.312	0.245

8.3.2.6 *Wood density*

Wood density was changed from 410 $\mathrm{kg\,m^{-3}}$ to the mean value for *Populus deltoides* (411 $\mathrm{kg\,m^{-3}}$) based on the global wood density database referred to by Chave et al. (2009), (Zanne et al., 2009, and references therein).

8.3.2.7 *Ratio of height to diameter (σ_{timber})*

This value was changed from 68.55 to 70.31. This figure was arrived at by dividing Beaupré tree heights by D_{bh}; the median was taken for values derived from measurements taken from trees of at least 7 years of age (and multiplied by 100).

It was observed that after the age of about 7 years, σ_{timber} was found to have settled, and that including earlier values would bias this parameter (Figure 8.6).[2]

2 Future work may be improved by applying a function to model the relationship depicted in Figure 8.6. That said, Yield-SAFE outputs for these early years are likely to be far less useful than those of latter years.

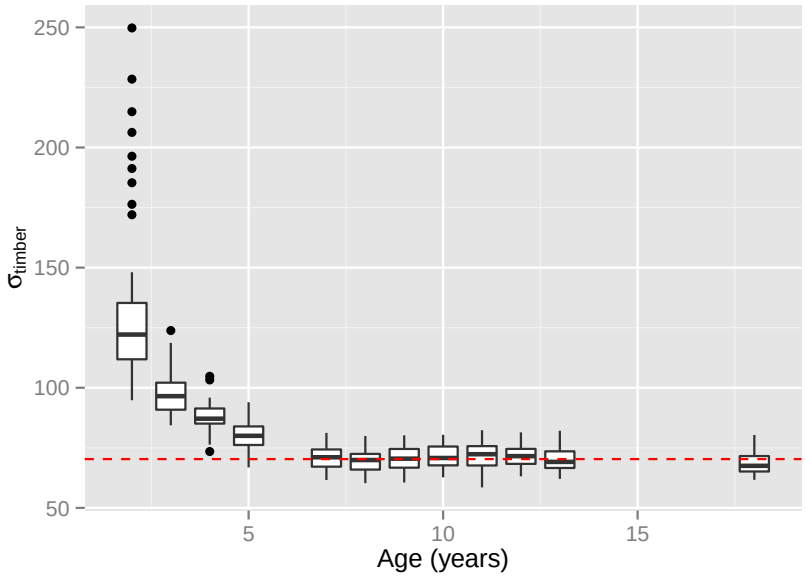

Figure 8.6: Ratio of tree height to diameter at breast height (D_{bh}) for Beaupré trees (σ_{timber}), based on measurements at the Silsoe silvoarable trial between 1992 and 2011.0 Red line indicates median (70.31) of trees greater than 7 years old.

Table 8.3: Initial and final parameters and initial conditions used in Yield-SAFE following parameterisation based on the Silsoe silvoarable trial (AGF). Initial values are based on Graves et al. (2010).

Parameter	Description	Units	Graves et al. (2010)	New value
t_{plant}	Date of year – pruning	J. day	2	2
t_{prune}	Date of year – pruning	J. day	350	350
h_{prune}	Pruning height	m	1.5	1.5
π_b	Proportion of biomass removed per prune		0.1	0.1
π_s	Proportion of shoots removed per prune		0.2	0.2
π_{bole}	Maximum proportion of bole		0.5	0.5
B_{height}	Maximum bole height		8.00	8.68
$t_{thinning}$	Date of year – thinning		300	300
M	Management Factor		1	1
Initial conditions				
ρ_t	Number of tree per m^2	m^2	0.0156	0.0156
$(N_t)_0$	Number of shoots per tree	tree^{-1}	0.6225	0.6225
$(B_t)_0$	Biomass of tree	g tree^{-1}	100	55
$(H_{bole})_0$	Initial bole height	m	0	0
$(LA_t)_0$	Initial leaf area of tree	m² tree^{-1}	0	0

Table 8.4: Initial and final parameters and initial conditions used in Yield-SAFE following parameterisation based on the Silsoe silvoarable trial (AGF). Initial values are based on Graves et al. (2010).

Parameter	Description	Units	Graves et al. (2010)	New value
q	Exponent relating tree diameter to height		1	1
$t_{budbirst}$	Time of bud burst	days	100	100
$t_{leaffall}$	Time of leaf fall	days	300	300
ϵ_t	Radiation use efficiency	$g\,MJ^{-1}$	1.4086	1.3
F	Form factor		0.367	0.367
γ_t	water needed to produce 1 g of tree biomass	$m^3\,g^{-1}$	0.0004	0.000 53
k_t	Light extinction coefficient		0.8	0.8
a	Fraction of biomass needed for maintenance respiration		0.0001	0.0003
LA_{tree}^{max}	Maximum leaf area	m^2	500	223.4
$LA_{tree}^{max}ratio$	Ratio		200 000	23 000
π_{ratio}	Ratio of branches to total biomass		0.15	0.306
π_{timber}	Ratio of timber to total biomass		0.85	0.694
ρ_{timber}	Wood density	$g\,m^{-3}$	410 000	411 000
$(pF_c)_t$	Critical pF value for tree	$\log_{10}$ cm	4	1.8
$(PF_{pwp})_t$	Permanent wilting point for trees	$\log_{10}$ cm	4.2	4.2
σ_{timber}	Ratio of height to diameter		68.556	70.31
$\frac{\Delta\sigma_{height}}{\Delta\rho_t}$	Response of Ht/diameter to density		0	0
σ_{canopy}	Ratio of maximum width to canopy depth		0.6	0.53
τ_t	Number of days after budburst to reach 63.2% of final leaf area	J. days	10	10
π_{SR}	Ratio of root mass to aboveground mass		0.22*	0.22
r	Fine root length per unit mass structural root	$m\,g^{-1}$	30.6378*	30.6378
k_r	Root absorption extinction coefficient		1*	0.0007

*These values were not present in the original (Graves et al., 2010) model; k_r was set to 1, setting root absorption to the maximum (i.e. the same as had the new root parameters not been included in the model).

8.3.3 *Meteorological data*

8.3.3.1 *Silsoe*

Meteorological data between 1992 and 2007 were obtained from the weather station at Silsoe College (Lat: 52.01, Long: −0.41, Elevation: 59 m asl). A gap in daily solar radiation values between 24 May 1992 and 4 June 1992 was filled with the mean of all extant measurements for May and June in 1992 (19.7 MJ m^{-2}).

Data for between January 2008 and January 2012 were obtained from the MIDAS Land Surface Stations data (UK Meteorological Office, 2013). Instrumentation and the nature of the data recorded at MIDAS stations differ, hence data from a number of stations within a 20 mile radius were used.

Temperature data were taken predominantly from the Woburn MIDAS station (ID: 458, Lat: 52.01, Long: −0.59, Elevation: 89 m); where gaps in the records exist, these were filled from data recorded at the Bedford MIDAS station (ID: 461, Lat: 52.23, Long: −0.46, Elevation: 85 m asl).

Precipitation data were obtained from data recorded at the Woburn Sands MIDAS station (ID: 4326, Lat: 52.02, Long: −0.66, Elevation: 85 m asl). Missing data were taken from the Wilstead MIDAS station (ID: 4363, Lat: 52.08, Long: −0.43, Elevation: 37 m asl).

Solar radiation values from MIDAS stations in Bedfordshire were found to be inconsistent, hence, solar radiation data were taken from the Rothamsted MIDAS station (ID: 471, Lat: 51.81, Long: −0.36, Elevation: 128 m asl)[3].

For meteorological values between 2012 and 2022, values between 2007 and 2012 (derived from MIDAS stations) were simply repeated (Figure 8.7).

8.3.3.2 *Leeds*

Obtaining complete weather data for the silvoarable network site operated by Leeds University at Headley Hall was challenging. A complete set of solar radiation measurements were not available from any UK Met Office (UKMO) station at approximately the same latitude as the Headley Hall site[4]. Partial records from several station were thus pooled. The years 1993–2009 (excluding 2002, and 2007 which were anomalous), 2002–2008, and 1994–2006 (excluding 1995, 1997, and 2003) were used from UKMO MIDAS stations: Leconfield (ID: 370, Lat: 53.87, Long: −0.44, Elevation: 7 m asl), Church Fenton (ID: 533, Lat: 53.84, Long: −1.20, Elevation: 8 m asl), and Cawood (ID: 535, Lat: 53.83, Long: −1.15, Elevation: 6 m asl) respectively. The complete rainfall and temperature data were used from the Church Fenton weather station.

Large numbers of missing values remained however. Solar radiation records from 1993 were duplicated for the year 1992, whilst the years 2009–2014 were

3 There was some doubt over the validity of solar radiation values collected at Silsoe, so the values from 1992–2006 were compared to the mean solar radiation from the UK Meteorological Office stations which recorded solar radiation in Bedfordshire, Buckinghamshire, Cambridgeshire, and Hertfordshire ($n = 7$). Values recorded at Silsoe lay within one standard deviation of the mean of these combined values

4 In fact, no complete record of solar radiation data exists from any UKMO station in North, South, East, or West Yorkshire, Greater Manchester, or Merseyside.

simply repeated to give a complete record until the end of 2028[5]. Missing values throughout were replaced with values interpolate by linear spline using the `na.approx()` function in the `zoo` (Zeileis and Grothendieck, 2005) package for the `R` statistical environment.

8.3.4 *Cropping regime*

The cropping regime for the cropped agroforestry and pure arable system was specified in accordance with the actual cropping that occurred between 1992 and 2004 at Leeds and Silsoe. Where parameters have not been specified in the model, the closest alternative was used instead (Table 8.5).

5 Note that predicted data from the EU ENSEMBLES project (http://www.ensembles-eu.org/) for the A1B climate scenario was used initially, but showed a poor fit to the observed climate data, and so was abandoned in favour of the repeated data. Future work may benefit from data generated from a stochastic model such as WGEN or LARS-WG (Semenov and Brooks, 1998)

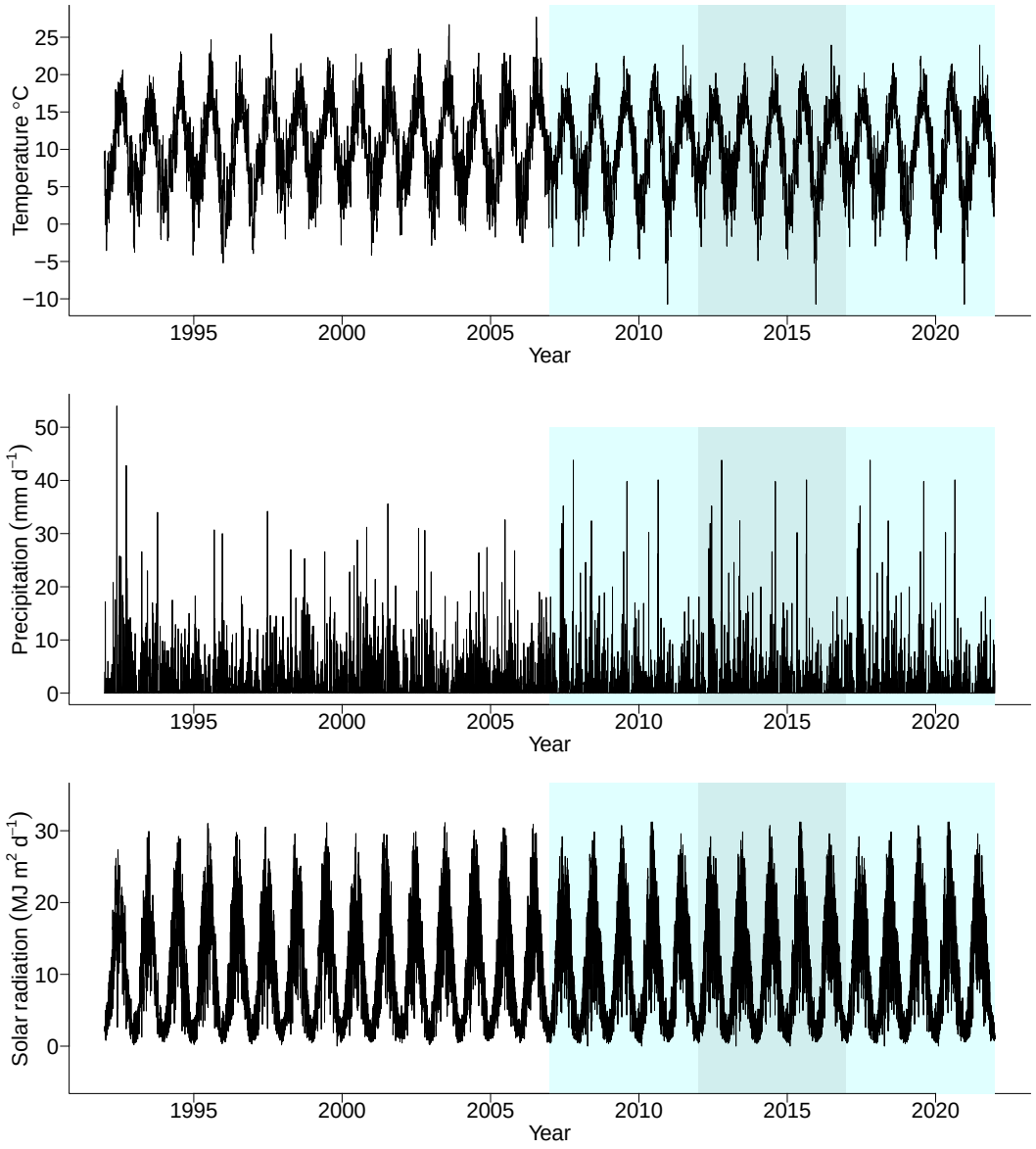

Figure 8.7: Weather data used in Yield-SAFE for modelling poplar growth. See text for a description of the sources used. Shaded regions indicate where data have been repeated.

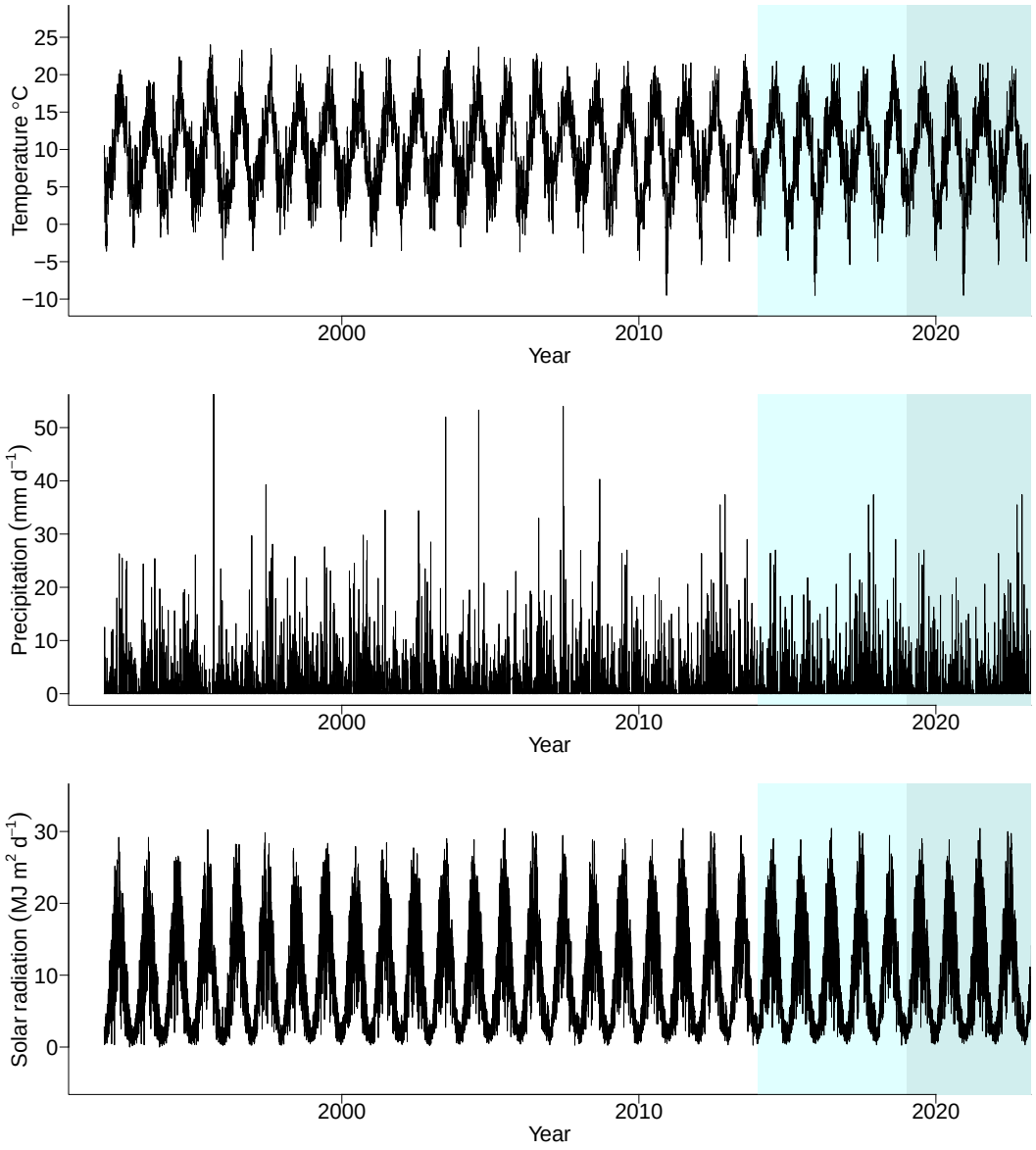

Figure 8.8: Weather data used in Yield-SAFE for modelling poplar growth at the Leeds site. See text for a description of the sources used. Shading indicates here data has been repeated.

Table 8.5: Actual cropping regime, and that specified in Yield-SAFE for the Silsoe and Leeds sites. OSR = Oilseed rape.

Year	Actual Crop	Yield-SAFE Crop
	Silsoe	
1992	Winter wheat	Winter wheat
1993	Linseed	Winter wheat
1994	Spring wheat	Spring barley
1995	Winter wheat	Winter wheat
1996	Winter wheat	Winter wheat
1997	Winter wheat	Winter wheat
1998	Winter beans	Winter beans
1999	Spring barley	Spring barley
2000	Winter wheat	Winter wheat
2001	Fallow	Fallow
2002	Winter barley	Winter barley
2003	Spring beans	Spring beans
2004	Fallow	Fallow
2005+	Annual grass	Annual grass
	Leeds	
1992	Spring barley	Winter barley
1993	Peas	Winter beans
1994	Winter wheat	Winter wheat
1995	Winter wheat	Winter wheat
1996	Winter barley	Winter barley
1997	Spring mustard	Spring OSR
1998	Winter wheat	Winter wheat
1999	Winter barley	Winter barley
2000	Winter wheat	Winter wheat
2001	Winter wheat	Winter wheat
2002	Winter barley	Winter barley
2003	Oil seed rape	Spring OSR
2004	Fallow	Fallow
2005+	Annual grass	Annual grass

8.3.5 *Model fitting*

After the aforementioned changes were made to those parameters which could be adjusted according to field data, five parameters were adjusted within a specified range until a good fit for the Silsoe data was found (Table 8.6).

Table 8.6: Yield-SAFE parameters which were adjusted to provide a good fit between modelled and field-observed data.

Parameter	Description	Range
k_r	Extinction coefficient to describe the interception of water by fine roots.	0.0001–0.001
γ_t	Water used to produce 1 g of aboveground biomass ($m^3\,g^{-1}$)	0.0001–0.001
ϵ_t	Radiation use efficiency for trees ($g\,MJ^{-1}$).	0.8–1.3
α	Fraction of biomass needed for maintenance respiration of aboveground dry matter.	0.0001–0.005
$LA^{max}_{tree}ratio$	Ratio by which LA^{max}_{tree} is divided to give n^{max}_{shoots}.	20 000–200 000

The fit of the model was assessed on the basis of three statistics: normalised Root Mean Squared Error (nRMSE) - a measure of the average deviation of observed values from the predicted (expressed as a percentage, Equation 8.20); d-index - a similar measure presented by Willmott et al. (1985) and Wellens et al. (2013) which presents the average difference as a value between zero and one (Equation 8.21). In the case of nRMSE a smaller number indicates a smaller deviation from the observed data. Jamieson et al. (1991) suggest that values of $< 10\%$ can be considered as an excellent fit to the observed data, between 10% and 20% can be considered good, between 20% and 30% considered fair, whilst values above 40% should be considered a poor fit. For d-index, values close to one indicates a good fit of modelled to observed data. Regression of observed and modelled data, and comparison to a 1:1 line can also be informative in assessing model performance, and this was conducted for arguably the most important model output of timber volume.

$$nRMSE = \left[\frac{\sum_{i=1}^{n}(p_i - y_i)^2}{n}\right]^{0.5} \times \frac{100}{\bar{y}} \tag{8.20}$$

$$d = 1 - \left[\frac{\sum_{i=1}^{n}(p_i - y_i)^2}{\sum_{i=1}^{n}(|p_i - \bar{y}| + |y_i - \bar{y}|)^2}\right] \tag{8.21}$$

p = modelled values.
y = field observed values.
$\bar{y}$ = mean of field observed values.
n = number of observations.

These statistics were applied to five model outputs: height, D_{bh}, volume, current annual increment (CAI), and mean annual increment (MAI). Annual increment can be expressed in two ways: CAI (m^3 ha^{-1} $year^{-1}$), which is the current rate of volume change over a given period (essentially a rolling mean), and MAI, which is the average rate of growth over the life of the tree. The formulae for these expressions are given in Equation 8.22 and Equation 8.23 (Savill et al., 1997).

$$CAI = \frac{v_n - v_0}{n} \tag{8.22}$$

v_0 = volume at the beginning of the period of n years (m^3).
n = number of years between measurements of v_n and v_0.

$$MAI = \frac{v}{a} \tag{8.23}$$

v = volume of tree (m^3).
a = age in years.

It is by using maximum MAI over the rotation length of the tree, that yield classes are assigned. Hence a tree in yield class 12 would be expected to produce a maximum MAI, over a given rotation length, of 12 m^3/ha $year^{-1}$ (Hamilton, 1996).

8.3.5.1 *Model sensitivity to drought*

Early attempts to parameterise the model indicated that the tree component was insufficiently sensitive to accurately model the impact of competition for water between the crop and the tree components. Simply put: the presence of an annual crop made almost no difference on the growth of the trees.

To address this problem it was necessary to make the trees substantially more sensitive to drought conditions, hence pF_c – the soil water potential at which trees begin to reduce biomass accretion – was reduced from -1.0 MPa ($pF = 4$) to -6.3 kPa ($pF = 1.8$). This parameter change impacted trees in the cropped and fallow treatments alike, and was not sufficient to generate the observed differences between the treatments. Therefore, it was necessary to alter soil parameters which impact evaporation rates; in this way it was possible to reduce the amount of water lost by the soil under bare fallow conditions, thus creating sufficient difference between treatments to match that observed.

Evaporation from the soil typically occurs in two phases: in the first phase evaporation is determined by the atmospheric conditions until a threshold soil moisture content is reached, after which the rate of evaporation slows in accordance with the rate at which water is transported from deeper soil levels to the soil surface (Ritchie, 1972).

In Yield-SAFE this relationship is modelled in the same way that potential tree and crop growth is limited by water availability (Figure 8.1); hence, when the soil water potential pF drops below a critical value pF_cE, evaporation from the soil declines at a rate proportional to the difference between pF_cE and a further threshold value pF_{Eoff} above which evaporation from the soil ceases completely. The onset of soil limited evaporation was changed from 20 kPa ($pF = 2.3$) to 1

kPa ($pF = 1.0$). The threshold for ceasing evaporation was changed from 1.5 MPa ($pF = 4.2$) to 63 kPa ($pF = 2.8$, Figure 8.9).

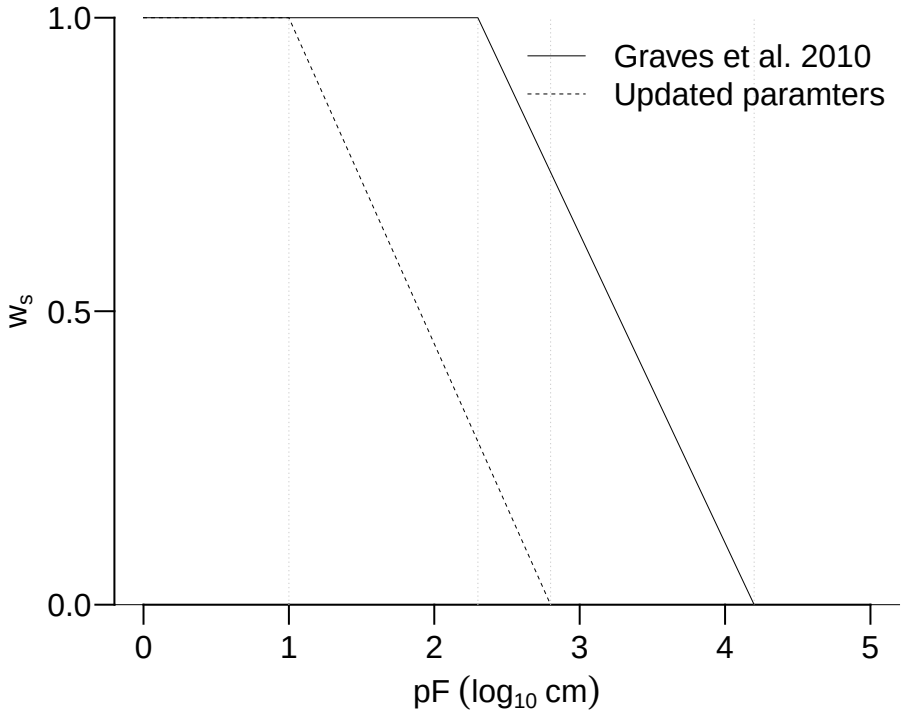

Figure 8.9: Influence of soil water potential (pF) on w_s: a factor used to scale evaporation (E_{act}). The original parameters (Graves et al., 2010) are included alongside the updated set of parameters.

Yield-SAFE's treatment of soil evaporation is extremely simple, as it assumes an even rate of evaporation from the entire soil profile (150 cm in the present case). More complicated models, for instance AquaCrop, divide the soil into two zones for the purposes of calculating evaporation, hence allowing rates to be set deferentially (Raes et al., 2012, Chapter 3). Lower values may therefore be more appropriate for Yield-SAFE, as otherwise soil evaporation may be over-estimated. *link this paragraph*

Aydin et al. (2005) proposed a similar model to describe soil evaporation with two thresholds. They calculated that actual evaporation (E_{act}) would stay the same as the potential if the ψ_p of the top 1 cm of soil was above -1.5 kPa ($pF = 1.2$) for sand, and -6.0 kPa ($pF = 1.8$) for clay.

8.3.5.2 *Carbon storage*

Since Yield-SAFE calculates biomass directly, it is simple to output carbon storage by converting biomass (g dry matter) to carbon by multiplication by a conversion factor. In the original Yield-SAFE model, a tree carbon content of 50% is assumed; in the updated version, this was changed according to measurements of total organic carbon (presented in Chapter 7) to the weighted mean carbon content of 47.94%.

Total aboveground carbon is a rather simplistic way of looking at carbon storage at the Silsoe silvoarable trial, and was improved by considering carbon stored in

different types of tree tissues, and assuming a longevity for each. Woody biomass was split into above and belowground fractions; on harvesting, belowground biomass was assumed to decompose whilst harvested aboveground biomass is processed into woody products, which also degrade over a time-span of years or decades, depending on what use the harvested material is put to.

Different scenarios with varying estimates for the longevity of resulting woody products could then be compared offering a range of outcomes dependent on the quality of timber and the potential market. Carbon storage was modelled over 100 years, with three consecutive rotations of 30 years each.

Decomposition of root matter and woody products were modelled with an exponential decay function equivalent to Dewar (1990), applied to the maximum above and belowground biomass for each rotation on the day of harvest (Equation 8.24).

$$rC_i = B_t \cdot C_w \cdot \rho \cdot 10^{-6} \cdot e^{-ki} \tag{8.24}$$

rC_i = residual carbon fraction on day i (t C ha^{-1}).
B_t = maximum aboveground biomass on the day of harvest (g tree^{-1}).
k = exponential coefficient.
C_w = weight mean carbon content (0.4794).
i = day since harvest.
ρ = tree planting density (trees ha^{-1}).

For root biomass, the shape of the exponential curve was based on Fahey and Arthur (1994) who demonstrate that within 4 years, 45–63% dry weight was lost from large woody roots in a northern hardwood ($k = 0.175$). These values serve as a starting point in the absence of more locally specific studies.

For woody products, the literature appear to be relatively sparse on the potential longevity of different woody products; for that reason, a range of values were used: 10, 25, 50 and 100, and 150 years. Coefficients were chosen to ensure that all the stored carbon had been lost by the end of each period. The lower end of this spectrum agrees with the estimates used by Thompson and Matthews (1989) for longevity of C in pulpwood. More durable products in the construction industry might persist for 80 years (Bowyer et al., 2004) or longer; indeed Thompson and Matthews (1989) use values of around a 40% loss in stored carbon over 90 years when used in the mining industry.

8.4 RESULTS

8.4.1 *Parameterisation*

Using the parameters listed in Table 8.3 and 8.4, it was possible to achieve a good fit between the model outputs for the cropped agroforestry system and the field data from the Silsoe agroforestry trial. These data are displayed in Figure 8.10 and Figure 8.11.

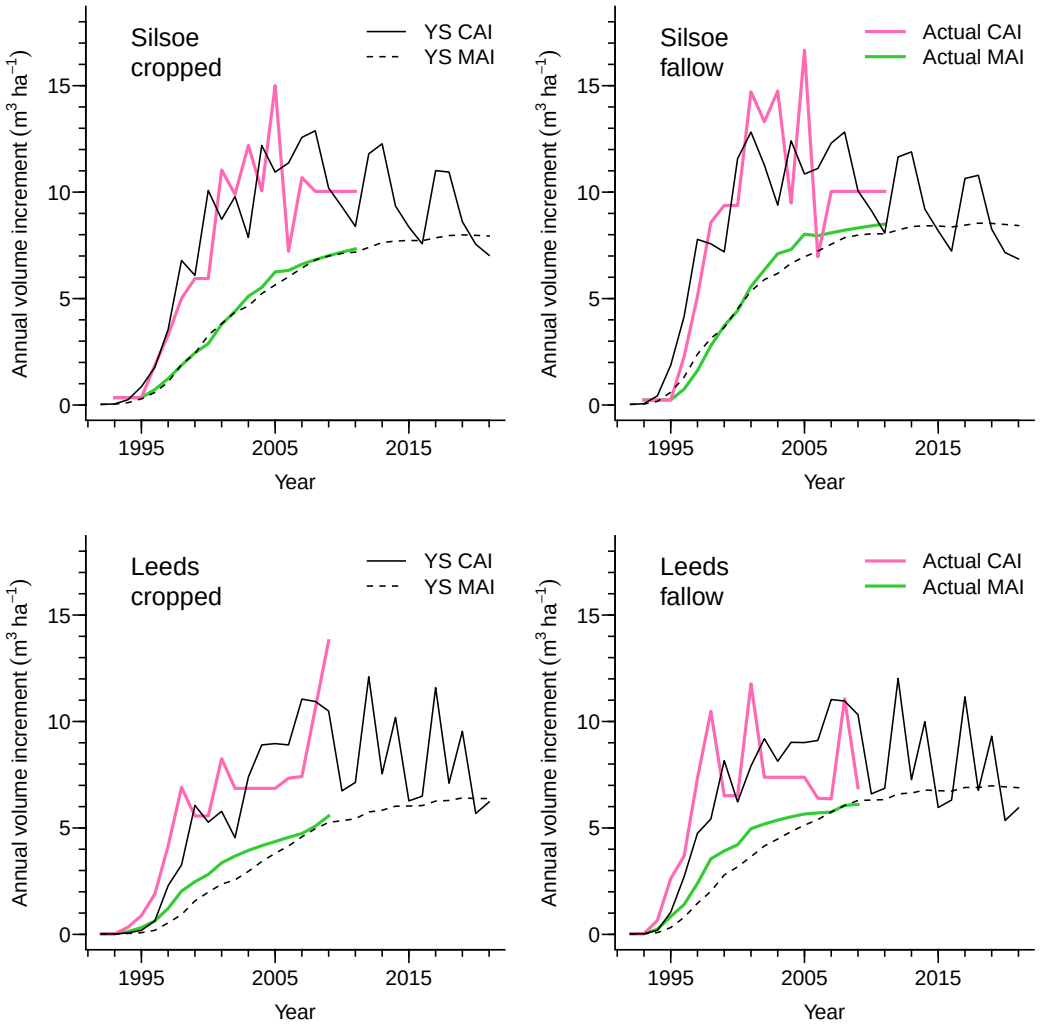

Figure 8.10: Current current annual increment (CAI) and mean annual volume measurement mean annual increment (MAI) ($m^3\,ha^{-1}$) from field measurements and modelling in Yield-SAFE for the Cropped (C) and Fallow (F) treatments respectively at Silsoe (top) and Leeds(bottom).

Consideration of the nRMSE and *d*-index indicate that the modelled values generally show a good fit to the calibration data. On average, model outputs for volume deviate by just 3–4% from those observed. Volume expressed as both CAI and MAI show the worst fit to the data, with deviations of between 12 and 20%. This is unsurprising, as these values are more closely affected by meteorological changes

in a given year. Whilst these values better reflect the ability of the model to predict annual variations and are therefore useful for assessing fit, in practice it is the absolute volume values that is of commercial value, and by this measurement the models fit the observed data extremely well.

Table 8.7: Modelled and Actual mean annual increment (MAI) (m^3/ha $year^{-1}$) for the Cropped and Fallow treatments at Silsoe and Leeds.

	Silsoe		Leeds	
	Cropped	Fallow	Cropped	Fallow
Actual: 19 years	7.3	8.5	5.6	6.1
Modelled: 19 years	7.1	8.0	5.3	6.3
Modelled: 30 years	8.0	8.5	6.4	7.0

Table 8.8: Percentage Root Mean Squared Error (nRMSE), *d*-index, and number of observations compared (n) for comparisons between model outputs and observed data for current annual increment (CAI), MAI, diameter at breast height (D_{bh}), height, and volume

	Silsoe			Leeds		
*nRMSE**	Cropped	Fallow	n	Cropped	Fallow	n
CAI	19.9	19.4	19	26.3	24.6	18
MAI	12.8	14.8	19	37.1	28.0	18
D_{bh}	4.8	6.0	13	9.8	8.9	18
Height	7.9	6.0	14	10.1	8.3	13
Volume	3.5	3.3	12	7.2	5.9	13
d-index**						
CAI	0.92	0.90	19	0.93	0.88	18
MAI	1.00	0.99	19	0.97	0.97	18
D_{bh}	1.00	0.99	13	0.98	0.98	18
Height	0.99	1.00	14	0.99	0.99	13
Volume	1.00	1.00	12	0.99	0.99	13

*nRMSE – average deviation of modelled from observed values, expressed as a percentage.

**d-index – a value close to 1.00 indicates a good fit.

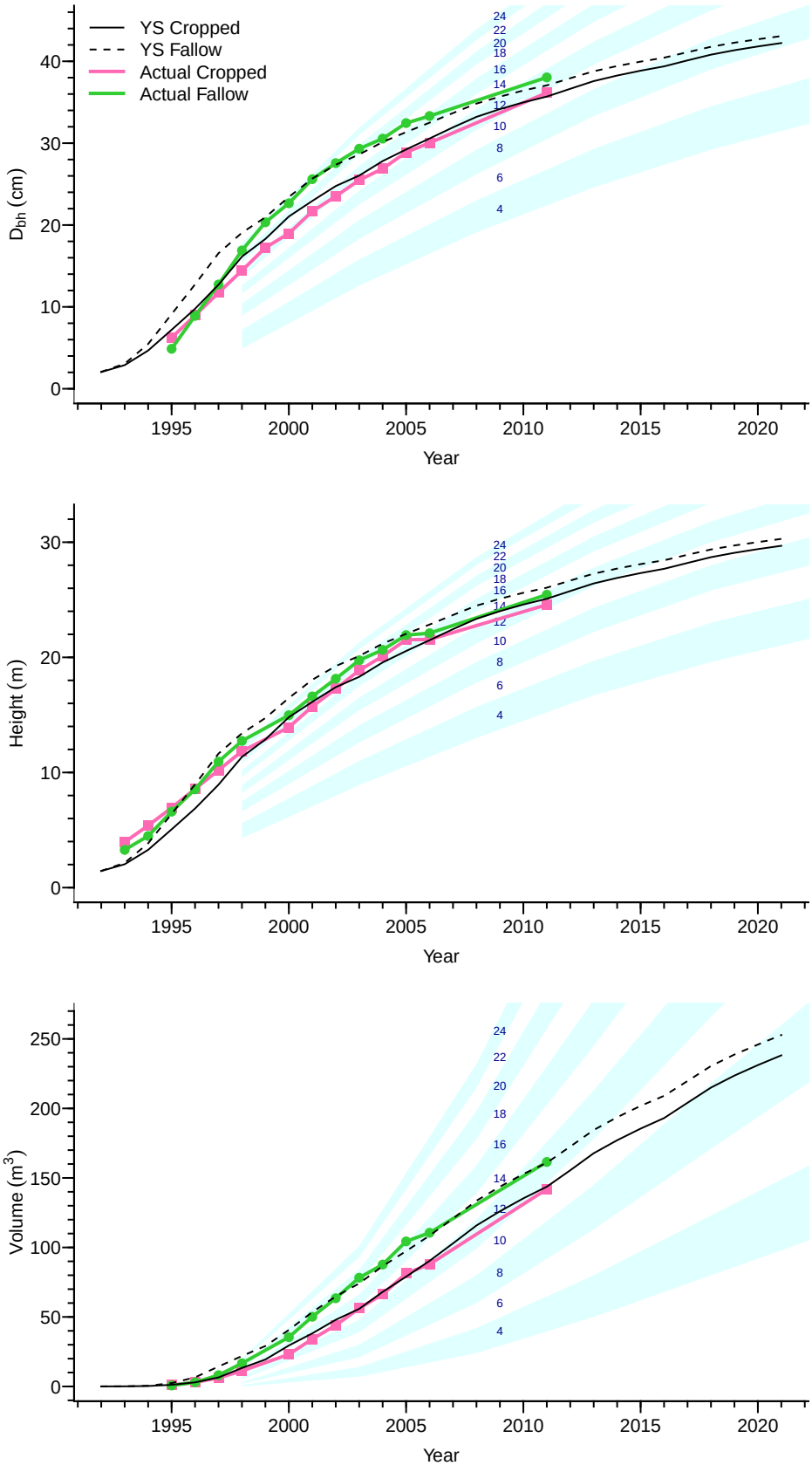

Figure 8.11: Comparison of diameter at breast height (D_{bh}) (cm), height (m), and volume (m^3) from actual measurements at the Silsoe silvoarable site, and outputs from Yield-SAFE.

8.4.2 *Validation*

Following parameterisation of the model using the Silsoe data, the model was validated against data collected from an identical experiment conducted at a different location: Headley Hall, North Yorkshire (53°52′20.4″N, 1°20′3.3″W): an experiment administered by Leeds University[6]. The silvoarable trial was set up at the same time as the Silsoe site (April 1992). The site is gently sloping, with a West-north-west aspect, at an altitude of 50 m asl. The site has shallow sandy clay loam soils of the Aberford series, sitting on top of Magnesium limestone (Burgess et al., 2003). Rainfall at the Leeds (629 mm) and Silsoe site (634 mm) were similar, although mean air temperature was lower at Leeds (9.3°C) than Silsoe (9.8°C) for the first seven years of the experiment (1992–1998) (Burgess et al., 2003).

Just two changes to the model parameters were made for the Leeds site: the effective soil depth was changed from 1500 cm to 500 cm, and weather data from the local area were used. Note that there were some inconsistencies in the height measurements from the Leeds data, hence some values were removed[7]. A summary of the data from Leeds used in validation is included in Appendix Table D.2.

Model outputs for the Leeds site remain excellent for volume, height and D_{bh}, but somewhat less good for annual increments. Values for MAI in the cropped treatment would be considered 'poor' according to Jamieson et al. (1991), though as noted MAI and CAI in particular are most likely to deviate from the actual values as they are heavily influenced by annual variation. Conversely, the nRMSE for volume was under 10% indicating an excellent fit to the data despite deviations in the early years of growth (Figure 8.13). In addition, the *d*-index values are uniformly greater than 0.9 except in the case of CAI (Table 8.8).

Model outputs for volume were further analysed by regression (Figure 8.12) indicating only small deviations from the 1:1 line. In addition, correlation coefficients (R^2) for each of the linear models were uniformly 0.99 or greater.

8.4.3 *Crop modelling*

One important question arising from the changes to the soil evaporation values, is whether or not this has marked effect on the ability of the model to predict crop yields. No changes were made to the crop profiles, so crop productivity in the Silsoe and Leeds models have simply been compared to a reference scenario based on Graves et al. (2010).

As can be seen in Figure 8.14, changes to the soil parameters have had negligible effect on crop productivity in the arable control; output values remain identical to the reference values. Some small reduction in yield is evident in the cropped treatments, however these reductions seem to have improved the quality of the model fit for some years; certainly it does not appear that changes to the fit of the crop outputs are significantly worse.

6 Data from 2005–2012 were kindly provided by Dr. David Pilbeam, Leeds University.

7 Some measurements indicated that the trees had declined in height from one year to the next, these were replaced with `NA`. Removal of so many values from the data affected the yearly means so as to make them implausible (less than the previous year), hence the final three years of height measurements in the fallow treatment were removed entirely.

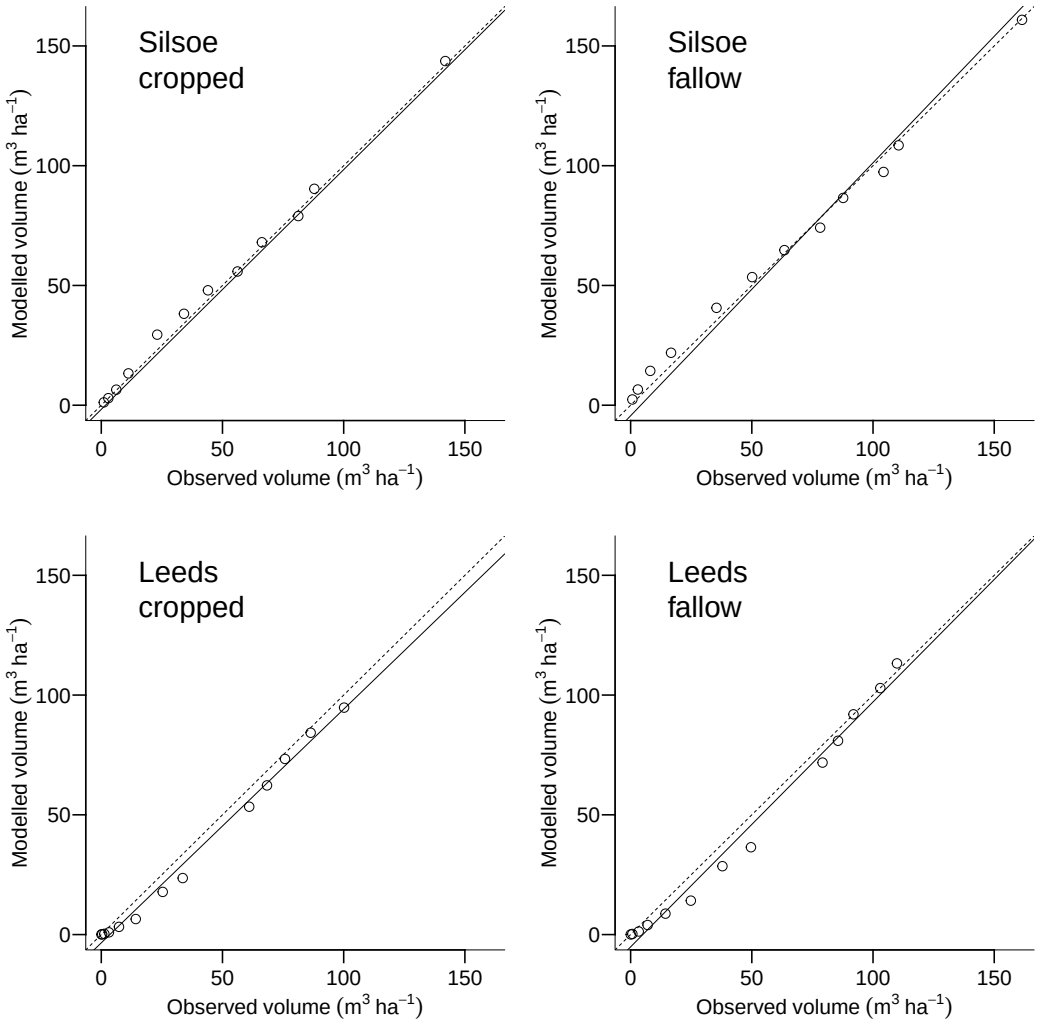

Figure 8.12: Regression of observed and Yield-SAFE outputs for volume from the cropped and fallow treatments at Silsoe and Leeds. Dashed line follows a 1:1 relationship, solid line indicates the actual regression between observed and expected.

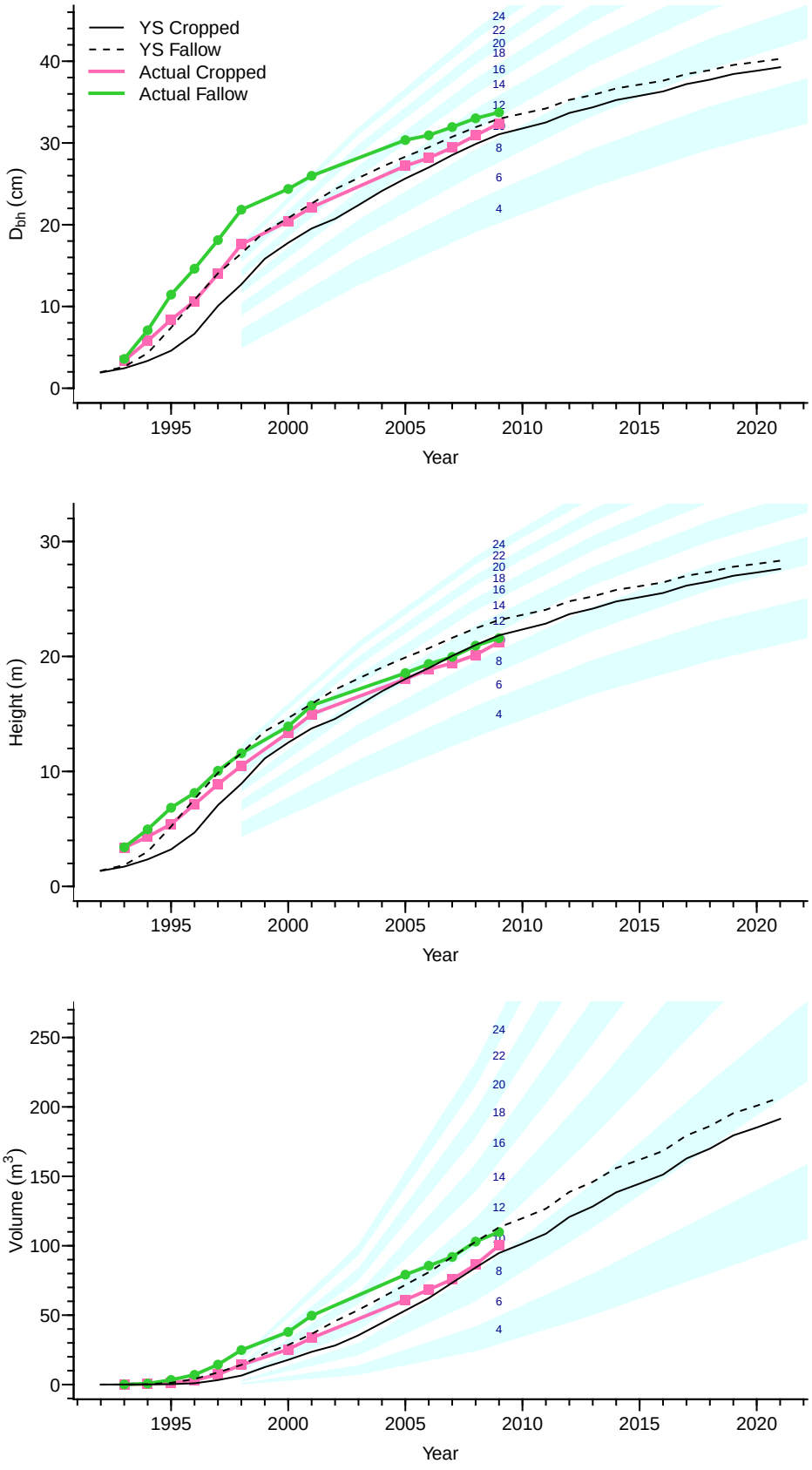

Figure 8.13: Comparison of diameter at breast height (D_{bh}) (cm), height (m), and volume (m^3) from actual measurements taken at the Leeds silvoarable trial, and outputs from Yield-SAFE parameterised using data from the Silsoe silvoarable trials.

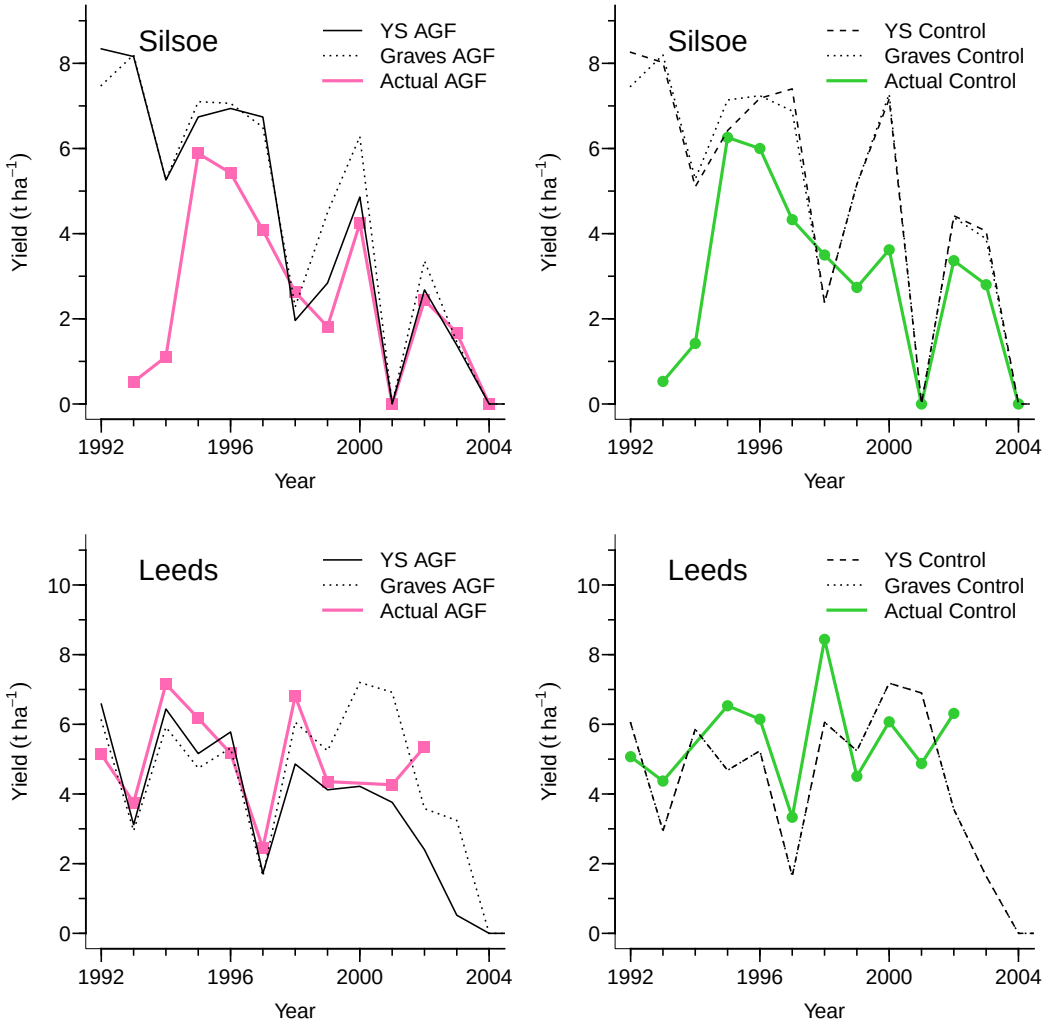

Figure 8.14: Comparison of Yield-SAFE outputs for crop yield and actual observed crop yields in the control and cropped treatments at the Silsoe and Leeds silvoarable trials. Yield-SAFE outputs derived from the poplar tree and soil parameters used by Graves et al. (2010) are included for reference. Note that no crop was grown in 2001 at Silsoe, and yields were particularly poor at Silsoe in 1993 and 1994.0

8.4.4 *Carbon storage*

Carbon storage values output by Yield-SAFE tended to be lower than the actual values collected from trees destructively sampled at Silsoe. In both the cropped and the fallow treatment however, modelled values lay within one standard deviation and the 95% confidence intervals of the observed means (Figure 8.15).

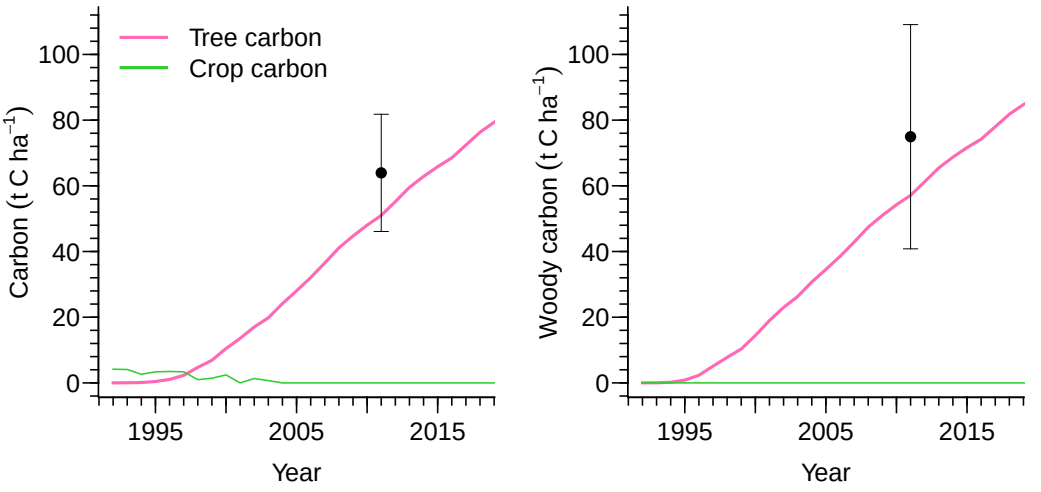

Figure 8.15: Carbon accumulation in the tree (above and belowground) and crop components as predicted by the Yield-SAFE model using parameters listed in Tables 8.3 and 8.3. Actual mean and 95% confidence intervals from destructive harvests conducted at the Silsoe silvoarable trial have been included.

Table 8.9: Effect of the assumed decomposition coefficient (k_d) and the associated longevity of product (years) on maximum and mean C storage in trees and woody products (t C ha^{-1}) in the cropped and fallow treatments.

		Cropped		Fallow	
k_d	Years	Max	Mean	Max	Mean
0.50	10	65.2	24.5	69.2	27.4
0.20	25	65.2	28.3	69.2	31.5
0.11	50	67.2	28.9	71.3	31.8
0.05	100	79.6	30.2	84.5	32.9
0.03	150	95.3	32.4	101.1	35.1

From Yield-SAFE outputs, it is possible to predict that the trees in the cropped and fallow treatments would have sequestered 82.0 t C ha^{-1} year^{-1} and 87.3 t C ha^{-1} year^{-1} over the course of a 30 year rotation. This equates to 2.7 and 2.9 t C ha^{-1} year^{-1}. Taken as a hundred year average however, assuming three consecutive rotations of thirty years each, this would equate to a mean storage at the site of just 20.0 t C ha^{-1} in the cropped treatment, and 22.6 t C ha^{-1} in the cropped treatment.

Including root residues remaining from harvests and woody products with different assumed longevity (between 10 and 150 years) increases the hundred year

mean carbon storage to between 24.5 and 32.4 t C ha^{-1} $year^{-1}$ and 27.4 and 35.1 t C ha^{-1} $year^{-1}$ from the cropped and fallow treatment respectively (Table 8.9).

Values assuming the 10, 50, and 100 year lifetime of woody products are presented in Figure 8.16 for the cropped treatment only. Crop carbon is included in these plots assuming a five year lifetime of harvest carbon, although these values are not included in those quoted in Table 8.9.

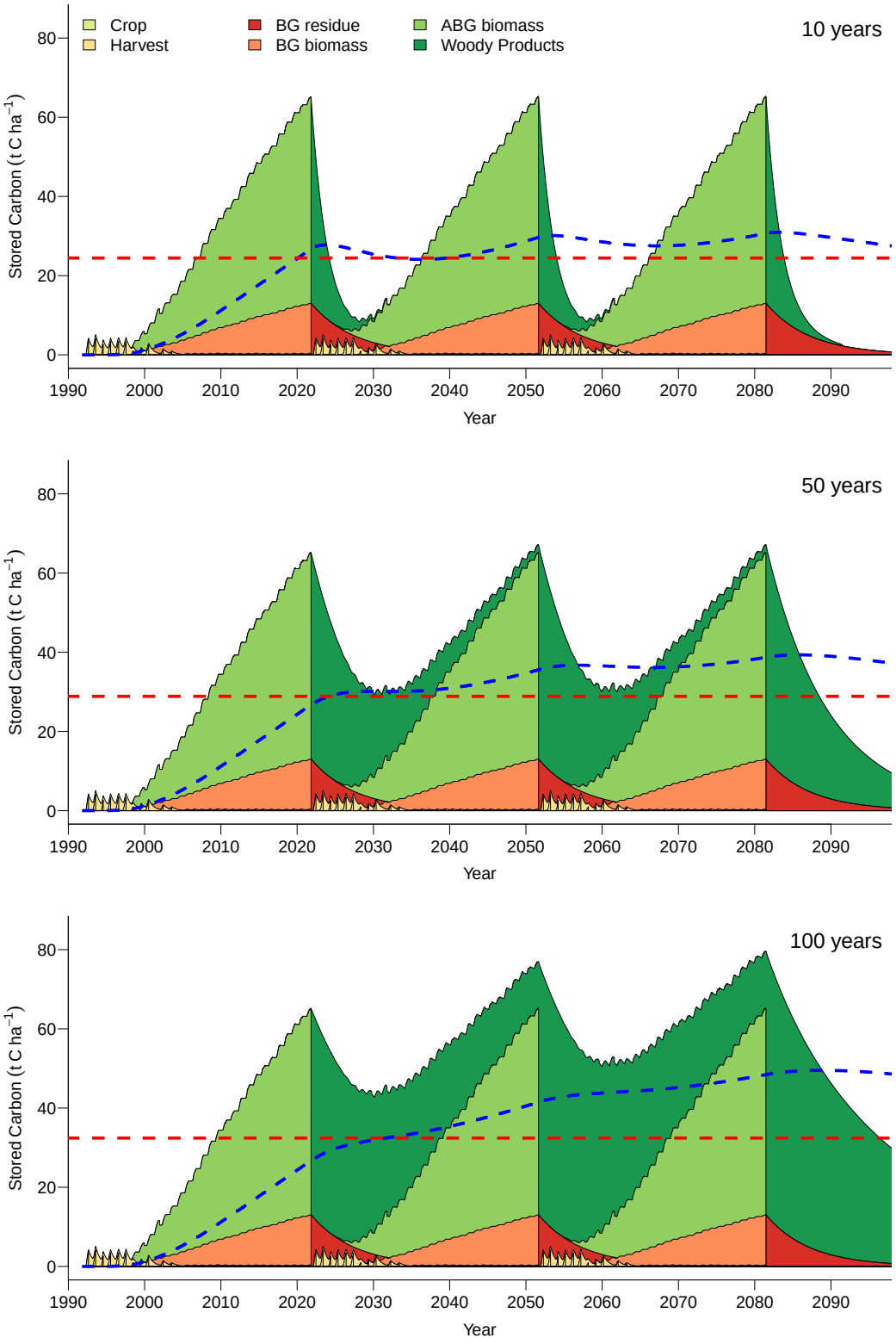

Figure 8.16: Three carbon fate scenarios assuming a woody product life of 10 (top), 50 (middle), and 100 (bottom) years, based on Yield-SAFE outputs from the cropped treatment at Silsoe. Dashed red line indicates hundred year mean carbon storage (t C ha^{-1}). Dashed blue line indicates cumulative mean carbon storage (t C ha^{-1}).

8.5 DISCUSSION

8.5.1 *Calibration and validation*

Analysis of Yield-SAFE outputs indicates that calibration and validation of the model to fit observed data was largely successful. Successful validation indicates that increasing the sensitivity of trees to water stress was justified, and that without doing so neither data from Silsoe nor Leeds could be accurately modelled in terms of the differences between cropped and fallow treatments. This discovery is potentially important for future work using the Yield-SAFE model.

The results also indicate that including functions to take account of root growth are justified, indeed model outputs are (at least initially) highly sensitive to this parameter, and allow the early stages of growth to be more accurately modelled. Above ground, canopy models have made use of leaf area index and a light extinction coefficient to describe the capacity of leaves to intercept solar radiation. It is logical that the capacity of roots to intercept water is also a function of the fine root length, and an analogous water extinction coefficient.

Indeed, results presented in Table 4.3 (Chapter 4) demonstrates the development of (coarse) roots with increasing age, and it is likely that there is a similar development of fine root penetration, whilst Nixon et al. (2001) note of a tea crop that responses to drought in young and mature plants are driven to a large extent by greater root penetration at depth. The inclusion of a root growth function thus allows for these effects to be modelled for the first time in Yield-SAFE.

Note that there is relatively poor agreement (at least for D_{bh}) between the model and observed for the early growth period at the Leeds site. This could potentially have been corrected by adjustment of the extinction coefficient k_r parameter, at the expense of the fit with Silsoe data. However, the later part of the growth curve and particularly volume measurements were excellent, despite early inconsistencies.

8.5.2 *Tree growth predictions*

Model outputs continue the trend noted in Chapter 7: despite initially promising growth rates, the performance of the trees declined markedly at both the Silsoe and Leeds sites.

At Silsoe, the model predicts that after thirty years, trees in the cropped treatment would be of yield class 8. Following the predictions of yield tables based on the final measurements in 2011 (Figure 8.11), this indicates that 19 years after planting, yield tables (Christie, 1994) over-estimate growth by four and two yield classes in the fallow and cropped treatments respectively. Note that the final values predicted by Yield-SAFE are close to the current maximum MAI (Table 8.7) indicating that at the time of measurement aged 19 years, trees in the fallow treatment have already reached their maximum rate of growth, whilst trees in the cropped treatment were close to it.

At Leeds, Yield-SAFE predicts that the trees will attain a yield class of six and seven for the cropped and fallow treatment respectively. This is also a substantial reduction from the yield class ten for volume predicted by yield tables for trees of

this size. All predicted yields are well below the yield class 14 for Silsoe and 12 for Leeds predicted by Burgess et al. in 2003.

At both sites, Yield-SAFE predicts that the volume difference between the cropped and fallow treatments after 30 years would be less than 1 $m^3\,ha^{-1}$ (Table 8.7), and that the magnitude of this difference remains relatively unaltered since the trees were about 10 years old. Whilst the fallow cannot be considered as a true forestry control, as it is likely that many more trees would be planted and then successively thinned (Christie, 1994), and because a true forestry control would not be ploughed to maintain a bare fallow; this finding is positive for silvoarable agroforestry, as it indicates that over the whole rotation arable cropping for ten years had relatively little influence on tree yield.

8.5.3 *Biological rotation age*

The biological rotation age is the age at which the CAI and MAI intersect, and marks the point at which it would be more economic in terms of volume accretion (and not necessarily market value) to harvest the trees and replant.

Outputs from Yield-SAFE suggest that the biological rotation age for the Silsoe trees varies with treatment (Figure 8.10). In Figure 8.10 CAI is presented as annual values for the purposes of model fitting, but more generally CAI is calculated as a rolling mean over a longer period to smooth inter-annual variations. When CAI is calculated as a two or three year rolling mean (not pictured), the biological rotation age in both treatments at both sites is approximately 29 years; if a larger period is used, the biological rotation age is not reached over a 30 year model run.

8.5.4 *Carbon storage*

Although still a highly simplified model, the presentation of hundred year average values provides a better estimate of carbon storage than a simple record of total carbon accretion in woody tissues.

With the exception of the soil, the majority of carbon stored in a plantation is within woody tissues, which are almost entirely removed at the end of the rotation, under a traditional clear-fell – replant system. Since the amount of carbon stored in each rotation is fairly constant, the most important factors that affect the rate of carbon storage are the rate at which tree roots decompose, and the rate at which woody products are returned to the atmosphere as CO_2. As can be seen from Table 8.9, an order of magnitude increase in the lifetime of woody products derived from tree harvest results in only a relatively small increase in the total carbon storage at the site. This difference will increase however over subsequent rotations until stabilising, so long as the longevity of woody products is greater than the subsequent rotation length (Figure 8.16).

Prioritising high quality timber that is likely to be turned into durable woody products with a long lifetime, is therefore a determinant factor in the efficacy of tree planting in agroforestry systems for carbon storage. Of greater importance is undoubtedly *carbon substitution* – i.e. substitution of timber for more carbon intensive materials. Perez-Garcia et al. (2005) indicate for example, that the reductions

in greenhouse gas (GHG) emissions from the substitution of pine for concrete in the building industry could be twice as great than the carbon stored in the forest stand before harvesting. Whilst methodologically difficult, these calculations would be necessary to gain a true understanding of the carbon storage potential of agroforestry systems.

Other improvements to these calculations might include estimates of carbon storage in leaf litter, validation of root matter decay, and the use of future climate data (e.g. from the EU ENSEMBLES project). A carbon accounting 'bolt-on' to Yield-SAFE could also take account of changes in soil carbon: linking Yield-SAFE outputs to an existing soil carbon models, for instance RothC may be an option.

Hypothesis

6. Using traditional forestry yield tables to predict the growth of trees in agroforestry systems and farm woodlands (which are typically planted at much wider spacings) will over-estimate yield.

Model predictions mde in this chapter corroborate the results from Chapter 7 which indicate that the Christie (1994) yield tables are not appropriate for the silvoarable agroforestry system at Silsoe, or Leeds. The reasons behind this are not clarified in this chapter, but it is possible that annual disruption of surface roots by cultivation of the arable rows may have had an impact. It is also possible that the Christie (1994) yield tables over-estimate yield in all cases.

9

ASH GROWTH PATTERN

This chapter is concerned with measurements of ash trees planted on former agricultural land in Bedfordshire. Data from mensuration and destructive harvests are presented and compared to existing yield tables. Allometric models for above-ground mass and carbon content of ash trees are presented.

9.1 HYPOTHESES

This chapter aims to falsify the following hypothesis.

Hypothesis

6. Using traditional forestry yield tables to predict the growth of trees in agroforestry systems and farm woodlands (which are typically planted at much wider spacings) will over-estimate yield.

9.2 INTRODUCTION

One of the ways in which farms in the UK have diversified in the latter part of the 20thcentury is by planting farm woodlands (Ilbery, 1991). This was encouraged by the introduction of the Farm Woodland Scheme by the Forestry Commission in 1988 (Forestry Commission England, n.d.) in anticipation of changes to the Common Agricultural Policy (Evans and Ilbery, 1992). Many of these woodlands tended to be 'minimum intervention woodlands': woodlands planted at a lower-than-usual density than forestry systems – usually around 2–3 m. Such systems do not require the same level of management as more dense forestry systems, and hence are more appropriate for farms. The grant scheme favoured native broadleaf planting on arable or improved grassland, offering the greatest amount, and the longest duration of payments for this type of woodland (Forestry Commission England, n.d.).

As concern has grown about the possible impacts of climate change, interest in the potential C storage of these woodlands has grown. In 2011 the Woodland Carbon Code (WCC) was launched by the Forestry Commission to allow the validation of current and expected C storage within woodlands. At present, the WCC has registered 202 projects covering 15 400 ha of woodland, with an expectation that these woodlands will sequester 1.6 million t C (Darot, 2014). Most of the projects registered so far have been to create mixed native broadleaved species, planted at spacings of 2.5–3.0 m, with a mean area of 19 ha (Morison, J., personal communication, 14 February 2014).

Whilst a number of methods of quantifying the C storage in these new woodlands are presented (Jenkins et al., 2011), some of the methods proposed rely on

the use of existing yield-tables. Yield tables rely on the 'site-index hypothesis' – the notion that stand mean height can be used as a measure of site productivity, and are a widely used by foresters and scientists (Skovsgaard and Vanclay, 2008). Yield-tables tend to have been designed for monitoring the stocks of dense forest plantations (Hamilton, 1996), but there is evidence that low stem densities may affect tree height, and that initial reductions in volume accretion due to wide spacing may not be recovered in later growth (Skovsgaard and Vanclay, 2008).

Quantification of C stocks in standing trees can also be conducted by applying allometric equations, which produce estimates of biomass based on proxy measurements, for example height, or stem diameter. One limitation of these models is that they are not generic, and should not be generalised for different species or for values outside the range used for calibration (Picard et al., 2012). Hence, if allometric models are to be widely applied for C quantification appropriate allometric equations must be developed.

In this chapter, measurements of ash trees from a number of recently planted woodlands on agricultural land are presented. These measurements are compared to Forestry Commission yield tables, and allometric equations developed for the quantification of ash tree biomass in widely spaced woodlands.

9.3 METHODS

9.3.1 *Selection of field sites*

In early 2012, three landowners gave permission for the use of their land for sampling of ash trees. These were Bedford Borough Council[1], the Forest of Marston Vale[2], and the Woodland Trust[3].

In total, eight woodlands were selected from a total of about twelve that were made available. The eight that were selected are summarised in Table 9.1, giving a range of ages from 7 to 21 years. Sites with trees planted at fixed spacing were favoured over variable spacing, to reduce variability in growth pattern.

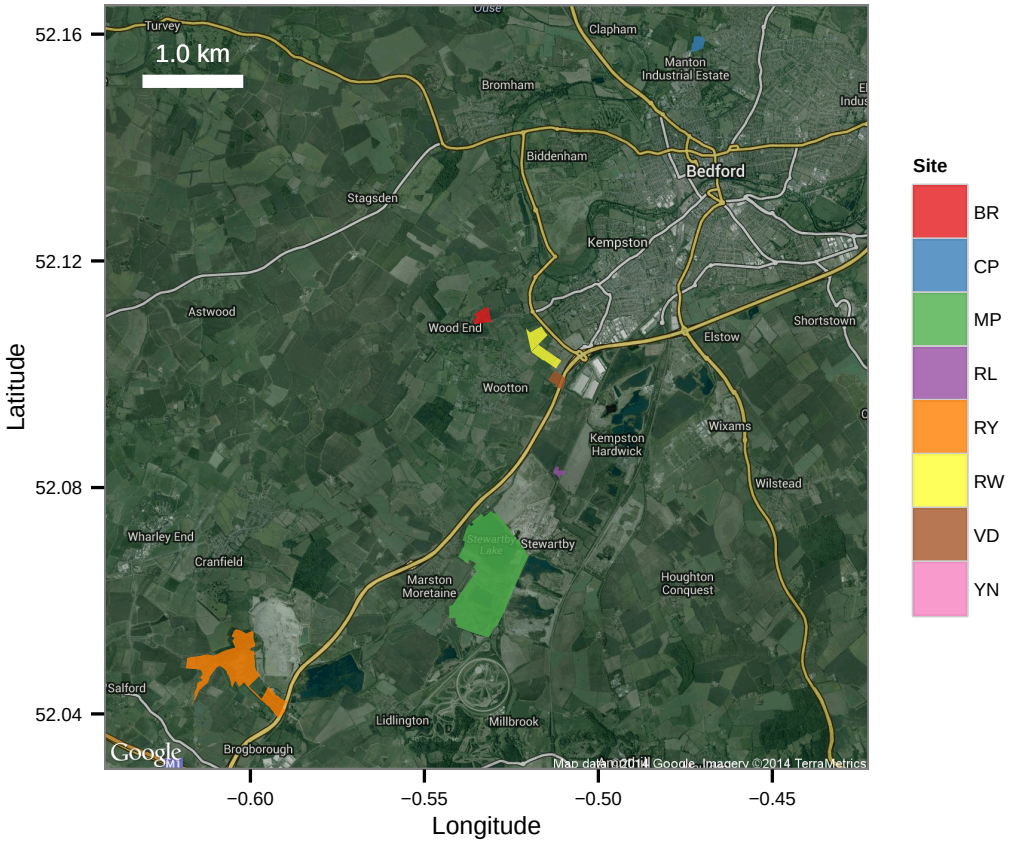

Figure 9.1: Location of the field sites used in sampling: Buttons Ramsay (BR), Clapham Park (CP), Millennium Country Park (MP), Randall's Farm (RL), Reynold's Wood (RY), Ridgeway Wood (RW), van Diemen's land (VD), and Yelnow New Wood (YN). Map data: Google © 2014 TerraMetrics

All sites were identified as belonging to soil series which contained a large proportion of clay (Table 9.2). This was confirmed by particle size determination (PSD), which classified most sites as 'clays', but two as 'clay loams' (Figure 9.2).

1 http://www.bedford.gov.uk/
2 http://marstonvale.org/
3 http://www.woodlandtrust.org.uk

Table 9.1: Details of field sites at which ash data were collected. Age refers to date of planting. BBC = Bedford Borough Council, FMV = The Forest of Marston Vale, WT = Woodland Trust.

Site name	Abbrev.	Age (years)	Spacing (m)	Owner
Buttons Ramsey	BR	7-8	1.25-5.0	FMV
Ridgeway Wood	RW	7-8	1.25-5.0	FMV
van Diemen's Land	VD	9-10	2.1	FMV
Clapham Park	CP	13-14	2.0-3.0	BBC
Millennium Country Park	MP	13-14	2.1	FMV
Randall's Farm	RL	18-19	2.2	BBC
Reynold's Wood	RY	18-19	3.0	WT
Yelnow New Wood	YN	20-21	3.0	BBC

Table 9.2: Results from PSD using the pipette method for the eight field sites: soil textural composition (to fine (0.06-0.2 mm), medium (0.2-0.6 mm), and coarse (0.6-2.0 mm) sand fractions. Sand refers to the total sand fraction (0.06-2.0 mm), whilst silt and clay refer to fractions 0.002-0.06 mm and <0.002 mm respectively. Soil series data were extracted using the NSRI LANDIS database (e.g. NSRI, 2012). For each site $n = 3$, except Clapham Park, were $n = 72$ (see Chapter 3, p.50).

Site	Series	Sand C	Sand M	Sand F	Sand	Silt	Clay
BR	Hanslope	9	23	13	45	24	31
CP	Evesham	3	12	11	26	32	42
RL	Evesham	1	9	4	15	1	84
RW	Evesham	4	17	11	33	27	41
RY	Hanslope	6	24	15	45	26	29
SH	Denchworth	3	7	12	22	30	48
VD	Evesham	3	16	10	29	29	42
YN	Hanslope	4	13	25	42	16	43

9.3.2 *Tree mensuration*

Comprehensive measurements of ash (*Fraxinus excelsior*) trees were taken in July-August 2012 at all sites listed in Table 9.1. One of the challenges related to sampling ash trees at these sites was that they were not plantations consisting solely of ash trees, but generally native broadleaf mixes generally comprising a range of species including oak (*Quercus robur*), birch (*Betulus* spp.), lime (*Tilia* spp.), field maple (*Acer campestre*), hawthorn (*Crataegus* spp.), cherry (*Prunus avium*), and occasionally alder (*Alnus glutinosa*). At some woodlands, a range of shrubby species were also planted at the woodland edges. These species included blackthorn (*Prunus spinosa*), spindle (*Euonymus europaeus*), guelder rose (*Viburnum opulus*) and dogwood (*Cornus sanguinea*).

In general, trees were planted in a grid pattern at spacings of 2.0-5.0 m. At some of the sites planted by the Forest of Marston Vale, trees were planted in a 'variable matrix', meaning that trees were still in general planted within a grid pattern, but

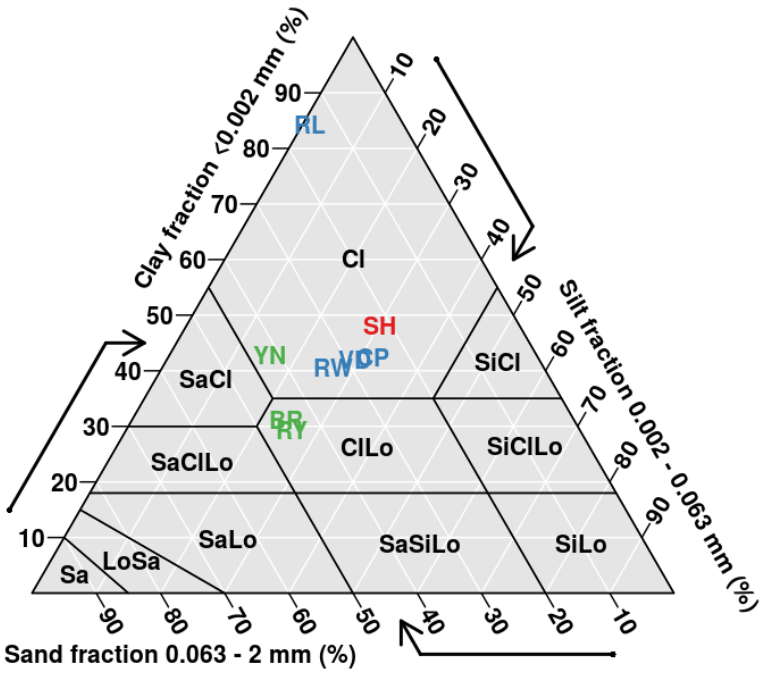

Figure 9.2: Soil texture triangle following the Soil Survey of England and Wales texture classification system. Site abbreviations follow the same pattern as Table 9.2. Text colour relates to the soil series to which soils at each of the sites belong: Red = Denchworth, Green = Hanslope, Blue = Evesham.

this grid pattern varied between 1.25-5.0 m, and incorporated open areas where no trees were planted at all.

Attempting to sample only the ash trees among these mixes was challenging, and made the use of a random sampling scheme difficult, hence a more systematic approach was taken. After an initial site visit to identify areas where ash trees were present, a number of transects were generated for each site bisecting these areas. These transects were then walked in the field with a map and compass, and ash trees within 3 m of either side of the transect were sampled for diameter at breast height (D_{bh}), diameter at 30 cm (D_{30}), height, and the number of adjacent trees (n_{adj}) present. D_{bh} was taken to be 130 cm above root flare, whilst n_{adj} was taken as a number between zero and eight relating to the number of trees present within the normal grid pattern on which the trees were planted. By recording n_{adj} it was hoped that it would be possible to capture the effect of the variable planting systems, by offering some measure of competition between trees (although ultimately this measure was not found to be useful).

Around 90 trees were measured at each site, with the exception of RL, RY, and CP. Fewer trees were sampled at RL due to constraints of the planting scheme which meant that only 74 trees could be sampled. More trees were sampled at RY since a high level of variation was observed at this site (possibly due to site topography), whilst additional trees were sampled at CP in order to effectively sample the two treatments described in Chapter 5.

Height was measured using a set of telescopic measuring poles (supplied by Forest Research) to the nearest cm. At both RL and RY, it was not always possible to measure the height of every tree, as larger trees exceeded the maximum height of the telescopic poles, but trees were planted too close together to accurately determine height using trigonometric methods.

Diameter was measured to the nearest mm using Masser[4] digital calipers provided by Forest Research. Two measurements of diameter were taken at right angles, and averaged to give a mean. Where trees were found to have two or more stems at 130 cm (or 30 cm – though this was much less common), each stem was was measured, and Equation 9.1 applied to the two measurements to produce a 'proxy' diameter measurement (British Standards Institute, 2012).

$$D_{bhmulti} = \sqrt{\sum_{i=i}^{n} d_i^2} \tag{9.1}$$

Data on the form of the tree can be extrapolated from diameter measurements, since it was recorded where co-dominant stems were present at D_{30} or D_{bh}. This is hereafter referred to as number of stems at 30 cm height (S_{30}) and number of stems at 130 cm height (S_{130}).

9.3.3 *Biomass sampling*

Using D_{bh} dbh data collected during tree mensuration, size classes were determined for biomass sampling. First, outliers were removed from the data, as determined by being greater or lower than 1.5 times the interquartile range than the $q_{0.75}$ and $q_{0.25}$. The $q_{0.33}$ and $q_{0.66}$ of the remaining D_{bh} values were calculated, and three size classes were determined by separating values above, below and between these values. This yielded nine values for D_{bh} which represented a cross-section of the sampled tree population (Table 9.3).

Trees which lay close to the D_{bh} values listed in Table 9.3 were identified at the appropriate site and felled. The height and D_{30} were recorded, and biomass partitioned into branch wood and stem wood. Canopy break was taken to be the point at which a main stem could not longer be distinguished, or the formation of a co-dominant stem, whichever came first.

Partitioned biomass was measured in-situ with a hand held balance precise to 50 g. Samples of stem wood were removed at 1, 1.3, 2, and 4 m, where possible. At least three branch samples were also collected (Figure 9.3b).

Trees at the minima and maxima of each size class identified in Table 9.3 were sampled in March-April 2013, before the trees had come into leaf.

4 Masser Oy, Jämytie 1, 96910 Rovaniemi, Finland (www.masser.fi.)

Table 9.3: Tree size classes as determined by D_{bh} measurements (mm), and approximate D_{bh} of three sample trees within each size class.

	Small			Medium			Large		
Site	Min	Med	Max	Min	Med	Max	Min	Med	Max
BR	8	28	32	34	36	41	43	48	67
CP	24	81	96	97	109	118	120	134	192
MC	28	61	76	78	91	101	103	115	156
RL	60	116	143	146	159	169	173	194	237
RW	6	9	12	14	15	18	20	22	39
RY	30	88	107	111	121	137	138	162	254
VD	15	24	27	29	31	33	35	37	46
YN	47	76	90	91	102	111	113	121	157

The intention was to complete a second round of sampling to measure the median tree from within each class, however time and labour constraints meant that it was not possible to complete the second round of sampling. No trees were sampled at RL or in the large class at RY, as these trees were found to be beyond the limits of what could reasonably be dealt with using hand tools.

In total 42 trees were destructively harvested from the planned 72. The actual D_{bh} values for these trees are included in Table 9.4. Note that all trees felled at the CP site were planted at 2.5 m spacing.

Table 9.4: Actual D_{bh} (mm) of trees sampled for biomass at each of the sites. Refer to Table 9.1 for site abbreviations. A zero indicates no data.

	Small			Medium			Large		
Site	Min	Med	Max	Min	Med	Max	Min	Med	Max
BR	23		33	34		41	42		68
CP	58	70	98	99	107	142	117	130	150
MC	50		72	80		77	104		116
RW	12		13	16		18	20		35
RY			87	109		132			
VD	12		30	27		49	35		46
YN	43		96	95		110	114		157

9.3.4 *Tree ring analysis*

Before felling a D_{bh} line was marked on each stem, and a 2-3 cm disk cut from each sampled tree, encompassing this line. Samples were immediately placed into a sealed plastic bag, and returned to the lab for refrigeration to prevent drying.

Three radii were selected at 120° from each other, and surface layers of the slice removed with a scalpel along these radii, in order to expose the rings more clearly. A series of digital images were then taken using a digital microscope[5] incorporating a scale object of known size. Using the software ImageJ (Rasband,

5 http://www.veho-world.com/

(a) Clockwise from top left: helmet, gloves, first aid kit, Japanese saws, digital balance, secateurs, hand held computer, large scale aerial photo, and felling wedge.

(b) For sampling purposes a 'step' cut was made at a height of 1 m, rather than a traditional felling cut at ground level.

Figure 9.3: A selection of hand tools used for biomass quantification (a), and making the first cut in a tree at Millennium Country Park (b).

2013), the width of each ring and the bark was calculated taking the scale object as a reference.

In order to ascertain a D_{bh} for a given age of the tree, an average of the values obtained from the three radii was used, then doubled. In order to calculate the expected bark width at a given age, a Michaelis-Menten function was fit to the under-bark diameter and bark width based on 72 measurements of branch and stem wood ranging from 1.3 to 147.0 mm underbark wood diameter. These measurements were taken exclusively from samples collected in April 2013 from sites MP, and YN, as it was not possible to accurately seperate wood from bark on samples taken prior to this (Figure 9.4a).

It was also necessary to establish a relationship between dry and wet wood diameter, as the first two slices, from trees 3 and 7 at CP, were erroneously dried at 105°C, and hence had shrunk. This relationship was established from 56 samples from trees collected at sites BR, CP, RW, and VD, which varied from 3.1 to 105.6 mm wet diameter (Figure 9.4b).

9.3.5 *Moisture content and specific gravity*

The moisture content of stem wood, stem bark, branch wood, and branch bark was calculated from samples collected at sites RY and MP. It was not possible to accurately separate the bark from the wood of samples taken from other sites, as they were collected over winter. Removal of bark from trees cut in the spring was

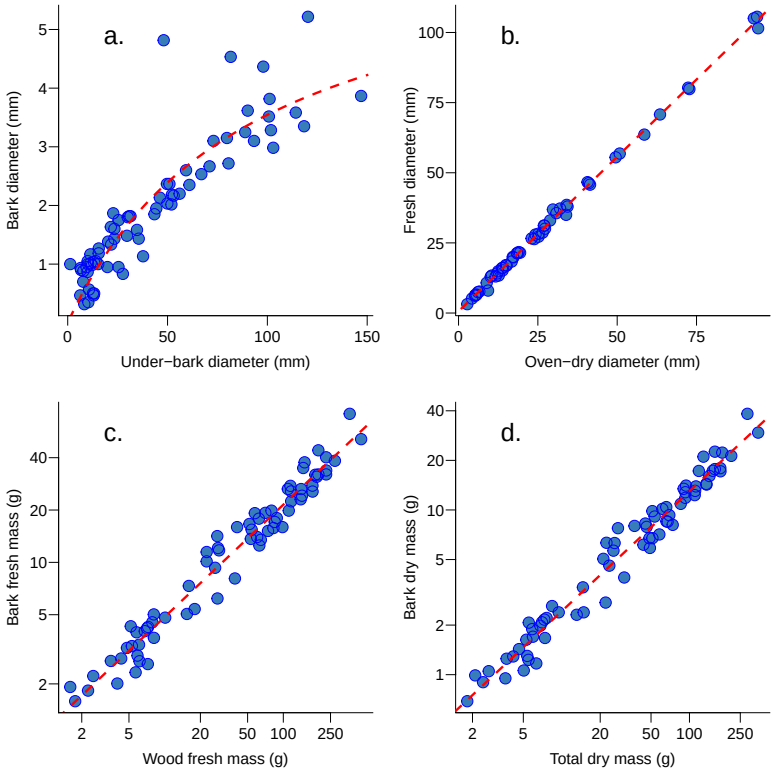

Figure 9.4: Ash bark diameter as a function of under-bark diameter (a.), and relationship between dry and wet diameter samples (b.), Ash bark dry mass as a function of dry under-bark (wood) mass (c.), and Ash bark dry mass as a function of total dry mass (d.). Dashed line in (a.) follows a curve described by a Michaelis-Menten function $y = ax/1 + \beta x$, where $\alpha = 6.841$ and $\beta = 92.997$, $R^2 = 0.92$. The regression line in (b.) follows the equation $y = 0.604 + 1.102x$, $R^2 = 1.00$. This relationship was used to translate the dry diameter of samples taken from trees 3 and 7 at Clapham Park into wet diameter, as tree ring measurements for these trees were completed after drying. Data in c. and d. have been plotted on $\log_{10}$ transformed axes. Regression lines follows the equation: $\log_{10}(y) = \alpha + \beta \log_{10}(x)$, where $\alpha = 0.04$ and $\beta = 0.646, \bar{R}^2 = 0.96$ (c), and $\alpha = -0.343$ and $\beta = 0.729, \bar{R}^2 = 0.97$ (d.).

facilitated by the movement of tree sap in the phloem directly between woody tissue and the bark.

Samples were weighed immediately on arrival at the laboratory, and again after drying to a constant weight at 105°C.

$$mc = \frac{(M_f - M_o)}{M_f} \tag{9.2}$$

M_f = fresh mass of sample in grams.
M_o = mass of sample in grams after drying in an oven at 105°C.

Basic specific gravity (G_b) of branch and stem sections (rings) was measured using the water displacement method using Equation 9.3 following the methods of Williamson and Wiemann (2010).

$$G_b = \frac{M_o / V_f}{P_{water}} \tag{9.3}$$

M_o = mass of sample in grams after drying in an oven at 105°C.
V_f = volume of fresh mass.
P_{water} = density of water (1 g cm^{-3}).

9.3.6 *Carbon content*

The proportional carbon content (C%) within each tree component (stem bark, stem wood, branch bark, branch wood) was determined by dry combustion using a Vario EL III Elemental Analyser[6]. The dried samples were ground to a particle size <0.5 mm with a flail grinder. A small amount of this sample was then weighed and packed inside a small foil envelope before oxidation at very high temperature in an elemental analyser.

Laboratory standard operating procedures (Appendix: A.5) were followed throughout.

9.3.7 *Data presentation and statistical analysis*

Statistical analyses were completed using the statistical development environment: R, version 3.0 (R Development Core Team, 2013). Analysis of variance was used to test for differences between groups, and model assumptions were checked using normality plots, histograms of the residuals and plots of residuals versus fitted values, created using commands in the basic R package.

Analysis of variance (ANOVA) was used to analyse the tree mensuration data, utilising the `aov()` function to compare the terms age, spacing, the number of neighbouring trees n_{adj}, number of stems at 130 cm height (S_{130}), and number of stems at 30 cm height (S_{30}). Interactions between the terms were also tested for. This was considered to be the 'maximal' model. Models were then simplified on the basis of the Aikake information criterion (AIC) following the model selection methodology detailed by Johnson and Omland (2004) and Crawley (2007).

Note due to the availability of field sites, this data were extremely imbalanced and non-orthogonal, meaning that a complete range of age × spacing interactions were not available (Figure 9.5). Analysis of D_{bh}, D_{30} and height, taking into account all sites was completed, however these results were badly confounded by the multicollinearity between the factors site, age, and spacing.

For these reasons, two further analyses were completed: a simple analysis of variance (ANOVA) considering only site (which remains confounded by age and spacing), and a more complicated model based only on data from the CP site. A maximal model involving the factors spacing, S_{130}, S_{30}, and the possible interactions was fitted to the data, and then simplified based on AIC until only the significant factors remained.

6 Elementar Analysensysteme GmbH, http://uk.elementar.de

Since trees were planted at four planting densities at CP: 2.0 m, 2.1 m, 2.5 m, and 3.0 m, it is possible to draw clearer conclusions about the impact of spacing from the analysis at this site. It should be noted however, that trees planted at 2.0 m spacing were in the silvopastoral blocks discussed in Chapter 5, and hence there remains a confounding influence. Treatment was not included as a factor (as in the soil carbon models), as it was implicit in spacing. In addition, tree height was not measured for trees spaced at 2.5 m.

Tree ring data were analysed using ANOVA incorporating a nested error term of the format age/site/tree/radius – where radius refers to one of three repeated measurements of ring width on each tree disc. This error term accounts for the pseudoreplication caused by the inclusion of all measurements at the tree and site level, and the temporal pseudoreplication inherent in the age term.

9.3.7.1 *Calculation of total organic carbon*

To calculate total organic carbon of each sample tree, mass of bark was first calculated for each tree component (branch and stem). A back-transformed log-log function (Equation 9.4), derived from regression (Figure 9.4), was used to estimate the proportion of each component that consisted of bark. This equation incorporates a correction factor (explained in more detail in section 9.3.7.2).

$$M_b = aM_t^b CF \tag{9.4}$$

M_b = estimated bark fresh mass.
M_t = total sample fresh mass.
a = 0.04
b = 0.646
CF = correction factor as Equation 9.8.

The resulting estimated bark mass (M_b) was then subtracted from total mass (M_t) to yield under-bark (wood) mass (M_w), (Equation 9.5)

$$M_w = M_t - M_b \tag{9.5}$$

Next, the dry mass (M_e) for each component was calculated using equation 9.6, using the appropriate moisture content (mc) for each tree component. From this, total carbon content for each component was calculated by multiplying the appropriate C% by the estimated dry mass M_e.

$$M_e = 1 - mc \times \ M_f \tag{9.6}$$

M_e = the estimated oven dry sample mass.

M_f = fresh mass of sample in grams.
mc = wood moisture content, calculated using Equation 9.2.

Total carbon content from each component was then summed.

9.3.7.2 *Biomass allometry*

The traditional allometric approach (Baskerville, 1972) was followed throughout for the modelling of allometric relationships. This approach applies a log-log linear model to the data (Equation 9.9), which is then back-transformed into a power relationship (Equation 9.10), and a correction applied CF, using the mean squared error (MSE) derived from the log-log model (Equation 9.7). Note that because the favoured transformation for this chapter has been log base-10, the mean-squared error of the regression must be converted to natural log prior to inclusion in the correction factor (Equation 9.8).

This correction factor is applied to correct biases in the regression error caused by the application of linear models on log transformed data (Baskerville, 1972; Mascaro et al., 2011; Sprugel, 1983)[7].

$$MSE = \sqrt{\frac{\sum(\log_{10} y - \log_{10} \bar{y})^2}{n-2}} \tag{9.7}$$

$$CF = e^{\frac{\log_{10} MSE}{2}} \tag{9.8}$$

$$\log_{10}(y) = \alpha + \beta \log_{10}(x) \tag{9.9}$$

$$y = \alpha x^{\beta} CF \tag{9.10}$$

Allometric models were established for the relationships between the independent variables: D_{bh}, D_{30}, and height (x in Equations 9.9 and 9.10), and the dependent variables: oven dry mass and carbon content of stem wood, stem bark, branch wood, and branch bark (y in Equations 9.9 and 9.10).

7 It is recognised that the nature of allometric relationships leads to an almost universal increase in variance with increasing diameter, hence future work would benefit from the inclusion of weighting to take account of this variant error structure (Mascaro et al., 2011). In addition, the use of non-linear models fitted following the methods of Picard et al. (2012) may improve model estimates. The evaluation of models which incorporate more than one variable as parameters may also yield more accurate results.

9.4 RESULTS

9.4.1 *Tree mensuration*

In total 952 trees were measured across the eight sites. Much variation in tree size was detected at the RY site, hence additional trees were sampled here. At CP, trees measured in a pilot study (without height measurements) were combined with trees measured in the later sampling effort, and an additional 74 trees were measured in the silvopastoral blocks.

Variation in tree size tended to increase with age, and was very large at some sites (Figure 9.5), particularly RY. Variation at this site may be to do with the varied topography of the site. Variance did not uniformly increase with age however, and site YN showed much more uniform growth than RY.

9.4.2 *Site, age and spacing*

9.4.2.1 *All sites*

Analyses showed that there were significant variations ($p < 0.001$) in the D_{bh}, D_{30}, and height of trees across all sites (Table 9.5). As noted in section 9.3.7, the factors site, age and spacing are strongly correlated, hence this observation is of limited value, and as a result significant differences ($p < 0.05$) were found between each site for all response variables (Table 9.6).

Table 9.5: Results from analysis of variance (ANOVA) of D_{bh}, D_{30}, and height for each site. Degrees of freedom and *F*-values are given with significance denoted by stars: $p <= 0.001$ (***), $p <= 0.01$ (**), $p <= 0.05$ (*). Note that it was necessary to $\log_{10}$ transform all response variables in order satisfy the usual normality assumptions of a linear model.

Term	DBH		D_{30}		Height	
	df	*F*-value	*df*	*F*-value	*df*	*F*-value
Site	7	694***	7	628***	5	997.28***
Residual	940		932		642	

9.4.2.2 *Clapham Park*

Analysis of variance ANOVA of tree mensuration data collected at the CP site, indicated that the response variables D_{bh}, D_{30} and height, were strongly correlated with tree spacing ($p < 0.001$), whilst D_{bh} and D_{30} were also strongly correlated with the presence of co-dominant stems at 130 cm ($p < 0.01$, Table 9.7).

Post-hoc tests completed on factors identified as significant, indicated that trees in the farm woodland (FW) treatment planted at a spacing of 2.1 and 2.5 m had significantly ($p < 0.05$) smaller diameters (both D_{bh} and D_{30}) than trees planted in the FW at 3 m spacing, and at 2 m spacing in the silvopasture (SP) treatment (Table 9.8). Conversely, trees planted at 2.1 m spacing were tallest ($p < 0.05$), no

Table 9.6: Mean, SE, and replication (n) for D_{bh}, D_{30}, and height at each site. Results from post-hoc testing is included as superscripts: means with different letters are significantly different. Values denoted with † were not included in the analysis. See section 9.3.7.

	D_{bh} (mm)			D_{30} (mm)			Height (cm)		
Site	Mean	SE	n	Mean	SE	n	Mean	SE	n
BR	37^{f}	1	94	55^{f}	1	94	375^{d}	7	94
CP	105^{c}	2	298	139^{c}	2	298	737^{c}	7	209
MC	90^{e}	3	88	127^{e}	4	76	793^{a}	15	73
RL	157^{a}	4	74	195^{a}	5	74	1128†	26	3
RW	16^{h}	1	88	28^{h}	1	92	199^{f}	5	92
RY	126^{b}	4	126	156^{b}	4	126	665†	21	20
VD	31^{g}	1	90	47^{g}	1	90	323^{e}	6	90
YN	100^{d}	2	90	127^{d}	3	90	780^{b}	15	90

Table 9.7: Minimum adequate models for D_{bh}, D_{30}, and height at the Clapham Park (CP) site, following simplification based on Aikake information criterion (AIC). Degrees of freedom and F-values are given with significance denoted by stars: $p <= 0.001$ (***), $p <= 0.01$ (**), $p <= 0.05$ (*). Note that it was necessary to $\log_{10}$ transform both diameter measurements in order satisfy the usual normality assumptions of a linear model. In addition, two outliers that showed uncharacteristically poor growth for the site were removed from the diameter models.

Term	D_{bh}		D_{30}		Height	
	df	F-value	df	F-value	df	F-value
Spacing	3	31.51***	3	37.34***	2	16.52***
S_{130}	3	6.21***	3	4.60**		
Residual	289		290		203	

difference being found between trees planted in the SP treatment at 2 m spacing, and trees planted in the FW treatment at 3 m ($p > 0.05$).

No clear patterns were established by post-hoc test results of D_{bh} and D_{30} in relation to S_{130}, although trees with two stems were found to have a larger ($p < 0.05$) D_{bh} than trees with three stems.

The proportion (%) of trees at the CP site with multiple stems at 130 cm (S_{130}) and 30 cm S_{30} are given in Table 9.9. Spacing was found by χ^2 test to have a highly significant ($\chi^2 = 17.34$, $p = 0.007$) effect on the number of stems at 130 cm height (S_{130}) and number of stems at 30 cm height (S_{30}) ($\chi^2 = 11.97$, $p = 0.006$): trees planted at a wider spacing tended to have more trees with multiple stems.

Table 9.8: Post-hoc tests results of spacing and S_{130} for D_{bh}, D_{30}, and height at Clapham Park (CP). Means ± standard error, and replication. Statistical significance is indicated by superscripts. Means with the same letter indicate a non-significant difference. Height measurements of trees at 2.5 m were not taken, whilst the effect of S_{130} on height was not tested.

	D_{bh} (mm)			D_{30} (mm)			Height (cm)		
Spacing	Mean	SE	*n*	Mean	SE	*n*	Mean	SE	*n*
2 (SP)	121^{a}	3	74^{a}	156	3	74	710^{b}	10	74
2.1	92^{b}	3	68^{b}	118	3	68	800^{a}	11	53
2.5	93^{b}	2	73^{b}	123	3	74	nd	nd	nd
3	113^{a}	3	81^{a}	158	4	81	731^{b}	11	79
S_{130}	Mean	SE	*n*	Mean	SE	*n*	Mean	SE	*n*
1	104^{ab}	2	147	132^{ab}	2	148	737^{ns}	9	100
2	111^{a}	3	106	146^{a}	4	106	743^{ns}	12	75
3	94^{b}	3	39	147^{a}	6	39	742^{ns}	19	27
4	108^{ab}	11	4	174^{a}	28	4	800^{ns}	19	4

Table 9.9: Number of trees with multiple stems at 130 cm (S_{130}) and 30 cm (S_{30}) at Clapham Park for each spacing (m)

	S_{130}			
Spacing	1	2	3	4
2.0 (SP)	46	24	4	0
2.1	36	24	7	2
2.5	39	25	10	0
3.0	28	33	18	2
	S_{30}			
Spacing	1	2	3	4
2.0 (SP)	73	1	0	0
2.1	60	9	0	0
2.5	64	10	0	0
3.0	64	15	2	0

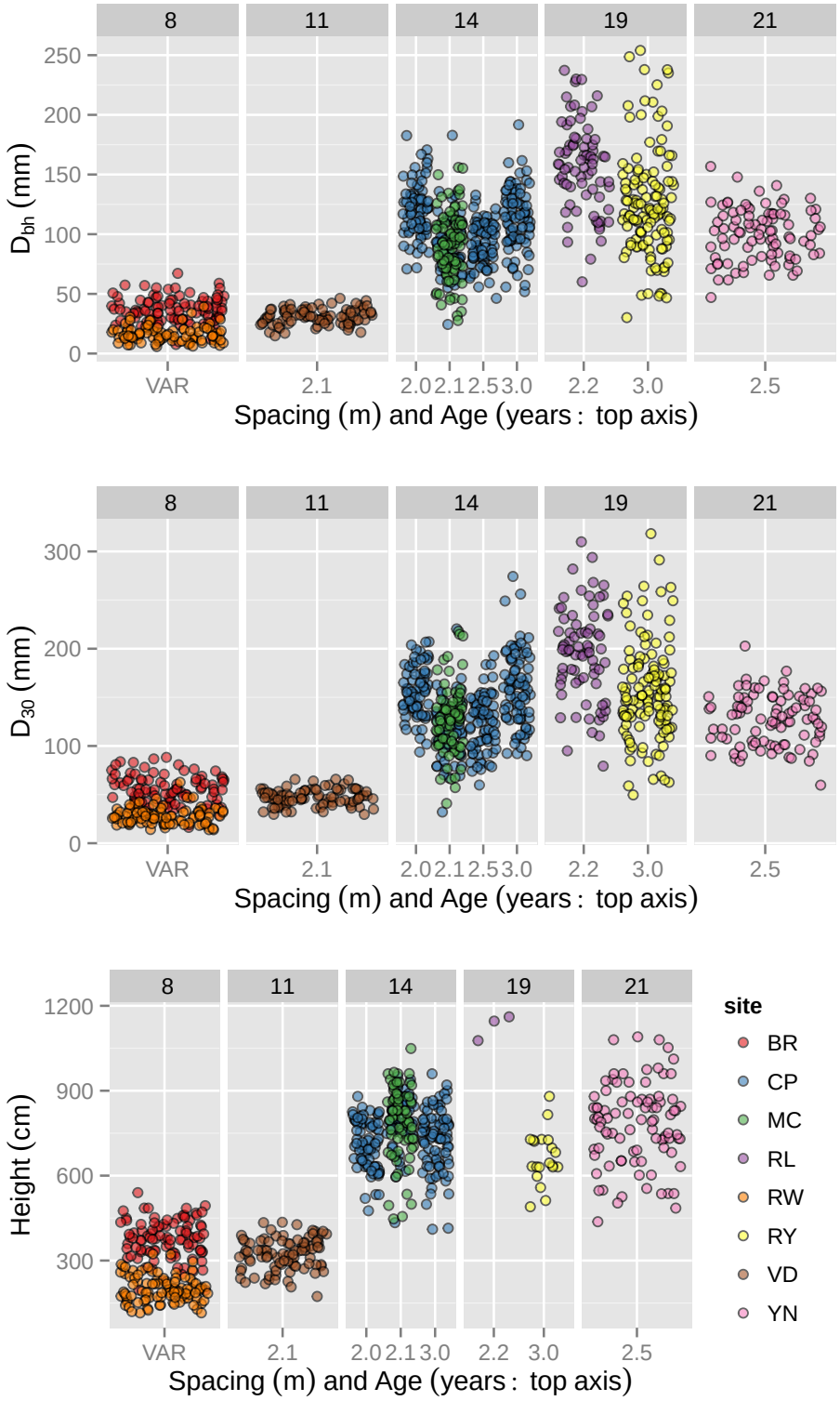

Figure 9.5: 'Jittered' plots showing D_{bh}, D_{30} and height as a function of tree age and tree spacing. Points are randomly distributed horizontally to alleviate crowding. Note that the size of trees at RY and RL meant that it was impossible to measure all but the smallest trees. Refer to Table 9.1 for site abbreviations.

9.4.3 *Tree ring analysis*

Tree ring widths varied between a minimum of 0.15 mm (consisting of just one row of early wood xylem) at the RW site, and a maximum of 9.11 mm at the CP site. Means of ring width measurements as D_{bh} are presented in Figure 9.6. Note that larger trees at sites RL and RY were not sampled for biomass, and hence were not available for tree ring analysis.

ANOVA of ring width measurements indicated that there were significant differences ($p < 0.001$) as a results of site[8]. Overall, the greatest ring widths were found at CP, whilst the smallest were found at site RW (Table 9.10).

Note that this analysis is confounded in that trees were of different ages when tree rings were measured, and although temporal pseudoreplication has been dealt with in the model, clearly a younger tree is likely to have smaller ring widths than an older tree. Furthermore, larger trees at sites RY were deliberately not sampled as they were beyond the range that could reasonably be dealt with by hand tools.

Table 9.10: Mean, SE, and replication of tree ring widths for each site (mm). results from multiple comparison tests are given as superscripts to the means. Difference letters indicates a significant difference.

Site	Age	Width	SE	n
BR	7-8	2.37^{cd}	0.12	125
CP	7-8	3.52^{a}	0.07	402
MC	9-10	3.26^{b}	0.11	194
RW	13-14	1.30^{f}	0.10	123
RY	13-14	2.51^{c}	0.09	201
VD	18-19	1.71^{e}	0.11	138
YN	20-21	2.27^{d}	0.07	354

Table 9.11: Maximum mean annual diameter increment MAI and age (years) for each site (mm year^{-1}), derived from tree ring measurements.

Site	Age	MMAI
BR	8	1.93
CP	14	5.16
MC	14	3.94
RW	8	1.14
RY	19	4.75
VD	10	1.51
YN	21	4.53

8 Anova table for this analysis is presented in Appendix E.1.

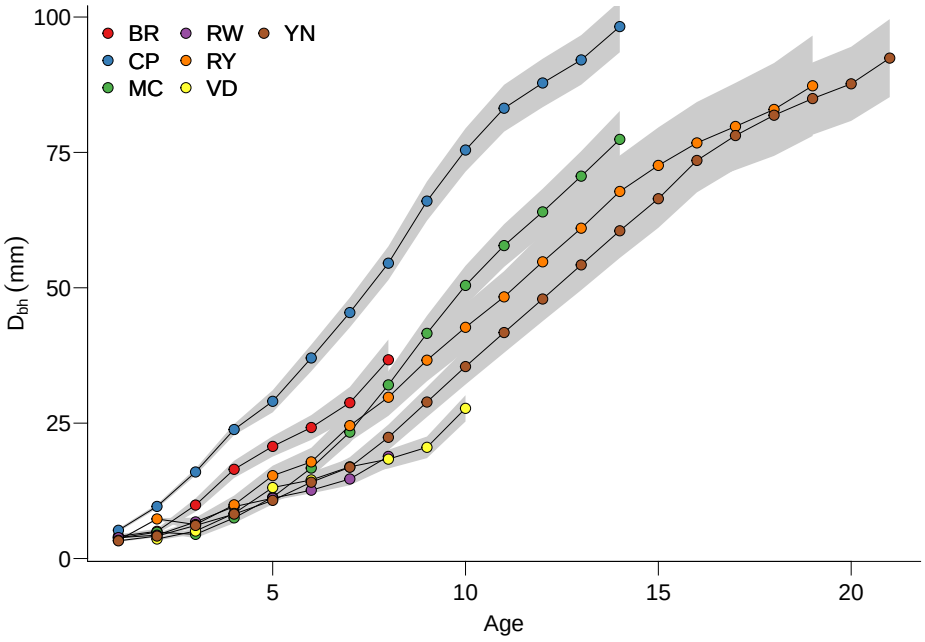

Figure 9.6: Mean D_{bh} for each site derived from tree ring measurements taken from trees sampled for biomass. At all sites $n = 6$, except RY ($n = 4$). Grey shading indicates standard error.

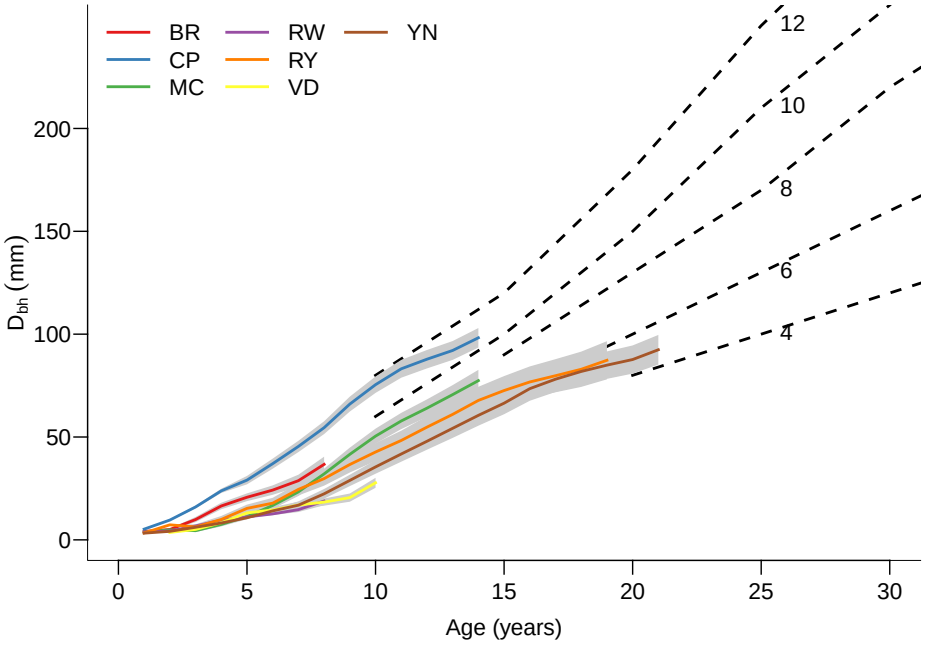

Figure 9.7: Mean D_{bh} for each site derived from tree ring measurements taken from trees sampled for biomass. At all sites $n = 6$, except RY ($n = 4$). Grey shading indicates standard error.Yield tables from the sycamore, ash, and birch (SAB) yield table are overlayed (Hamilton, 1996).

9.4.4 *Moisture and carbon content*

Moisture content for ash trees varied between 0.30 in the case of branch wood, and 0.67 in the case of leaves. Carbon contents were generally similar across woody tissues, and just under 50%. A summary of these results is given in Table 9.12.

Table 9.12: Mean, SE, and replication for moisture content (*mc*) carbon content (C%) of ash trees measured in 2012-2013.

Tissue	Mean	SE	*n*
Moisture content (*mc*)			
branch wood	0.304	0.003	42
stem wood	0.308	0.009	30
branch bark	0.513	0.005	42
stem bark	0.477	0.007	30
leaf	0.674	0.008	9
Carbon content (C%)			
branch wood	48.853	0.125	6
stem wood	48.636	0.108	6
branch bark	47.825	0.259	6
stem bark	47.783	0.241	6

9.4.5 *Total tree biomass and carbon*

Dry mass and carbon content of each tree component was calculated using the appropriate conversion factor. Results for mean total fresh mass, dry mass and carbon content for each site are given in Table 9.13. The mean proportion of total fresh mass, dry mass, and carbon content is given in Table 9.14.

Table 9.13: Mean, SE, and replication of total fresh mass, dry mass and carbon content of the above-ground components of the sampeld trees for each site.

	Fresh mass (kg)			Dry mass (kg)			C content (kg)		
Site	Mean	SE	*n*	Mean	SE	*n*	Mean	SE	*n*
BR	5.9	2.3	6	4.0	1.6	6	2.0	0.8	6
CP	58.0	11.3	10	39.9	7.8	10	19.4	3.8	10
MC	39.6	7.3	6	27.3	5.0	6	13.3	2.4	6
RW	1.7	0.6	6	1.2	0.4	6	0.6	0.2	6
RY	65.6	18.9	3	45.2	13.1	3	22.0	6.4	3
VD	5.3	1.5	6	3.6	1.0	6	1.8	0.5	6
YN	50.2	11.4	6	34.5	7.9	6	16.8	3.8	6

Table 9.14: Mean, SE, and replication of the proportion (%) of total fresh mass, dry mass and carbon content for each ash tree component.

Fresh mass (kg)	Mean	SE	n
Branch bark	2.3	0.2	43
Branch wood	35.8	2.0	43
Stem bark	3.4	0.4	43
Stem wood	58.6	1.9	43
Dry mass (kg)	**Mean**	**SE**	n
Branch bark	1.6	0.2	43
Branch wood	36.4	2.0	43
Stem bark	2.6	0.3	43
Stem wood	59.4	1.9	43
Carbon content (kg)	**Mean**	**SE**	n
Branch bark	1.6	0.1	43
Branch wood	36.5	2.0	43
Stem bark	2.5	0.3	43
Stem wood	59.3	1.9	43

9.4.5.1 *Ratio of branch mass to total mass(π_{branch})*

Field data collected at the CP field site was used to inform the ratio of branch mass to total mass (π_{branch}). Analysis of the data collected across the eight sampled sites indicated that a strong ($p < 0.05$) relationship existed between π_{branch} and age (Figure 9.8)[9]. This relationship is interesting as the value derived from the YN site was 0.54, indicating that more than half of the aboveground biomass was allocated to branch wood. This is in contrast with the 0.31 value determined for the 19 year old poplar trees at Silsoe, and probably reflects a lack of pruning and less apical dominance in the species.

Since it was unclear how far this relationship could be extrapolated beyond the data, the value of 0.54 taken from YN was used for π_{branch}.

Table 9.15: Model coefficients for regression of the ratio of dry branch to total mass (π_{branch}) compared to tree age. t-value is given with resulting p-value, denoted by stars: $p <= 0.001$ (***), $p <= 0.01$ (**), $p <= 0.05$ (*). Residual degrees of freedom (df), and Pearson's correlation coefficient (R^2) are also given.

Model	α	β	R^2	t-value	df
$\pi_{branch} = \alpha + \beta\ age$	0.20	0.01	0.21	3.07^{**}	35

9 Note that other independent variables, for instance spacing, and site, were excluded from this analysis to prevent their confounding effects, and hence it is not entirely clear how much of an impact these other independent variables have on this relationship.

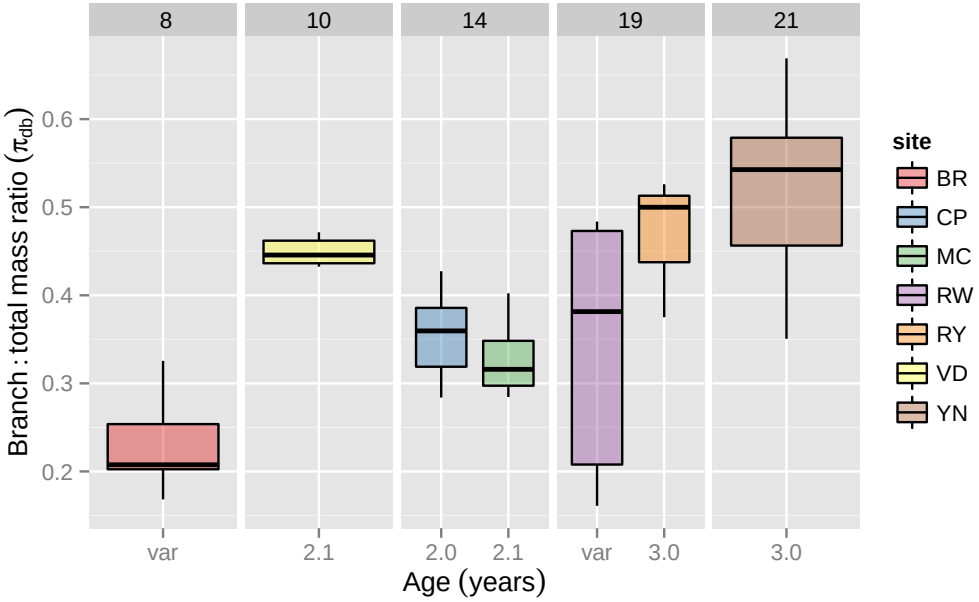

Figure 9.8: Ratio of dry branch mass to dry total mass (π_{branch}) as a function of age and spacing. In all cases $n = 6$, except at MP where one outlier was removed, and YN where $n = 3$.

9.4.6 *Allometric relationships*

9.4.6.1 *Tree height*

The correlations between D_{bh} and D_{30}, and height were found to be highly significant ($p < 0.001$). The D_{bh} model (Figure 9.9) was found to be a slightly better fit for the data in terms of R^2 (Table 9.16) than the D_{30} model (Figure 9.9).

Table 9.16: Model coefficients from log-log regression of D_{bh} (mm), D_{30} (mm), and height (cm). t-value is given with resulting p-value, denoted by stars: $p <= 0.001$ (***), $p <= 0.01$ (**), $p <= 0.05$ (*). Residual degrees of freedom (df), and Pearson's correlation coefficient (R^2) are also given.

Model	α	β	R^2	t-value	df
$\log_{10}(height) = \alpha + \beta \log_{10}(DBH)$	1.56	0.65	0.90	75.53^{***}	665
$\log_{10}(height) = \alpha + \beta \log_{10}(D30)$	1.26	0.75	0.87	65.95^{***}	659

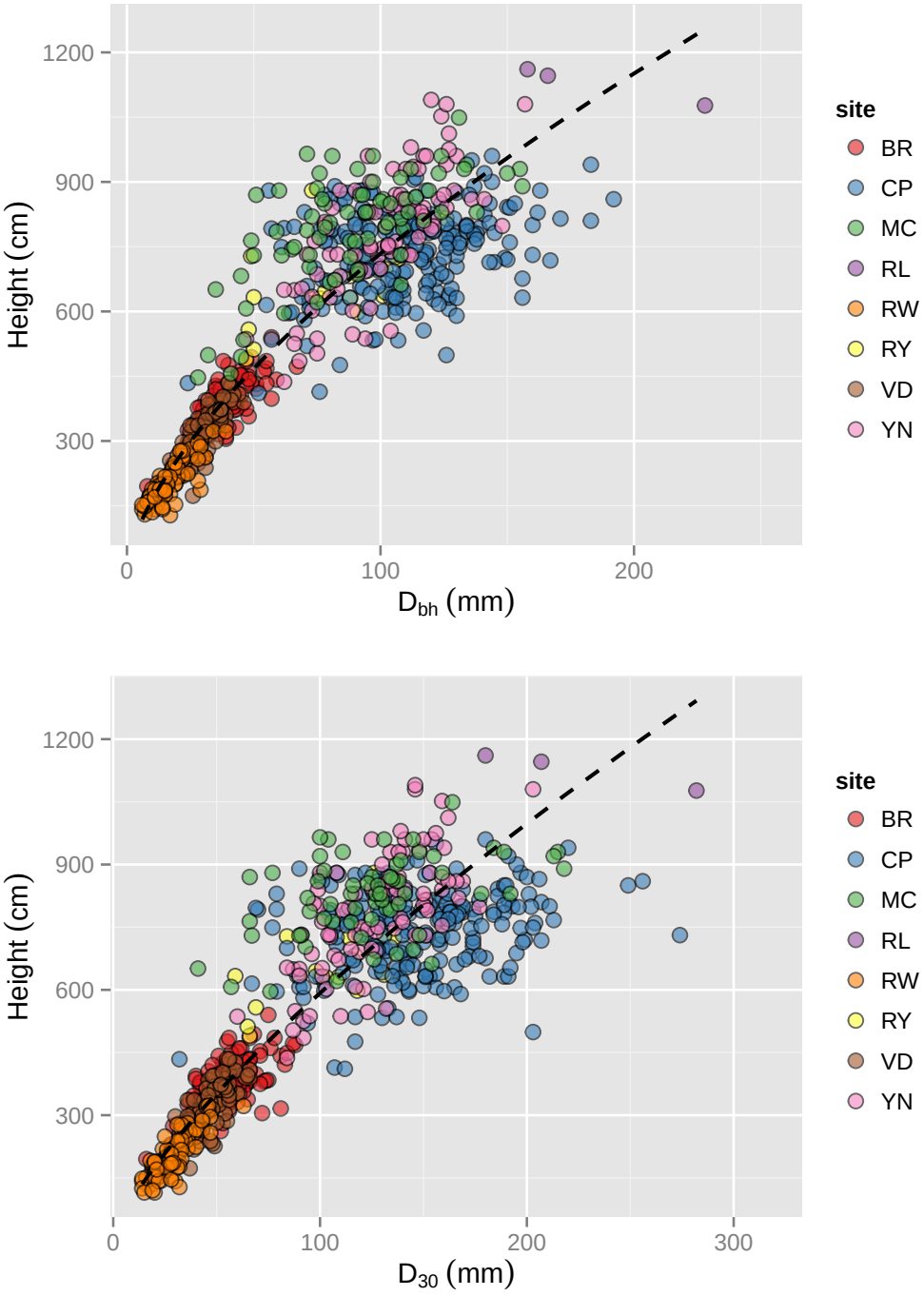

Figure 9.9: Ash height as a function of D_{bh} and D_{30} for all ash trees measured in 2012. The regression lines follow the equations $height = 36.57DBH^{0.65}$ ($R^2 = 0.8956$), and $height = 18.37DBH^{0.75}$ ($R^2 = 0.8684$). A correction factor using the mean squares error from the untransformed model (Equation 9.8), has been applied to correct for the bias resulting from the back-transformation of the log-log model (Baskerville, 1972; Sprugel, 1983).

9.4.6.2 *Dry mass and carbon content*

Histograms showing the distribution of ages and D_{bh} for all the destructively sampled trees are presented in Figure 9.10.

Highly significant ($p < 0.001$) allometric relationships were found between D_{bh}, D_{30}, and height (Figure 9.11), following the methods of Baskerville (1972). Of the dependent variables, D_{bh} was found to have the best fit with the independent variables based on R^2; coefficients from the log-log transformed models are given in Table 9.17.

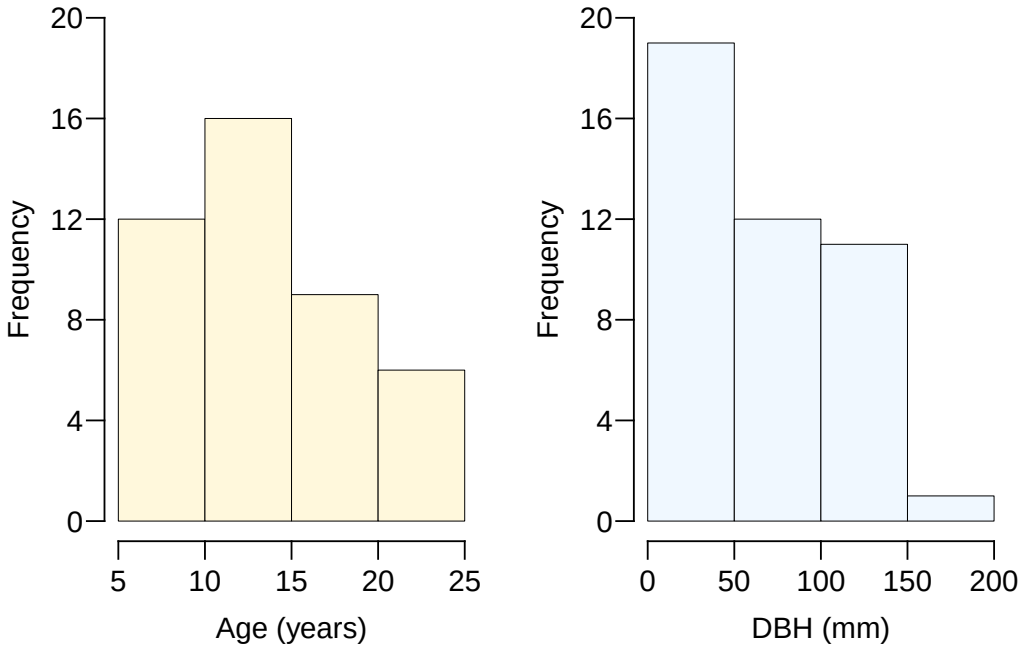

Figure 9.10: Age and D_{bh} distributions of trees sampled for biomass.

Table 9.17: Regression of dry mass and carbon content of aboveground components with D_{bh}, D_{30}, and height. Models were of the form $\log_{10}(y) = \alpha + \beta \log_{10}(x)$ and back-transformed into the format $y = \alpha x^{\beta} CF$ where CF is a correction factor of the form $e^{MSE/2}$, and MSE is the mean squared error of the log-log regression model. p-values are given as asterisks: ***= $p < 0.001$.

Component	α	β	df	t-value	R^2	CF
Dry mass (kg) ~ D_{bh} (mm)						
Branch wood	-3.551 ± 0.221	2.318 ± 0.124	41	18.63***	0.89	1.08
Branch bark	-3.426 ± 0.137	1.453 ± 0.077	41	18.81***	0.90	1.03
Stem wood	-2.905 ± 0.136	2.083 ± 0.076	41	27.33***	0.95	1.03
Stem bark	-3.006 ± 0.086	1.315 ± 0.048	41	27.21***	0.95	1.01
Total	-2.739 ± 0.122	2.124 ± 0.069	41	30.96***	0.96	1.02
Carbon content (kg) ~ D_{bh} (mm))						
Branch wood	-3.862 ± 0.221	2.318 ± 0.124	41	18.63***	0.89	1.08
Branch bark	-3.747 ± 0.137	1.453 ± 0.077	41	18.81***	0.90	1.03
Stem wood	-3.218 ± 0.136	2.083 ± 0.076	41	27.33***	0.95	1.03
Stem bark	-3.326 ± 0.086	1.315 ± 0.048	41	27.21***	0.95	1.01
Total	-3.053 ± 0.122	2.124 ± 0.069	41	30.95***	0.96	1.02
Dry mass (kg) ~ D_{30} (mm)						
Branch wood	-4.390 ± 0.313	2.603 ± 0.165	41	15.79***	0.86	1.11
Branch bark	-3.954 ± 0.194	1.632 ± 0.102	41	15.96***	0.86	1.04
Stem wood	-3.716 ± 0.187	2.369 ± 0.098	41	24.09***	0.93	1.04
Stem bark	-3.519 ± 0.118	1.497 ± 0.062	41	24.15***	0.93	1.02
Total	-3.546 ± 0.186	2.405 ± 0.098	41	24.62***	0.94	1.04
Carbon content (kg) ~ D_{30} (mm)						
Branch wood	-4.701 ± 0.313	2.603 ± 0.165	41	15.79***	0.86	1.11
Branch bark	-4.274 ± 0.194	1.632 ± 0.102	41	15.96***	0.86	1.04
Stem wood	-4.029 ± 0.187	2.369 ± 0.098	41	24.09***	0.93	1.04
Stem bark	-3.840 ± 0.118	1.497 ± 0.062	41	24.15***	0.93	1.02
Total	-3.860 ± 0.186	2.405 ± 0.098	41	24.61***	0.94	1.04
Dry mass (kg) ~ height (mm)						
Branch wood	-7.202 ± 0.556	2.794 ± 0.201	41	13.92***	0.83	1.14
Branch bark	-5.711 ± 0.348	1.750 ± 0.126	41	13.94***	0.83	1.05
Stem wood	-6.304 ± 0.358	2.554 ± 0.129	41	19.78***	0.91	1.06
Stem bark	-5.151 ± 0.227	1.612 ± 0.082	41	19.68***	0.90	1.02
Total	-6.158 ± 0.365	2.586 ± 0.132	41	19.62***	0.90	1.06
Carbon content (kg) ~ height (mm)						
Branch wood	-7.513 ± 0.556	2.794 ± 0.201	41	13.92***	0.83	1.14
Branch bark	-6.031 ± 0.348	1.750 ± 0.126	41	13.94***	0.83	1.05
Stem wood	-6.618 ± 0.358	2.554 ± 0.129	41	19.78***	0.91	1.06
Stem bark	-5.472 ± 0.227	1.612 ± 0.082	41	19.68***	0.90	1.02
Total	-6.473 ± 0.365	2.587 ± 0.132	41	19.62***	0.90	1.06

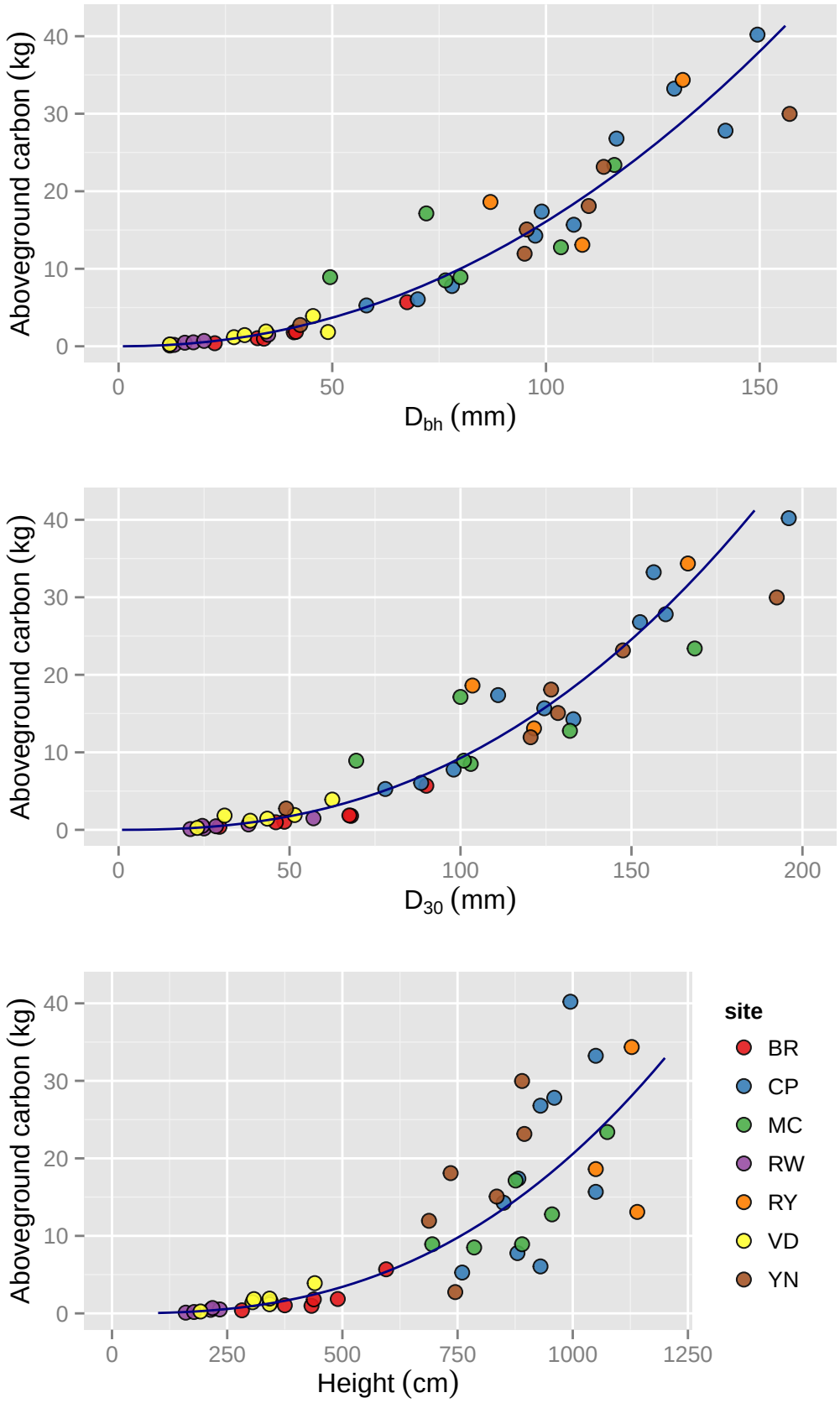

Figure 9.11: Relationship between D_{bh}, D_{30}, and height and aboveground carbon content (kg). Coefficients for each model are given in Table 9.17.

9.5 DISCUSSION

9.5.1 *Tree mensuration*

Due to the non-orthogonal nature of the mensuration data, it is difficult to draw many useful conclusions. Analysis of all sites (Table 9.6) indicated significant differences between all sites for dependent variable (D_{bh}, D_{30}, and height), but it was not possible to glean any link between planting density, or age. There is an increasing trend with age, but this is undermined somewhat by measurements of trees at the YN site.

Why trees at site YN experienced such poor growth relative to trees at other sites is unclear. It is possible that trees at sites RY and RL experienced better treatment after planting. The RL site is small, and whilst owned by Bedford Borough Council, is administered by the local wildlife trust, and therefore is much more intensively managed than any of the other sites. Furthermore, RY is administered by the Woodland Trust, and is also bisected by a major gas pipeline, for which reasons the site may also have received better management than YN. This speculation does not explain the poor performance of trees at YN relative to CP and MP however. It has not been possible to obtain records from tree stock suppliers from the time of planting, hence it is not possible to rule out genetic factors.

The analysis completed at Clapham Park is more informative, and agrees with well established forestry understanding: trees planted closer together tended to have a smaller diameter, but a greater height (Savill et al., 1997). This was not the case with trees planted at 2.0 m $\times$ 2.0 m spacing, as these trees were in the silvopastoral blocks. Interestingly, trees in the silvopastoral blocks, were equivalent in terms of mean diameter and height, to trees at 3 m $\times$ 3 m within the woodland plantation. This is presumably since these trees had better access to resources in terms of both light and water.

In terms of the number of multiple stems measured at 130 cm and 30 cm, it does not appear that the trees planted in the SP treatment had any worse form than the trees planted in the farm woodland treatment. At both measurement heights, a higher proportion of trees had only a single stem in the SP treatment. This is however, a very coarse indication of form, and a more comprehensive study may be more revealing. it should also be noted that during the early years, each SP block was fenced individually; this may have offered better protection against browsing animals[10] in the first few years following establishment.

9.5.1.1 *Quality of fit to yield tables*

At present, the Forestry Commission does not have a dedicated yield table for ash trees. Instead, it relies on a more general sycamore, ash, and birch (SAB) yield table (Hamilton, 1996). This yield table is based on a forestry situation with an initial planting density of either 1787 or 2949 trees ha^{-1}, with the expectation that thinning will take place every five years, reducing the final crop to a density of between 118 and 240 trees ha^{-1}.

10 Certainly there was evidence of small deer species (*Muntiacus reevesi* and probably *Capreolus capreolus*) throughout fieldwork in 2012–2014.

Clearly this is a scenario very different to that experienced by the trees sampled in this study. Furthermore, the SAB yield table begins at ten years, hence it is not possible to compare the majority of measurements taken in this study to the predictions made by Hamilton (1996).

That said, it appears from Figure 9.7 that the rates of growth recorded during tree ring analysis, are at least consistent with the range of yields predicted by Hamilton (1996). It remains to be seen if the trajectory of growth curves from these 'minimum intervention woodlands' are likely to be different to the growth pattern of the more intensively managed ash trees under the SAB yield table. The maximum mean annual increment (MAI) for each site, based on current measurements were no greater than five (Table 9.11).

Attempts to create a yield table based on the data collected in this study by fitting an equation (Equation 9.11[11] as used by Christie (1989)) to the height and D_{bh} data collected during mensuration and tree ring counts. An iterative nonlinear least-squares approach was used to estimate the parameters of the model. These attempts were ultimately unsuccessful however as models failed to converge. This is probably because the data, which are from very young trees, do not show signs of slowing growth; hence it was impossible to generate an estimate for the aymptote.

$$y = \alpha\beta^{(1+(\phi-1)e^{(\rho x)})}\frac{\gamma(x)-\gamma(0)}{1-\gamma(0)} \tag{9.11}$$

α = parameter (200).
β = asymptotic parameter related to the percentile of the population that is being represented by the model:

$$\begin{cases} \beta = 0.66 : q_{0.1} \\ \beta = 0.80 : q_{0.5} \\ \beta = 0.94 : q_{0.9} \end{cases}$$

γ = gompertz function of the form:
$\gamma(x) = e^{-e^{(\delta(\epsilon-x))}}$.
δ = parameter of the gompertz function (0.08).
ϵ = parameter of the gompertz function (0).
ϕ = polymorphic parameter (10).
ρ = polymorphic parameter (-0.17).

9.5.2 *Biomass allometry*

Attempts to establish an allometric relationship for aboveground carbon content were successful for each of the explanatory variables D_{bh}, D_{30}, and height. The models incorporating D_{bh} were found to provide the best fit to the data.

Comparison with other allometric relationships for aboveground dry mass found in the literature demonstrate the risk of using models to predict beyond the scope of the original data (Figure 9.12).

11 Starting values used to fit a non-linear least squares regression model are included in parentheses.

Of the five similar equations found in the literature (Table 9.18), two were developed from UK data (Bunce, 1968). These two models are derived from one site each in Cumbria, England, and are determined using the same log-log models[12] used here, based on just 15 samples each.

Despite finding very good correlation with his own data, the models derived by Bunce (1968) show a poor fit to data from the present study. For a tree with a D_{bh} of 150 mm, the present model predicts a total aboveground dry mass (not leaves) of 78 kg, whereas Bunce's models predict 4 kg (Roundsea) and 5 kg (Meathop).

Table 9.18: Comparison of allometric relationships for ash found in the literature. All equations follow the form $\log_{10} y = a + \beta \log_{10} x$ or $\ln y = a + \beta \ln x$ and were back-transformed to $y = \alpha x^{\beta} CF$ where α was transformed either with e or antilog_{10} and the correction factor (Equation 9.10). All the equations were calculated with D_{bh} in cm, except Blujdea et al. (2012) who appear to have used m, and the present study where D_{bh} was recorded in mm. Note that R^2 refers to the fit with the original data from which the model was derived, not data presented in the current study.

Source	α	β	R^2	n	CF	D_{bh} (mm)
This study	-2.739^a	2.1236	0.9590	42	1.02	12-157
Bunce	-5.3081[b]	2.4882	0.9940	15	1.01	90-1040
Bunce	-5.3870[b]	2.5466	0.9853	15	1.01	95-575
Alberti et al.	-2.69[b]	2.76	0.96	40	1.12	50-400
Blujdea et al.	3.4014[b]	3.2896	0.9649	14	1.08	<10-81

[a] $\log_{10}$ transformed
[b] ln transformed

Table 9.19: Additional information relating to sites at which allometric relationships were established (Table 9.18). Altitude (Alt: m above sea level), mean annual temperature (Temp: °C), and total annual precipitation (Prec: mm year^{-1}) and presented alongside the previous land use of the site, and the current form of the woodland - whether plantation or naturally regenerated secondary woodland. Refer to Table 9.18 for source references.

Source	Alt	Temp	Prec	Previous	Current
This study	58	10.2	652	Pasture	Plantation
Bunce	<50	na	na	Woodland	Secondary
Alberti et al.	600	10.0	2500	Grassland	Secondary
Blujdea et al.	100-300	10.5	<470	Agricultural	Plantation

It is possible that growing conditions for ash trees in the Cumbrian sites were less favourable than the milder climate of Bedfordshire resulting in a lower aboveground mass for a given D_{bh}. Certainly Kerr and Cahalan (2004) note that ash trees prefer 'warm' conditions with 'rich' or 'very rich' soil nutrient status. In addition

12 Note that in the discussion of the models developed by Bunce (1968) the models were back-transformed and the correction factor suggested by Baskerville (1972) applied, although this was not done in the original article.

ash trees can develop chlorotic foliage in the presence of high concentrations of calcium (Kerr and Cahalan, 2004); this may have been the case at both Cumbrian sites which lay on top of limestone bedrock (Bunce, 1968).

In a similar study, covering a range of D_{bh} values encompassed by the present study and with similar temperature and previous land-use (Table 9.19), Blujdea et al. (2012) present a model with a reasonable fit to our data ($R^2 = 0.83$, Figure 9.12). This model tends to under-estimate aboveground carbon content as measured in this study; Blujdea et al. (2012) predict that a tree of D_{bh} 80 mm would have an aboveground biomass of 16 kg, in comparison to 21 kg predicted by our model.

Alberti et al. (2005) present a model which also provides a reasonable fit to our data ($R^2 = 0.87$) but which was developed over a larger sample size incorporating a range of D_{bh} from 50–400 mm. Based on this model, a tree of 400 mm in diameter would be 2011 kg compared to 627 kg based on our model. Hence despite the great differences between our model, and the models presented by Bunce (1968), the trajectory is not unreasonably steep, although it would still be unwise to make predictions far beyond the scope of the original data based on this model.

9.5.3 *Ratio of stem to branch wood*

Biomass partitioning data (for which there is a relative paucity) collected in this study may help in the parameterisation of biophysical models , for instance Yield-SAFE. In the past a single value has been used for this parameter, however Figure 9.8 indicates that this may not be the best approach, as it appears that this ratio changes with age. Application of the equation given in table 9.15 may provide better estimates in future.

It should be noted however that as with other analyses presented in this study, this relationship is at least partly confounded by the effect of spacing. To avoid the confounding influence of other variables, only age was used as an independent variable in developing the regression relationship; future studies would benefit from sampling from a chronosequence of sites without changes in planting density.

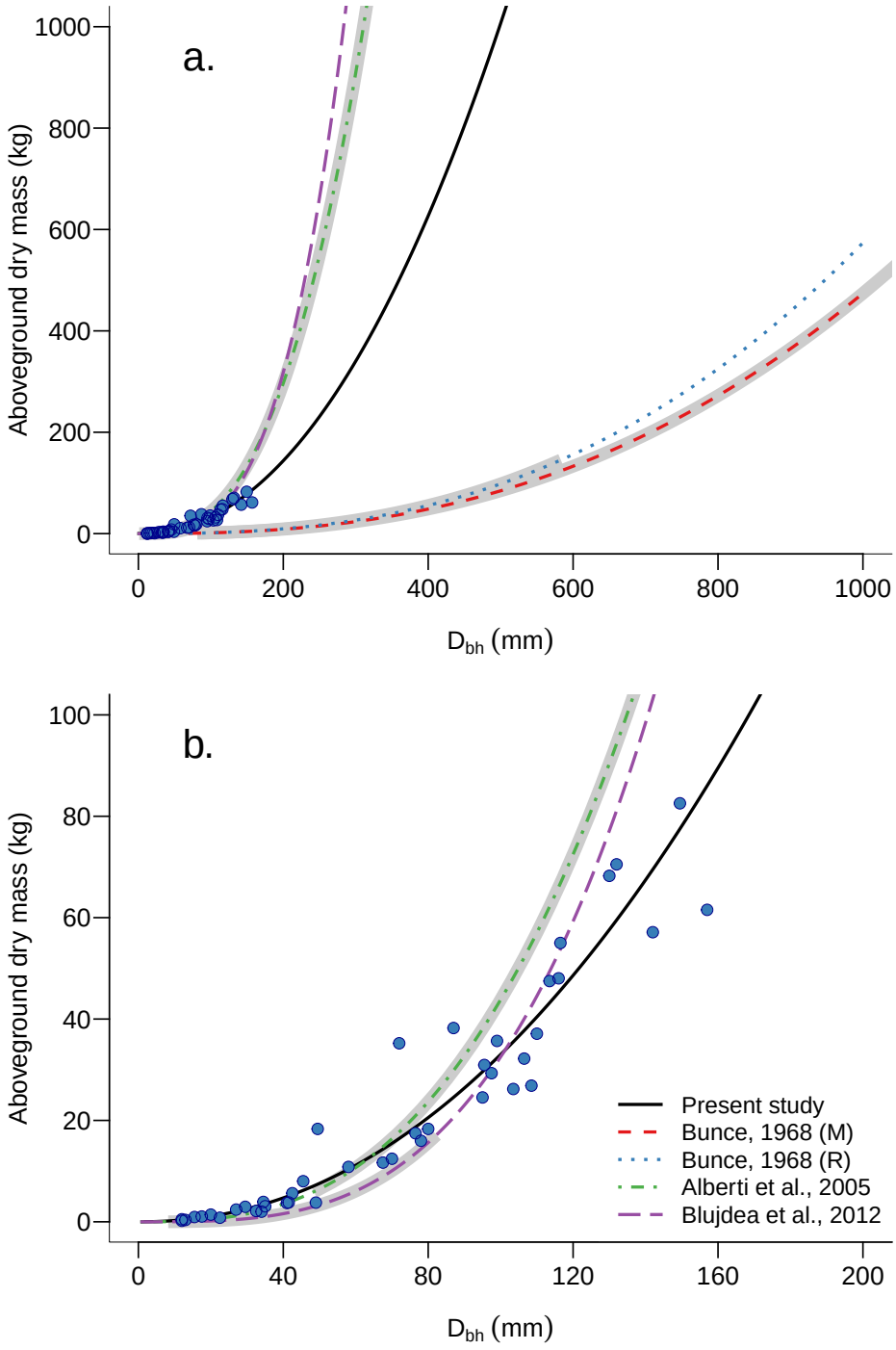

Figure 9.12: Comparison of allometric relationships of D_{bh} (mm) and aboveground dry mass (kg). See Table 9.18 for model coefficients. Grey shading (if present) represents that range of D_{bh} values to which the model was initially fit.

Hypothesis

6. Using traditional forestry yield tables to predict the growth of trees in agroforestry systems and farm woodlands (which are typically planted at much wider spacings) will over-estimate yield.

The woodlands measured in this chapter are generally younger than the earliest predictions made by the sycamore, ash, and birch (SAB) yield tables (Hamilton, 1996), hence it is not possible to draw any firm conclusions about the veracity of the above hypothesis. However, it appears to be the case that the predictions are roughly consistent with the early years of tree growth. It remaisn to be seen however whether the trajectory of tree growth will remain consistent with the yield tables as the trees get older.

Part IV

CONCLUSIONS

It is quite in keeping with man's
curious intellectual history, that the
simplest and most important questions
are those he asks least often.

— Sir Ralph Norman Angell (1872 - 1967)

10 SYNTHESIS

In this chapter each hypothesis is addressed in turn, and the findings from the relevant chapters combined to give a concerted answer to the two research questions. Soil organic carbon data from Part ii from the Silsoe silvoarable trial and Clapham Park are presented alongside tree biomass C measurements reported in Part iii. Additional crop yield data from Silsoe, and biomass C calculations from Clapham Park are presented for the first time. The combined C storage at each site is presented to provide a more complete picture of the C balance at the Silsoe silvoarable trial and Clapham Park.

10.1 HYPOTHESES AND RESEARCH QUESTIONS

As stated in the introduction (Chapter 1), considerable uncertainty exists about the efficacy of tree planting in agricultural environments as a strategy for C storage. This thesis aims to address these uncertainties by answering two research questions:

1. **What is the effect of tree planting on arable and pasture land on above and belowground C stocks?**
2. **What are the implications for carbon sequestration standards such as the Woodland Carbon Code?**

In order to answer these questions a number of hypotheses were developed based on the literature review. In this chapter each of these hypotheses is dealt with in turn, and a brief concerted answer to the two research questions is presented.

Outcomes for each hypothesis are colour coded as below:

Hypothesis

Hypothesis upheld.

Hypothesis

Not enough evidence to either uphold of falsify hypothesis.

Hypothesis

Hypothesis falsified.

Hypothesis

1. Establishing silvoarable agroforestry systems on arable land will increase soil organic carbon (SOC) stocks relative to a pure arable control.

Results presented in Chapter 4 indicate that, in line with the literature consensus, planting trees in arable enviroments leads to an increase in SOC stock. This increase was limited to only one depth increment however (0–40 cm), and was not found when the complete depth profile was considered.

Hypothesis

2. The incorporation of trees into the arable environment will lead to increases in soil organic carbon (SOC) storage at depth.

Results from the Silsoe silvoarable trial did not suggest that there were gains in SOC storage at depth as a result of tree planting in the arable environment. In fact, at one depth increment: 60–105 cm there were declines in SOC stock. This follows a pattern suggested by a number of studies that tree planting on arable land does not produce gains in subsoil C stocks, at least over the several-decade timescale (Jug et al., 1999; Richter et al., 1999; Vesterdal and Ritter, 2002), the exact reasons for this are unclear.

Results presented by Upson and Burgess (2013) were recalculated using the equivalent soil mass (ESM) method for quantifying SOC stock changes. The impact of applying this method was large, resulting in 19–25% lower SOC stock when the whole depth profile of 0–150 cm was considered. This echoes the findings of Lee et al. (2009), and indicates that the 'fixed-depth' method is unreliable for reporting SOC stock changes. Several versions of the ESM are reported in the literature; more research to clarify when to use each method, and what impact it may have, is required.

Hypothesis

3. Tree related SOC is more stable than arable crop or grass related SOC.

Fractionation completed on soils at the Silsoe silvoarable trial, which might have indicated a qualitative difference in the stability of C stored in the soil, did not indicate any differences between treatments, except in the carbon fraction related to sand and stable aggregates. This is most probably related to differences in soil texture between treatments.

Fractionation using the Zimmermann et al. (2007) technique is time consuming and costly, and for these reasons only a very small sample size was analysed (for each treatment and depth combination: $n = 3$) at Silsoe. Since the effect sizes are small relative to the variance, it is almost certain that the same low power problems experienced with analysis of bulk soil C affect this analysis. A similar analysis at Clapham Park is underway, limited to the top two depth increments where changes in organic carbon content ($C_o\%$) were detected, and consequently

with a larger sample size. It is hoped that this analysis will better explain changes in C_o% and SOC stocks at Clapham Park, and particular elucidate the question of whether changes have occurred mainly in the labile particulate organic matter (POM) fraction as Huang et al. (2011) found, or whether more significant changes in fractions likely to persists for much longer (e.g. chemically resistant soil organic carbon (rSOC)) were found.

Hypothesis

4. Planting trees on grassland will lead to a decline in SOC stock.

At Clapham Park, where trees were planted into a permanent pasture, tree planting was associated with a decline in SOC stock at 0–10 cm. Beneath this depth, and to the full 150 cm, no differences between treatments were found[1].

These findings agree with hypothesis 4, which was proposed based on a number of recent meta-analyses addressing the issue of SOC change following afforestation (Guo and Gifford, 2002; Laganiere et al., 2010; Paul and Polglase, 2002; Post and Kwon, 2000; Shi et al., 2013).

Results from power analyses indicate that for measurements of 0–40 cm at Silsoe and 0–20 cm at Clapham Park, sufficient replication was completed to constrain the Type II error rate to 0.2 or lower. This means that the chance of incorrectly concluding that there was no difference between treatments (if a similar experiment was replicated many times) was 20% or less – the nominal threshold assumed for hypothesis testing. At depths greater than these, there was an increased likelihood of incorrectly concluding that there was no difference between treatments. With this in mind, depths for which insufficient replication was completed should be viewed with considerable caution, and despite attempts to sample as intensively as possible, it was not possible to draw firm conclusions about the complete 150 cm profile (and indeed any cumulative depths greater than 40 cm in depth). Despite the availability of the so-called 'observed power' in many modern proprietary statistical software packages, it is not possible to retrospectively calculate power from a hypothesis test which failed to show a statistical difference. Since there is a relationship between the Type I error rate α and the Type II error rate β, attempting to calculate β from the observed p-value results in a value that is scaled to it 1:1 (Hoenig and Heisey, 2001; Thomas, 1997; Thomas and Krebs, 1997). This is known as the observed power fallacy.

1 It should be remembered that at both the Silsoe and Clapham Park experiments, the assumption has been made that the level of SOC across the sites was homogeneous before planting. Since the silvoarable experiment at Silsoe and Clapham Park were under a uniform land use since the 1880s prior to planting, this is a reasonable assumption. In the case of Silsoe however the measured changes in SOC may underestimate the true values, as a continuous grass sward was allowed to develop in the years after the end of cultivation. Measurements from Silsoe are therefore of the 'tree effect' only, and a better evaluation of the effect of silvoarable agroforestry on SOC would have measured the arable control before establishment of trees, and the same field 19 years later without C inputs to the arable control from grass. This problem is not so acute at Clapham Park because the pasture (PA) treatment has remained uniform since tree planting, and can be assumed to have remained at an equilibrium state.

Hypothesis

5. Losses of SOC from tree planting on grassland are dependent on the density of the tree planting.

Measurements from an adjacent mature grazed woodland suggested that in time the loss of SOC stock may recover, however it is not clear how long this would take, and it could simply be a site effect. Conceptually this is illustrated in Figure 10.1 using the actual values from the Clapham Park experiment and values derived from the adjacent mature grazed woodland Helen's Wood (for depths of 0–10 cm). Note that in this figure the recovery curves for both the silvopasture (SP) blocks and the farm woodland (FW) treatment have been shown to equilibriate at the same point – the SOC stock measured at Helen's Wood. This shows a possible end point for both treatments on a per-hectare basis although it may not be completely representative of future conditions[2].

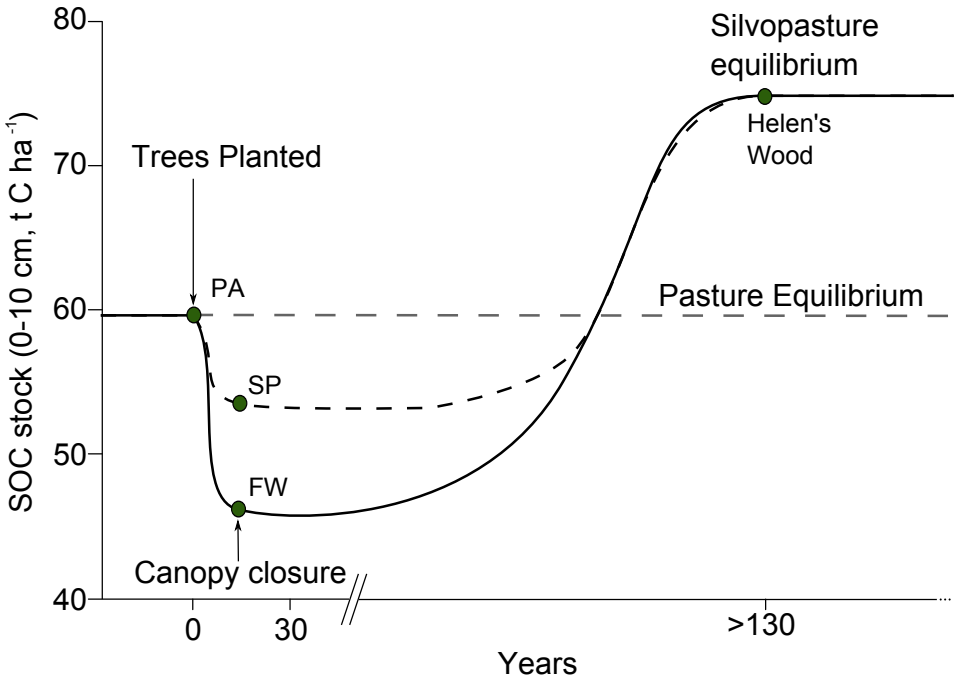

Figure 10.1: Conceptual diagram showing how soil organic carbon (SOC) stock changes resulting from tree planting may be recovered over time (0-10 cm). Actual data from the pasture (PA), silvopasture (SP) and farm woodland (FW) treatments and from the mature grazed woodland Helen's Wood have been included, however the trend is speculative, as is the time taken to recover carbon losses.

2 Note that there are a number of reasons to be cautious about assuming that Helen's Wood represents an 'equilibrium state' at which either the silvopasture blocks or the farm woodland treatment will climax. Firstly Helen's Wood is known to have been in continuous woodland cover since the 1880s, and probably very much longer, so it is not known how long the current SOC levels took to accumulate. Second, Helen's Wood is now an open woodland with a very limited age distribution. Hence, a high proportion of radiation reaches the woodland floor (Figure 3.10); it may not necessarily be representative therefore of the farm woodland as it matures, but nor is it representative of the silvopasture blocks.

An interesting finding arising from Clapham Park is that SOC declined more slowly in the silvopasture plots than the farm woodland. This finding may be consistent with hypothesis 5, if the loss of SOC stock in the farm woodland treatment is linked to the loss of understorey vegetation, as it appears to be. In silvopastoral systems, maintaining grass yields is an objective alongside producing good quality trees. At Clapham Park this was achieved by confining trees to SP blocks which were (at least initially) fenced. Another option is to plant trees throughout a pasture at a low enough density to ensure that light reaches the ground, for example at Glensaugh, Aberdeenshire (Figure 10.2).

Figure 10.2: Sycamore at a density of 200 trees ha^{-1} at the Glensaugh silvopastoral network site.

Maintaining a full sward beneath the trees would mean that such sites benefit from continued C inputs from grass root turnover and new inputs from tree roots and litter deposition in a similar way to the SP blocks at Clapham Park. Therefore, planting trees at higher densities results in reduced pasture production, and lower C inputs, but conversely higher inputs of C from tree sources. Eventually inputs from trees may become large enough to restore carbon lost in the years since planting, and potentially exceed the original inputs of C from the pasture. Whilst resulting in more rapid losses, higher density planting may offer greater gains in the long-term. This relationship is conceptualised in Figure 10.3. If woodlands are thinned, either deliberately or by attrition, the establishment of understory vegetation will also have an impact. It should be noted however, that the Clapham Park experiment in effect examines two densely planted tree treatments (one of which is able to maintain an understory) – and not low density planting more characteristic of silvopastoral systems. Given the relative dearth of research on

this topic particularly in the UK, research to understand the impact on SOC of different planting densities in silvopastoral systems would be highly informative.

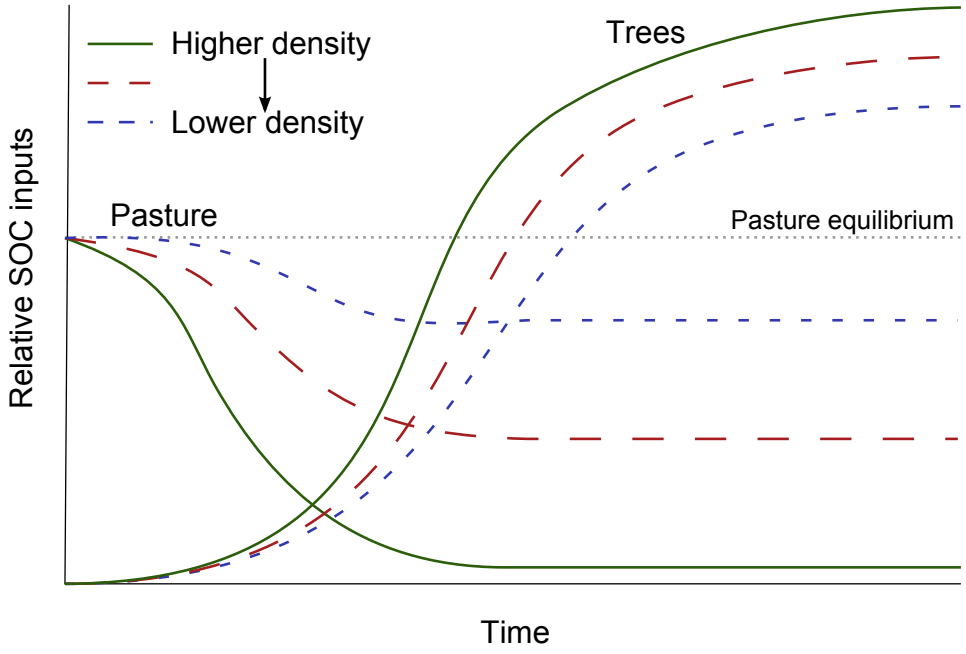

Figure 10.3: Conceptual diagram of how inputs of C to the soil might differ with different planting density in a silvopastoral system.

Hypothesis

6. Using traditional forestry yield tables to predict the growth of trees in agroforestry systems and farm woodlands (which are typically planted at much wider spacings) will over-estimate yield.

Forestry Commission yield tables are a widely used tool in the forestry sector, used to predict the final yield of trees from measurements taken at an earlier age. Since these yield tables were designed primarily with the focus of calculating merchantable timber at harvest from densely stocked plantations, they may not be appropriate for the much lower planting densities that are typical of agroforestry systems.

Results from Silsoe (in Chapter 7) and from Leeds (in Chapter 8) indicate that the existing yield tables for widely spaced poplar do not well represent the reality observed. These yield tables were titled provisional in 1994 (Christie, 1994), but no further updates to these tables have been produced. The exact reason for the poor fit of the yield tables is unclear, but it may not necessarily be the result solely of the different planting arrangement, competition with the crop, cultivation, or the incidence of *Melampsora* spp. rust experienced by the trees at Silsoe. The results presented here provide credence to observations by Tom Jenkins (personal communication, 25 May 2012) that the yields predicted in tables (Christie, 1994) are too optimistic. This observation has important implications for financial analyses based on these yield predictions.

At Clapham Park and the other woodlands measurements across Bedfordshire, measurements of ash trees were taken during one season only, so a record of measurements since planting was not available. By sampling woodlands of different ages at different sites, and by reproducing growth patterns by tree ring analysis, it was possible to approximate the growth pattern of the trees since planting. Forestry Commission yield tables do not include a single table for ash trees, instead they are catered for under the sycamore, ash, and birch (SAB) yield tables. The measurements of ash trees presented in this thesis appear to fit within the range of values predicted by the SAB yield table, however this is difficult to evaluate with certainty as the yield tables tend to begin later than many of measurements presented in Chapter 9.

Hypothesis

7. Small losses in SOC may offset a large proportion of gains of C in aboveground tree biomass.

Results obtained from the quantification of biomass C are presented here for the first time alongside values obtained from SOC determination. Tables 10.2 and 10.3 present combined C storage in the tree and soil components. At Silsoe, measurements of the crop and understory have been included, but at neither site has fine root C explicitly been included in the final totals, rather the assumption was made that fine root mass was incorporated into SOC measurements.

Totals for vegetation and soil C have been included as absolute values – a snapshot of actual C at the time of sampling, and as relative values, i.e. $treatment - control$, and hence the change in C storage over a 19 year (Silsoe) and 14 year (Clapham) period. As noted, these measurements assume that pre-planting SOC levels were uniform across treatments.

An additional column has been added to accompany per-hectare C (Table 10.3) storage values from the SP treatment at Clapham Park. This column represents values adjusted for the actual proportion of land use at the site. Since the tree blocks occupied just 3.76 % of the grassland, biomass C and SOC were reduced to reflect this, and SOC values from the PA treatment used to make up the remaining 96.24 % of the land.

Trees at Clapham Park are a mix of native broadleaved species (Burgess et al., 2000), but only ash trees were measured. In the absence of measurements from other trees, it was assumed that the ash trees were representative of the other species. Explanations of how values for crop, understory vegetation, and biomass C at Clapham Park have been included in Appendix: F. Biomass C totals derived from these methods are included in Table 10.1.

Note that statistical tests were conducted only on the tree biomass C component, and the SOC component in each table, and it was not possible to conduct statistical analyses on the absolute total values. Since in such an analysis the experimental unit is the treatment itself, there is only one 'replicate' each and therefore zero degrees of freedom. This makes it impossible to produce confidence intervals or complete statistical tests.

Table 10.1: Estimated biomass C at Clapham Park. Except where indicated, values are given in C . Note that part of the difference between C totals is accounted for by the increased planting density in the SP plots: trees were planted with 2 × 2 m spacing, as opposed to 2.5 × 2.5 m spacing in the FW treatment.

		Aboveground (kg tree^{-1})		Belowground (kg tree^{-1})		Total (t C ha^{-1} of trees)		
Treat	D_{bh} (mm)	Mean	SE	Mean	SE	Mean	SE	n
FW	92	14.09	0.65	8.35	0.38	35.90	1.64	74
SP	121	24.98	1.17	14.78	0.69	99.41	4.65	74

Results from analyses of SOC are presented in Chapter 4 and indicated that there were no significant differences between treatments for the full depth profile ($p > 0.05$) at either site. Nor were any differences found at Silsoe in tree C between treatments (Paired t-test: $t = -2.34$, $df = 2.00$, $p = 0.14$). On a per-hectare basis (not taking into account the true proportions of tree and grassland in the SP treatment) the SP blocks at Clapham Park were found to be storing significantly more biomass C ($t = 12.87$, $df = 90.90$, $p < 0.001$). No differences in SOC were found for the whole profile ($p > 0.05$, Chapter 5).

Results presented in Table 10.2 and 10.3 show that C storage in the tree components is much smaller than in SOC stock (to 150 cm), and typically accounts for between just 18–30% of the SOC stock, and just 2% when the SP treatment is considered to include the correct proportion of pasture and trees.

One important finding arising from Table 10.3 is that it appears that the equivalent of −42% of the biomass C stored in the FW treatment in tree biomass, has been lost in changes to the SOC stock. In fact, this whole profile (0–150 cm) value masks the true significance of this result[3], as in the top 0–10 cm alone one can say with some confidence that −37% of aboveground C gains were lost in associated changes in SOC stock in the FW treatment. For the SP blocks (when considered in the correct proportions of land use) twice as much C was lost in the soil (0–10 cm) than was gained in tree planting after 14 years.

Hypothesis

8. Frequentist hypothesis testing is an appropriate tool to determine differences in SOC in newly planted woodlands.

As noted in Chapter 6, assessing the assumptions made in the Woodland Carbon Code with regard to SOC is not simple, since the Woodland Carbon Code deals with more typical afforestation regimes, and not agroforestry in particular. The results from the Silsoe trial indicate however that the broad assumption of an increase in SOC following tree planting in arable land is correct.

At Clapham Park however, the farm woodland treatment – a native broadleaf mix planted on pastoral land at a minimum intervention density – is fairly typi-

3 A significant difference between each treatment was detected at the cumulative 0–10 cm, and we know from power analyses that sufficient replication was completed at this depth. It is therefore probably more appropriate to use 0–10 instead of 0–150 cm.

Table 10.2: Total C storage at the experiment at Silsoe (2011) for 19 years including arable cropping for 10 years. All values in (t C ha^{-1}). Tests of statistical significance were completed for differences between the woody biomass C (see Appendix F) and the SOC (presented in Chapter 4), in neither case were the differences found to be statistically significant ($p > 0.05$). Relative measurements (italics) are relative to the control.

	Agroforestry Cropped			Agroforestry Fallow			Arable Control		
Component	Mean	SE	*n*	Mean	SE	*n*	Mean	SE	*n*
Leaves	0.85	0.11	3	1.08	0.28	3	_	_	_
Tree (woody)	63.94	7.18	3	74.95	13.74	3	_	_	_
understory	0.53	0.05	6	0.42	0.30	6	0.73	0.33	4
Harvested crop	15.73	0.29	10	_	_	_	21.60	0.53	10
Absolute vegetative	81.05	7.28	_	76.45	19.66	_	22.33	3.45	_
Relative vegetative	*58.72*	_	_	*54.12*	_	_	_	_	_
Absolute SOC	173.47	10.43	3.00	163.80	3.81	3.00	174.56	9.06	6.00
Relative SOC	*−1.09*	_	_	*−10.76*	_	_	_	_	_
Absolute Total	254.52	19.44	_	240.25	15.24	_	196.89	9.06	_
Relative Total	*62.85*	_	_	*64.19*	_	_	_	_	_

cal of projects registered with the Woodland Carbon Code. For this situation the Woodland Carbon Code assumes no change in SOC stock. Although it is expected that there will be an initial drop in SOC associated with tree planting, it is anticipated that this will later be recovered through C inputs from the trees. The results presented in Chapter 5 support this assumption – tree planting was indeed associated with an initial loss of SOC, and results from the mature grazed woodland (Helen's Wood) indicate that there may be a recovery of soil C over an unspecified time period.

With regard to the second method of soil C accounting suggested by the Woodland Carbon Code (WCC): making a SOC assessment before and after afforestation, the results from Chapter 6 offer some insights. If results from the farm woodland at Clapham Park can be generalised to the afforestation of permanent pasture elsewhere, it may not be possible to statistically test for changes in SOC stocks with the nominally accepted error rates for depths greater than 20 cm in woodlands < 15 years old without a prohibitively expensive sampling effort. For this reason, traditional frequentist hypothesis testing does not seem to be an appropriate choice of statistical method.

It is likely that if SOC stock assessment becomes the norm for C validation schemes such as the Woodland Carbon Code, adopting a lower burden of proof would be necessary. The re-sampling study conducted in Chapter 6 demonstrated that to capture most of the variation before and after afforestation in the farm woodland treatment at Clapham Park would still require non-trivial cost to get a reasonably robust answer. It is important that steps are made to quantify changes

Table 10.3: Total C storage at Clapham Park from measurements taken in 2012–2013 all values in t C ha^{-1}. Statistical tests were conducted on Tree C and Absolute SOC values; statistically significant differences ($p < 0.05$) were found between trees in the silvopasture (SP) plots and the FW at a per-hectare basis, but no differences were found between treatments for SOC for the full depth profile ($p > 0.05$). An additional column (Mean[a]) has been included to present the SP treatment in the actual proportions of tree and pasture present at the site. Relative measurements (in italics) are relative to the pasture control.

	Farm Woodland			Silvopasture trees				Pasture		
Component	Mean	SE	*n*	Mean	SE	*n*	Mean[a]	Mean	SE	*n*
Tree	35.90	1.64	74	99.41	4.65	74	3.74	_	_	_
Absolute SOC	189.63	6.29	20	205.84	8.19	20	204.89	204.85	5.45	40
Relative SOC	*−15.22*	_	_	*0.99*	_	_	*0.04*	_	_	_
Absolute Total	225.53	31.48	_	305.25	54.25	_	208.66	204.85	5.45	40
Relative Total	*20.68*	_	_	*100.4*	_	_	*3.77*	_	_	_

in SOC stock accurately however, since even relatively small changes can negate many years of biomass C accretion due to the relative size of the biomass and soil C pools.

One solution to overcoming these limitations may be to adopt the methods suggested by Kravchenko and Robertson (2011): dealing with each depth increment individually. Significant differences between individual depths from treatments or successive measurements would be summed to give the whole soil profile change. Evaluating this method should be considered an important area of future research, as it would help to improve the present situation of unacceptably large Type II errors which have been identified as an issue in this thesis.

Related to this is a further insight that has not been discussed so far: the size of the depth increments used to calculate whole profile changes. In this study, the two deepest depth increments were also the largest (45 cm), which is logical insofar as the largest changes in SOC stock occur in the most shallow depth increments. Samples from deep in the soil profile were typically very low in C_o% but high in inorganic C, which was removed by reaction with HCl. An updated method was adopted for ensuring that all the inorganic C was removed prior to analysis (Appendix B.4.2). However, since the C_o% at this depth was so low (and at times below the detection limit of the elemental analyser), the effect size will also be very small relative to the natural variation (and variation caused by measurement inaccuracies). It would be wise therefore to reduce the size of the depth increments so that when SOC stocks are calculated from C_o%, the increments about which there is likely to be least certainty do not have an undue influence over the whole profile SOC stocks.

10.2 NEW RESEARCH

A summary of the principal novel aspects of this thesis is included here.

- Attempting to quantify SOC stock in a UK silvoarable and silvopastoral system to a depth of 150 cm. Literature searches indicate that the work presented in Chapters 4 and 5 are the most comprehensive studies of bulk SOC stock in UK agroforestry systems to date.
- In chapter 7 it was observed that poplar yields at the Silsoe silvoarable system were poorly reflected by existing Forestry Commission yield tables. This is the first time that this observation has been made for UK agroforestry systems.
- The calibration of the Yield-SAFE model in Chapter 8 based on 19 years of poplar measurements and destructive harvests incorporating above and belowground measurements, and the inclusion of terms to account for fine root length expansion are advances in the development of the model.
- Development of allometric models for UK ash trees at 'minimum intervention' woodland densities. Whilst such relationships have been established in other countries, Chapter 9 presents what appears to be the first allometric relations for aboveground biomass (or C) from diameter at breast height (D_{bh}) for ash tree plantations at wider-than-usual spacings (c. 2.5 m) in the UK.

10.3 FUTURE RESEARCH

The following areas for future research have been highlighted by the work completed in this thesis.

- New approaches for dealing with the statistical problems related to sampling whole profile SOC changes should be evaluated: for example those suggested by Kravchenko and Robertson (2011). Without addressing this problem, or at least presenting post-hoc power analyses, studies of deep SOC changes risk drawing the wrong conclusions.
- The long term changes in SOC following afforestation of permanent pasture and grassland should be investigated further. There is evidence that SOC stock will return to pre-planting levels, but further evidence is required to clarify this point. If SOC levels do not recover, planting trees on permanent pasture or grassland as a strategy for C sequestration should be considered critically, taking account of the differences in stability of C stored in tree biomass and products, and the soil.
- In the study of SOC at Clapham Park, tree planting reduced the prevalence of understory vegetation, and this may have been a cause of SOC losses. Many silvopastoral systems are composed of low density plantings across pastures, rather than small blocks of higher density planting. Hence, a question that arises from this work is what effect low density planting more typical of silvopastoral systems has on SOC stock, if the grass understory remains relatively unaffected.

REFERENCES

AGFORWARD (2014). What is agroforestry. [Accessed: 11/07/2014] http://www.agforward.eu/index.php/en/.

Alberti, G, Candido, P, and Peressotti, A (2005). Aboveground biomass relationships for mixed ash (*Fraxinus excelsior* L. and *Ulmus glabra* Hudson) stands in Eastern Prealps of Friuli Venezia Giulia (Italy). *Annals of Forest Science*, 62, 831–836.

Alexander, L, Allen, S, Bindoff, NL, Bréon, FM, Church, J, Cubasch, U, Emori, S, Forste, P, Friedlingstein, P, Gillett, N, Gregory, J, Hartmann, D, Jansen, E, Kirtman, B, Knutti, R, Kanikicharla, KK, Lemke, P, Marotzke, J, Meehl, VMDG, Mokhov, I, Piao, S, Plattner, GK, Dahe, Q, Ramaswamy, V, Randall, D, Rhein, M, Rojas, M, Sabine, C, Shindell, D, Stocker, TF, Talley, L, Vaughan, D, and Xie, SP (2013). *Working Group I Contribution to the IPCC Fifth Assessment Report Climate Change 2013: The Physical Science Basis Summary for Policymakers*.

Angelsen, A, Brockhaus, M, Kanninen, M, Sills, E, Sunderlin, WD, and Wertz-Kanounnikoff, S (eds.) (2009). *Realising REDD+*. CIFOR, Bogor, Indonesia.

Arrhenius, S (1896). On the influence of carbonic acid in the air upon the temperature of the ground. *The London, Edinburgh, and Dublin Philosophical Magazine*, 41, 237–276.

Ashby, Z (2001). Effect of soil characteristics on poplar growth. Thesis, Cranfield University, Cranfield University.

Aves, C (2002). Factors influencing cereal establishment in a silvoarable system. Thesis.

Aydin, M, Yang, SL, Kurt, N, and Yano, T (2005). Test of a simple model for estimating evaporation from bare soils in different environments. *Ecological Modelling*, 182 (1), 91–105.

Balesdent, J and Balabane, M (1996). Major contribution of roots to soil carbon storage inferred from maize cultivated soils. *Soil Biology and Biochemistry*, 28 (9), 1261–1263.

Bambrick, AD, Whalen, JK, Bradley, RL, Cogliastro, A, Gordon, AM, Olivier, A, and Thevathasan, NV (2010). Spatial heterogeneity of soil organic carbon in tree-based intercropping systems in Quebec and Ontario, Canada. *Agroforestry Systems*, 79 (3), 343–353.

Baskerville, G (1972). Use of logarithmic regression in the establishment of plant biomass. *Canadian Journal of Forest Research*, 2, 49–53.

Batjes, NH (1996). Total carbon and nitrogen in the soils of the world. *European Journal of Soil Science*, 47, 151–163.

Beheshti, A, Raiesi, F, and Golchin, A (2012). Soil properties, C fractions and their dynamics in land use conversion from native forests to croplands in northern Iran. *Agriculture, Ecosystems & Environment*, 148, 121–133.

Bellamy, PH, Loveland, PJ, Bradley, RI, Lark, RM, Kirk, GJD, and Guy, JD (2005). Carbon losses from all soils across England and Wales 1978-2003. *Nature*, 437 (7056), 245–8.

Benjamini, Y and Hochberg, Y (1995). Controlling the false discovery rate: a practical and powerful approach to multiple testing. *Journal of the Royal Statistical Society*, 57 (1), 289–300.

Betts, RA, Falloon, PD, Goldewijk, KK, and Ramankutty, N (2007). Biogeophysical effects of land use on climate: Model simulations of radiative forcing and large-scale temperature change. *Agricultural and Forest Meteorology*, 142 (2-4), 216–233.

Black, KE, Harbron, CG, Franklin, M, Atkinson, D, and Hooker, JE (1998). Differences in root longevity of some tree species. *Tree Physiology*, 18 (4), 259–264.

Blujdea, V, Pilli, R, Dutca, I, Ciuvat, L, and Abrudan, I (2012). Allometric biomass equations for young broadleaved trees in plantations in Romania. *Forest Ecology and Management*, 264, 172–184.

Bohm, W (1979). *Methods of Studying Root Systems*. Springer-Verlag, Heidelberg.

Borden, KA (2013). Tree Roots in Agroforestry : Evaluating Biomass and Distribution with Ground Penetrating Radar by Tree Roots in Agroforestry : Evaluating Biomass and Distribution with Ground Penetrating Radar. Thesis.

Bowyer, J, Briggs, D, Lippke, B, Perez-Garcia, J, and Wilson, J (2004). *Life cycle environmental performance of renewable building materials in the context of residential construction: CORRIM Phase I Research Report*, volume 1. Seattle, WA.

Bradley, R, Milne, R, Bell, J, Lilly, A, Jordan, C, and Higgins, A (2005). A soil carbon and land use database for the United Kingdom. *Soil Use and Management*, 21 (4), 363–369.

Brady, NC and Weil, RR (2008). *The Nature and Properties of Soils*. Prentice Hall, Upper Saddle River, N.J., 14th edition.

British Standards Institute (1990). BS 1377-3: 1990 Methods of test for: Soils for civil engineering purpose –Part 3: Chemical and electro-chemical tests.

British Standards Institute (2012). BS5837:2012 Trees in relation to design , demolition and construction – Recommendations.

Buchanan, A and Levine, S (1999). Wood-based building materials and atmospheric carbon emissions. *Environmental Science & Policy*, 2, 427–437.

Bukhari, Y (1998). Tree-root influence on soil physical conditions, seedling establishment and natural thinning of *Acacia seyal* var. seyal on clays of Central Sudan. *Agroforestry systems*, 42, 33–43.

Bunce, RGH (1968). Biomass and production of trees in a mixed deciduous woodland. I. Girth and height as parameters for the estimation of tree dry weight. *Journal of Ecology*, 56 (3), 759–775.

Burgess, P, Graves, AR, Goodall, GR, and Brierly, EDR (2000). Bedfordshire Farm Woodland Demonstration Project: Final Report to the European Commission.

Burgess, P, Incoll, LD, Corry, DT, Beaton, A, and Hart, BJ (2004). Poplar (Populus spp) growth and crop yields in a silvoarable experiment at three lowland sites in England. *Agroforestry Systems*, 63 (63), 157–169.

Burgess, P, Incoll, LD, Hart, BJ, Beaton, A, Piper, RW, Seymour, I, Reynolds, FH, Wright, C, Pillbeam, DJ, and Graves, AR (2003). *The Impact of Silvoarable Agroforestry with Poplar on Farm Profitability and Biological Diversity Final Report to DEFRA*. Institute of Water and Environment, Cranfield University, Silsoe.

Burgess, P, Moffat, AJ, and Matthews, RB (2010). Assessing climate change causes, risks and opportunities in forestry. *Outlook on Agriculture*, 39 (4), 263–268.

Burgess, P, Nkomaula, J, and Medeiros Ramos, A (1997). Root distribution and water use in a four-year old silvoarable system. *Agroforestry Forum*, 8 (3), 15–19.

Burgess, P, Stephens, W, Anderson, G, and Durston, J (1996). Water use by a poplar-wheat agroforestry system. *Aspects of Applied Biology*, 44, 129–136.

Burgess, PJ, Reinhard, BR, and Pasturel, P (2006). Compatible measurements of volumetric soil water content using a neutron probe and Diviner 2000 after field calibration. *Soil Use and Management*, 22, 401–404.

Cambardella, C, Gajda, A, Doran, JW, Wienhold, B, and Kettler, T (2000). Estimation of particulate and total organic matter by weight loss-on-ignition. *In* Lal, R, Kimble, J, Follett, R, and Stewart, B (eds.), *Assessment Methods for Soil Carbon (Advances in Soil Science)*, CRC Press, Boca Raton, USA. 696.

Canadell, J, Jackson, RB, Ehleringer, JR, Mooney, HA, Sala, OE, and Schulze, E (1996). Maximum Rooting Depth of Vegetation Types at the Global Scale. *Oecologia*, 108 (4), 583–595.

Cannell, M, Van Noordwijk, M, and Ong, C (1996). The central agroforestry hypothesis: the trees must acquire resources that the crop would not otherwise acquire. *Agroforestry systems*, 34 (1), 27–31.

Carney, KM, Hungate, Ba, Drake, BG, and Megonigal, JP (2007). Altered soil microbial community at elevated CO2 leads to loss of soil carbon. *Proceedings of the National Academy of Sciences of the United States of America*, 104 (12), 4990–4995.

Cerri, C, Bernoux, M, Cerri, C, and Feller, C (2004). Carbon cycling and sequestration opportunities in South America: the case of Brazil. *Soil Use and Management*, 20 (2), 248–254.

Chan, K, Heenan, D, and Oates, A (2002). Soil carbon fractions and relationship to soil quality under different tillage and stubble management. *Soil and Tillage Research*, 63 (3-4), 133–139.

Charalambides, CA (2002). *Enumerative Combinatorics*. CRC Press.

Chave, J, Coomes, D, Jansen, S, Lewis, SL, Swenson, NG, and Zanne, AE (2009). Towards a worldwide wood economics spectrum. *Ecology letters*, 12 (4), 351–66.

Christensen, B (2001). Physical fractionation of soil and structural and functional complexity in organic matter turnover. *European Journal of Soil Science*, 52, 345–353.

Christie, JM (1989). *A study of the growth of free growing Ash trees in southern England*. Farnham.

Christie, JM (1994). *Provisional yield tables for poplar in Britain*. Forestry Commission, Edinburgh.

Cohen, J (1962). The statistical power of abnormal-social psychological research: A review. *Journal of Abnormal and Social Psychology*, 65 (3), 145–153.

Cohen, J (1992). A power primer. *Psychological bulletin*, 112 (1), 155–159.

Confalonieri, U, Menne, B, Akhtar, R, Ebli, K, Hauengue, M, Kovats, R, Revich, B, and Woodward, A (2007). Human health. *In* Parry, M, Canziani, O, Palutikof, J, van der Linden, P, and Hansen, C (eds.), *Climate Change 2007: Impacts, Adaptation and Vulnerability. Contribution of Working Group II to the Fourth Assessment Report of the Intergovernmental Panel on Climate Change*, Cambridge University Press, Cambridge, UK. 391–431.

Conover, WJ (1971). *Practical Nonparametric Statistics*. John Wiley & Sons Inc., New York.

Cranfield University (2014). The Soils Guide. [Accessed: 23/02/2014] https://www.landis.org.uk/.

Crawley, M (2007). *The R book*. Wiley, Chichester.

Crowley, TJ (2000). Causes of Climate Change Over the Past 1000 Years. *Science*, 289 (5477), 270–277.

Darot, J (2014). *Woodland Carbon Code Statistics: Data to March 2014*. Economics & Statistics, Forestry Commission, Edinburgh.

Das, DK and Chaturvedi, OP (2005). Structure and Function of Populus deltoides Agroforestry Systems in Eastern India: 1. Dry matter dynamics. *Agroforestry Systems*, 65 (3), 215–221.

Delgado, JA and Mosier, AR (1996). Mitigation Alternatives to Decrease Nitrous Oxides Emissions and Urea-Nitrogen Loss and Their Effect on Methane Flux. *Journal of Environment Quality*, 25 (5), 1105.

Denman, K, Brasseur, G, and Chidthaisong, A (2007). Couplings between changes in the climate system and biogeochemistry. *In* Solomon, S, Qin, D, Manning, M, Chen, Z, Marquis, M, Averyt, KB, Tignor, M, and Miller, H (eds.), *Climate change*, Cambridge University Press, Cambridge, United Kingdom, and New York, NY, USA., chapter 7.

Dessler, AE, Zhang, Z, and Yang, P (2008). Water-vapor climate feedback inferred from climate fluctuations, 2003–2008. *Geophysical Research Letters*, 35 (20), L20704.

Dewar, RC (1990). A model of carbon storage in forests and forest products. *Tree Physiology*, 6 (4), 417–28.

Dewar, RC (1991). Analytical model of carbon storage in the trees, soils, and wood products of managed forests. *Tree Physiology*, 8 (3), 239–58.

Dewar, RC and Cannell, MG (1992). Carbon sequestration in the trees, products and soils of forest plantations: an analysis using UK examples. *Tree Physiology*, 11 (1), 49–71.

Dodd, J and Boddington, C (2000). Mycelium of arbuscular mycorrhizal fungi (AMF) from different genera: form, function and detection. *Plant and Soil*, 226, 131–151.

Donkin, C (2001). Effect of vegetation and cultivation practice on soil organic matter in a silvoarable trial. Thesis, Cranfield.

Easterling, W, Aggarwal, P, Batima, P, Brander, K, Erda, L, Howden, S, Kirilenko, A, Morton, J, Soussana, JF, Schmidhuber, J, and Tubiello, F (2007). Food, fibre and forest products Coordinating. *In* Parry, M, Canziani, O, Palutikof, J, van der Linden, P, and Hanson, C (eds.), *Climate Change 2007: Mitigation. Contribution of Working Group II to the Fourth Assessment Report of the Intergovernmental Panel on Climate Change*, Cambridge University Press, Cambridge, UK, chapter 5. 273–313.

Eddy, JA (1976). The maunder minimum. *Science (New York, N.Y.)*, 192 (4245), 1189–202.

Edwards, PN and Christie, JM (1981). *Yield Models for Forest Management*. Forestry Commission, Edinburgh.

Eichhorn, MP, Paris, P, Herzog, F, Incoll, LD, Liagre, F, Mantzanas, K, Mayus, M, Moreno, G, Papanastasis, VP, Pilbeam, DJ, Pisanelli, A, and Dupraz, C (2006). Silvoarable Systems in Europe - Past, Present and Future Prospects. *Agroforestry Systems*, 67 (1), 29–50.

Elementar Analysensysteme GmbH (2002). Operating Instructions vario EL III CHNOS Elemental Analyzer.

Ellert, B and Bettany, J (1995). Calculation of organic matter and nutrients stored in soils under contrasting management regimes. *Canadian Journal of Soil Science*, 75 (4), 529–538.

Erdfelder, E, Faul, F, and Buchner, A (1996). GPOWER: A general power analysis program. *Behavior Research Methods, Instruments, & Computers*, 28 (1), 1–11.

Evans, N and Ilbery, B (1992). Farm-based accommodation and the restructuring of agriculture: Evidence from three English counties. *Journal of Rural Studies*, 8 (1), 85–96.

Evelyn, J (1729). *Sylva, or a Discourse on Forest Trees*. The Project Gutenberg, London, 4th edition.

Fahey, TJ and Arthur, MA (1994). Further Studies of Root Decomposition Following Harvest of a Northern Hardwoods Forest. *Forest Science*, 40 (4), 618–629.

FAO (2003). *World agriculture: towards 2015/2030. An FAO perspective*. Food and Agriculture Organization, Rome.

Farrar, J, Hawes, M, Jones, D, and Lindow, S (2003). How roots control the flux of carbon to the rhizosphere. *Ecology*, 84 (4), 827–837.

Fernandez, I, Mahieu, N, and Cadisch, G (2003). Carbon isotopic fractionation during decomposition of plant materials of different quality. *Global Biogeochemical Cycles*, 17 (3), 1–9.

Fleming, J (1998). Arrhenius and current climate concerns: Continuity or a 100–year gap? *Eos, Transactions American Geophysical Union*, 79 (34), 1996–1999.

Fontaine, S, Barot, S, Barré, P, Bdioui, N, Mary, B, and Rumpel, C (2007). Stability of organic carbon in deep soil layers controlled by fresh carbon supply. *Nature*, 450 (7167), 277–80.

Fontaine, S, Henault, C, Aamor, A, Bdioui, N, Bloor, J, Maire, V, Mary, B, Revaillot, S, and Maron, P (2011). Fungi mediate long term sequestration of carbon and nitrogen in soil through their priming effect. *Soil Biology and Biochemistry*, 43 (1), 86–96.

Forestry Commission (2013). Woodland Carbon Code - About the Code - Guidance - 3.4 Project Carbon Sequestration. [Accessed: 26/02/14] http://www.forestry.gov.uk/forestry/INFD-8JUE9T.

Forestry Commission England (n.d.). Farm Woodland Scheme. []http://www.forestry.gov.uk/forestry/INFD-6ZCGFZ.

Foster, P, Ramaswamy, V, Artaxo, P, Bernsten, T, Betts, R, Fahey, D, Haywood, J, Lean, J, Lowe, D, Myhre, G, Nganha, J, Prinn, R, Raga, G, Schulz, M, and Van Dorland, R (2007). Changes in Atmospheric Constituents and in Radiative Forcing. *In* Solomon, S, Qin, D, Manning, M, Chen, Z, Marquis, M, Averyt, KB, Tignor, M, and Miller, H (eds.), *Climate Change 2007: The Physical Science Basis. Contribution of Working Group I to the Fourth Assessment Report of the Intergovernmental Panel on Climate Change*, Cambridge University Press, Cambridge, United Kingdom, and New York, NY, USA. 130–234.

Fourcaud, T, Hruska, J, Cermak, J, Nadyezhdin, V, and Praus, L (2002). An evaluation of different methods to investigate root system architecture or urban trees in situ: I . Ground-penetrating radar. *Journal of Arboriculture*, 28, 2–10.

Friend, A, Scarascia-Mugnozza, G, Isebrands, JG, and Heilman, PE (1991). Quantification of two-year-old hybrid poplar root systems: morphology, biomass, and 14C distribution. *Tree Physiology*, 8 (2), 109–19.

Gaudinski, JB, Trumbore, SE, Eric, A, and Zheng, S (2000). Soil carbon cycling in a temperate forest : radiocarbon-based estimates of residence times , sequestration rates and partitioning of fluxes. *Biogeochemistry*, 51, 33–69.

van Genuchten, M (1980). A closed-form equation for predicting the hydraulic conductivity of unsaturated soils. *Soil Science Society of America*, 44 (5), 892–898.

George, SJ, Kelly, RN, Greenwood, PF, and Tibbett, M (2010). Soil carbon and litter development along a reconstructed biodiverse forest chronosequence of South-Western Australia. *Biogeochemistry*, 101 (1-3), 197–209.

Gielen, B, Calfapietra, C, Lukac, M, Wittig, VE, De Angelis, P, Janssens, Ia, Moscatelli, MC, Grego, S, Cotrufo, MF, Godbold, DL, Hoosbeek, MR, Long, SP, Miglietta, F, Polle, A, Bernacchi, CJ, Davey, PA, Ceulemans, R, and Scarascia-Mugnozza, GE (2005). Net carbon storage in a poplar plantation (POPFACE) after three years of free-air CO2 enrichment. *Tree Physiology*, 25 (11), 1399–408.

Golchin, A, Oades, J, Skjemstad, J, and Clarke, P (1994). Study of free and occluded particulate organic matter in soils by solid state 13 C Cp/MAS NMR spectroscopy and scanning electron microscopy. *Australian Journal of Soil Research*, 32 (2), 285.

Goosse, H (2005). Modelling the climate of the last millennium: What causes the differences between simulations? *Geophysical Research Letters*, 32 (6), L06710.

Gordon, AM, Naresh, RPF, and Thevathasan, V (2006). How much carbon can be stored in Canadian agroecosystems using a silvopastoral approach. *In* Mosquera-Losada, M and Mcadam, JH (eds.), *Silvopastoralism and Sustainable Land Management: Proceedings of an International Congress on Silvopastoralism and Sustainable Management Held in Lugo Spain, in April 2004*, CABI Publishing. 210–218.

Graves, A, Burgess, P, Palma, J, Keesman, K, van der Werf, W, Dupraz, C, van Keulen, H, Herzog, F, and Mayus, M (2010). Implementation and calibration of the parameter-sparse Yield-SAFE model to predict production and land equivalent ratio in mixed tree and crop systems under two contrasting production situations in Europe. *Ecological Modelling*, 221 (13-14), 1744–1756.

Graves, AR, Burgess, P, Palma, J, Herzog, F, Moreno, G, Bertomeu, M, Dupraz, C, Liagre, F, Keesman, K, Vanderwerf, W, and Werf, WVD (2007). Development and application of bio-economic modelling to compare silvoarable, arable, and forestry systems in three European countries. *Ecological Engineering*, 29 (4), 434–449.

Gregorich, EG, Beare, MH, McKim, UF, and Skjemstad, JO (2006). Chemical and Biological Characteristics of Physically Uncomplexed Organic Matter. *Soil Science Society of America Journal*, 70 (3), 975–985.

Guo, LB and Gifford, RM (2002). Soil carbon stocks and land use change: a meta analysis. *Global Change Biology*, 8, 345–360.

Guo, LB, Halliday, MJ, Siakimotu, SJM, and Gifford, RM (2005). Fine root production and litter input: Its effects on soil carbon. *Plant and Soil*, 272 (1-2), 1–10.

Guo, LB, Wang, M, and Gifford, RM (2007). The change of soil carbon stocks and fine root dynamics after land use change from a native pasture to a pine plantation. *Plant and Soil*, 299 (1-2), 251–262.

Gustavsson, L and Sathre, R (2006). Variability in energy and carbon dioxide balances of wood and concrete building materials. *Building and Environment*, 41 (7), 940–951.

Hamilton, GJ (1996). *Forest Mensuration: Forestry Commission Booklet 39*. HMSO, Norwich, 4th edition.

Hansen, MC, Potapov, PV, Moore, R, Hancher, M, Turubanova, Sa, Tyukavina, A, Thau, D, Stehman, SV, Goetz, SJ, Loveland, TR, Kommareddy, A, Egorov, A, Chini, L, Justice, CO, and Townshend, JRG (2013). High-resolution global maps of 21st-century forest cover change. *Science (New York, N.Y.)*, 342 (6160), 850–3.

Harper, R, Okom, A, Stilwell, A, Tibbett, M, Dean, C, George, S, Sochacki, S, Mitchell, C, Mann, S, and Dods, K (2012). Reforesting degraded agricultural landscapes with Eucalypts: Effects on carbon storage and soil fertility after 26years. *Agriculture, Ecosystems & Environment*, 2050, 3–13.

Harper, RJ and Tibbett, M (2013). The hidden organic carbon in deep mineral soils. *Plant and Soil*, 368 (1-2), 641–648.

Hartmann, D, Klein Tank, A, Rusticucci, M, Alexander, L, Brönnimann, S, Charabi, Y, Dentener, F, Dlugokencky, E, Easterling, D, Kaplan, A, Soden, B, Thorne, P, Wild, M, and Zhai, P (2013). Observations: Atmosphere and Surface. *In* Stocker, T, Qin, D, Plattner, G, Tignor, M, Allen, S, Boschung, J, Nauels, A, Xia, Y, Bex, V, and Midgley, P (eds.), *Climate Change 2013: The Physical Science Basis. Contribution of Working Group I to the Fifth Assessment Report of the Intergovernmental Panel on Climate Change*, Cambridge University Press, Cambridge, United Kingdom and New York, NY, USA. 159–254.

Hays, JD, Imbrie, J, and Shackleton, NJ (1976). Variations in the Earth's Orbit: Pacemaker of the Ice Ages. *Science (New York, N.Y.)*, 194 (4270), 1121–32.

Hegerl, G, Zwiers, F, Braconnot, P, Gillet, N, Luo, Y, Marengo Orsini, J, Nicholls, N, Penner, J, and Stott, P (2007). Understanding and attributing climate change. *In* Solomon, S, Qin, D, Manning, M, Chen, Z, Marquis, M, Averyt, KB, Tignor, M, and Miller, H (eds.), *Climate Change 2007: The Physical Science Basis. Contribution of Working Group I to the Fourth Assessment Report of the Intergovernmental Panel on Climate Change*, Cambridge University Press, Cambridge, United Kingdom and New York, NY, USA.

Hein, S and Spiecker, H (2008). Crown and tree allometry of open-grown ash (*Fraxinus excelsior* L.) and sycamore (*Acer pseudoplatanus* L.). *Agroforestry Systems*, 73 (3), 205–218.

Hirano, Y, Dannoura, M, Aono, K, Igarashi, T, Ishii, M, Yamase, K, Makita, N, and Kanazawa, Y (2008). Limiting factors in the detection of tree roots using ground-penetrating radar. *Plant and Soil*, 319 (1-2), 15–24.

Hoenig, JM and Heisey, DM (2001). The Abuse of Power : The Pervasive Fallacy of Power Calculations for Data Analysis. *The American Statistician*, 55 (1), 1–6.

Hoogmoed, M, Cunningham, S, Thomson, J, Baker, P, Beringer, J, and Cavagnaro, T (2012). Does afforestation of pastures increase sequestration of soil carbon in Mediterranean climates? *Agriculture, Ecosystems & Environment*, 159, 176–183.

Hoosbeek, MR, Lukac, M, van Dam, D, Godbold, DL, Velthorst, EJ, Biondi, Fa, Peressotti, A, Cotrufo, MF, de Angelis, P, and Scarascia-Mugnozza, G (2004). More new carbon in the mineral soil of a poplar plantation under Free Air Carbon Enrichment (POPFACE): Cause of increased priming effect? *Global Biogeochemical Cycles*, 18 (1), 1–7.

Huang, Z, Davis, MR, Condron, LM, and Clinton, PW (2011). Soil carbon pools, plant biomarkers and mean carbon residence time after afforestation of grassland with three tree species. *Soil Biology and Biochemistry*, 43 (6), 1341–1349.

Hungate, B, Jackson, R, Field, C, and Stuart Chapin, F (1995). Detecting changes in soil carbon in CO2 enrichment experiments. *Plant and Soil*, 187, 135–145.

Hurlbert, S (1984). Pseudoreplication and the design of ecological field experiments. *Ecological Monographs*, 54 (2), 187–211.

Ilbery, BW (1991). Farm diversification as an adjustment strategy on the urban fringe of the West Midlands. *Journal of Rural Studies*, 7 (3), 207–218.

IPCC (2000*a*). *IPCC Special Report: Emissions Scenarios: Summary for Policymakers*. Cambridge University Press, Cambridge, UK.

IPCC (2000*b*). *Land Use, Land-Use Change and Forestry*. Cambridge University Press, Cambridge, UK.

IPCC (2007). *Contribution of Working Groups I, II and III to the Fourth Assessment Report of the Intergovernmental Panel on Climate Change: Synthesis Report*. November. IPCC, Geneva, Switzerland.

Jackson, RB, Mooney, HA, and Schulze, ED (1997). A global budget for fine root biomass, surface area, and nutrient contents. *Proceedings of the National Academy of Sciences of the United States of America*, 94 (14), 7362–6.

Jamieson, P, Porter, J, and Wilson, D (1991). A test of the computer simulation model ARCWHEAT1 on wheat crops grown in New Zealand. *Field crops research*, 27, 337–350.

Jandl, R, Lindner, M, Vesterdal, L, Bauwens, B, Baritz, R, Hagedorn, F, Johnson, DW, Minkkinen, K, and Byrne, Ka (2007). How strongly can forest management influence soil carbon sequestration? *Geoderma*, 137 (3-4), 253–268.

Janzen, H (2005). Soil carbon: A measure of ecosystem response in a changing world? *Canadian Journal of Soil Science*, 85, 467–480.

Janzen, HH, Campbell, CA, Brandt, SA, Lafond, GP, and Townley-Smith, L (1992). Light-Fraction Organic Matter in Soils from Long-Term Crop Rotations. *Soil Science Society of America Journal*, 56 (6), 1799.

Jastrow, JD, Amonette, JE, and Bailey, VL (2006). Mechanisms controlling soil carbon turnover and their potential application for enhancing carbon sequestration. *Climatic Change*, 80 (1-2), 5–23.

Jenkins, T, Mackie, E, Matthews, R, Miller, G, Randle, T, and White, M (2011). *FC Woodland Carbon Code : Carbon Assessment Protocol*. Forestry Commission.

Jenkinson, DS, Adams, DE, and Wild, A (1991). Model estimates of CO2 emissions from soil in response to global warming. *Nature*, 351 (6324), 304–306.

Jobbágy, E, Jackson, RRB, and Jobbagy, EG (2000). The vertical distribution of soil organic carbon and its relation to climate and vegetation. *Ecological Applications*, 10, 423–436.

Joffre, R, Rambal, S, and Ratte, JP (1999). The dehesa system of southern Spain and Portugal as a natural ecosystem mimic. *Agroforestry Systems*, 45, 57–79.

Johnson, C, Henshaw, J, and Mclnnes, G (1992). Impact of aircraft and surface emissions of nitrogen oxides on tropospheric ozone and global warming. *Nature*, 355 (6355), 69–71.

Johnson, JB and Omland, KS (2004). Model selection in ecology and evolution. *Trends in Ecology & Evolution*, 19 (2), 101–8.

Jones, DL, Nguyen, C, and Finlay, RD (2009). Carbon flow in the rhizosphere: carbon trading at the soilâroot interface. *Plant and Soil*, 321 (1-2), 5–33.

Jose, S (2009). Agroforestry for ecosystem services and environmental benefits: an overview. *Agroforestry Systems*, 76 (1), 1–10.

Joslin, J, Wolfe, MH, and Hanson, P (2000). Effects of altered water regimes on forest root systems. *New Phytologist*, 147, 117–129.

Jug, a, Makeschin, F, Rehfuess, K, and Hofmann-Schielle, C (1999). Short-rotation plantations of balsam poplars, aspen and willows on former arable land in the Federal Republic of Germany. III. Soil ecological effects. *Forest Ecology and Management*, 121 (1-2), 85–99.

Kerr, G and Cahalan, C (2004). A review of site factors affecting the early growth of ash (*Fraxinus excelsior* L.). *Forest Ecology and Management*, 188 (1-3), 225–234.

Kiehl, JT and Trenberth, KE (1997). Earth's Annual Global Mean Energy Budget. *Bulletin of the American Meteorological Society*, 78 (2), 197–208.

King, J, Gay, A, Sylvester-Bradley, R, Bingham, I, Foulkes, J, Gregory, P, and Robinson, D (2003). Modelling Cereal Root Systems for Water and Nitrogen Capture: Towards an Economic Optimum. *Annals of Botany*, 91 (3), 383–390.

King, K (1987). The history of agroforestry. *In* Steppler, H and Nair, P (eds.), *Agroforestry: a decade of development.*, Internation Council for Research in Agroforestry, Nairobi, chapter 1. 3–11.

Kirby, KR and Potvin, C (2007). Variation in carbon storage among tree species: Implications for the management of a small-scale carbon sink project. *Forest Ecology and Management*, 246 (2-3), 208–221.

Kirschbaum, MU, Guo, LB, and Gifford, RM (2008). Why does rainfall affect the trend in soil carbon after converting pastures to forests? *Forest Ecology and Management*, 255 (7), 2990–3000.

Kirschbaum, MUF (2004). Direct and indirect climate change effects on photosynthesis and transpiration. *Plant Biology*, 6 (3), 242–53.

Kirschbaum, MUF, Whitehead, D, Dean, SM, Beets, PN, Shepherd, JD, and Ausseil, aGE (2011). Implications of albedo changes following afforestation on the benefits of forests as carbon sinks. *Biogeosciences*, 8 (12), 3687–3696.

Klaa, K, Mill, PJ, and Incoll, LD (2005). Distribution of small mammals in a silvoarable agroforestry system in Northern England. *Agroforestry Systems*, 63, 101–110.

Kleber, M, Mikutta, R, Torn, MS, and Jahn, R (2005). Poorly crystalline mineral phases protect organic matter in acid subsoil horizons. *European Journal of Soil Science*, 56, 717–725.

Kleidon, A, Fraedrich, K, and Heimann, M (2000). A green planet versus a desert world: estimating the maximum effect of vegetation on the land surface climate. *Climatic Change*, 44, 471–493.

Klute, A (1986). *Methods of Soil Analysis: Part 1 - Physical and Mineralogical Methods*. American Society of Agronomy, Wisconsin, USA, 2nd edition.

Koga, N, Sawamoto, T, and Tsuruta, H (2006). Life cycle inventory-based analysis of greenhouse gas emissions from arable land farming systems in Hokkaido, northern Japan. *Soil Science and Plant Nutrition*, 52 (4), 564–574.

Kramer, C, Trumbore, S, Froberg, M, Cisneros Dozal, L, Zhang, D, Xu, X, Santos, GM, and Hanson, PJ (2010). Recent leaf litter is not a major source of microbial carbon in a temperate forest mineral soil. *Soil Biology and Biochemistry*, 42 (7), 1028–1037.

Kravchenko, AN and Robertson, GP (2011). Whole-Profile Soil Carbon Stocks: The Danger of Assuming Too Much from Analyses of Too Little. *Soil Science Society of America Journal*, 75 (1), 235–240.

Kubin, E (1998). Leaching of nitrate nitrogen into the groundwater after clear felling and site preparation. *Boreal Environment Research*, 3, 3–8.

Kurz, Wa, Dymond, CC, Stinson, G, Rampley, GJ, Neilson, ET, Carroll, aL, Ebata, T, and Safranyik, L (2008). Mountain pine beetle and forest carbon feedback to climate change. *Nature*, 452 (7190), 987–90.

Labitzke, K and Matthes, K (2003). Eleven-year solar cycle variations in the atmosphere: observations, mechanisms and models. *The Holocene*, 13 (3), 311–317.

Laganiere, J, Angers, DA, and Pare, D (2010). Carbon accumulation in agricultural soils after afforestation: a meta-analysis. *Global Change Biology*, 16 (1), 439–453.

Landmark Information Group (2004). Ordnance Survey County Series 1st Edition [TIFF geospatial data], Scale 1:2500, Bedfordshire, 1883.

Landmark Information Group (2011*a*). 1960 map of Clapham Park [PNG map] created using: Edina Historic Digimap Service, Ordnance Survey County Series 1:10560, 3rd Revision 1922-1969 [TIFF geospatial data], Published 1960.

Landmark Information Group (2011*b*). 1970s Map of Clapham Park [PNG map] created using: Edina Historic Digimap Service, Ordnance Survey N.G. 1:10000 [TIFF geospatial data], Published 1972.

Le Treut, H, Somerville, R, Cubasch, U, Ding, Y, Mauritzen, C, Mokssit, A, Peterspn, T, and Prather, M (2007). Historical Overview of Climate Change. *In* Solomon, S, Qin, D, Manning, M, Chen, Z, Marquis, M, Averyt, K, Tignor, M, and Miller, H (eds.), *Climate Change 2007: The Physical Science Basis. Contribution of Working Group I to the Fourth Assessment Report of the Intergovernmental Panel on Climate Change*, Cambridge University Press, Cambridge, United Kingdom, and New York, NY, USA. 94–127.

Lee, J, Hopmans, JW, Rolston, DE, Baer, SG, and Six, J (2009). Determining soil carbon stock changes: Simple bulk density corrections fail. *Agriculture, Ecosystems & Environment*, 134 (3-4), 251–256.

Lemke, P, Ren, J, Alley, R, Allison, I, Carrasco, J, Flato, G, Fujii, Y, Kaser, G, Mote, P, Thomas, R, and Zhang, T (2007). Observations: Changes in snow, ice and frozen ground. *In* Solomon, S, Qin, D, Manning, M, Chen, Z, Marquis, M, Averyt, K, Tignor, M, and Miller, H (eds.), *Climate Change 2007: The Physical Science Basis. Contribution of Working Group I to the Fourth Assessment Report of the Intergovernmental Panel on Climate Change*, Cambridge University Press, Cambridge.

Lodhiyal, L, Singh, RP, and Singh, S (1995*a*). Structure and Function of an Age Series of Poplar Plantations in Central Himalaya: I Dry Matter Dynamics. *Annals of Botany*, 76, 191–199.

Lodhiyal, LS and Lodhiyal, N (1997). Variation in biomass and net primary productivity in short rotation high density central Himalayan poplar plantations. *Forest Ecology and Management*, 98, 167–179.

Lodhiyal, LS, Singh, RP, and Singh, S (1995*b*). Structure and Function of an Age Series of Poplar Plantations in Central Himalaya. II Nutrient Dynamics. *Annals of Botany*, 76, 201–210.

Lundgren, B (1982). What is Agroforestry? *Agroforestry Systems*, 1 (1), 7–12.

Lundmark-Thelin, A and Johansson, M (1997). Influence of mechanical site preparation on decomposition and nutrient dynamics of Norway spruce (Picea

abies(L.) Karst.) needle litter and slash needles. *Forest Ecology and Management*, 96, 101–110.

von Lützow, M, Kögel-Knabner, I, Ekschmitt, K, Flessa, H, Guggenberger, G, Matzner, E, and Marschner, B (2007). SOM fractionation methods: Relevance to functional pools and to stabilization mechanisms. *Soil Biology and Biochemistry*, 39 (9), 2183–2207.

Madari, B, Machado, PL, Torres, E, de Andrade, AG, and Valencia, LI (2005). No tillage and crop rotation effects on soil aggregation and organic carbon in a Rhodic Ferralsol from southern Brazil. *Soil and Tillage Research*, 80 (1-2), 185–200.

Magnusson, K (2013). Creating a typical textbook illustration of statistical power using either ggplot or base graphics. [Accessed: 27/05/2014] http://goo.gl/qgzE2V.

Makkonen, K and Helmisaari, Hs (1999). Assessing fine-root biomass and production in a Scots pine stand - comparison of soil core and root ingrowth core methods. *Plant and Soil*, 210, 43–50.

Marschner, B and Kalbitz, K (2003). Controls of bioavailability and biodegradability of dissolved organic matter in soils. *Geoderma*, 113 (3-4), 211–235.

Mascaro, J, Litton, CMC, Hughes, RF, Uowolo, A, and Schnitzer, SA (2011). Minimizing Bias in Biomass Allometry: Model Selection and Log-Transformation of Data. *Biotropica*, 43, 1–5.

Masera, OR, Garza-Caligaris, J, Kanninen, M, Karjalainen, T, Liski, J, Nabuurs, G, Pussinen, A, de Jong, B, and Mohren, G (2003). Modeling carbon sequestration in afforestation, agroforestry and forest management projects: the CO2FIX V.2 approach. *Ecological Modelling*, 164 (2-3), 177–199.

Matthews, R (2002). Introduction. *In* Matthews, R and Stephens, W (eds.), *Crop-soil Simulation Models. Applications in Developing Countries*, CABI Publishing, Wallingford, chapter 1. 277.

McKay, H (2011). *Short Rotation Forestry : Review of growth and environmental impacts*. Edinburgh.

McKay, H, Hudson, JB, and Hudson, RJ (2003). Woodfuel Resource In Britain Part 2: Appendices.

Mead, R and Willey, RW (1980). The Concept of a 'Land Equivalent Ratio' and Advantages in Yields from Intercropping. *Experimental Agriculture*, 16 (03), 217.

Meehl, G, Stocker, T, Collins, W, Friedlingstein, P, Gaye, A, Gregory, J, Kitoh, A, Knutti, R, Murphy, J, Noda, A, Raper, S, Watterson, I, Weaver, A, and Zhao, ZC (2007). Global climate projections. *In* Solomon, S, Qin, D, Manning, M, Chen, Z, Marquis, M, Averyt, KB, Tignor, M, and Miller, H (eds.), *Climate Change 2007: The Physical Science Basis. Contribution of Working Group I to the Fourth Assessment Report of the Intergovernmental Panel on Climate Change*, Cambridge University Press, Cambridge, United Kingdom and New York, NY, USA.

de Mendiburu, F (2010). agricolae: Statistical Procedures for Agricultural Research: R package version 1.1-3. []http://cran.r-project.org/package=agricolae.

Messing, I, Alriksson, A, and Johansson, W (1997). Soil physical properties of afforested and arable land. *Soil Use and Management*, 13 (4), 209–217.

Mobbs, D, Lawson, G, Friend, A, Crout, N, Arah, J, and Hodnett, M (1999). HyPAR model for agroforestry systems. *In Technical Manual Model Description for Version 3.0. DFID Forestry Research Programme R5652 Penicuik*, Institute of Terrestrial Ecology, Edinburgh.

Montagnini, F and Nair, PKR (2004). Carbon sequestration: an underexploited environmental benefit of agroforestry systems. *Agroforestry Systems*, 61, 281–295.

Moore, T and Knowles, R (1989). The influence of water table levels on methane and carbon dioxide emissions from peatland soils. *Canadian Journal of Soil Science*, 69 (1), 33–38.

Moreno, G, Obrador, J, Cubera, E, and Dupraz, C (2005). Fine Root Distribution in Dehesas of Central-Western Spain. *Plant and Soil*, 277 (1-2), 153–162.

Morison, J, Matthews, R, Miller, G, Perks, M, Randle, T, Vanguelova, E, White, M, Yamulki, S, and Lodge, AH (2012). *Understanding the Carbon and Greenhouse Gas Balance of UK Forests*. Edinburgh.

Mosquera-losada, R, Freese, D, and Rigueiro-Rodriguez, A (2011). Carbon Sequestration in European Agroforestry Systems. *In* Kumar, BM and Nair, PKR (eds.), *Carbon Sequestration Potential of Agroforestry Systems*. 1st edition, 43–59.

Mulia, R and Dupraz, C (2006). Unusual Fine Root Distributions of Two Deciduous Tree Species in Southern France: What Consequences for Modelling of Tree Root Dynamics? *Plant and Soil*, 281 (1-2), 71–85.

Nabuurs, G, Masera, O, Andrasko, K, Benitez-Ponce, P, Boer, R, Dutschke, M, Elsiddig, E, Ford-Robertson, J, Frumhoff, P, Karjalainen, T, Krankina, O, Kurz, W, Matsumoto, M, Oyhantcabal, W, Ravindranath, N, Sanz Sanchez, M, and Zhang, X (2007). Forestry. *In* Metz, B, Davidson, OR, Bosch, P, Dave, R, and Meyer, L (eds.), *Climate Change 2007: Mitigation. Contribution of Working Group III to the Fourth Assessment Report of the Intergovernmental Panel on Climate Change*, Cambridge University Press, Cambridge, United Kingdom and New York, NY, USA.

Nair, P (1993). *An introduction to agroforestry*. Kluwer academic, Dordrecht.

Nair, P, Nair, V, B., MK, and Showalter, JM (2010). Chapter Five – Carbon Sequestration in Agroforestry Systems. *In Advances in Agronomy*, volume 108. 237–307.

Nair, PKR (2011). Carbon sequestration studies in agroforestry systems: a reality-check. *Agroforestry Systems*, 68 (2), 243–253.

Nair, PKR, Kumar, BM, and Nair, VD (2009). Agroforestry as a strategy for carbon sequestration. *Journal of Plant Nutrition and Soil Science*, 172 (1), 10–23.

Natural_England (2008). *Natural England Technical Information Note TIN037: Soil Texture*. February.

Newman, EI (1966). A Method of Estimating the Total Length of Root in a Sample. *Journal of Applied Ecology*, 3 (1), 139–145.

Newman, S, Wainwright, J, Hutton, N, Wu, Y, Marshall, C, Amatya, S, Ranasinghe, D, and Morris, R (1995). Spacing and variety effects on poplar silvoarable systems in the UK. *Agroforestry forum*, 6 (2), 37–43.

Nixon, D, Burgess, P, Sanga, B, and Carr, M (2001). A comparison of the responses of mature and young clonal tea to drought. *Experimental Agriculture*, 37 (3), 391–402.

Nkomaula, JC (1996). *Root distribution of Four-Year-Old Poplar in a Silvo-Arable System*. Thesis, Cranfield University, Cranfield.

van Noordwijk, M, Lusiana, B, and Khasanah, N (2004). WaNuLCAS 3.01 Background on a model of water, nutrient and light capture in agroforestry systems.

Norby, RJ, Delucia, EH, Gielen, B, Calfapietra, C, Giardina, CP, King, JS, Ledford, J, McCarthy, HR, Moore, DJP, Ceulemans, R, De Angelis, P, Finzi, AC, Karnosky, DF, Kubiske, ME, Lukac, M, Pregitzer, KS, Scarascia-Mugnozza, GE, Schlesinger, WH, and Oren, R (2005). Forest response to elevated CO2 is conserved across a broad range of productivity. *Proceedings of the National Academy of Sciences of the United States of America*, 102 (50), 18052–6.

NSRI (2012). *Full Soils Site Report for location 504812E, 252514N, 1km x 1km,*. July.

Oelbermann, M and Voroney, RP (2007). Carbon and nitrogen in a temperate agroforestry system: Using stable isotopes as a tool to understand soil dynamics. *Ecological Engineering*, 29 (4), 342–349.

Ordnance Survey GB (2011). 10K Raster [TIFF geospatial data], Scale 1:10,000, Tile: tl05sw.

Pacala, S and Socolow, R (2004). Stabilization wedges: solving the climate problem for the next 50 years with current technologies. *Science (New York, N.Y.)*, 305 (5686), 968–72.

Page, W (1912). Parishes - Clapham. *In A History of the County of Bedford*. 128–132.

Pallardy, SG, Gibbins, DE, and Rhoads, JL (2003). Biomass production by two-year-old poplar clones on floodplain sites in the Lower Midwest , USA. *Agroforestry Systems*, 59, 21–26.

Palma, J, Graves, A, Bunce, R, Burgess, P, de Filippi, R, Keesman, KJ, van Keulen, H, Liagre, F, Mayus, M, Moreno, G, Reisner, Y, and Herzog, F (2007*a*). Modeling environmental benefits of silvoarable agroforestry in Europe. *Agriculture, Ecosystems and Environment*, 119 (3-4), 320–334.

Palma, J, Graves, A, Burgess, P, Keesman, K, van Keulen, H, Mayus, M, Reisner, Y, and Herzog, F (2007*b*). Methodological approach for the assessment of environmental effects of agroforestry at the landscape scale. *Ecological Engineering*, 29 (4), 450–462.

Pandey, D (2002). Carbon sequestration in agroforestry systems. *Climate Policy*, 2 (4), 367–377.

Pasturel, P (2004). Light and Water Use in a Poplar Silvoarable System. Thesis, Cranfield.

Paul, K and Polglase, P (2002). Change in soil carbon following afforestation. *Forest Ecology and Management*, 168 (June 2001), 241–257.

Paul, K, Polglase, P, and Richards, G (2003). Predicted change in soil carbon following afforestation or reforestation, and analysis of controlling factors by linking a C accounting model (CAMFor) to models of forest growth (3PG), litter decomposition (GENDEC) and soil C turnover (RothC). *Forest Ecology and Management*, 177 (1-3), 485–501.

Paustian, K, Babcock, B, Hatfield, J, and Lal, R (2004). *Agricultural Mitigation of Greenhouse Gases: Science and Policy Options. CAST (Council on Agricultural Science and Technology) Report, R141 2004*.

Peichl, M, Thevathasan, NV, Gordon, AM, Huss, J, and Abohassan, Ra (2006). Carbon Sequestration Potentials in Temperate Tree-Based Intercropping Systems, Southern Ontario, Canada. *Agroforestry Systems*, 66 (3), 243–257.

Peng, R and Sutton, S (1996). The activity and diversity of ground arthropods in an agroforestry system. *In Proceedings of the New Zealand Plant Protection Conference*. New Zealand Plant Protection Society Inc., 309–313.

Perez-Garcia, J, Lippke, B, and Comnick, J (2005). An assessment of carbon pools, storage, and wood products market substitution using life-cycle analysis results. *Wood and Fiber*, 37, 140–148.

Picard, N, Saint-Andre, L, and Henry, M (2012). *Manual for building tree volume and biomass allometric equations: From field measurement to prediction*. Rome.

Pietola, L and Alakukku, L (2005). Root growth dynamics and biomass input by Nordic annual field crops. *Agriculture, Ecosystems & Environment*, 108 (2), 135–144.

Piirainen, S, Finér, L, Mannerkoski, H, and Starr, M (2007). Carbon, nitrogen and phosphorus leaching after site preparation at a boreal forest clear-cut area. *Forest Ecology and Management*, 243 (1), 10–18.

Poeplau, C, Don, A, Vesterdal, L, Leifeld, J, Van Wesemael, B, Schumacher, J, and Gensior, A (2011). Temporal dynamics of soil organic carbon after land-use change in the temperate zone - carbon response functions as a model approach. *Global Change Biology*, 17 (7), 2415–2427.

Polmear, GI (2010). Stratified Random Point Sampler.

Post, WM and Kwon, KC (2000). Soil carbon sequestration and land-use change: processes and potential. *Global Change Biology*, 6 (3), 317–327.

Puri, S, Singh, V, Bhushan, B, and Singh, S (1994). Biomass production and distribution of roots in three stands of Populus deltoides. *Forest Ecology and Management*, 65 (2-3), 135–147.

R Development Core Team (2013). R: A language and environment for statistical computing. []http://www.r-project.org.

Raes, D, Steduto, P, Hsiao, TC, and Fereres, E (2012). *AquaCrop Version 4.0 Reference Manual*. June. Food and Agriculture Organization, Rome.

Rasband, W (2013). ImageJ. []http://imagej.nih.gov/ij/.

Rasse, DP, Rumpel, C, and Dignac, MF (2005). Is soil carbon mostly root carbon? Mechanisms for a specific stabilisation. *Plant and Soil*, 269 (1-2), 341–356.

Recous, S, Coppens, F, Abiven, S, Garnier, P, and Merckx, R (2008). Carbon and Nitrogen Dynamics in Soils: Effects of Residue Quality and Localization. *In Systems for Enhancing Management of Agroforestry Systems*, International Atomic Eneregy Agency, Vienna, November. 99.

Richter, DD, Markewitz, D, Trumbore, SE, and Wells, CG (1999). Rapid accumulation and turnover of soil carbon in a re-establishing forest. *Ecosystems*, 400, 14–16.

Rillig, M, Wright, S, Nichols, K, Schmidt, W, and Torn, M (2001). Large contribution of arbuscular mycorrhizal fungi to soil carbon pools in tropical forest soils. *Plant and Soil*, 233, 167–177.

Ritchie, J (1972). Model for predicting evaporation from a row crop with incomplete cover. *Water Resources Research*, 8 (5), 1204–1213.

Ritchie, J (1998). Soil water balance and plant water stress. *In* Tsuji, GY, Hogenboom, G, and Thornton, PK (eds.), *Understanding options for agricultural production*, Kluwer Academic Publishers, Dordrecht. 41–54.

Rogner, HH, Zhou, D, Bradley, P, Crabbé, P, Edenhofer, O, Hare, B, Kuijpers, L, and Yamaguchi, M (2007). Introduction. *In* Metz, B, Davidson, OR, Bosch, P, Dave, R, and Meyer, L (eds.), *Climate Change 2007: Mitigation. Contribution of Working Group III to the Fourth Assessment Report of the Intergovernmental Panel on Climate Change*, Cambridge University Press, Cambridge, United Kingdom and New York, NY, USA., chapter 1.

Rosell, R, Gasparoni, J, and Galantini, J (2001). Soil organic matter evaluation. *In* Lal, R, Kimble, J, Follett, R, and Stewart, B (eds.), *Assessment Methods for Soil Carbon*, Lewis Publishers, Boca Raton, Florida, chapter 21. 311–322.

RStudio (2012). RStudio: Integrated development environment for R (Version 0.97.248). []http://www.rstudio.org.

Rumpel, C, Kögel-Knabner, I, and Bruhn, F (2002). Vertical distribution, age, and chemical composition of organic carbon in two forest soils of different pedogenesis. *Organic Geochemistry*, 33 (10), 1131–1142.

Salehi, M, Beni, OH, Harchegani, HB, Borujeni, IE, and Motaghian, H (2011). Refining Soil Organic Matter Determination by Loss-on-Ignition. *Pedosphere*, 21 (4), 473–482.

Savill, P, Evans, J, Auclair, D, and Falck, J (1997). *Plantation Silviculture in Europe*. Oxford University Press.

Sayer, E, Heard, S, Grant, H, Marthew, T, and Tanner, E (2011). Soil carbon release enhanced by increased tropical forest litterfall. *Nature Climate Change*, 1, 304–307.

Schöning, I and Kögel-Knabner, I (2006). Chemical composition of young and old carbon pools throughout Cambisol and Luvisol profiles under forests. *Soil Biology and Biochemistry*, 38 (8), 2411–2424.

Schultz, R, Isebrands, J, and Kormanik, P (1983). Mycorrhizae of Poplars. *USDA Forest Service General Technical Report*, 91, 17–28.

Schulze, ED (2000). Managing Forests After Kyoto. *Science*, 289 (5487), 2058–2059.

Schumacher, BA (2002). *Methods for the Determination of Total Organic Carbon (TOC) in Soils and Sediments*. April.

Schuur, EAG, Bockheim, J, Canadell, JG, Euskirchen, E, Field, CB, Goryachkin, SV, Hagemann, S, Kuhry, P, Lafleur, PM, Lee, H, Mazhitova, G, Nelson, FE, Rinke, A, Romanovsky, VE, Shiklomanov, N, Tarnocai, C, Venevsky, S, Vogel, JG, and Zimov, Sa (2008). Vulnerability of Permafrost Carbon to Climate Change: Implications for the Global Carbon Cycle. *BioScience*, 58 (8), 701.

Seattle, M (2012). Building materials: Wooden skyscrapers. [Accessed: 15/07/2014]http://www.economist.com/blogs/babbage/2012/08/building-materials.

Semenov, M and Brooks, R (1998). Comparison of the WGEN and LARS-WG Stochastic Weather Generators for Diverse Climates. *Climate Research*, 10, 95–107.

Seobi, T, Anderson, SH, Udawatta, RP, and Gantzer, CJ (2005). Influence of Grass and Agroforestry Buffer Strips on Soil Hydraulic Properties for an Albaqualf. *Soil Science Society of America Journal*, 69 (3), 893.

Sharrow, S and Ismail, S (2004). Carbon and nitrogen storage in agroforests, tree plantations, and pastures in western Oregon, USA. *Agroforestry Systems*, 60 (2), 123–130.

Sheldrick, R and Auclair, D (2000). Origins of agroforestry and recent history in the UK. Bulletin 122. *In* Hislop, M and Claridge, J (eds.), *Agrofestry in the UK*, Edinburgh, chapter 2. 136.

Shi, S, Zhang, W, Zhang, P, Yu, Y, and Ding, F (2013). A synthesis of change in deep soil organic carbon stores with afforestation of agricultural soils. *Forest Ecology and Management*, 296, 53–63.

Shoji, S, Delgado, J, Mosier, A, and Miura, Y (2001). Use of controlled release fertilizers and nitrification inhibitors to increase nitrogen use efficiency and to conserve air and water quality. *Communications in Soil Science and Plant Analysis*, 32 (7-8), 1051–1070.

Sibbald, A, Eason, W, McAdam, J, and Hislop, A (2001). The establishment phase of a silvopastoral national network experiment in the UK. *Agroforestry systems*, 39, 39–53.

Silva, J and Rego, F (2003). Root distribution of a Mediterranean shrubland in Portugal. *Plant and Soil*, 255 (2), 529–540.

Sims, R, Schock, R, Adegbululgbe, A, Fenhann, J, Konstantinaviciute, I, Moomaw, W, Nimir, H, Schlamadinger, B, Torres-Martínez, J, Turner, C, Uchiyama, Y, Vuori, S, Wamukonya, N, and X. Zhang (2007). Energy Supply. *In* Metz, B, Davidson, O, Bosch, P, Dave, R, and Meyer, L (eds.), *Climate Change 2007: Mitigation. Contribution of Working Group III to the Fourth Assessment Report of the Intergovernmental Panel on Climate Change*, Cambridge University Press, Cambridge, United Kingdom and New York, NY, USA.

Skovsgaard, JP and Vanclay, JK (2008). Forest site productivity: a review of the evolution of dendrometric concepts for even-aged stands. *Forestry*, 81 (1), 13–31.

Smith, P, Martino, D, Cai, Z, Gwary, D, Janzen, H, Kumar, P, McCarl, B, Ogle, S, O'Mara, F, Rice, C, Scholes, B, and Sirotenko, O (2007). Agriculture. *In* Metz, B, Davidson, OR, Bosch, P, Dave, R, and Meyer, L (eds.), *Climate Change 2007: Mitigation. Contribution of Working Group III to the Fourth Assessment Report of the Intergovernmental Panel on Climate Change*, Cambridge University Press, Cambridge, United Kingdom, chapter 8. 497–540.

Souch, CA and Stephens, W (1998). Growth, productivity and water use in three hybrid poplar clones. *Tree Physiology*, 18 (12), 829–835.

Sprugel, D (1983). Correcting for bias in log-transformed allometric equations. *Ecology*, 64 (1), 209–210.

Stephenson, NL, Das, AJ, Condit, R, Russo, SE, Baker, PJ, Beckman, NG, Coomes, Da, Lines, ER, Morris, WK, Rüger, N, Alvarez, E, Blundo, C, Bunyavejchewin, S, Chuyong, G, Davies, SJ, Duque, A, Ewango, CN, Flores, O, Franklin, JF, Grau, HR, Hao, Z, Harmon, ME, Hubbell, SP, Kenfack, D, Lin, Y, Makana, JR, Malizia, A, Malizia, LR, Pabst, RJ, Pongpattananurak, N, Su, SH, Sun, IF, Tan, S, Thomas, D, van Mantgem, PJ, Wang, X, Wiser, SK, and Zavala, MA (2014). Rate of tree carbon accumulation increases continuously with tree size. *Nature*, 507 (7490), 90–3.

Stocker, T, Qin, D, Plattner, GK, Alexandeer, L, Allen, S, Bindoff, N, Breon, F, Church, J, Cubasch, U, Emori, S, P.Forster, Friedlingstein, P, Gillet, N, Gregory,

J, Hartmann, D, Jansen, E, Kirtman, B, Knutti, R, Krishna Kumar, K, Lemke, P, Marotzke, J, Masson-Delmotte, V, Meehl, G, Mokhov, I, Piao, S, Ramaswamy, V, Randall, D, Rhein, M, Rojas, M, Sabine, C, Schindell, D, Talley, L, Vaughan, D, and Xie, SP (2013). Technical Summary. *In* Stocker, T, Qin, D, Plattner, G, Tignor, M, Allen, S, Boschung, J, Nauels, A, Xia, Y, Bex, V, and Midgley, P (eds.), *Climate Change 2013: The Physical Science Basis. Contribution of Working Group I to the Fifth Assessment Report of the Intergovernmental Panel on Climate Change*, Cambridge University Press, Cambridge, United Kingdom and New York, NY, USA. 33–115.

Stockmann, U, Adams, MA, Crawford, JW, Field, DJ, Henakaarchchi, N, Jenkins, M, Minasny, B, McBratney, AB, Courcelles, VDRD, Singh, K, Wheeler, I, Abbott, L, Angers, Da, Baldock, J, Bird, M, Brookes, PC, Chenu, C, Jastrow, JD, Lal, R, Lehmann, J, O'Donnell, AG, Parton, WJ, Whitehead, D, and Zimmermann, M (2013). The knowns, known unknowns and unknowns of sequestration of soil organic carbon. *Agriculture, Ecosystems & Environment*, 164, 80–99.

Stone, E and Kalisz, P (1991). On the maximum extent of tree roots. *Forest Ecology and Management*, 46 (1-2), 59–102.

Szott, L (1991). Soil-plant interactions in agroforestry systems. *Forest Ecology and Management*, 45 (1-4), 127–152.

Thomas, L (1997). Retrospective power analysis. *Conservation Biology*, 11 (1), 276–280.

Thomas, L and Krebs, C (1997). A review of statistical power analysis software. *Bulletin of the Ecological Society of America*, 78 (2), 128–139.

Thompson, D and Matthews, R (1989). *Research Information Note 160. The storage of carbon in trees and timber*. Forestry Commission Research Divison.

Tiessen, H, Cuevas, E, and Chacon, P (1994). The role of soil organic matter in sustaining soil fertility. *Nature*, 371 (6500), 783–785.

Trenberth, K, Jones, P, Ambenje, P, Bojariu, R, Easterling, D, Klein Tank, A, Parker, D, Rahimzadeh, F, Renwick, J, Rusticucci, M, Soden, B, and Zhai, P (2007). Observations: surface and atmospheric climate change. *In* Solomon, S, Qin, D, Manning, M, Chen, Z, Marquis, M, Averyt, KB, Tignor, M, and Miller, H (eds.), *Climate Change 2007: The Physical Science Basis. Contribution of Working Group I to the Fourth Assessment Report of the Intergovernmental Panel on Climate Change*, Cambridge University Press, Cambridge, United Kingdom, and New York, NY, USA. 235–336.

Treseder, K and Allen, M (2000). Mycorrhizal fungi have a potential role in soil carbon storage under elevated CO2 and nitrogen deposition. *New Phytologist*, 147, 189–200.

Trumbore, S (1993). Comparison of carbon dynamics in tropical and temperate soils using radiocarbon measurements. *Global Biogeochemical Cycles*, 7 (2), 275–290.

UK Meteorological Office (2013). Met Office Integrated Data Archive System (MIDAS) Land and Marine Surface Stations Data (1853-current), NCAS British Atmospheric Data Centre.

UNEP (2011). *Bridging the Emissions Gap*.

UNESA (2004). *World Population to 2300*. New York.

UNFAO (2009). *Food Security and Agricultural Mitigation in Developing Countries: Options for Capturing Synergies*. Rome.

Upson, MA and Burgess, P (2013). Soil organic carbon and root distribution in a temperate arable agroforestry system. *Plant and Soil*, 373 (1-2), 43–58.

Vanguelova, EI, Nisbet, TR, Moffat, aJ, Broadmeadow, S, Sanders, TGM, and Morison, JIL (2013). A new evaluation of carbon stocks in British forest soils. *Soil Use and Management*, 29 (2), 169–181.

Veen, JV and Ladd, J (1985). Turnover of carbon and nitrogen through the microbial biomass in a sandy loam and a clay soil incubated with glucose and (NH4) 2SO4 under different moisture regimes. *Soil Biology and Biochemistry*, 17 (6), 747–756.

Verma, K and Bradley, R (1988). *Soils of Silsoe College Farm*. Cranfield University, Silsoe.

Vesterdal, L and Ritter, E (2002). Change in soil organic carbon following afforestation of former arable land. *Forest Ecology and Management*, 169, 137–147.

Vylupek, O (2010). *Biophysical Modelling of Cider Orchard Intercropping*. Thesis, Cranfield University.

Walkley, A and Black, I (1934). An examination of the Degtjareff method for determining soil organic matter, and a proposed modification of the chromic acid titration method. *Soil Science*, 37 (1), 29–38.

Wang, X, Wang, J, and Zhang, J (2012). Comparisons of three methods for organic and inorganic carbon in calcareous soils of northwestern China. *Plos One*, 7 (8), e44334.

Wang, Y, Amundson, R, and Trumbore, S (1995). Radiocarbon Dating of Soil Organic Matter. *Quarternary Research*, 45 (3), 282–288.

Wellens, J, Raes, D, Traore, F, Denis, A, Djaby, B, and Tychon, B (2013). Performance assessment of the FAO AquaCrop model for irrigated cabbage on farmer plots in a semi-arid environment. *Agricultural Water Management*, 127, 40–47.

Wenhua, L (2004). Degradation and restoration of forest ecosystems in China. *Forest Ecology and Management*, 201 (1), 33–41.

van der Werf, W, Keesman, K, Burgess, P, Graves, A, Pilbeam, D, Incoll, LD, Metselaar, K, Mayus, M, Strappus, R, van Keulen, H, Palma, J, and Dupraz, C (2007). Yield-SAFE: A parameter-sparse, process-based dynamic model for predicting

resource capture, growth, and production in agroforestry systems. *Ecological Engineering*, 9 (340), 419–433.

West, V (2011). *Soil carbon in the Woodland Carbon Code*. July. Forestry Commission, Edinburgh.

Wielopolski, L, Hendrey, G, Daniels, J, and McGuigan, M (2000). Imaging tree root systems in situ. *In Eighth International Conference on Ground Penetrating Radar*. volume 4084, 642–646.

Williams-Guillen, K, Perfecto, I, and Vandermeer, J (2008). Bats Limit Insects in a Neotropical Agroforestry System. *Science*, 320, 2008.

Williamson, GB and Wiemann, MC (2010). Measuring wood specific gravity...Correctly. *American Journal of Botany*, 97 (3), 519–24.

Willmott, CJ, Ackleson, SG, Davis, RE, Feddema, JJ, Klink, KM, Legates, DR, O'Donnell, J, and Rowe, CM (1985). Statistics for the evaluation and comparison of models. *Journal of Geophysical Research*, 90 (C5), 8995.

Winton, M (2006). Surface Albedo Feedback Estimates for the AR4 Climate Models. *Journal of Climate*, 19 (3), 359–365.

World Agroforestry Centre (n.d.). Wood Density Database.

Wösten, J, Lilly, A, Nemes, A, and Bas, CL (1999). Development and use of a database of hydraulic properties of European soils. *Geoderma*, 90, 169–185.

Wright, S and Upadhyaya, A (1998). A survey of soils for aggregate stability and glomalin, a glycoprotein produced by hyphae of arbuscular mycorrhizal fungi. *Plant and soil*, 198, 97–107.

Wulfsohn, D and Nyengaard, J (1999). Simple stereological procedure to estimate the number and dimensions of root hairs. *Plant and Soil*, 209, 129–136.

Xie, Y (2012). knitr: A general purpose package for dynamic report generation in R. R package version 1.1. []http://yihui.name/knitr/.

Zaehle, SS, Ciais, P, Friend, AD, and Prieur, V (2011). Carbon benefits of anthropogenic reactive nitrogen offset by nitrous oxide emissions. *Nature Geoscience*, 4 (9), 601–605.

Zanne, A, Lopez-Gonzalez, G, Coomes, D, Ilic, J, Jansen, S, Lewis, S, Miller, R, Swenson, N, Wiemann, M, and Chave, J (2009). Data from: Towards a worldwide wood economics spectrum. *Dryad Digital Repository*.

Zeileis, A and Grothendieck, G (2005). zoo: S3 infrastructure for regular and irregular time series. *Journal of Statistical Software*, 14 (6).

Zenone, T, Morelli, G, and Teobaldelli, M (2008). Preliminary use of ground-penetrating radar and electrical resistivity tomography to study tree roots in pine forests and poplar plantations. *Functional Plant Biology*, 35 (10), 1047–1058.

Zhu, YG and Michael Miller, R (2003). Carbon cycling by arbuscular mycorrhizal fungi in soilâplant systems. *Trends in plant science*, 8 (9), 407–9.

Zimmermann, M, Leifeld, J, Schmidt, MWI, Smith, P, and Fuhrer, J (2007). Measured soil organic matter fractions can be related to pools in the RothC model. *European Journal of Soil Science*, 58 (3), 658–667.

Part V

APPENDIX

A

APPENDIX TO CHAPTER 4

A.1 THE INTERSECTION METHOD FOR FINE ROOT LENGTH DETERMINATION

A grid of 1 cm squares was printed out onto an A4 piece of paper and then positioned beneath a large, shallow plastic dish. The sample was poured into the dish and positioned randomly above the sheet. The number of intersections of the roots with the grid was counted (Figure A.1).

Figure A.1: Fine root sample overlaid onto 1 cm grid. This sample was from a depth of 105 cm and at a distance of 4 m from the tree, hence there are relatively few intersections.

The number of root intersections was converted into a root length density ( ) by multiplying a constant (11/14) by the number of intersections (I) and the distance (U) between grid lines in cm – in this case 1. The resulting value was then divided by the volume of the soil sample from which the roots released (Equation A.1).

$$FRLD = \frac{\frac{11}{14} \cdot I \cdot U}{V} \tag{A.1}$$

A.2 COMPARISON OF METHODS OF DETERMINING OCC

Table A.1: Results from regression of C_o% determination methods

	Dependent variable:	
	DryCombustion	Rothamsted
	(1)	(2)
Titration	0.865***	0.782***
	(0.071)	(0.051)
Constant	0.252	0.158
	(0.159)	(0.111)
Observations	27	18
R^2	0.856	0.936
Adjusted R^2	0.851	0.932
Residual Std. Error	0.429 (df = 25)	0.255 (df = 16)
F Statistic	149.000*** (df = 1; 25)	233.300*** (df = 1; 16)
Note:		*p<0.1; **p<0.05; ***p<0.01

Table A.2: Results from ANOVA of different methods of C_o% determination. C_o% × determination method, depth, distance, and interractions thereof.

	Df	Sum Sq	Mean Sq	F value	Pr(>F)
Residuals	2	1.79	0.90		
method	2	1.39	0.69	4.77	0.013
treat	2	0.24	0.12	0.82	0.448
depth	2	73.47	36.74	252.66	0.000
method:treat	3	0.48	0.16	1.10	0.360
method:depth	4	0.80	0.20	1.37	0.259
treat:depth	4	1.44	0.36	2.47	0.058
method:treat:depth	6	0.09	0.01	0.10	0.996
Residuals	46	6.69	0.15		

Table A.3: Summary statistics for LSD test of C_o% (100) × determination method.

	OCC	std	r	LCL	UCL	Min	Max
OCC_ea	1.91	1.11	27	1.76	2.05	0.44	3.84
OCC_roth	1.59	0.98	18	1.41	1.77	0.43	3.06
OCC_t	1.91	1.19	27	1.77	2.06	0.30	3.78

Table A.4: Groups of statistical similarity for $C_o\%$ (100) $\times$ determination method. Different letters indicate a significant difference $p < 0.05$.

trt	means	M
OCC_t	1.91	a
OCC_ea	1.91	a
OCC_roth	1.59	b

Results from dry combustion completed at Cranfield, and by Rothamsted closely matched those given by the titration method (Figure A.2). One potential outlier was identified and removed from the cropped treatment at the lowest depth increment. A regression of the results from the two methods indicates that there is a highly significant correlation between both sets of results from dry combustion ($p < 0.001$). A high coefficient of determination of at least 0.92 indicates a good fit between the datasets (Figure A.2). The absolute mean differences between the results gained through titrimetry and those determined by elemental analysis at Cranfield and Rothamsted were 0.35 and 0.30 g 100 g^{-1} respectively.

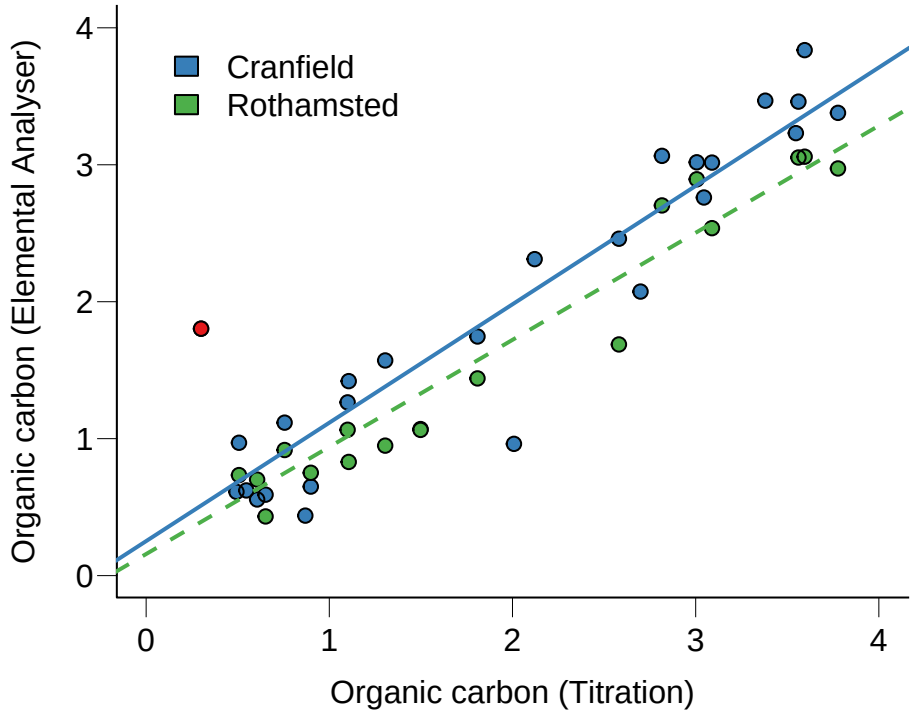

Figure A.2: Scatterplot of the carbon content results from the Walkley-Black method and results from dry combustion in an elemental analyser conducted at Cranfield and Rothamsted (all units in g 100 g^{-1}). One outlier from dry combustion at Cranfield has been removed (indicated by a red circle). Regression analysis of titration results vs. Cranfield elemental analysis (solid blue line) follows the equation $y = 0.252 + 0.865x$, $R^2 = 0.85$. Dashed green line indicates regression analysis of results from titration and elemental analysis conducted at Rothamsted ($y = 0.158 + 0.782x$, $R^2 = 0.93$).

To further investigate the relationship between the two variables, analysis of variance was used to compare the means of results from the three methods, including the variables treatment, depth and an error term to account for the experimental blocking (Table A.2). Results from this analysis indicate that whilst differences in C_o% measurements gained through elemental analysis and titrimetry at Cranfield did not differ, significantly less carbon was recovered using the elemental analysis completed at Rothamsted.

A.3 COMPARISON OF OCC DATA COLLECTED IN 2001 AND 2011 AT SILSOE

Data collected by Donkin (2001) can be compared to data from the present study to gain some indication of the changes in organic carbon content over time.

Data were collected at two depths (15 and 30 cm) and at three distances from the tree (0, 2 and 4 m); these are compared with the same depths at distances of 0.5, 2.5 and 4.5 m. Donkin collected data at two distances from the tree along the tree row; both have been used for comparison with the present data.

Since the sequential nature of the measurements could violate the assumption of independence, year was modelled as a random effect.

Block was also modelled as a random effect using the same blocking as reported in Appendix B of Donkin's thesis. Because block was not specified for the control samples, results from the control plots were not tested.

A.3.1 *Analysis of penetrometer data from Aves, 2002*

Aves (2002) completed a study of soil resistance using a cone penetrometer at one metre intervals across the intercropped alleys (Table A.5). Whilst no statistical analyses were completed in the original thesis, Aves's are analysed here.

Table A.6:

Table A.5: Summary of penetrometer resistance () data collected by Aves (2002). Note that depth has been limited to 23.1 cm as data beneath this depth were incomplete.

	Distance (m)							
Depth (cm)	1	2	3	4	5	6	7	8
3.3	332	283	448	467	578	465	407	394
6.6	522	507	621	700	755	647	592	556
9.9	602	542	658	758	754	798	617	585
13.2	795	721	733	766	742	858	638	611
16.5	958	760	852	705	782	842	649	670
19.8	1110	840	931	742	837	822	736	774
23.1	1182	1015	989	803	837	893	812	847

First, the data were limited to a depth of 23.1 cm to exclude missing values at greater depths. The remaining data were analysed using ANOVA, including the block from which measurements were made, as a random effect. This accounted for the spatial pseudoreplication inherent in the experimental design.

Results from the ANOVA indicate that there were significant variations in penetrometer resistance as a result of the distance across the arable alley and depth. A highly significant interaction was also found between distance and depth (Table A.6).

Table A.6: Results from ANOVA of soil prenetrometer resistance (kPa) × depth, distance, and interractions thereof.

	Df	Sum Sq	Mean Sq	F value	Pr(>F)
Residuals	1	25457.79	25457.79		
dist	1	318633.37	318633.37	14.75	0.000
depth	6	7879730.02	1313288.34	60.80	0.000
dist:depth	6	874858.98	145809.83	6.75	0.000
Residuals	321	6933650.41	21600.16		

Table A.7: Summary statistics for LSD test of Penetrometer resistance (kPa) × distance.

	res	std	r	LCL	UCL	Min	Max
1	785.60	318.15	42	740.98	830.21	240.00	1470.00
2	666.86	245.08	42	622.24	711.47	180.00	1360.00
3	747.62	213.26	42	703.00	792.24	320.00	1140.00
4	705.71	197.96	42	661.10	750.33	240.00	1120.00
5	755.00	164.20	42	710.38	799.62	410.00	1190.00
6	760.83	201.61	42	716.22	805.45	330.00	1210.00
7	635.71	158.17	42	591.10	680.33	340.00	960.00
8	633.86	164.10	42	589.24	678.47	350.00	1030.00

Table A.8: Groups of statistical similarity for Penetrometer resistance (kPa) × distance. Different letters indicate a significant difference $p < 0.05$.

trt	means	M
1	785.60	a
6	760.83	ab
5	755.00	ab
3	747.62	ab
4	705.71	bc
2	666.86	cd
7	635.71	d
8	633.86	d

Table A.9: Summary statistics for LSD test of Penetrometer resistance (kPa) × depth.

	res	std	r	LCL	UCL	Min	Max
13.2	732.98	143.81	48	691.24	774.71	460.00	1170.00
16.5	777.29	168.71	48	735.56	819.03	490.00	1210.00
19.8	848.96	188.82	48	807.22	890.69	450.00	1470.00
23.1	922.33	196.12	48	880.60	964.07	430.00	1360.00
3.3	421.77	132.55	48	380.04	463.51	180.00	750.00
6.6	612.29	125.65	48	570.56	654.03	420.00	990.00
9.9	664.17	129.78	48	622.43	705.90	470.00	1030.00

Table A.10: Groups of statistical similarity for Penetrometer resistance (kPa) × depth. Different letters indicate a significant difference $p < 0.05$.

trt	means	M
23.1	922.33	a
19.8	848.96	b
16.5	777.29	c
13.2	732.98	c
9.9	664.17	d
6.6	612.29	d
3.3	421.77	e

Depth was found to be the best predictor of soil resistance, which increased significantly at each depth increment ($p < 0.05$, Table A.6).

Soil resistance was also found to vary significantly across the tree row ($p < 0.05$). Almost uniformly, the greatest soil resistance was found towards the centre of the alley. Resistance at metres to ere significantly greater than distances closer to the tree row, with the exception of metre 1, which showed the highest overall mean resistance (Table A.8).

A.4 PROTOCOLS AND ADDITIONAL METHODS

A.4.1 *Soil organic matter (carbon) by dichromate digest: NR-SAS / SOP4 / Version 1*

A.4.1.1 *Source*

This SOP is based on Method 3 of British Standard BS 1377-3:1990 - Soils for civil engineering purposes - part 3: chemical and electro-chemical tests and method 56 of the MAFF Reference Book RB427 (1986) Analysis of Agricultural Materials.

A.4.1.2 *Scope*

This SOP describes a method for the determination of organic matter (carbon). This SOP is applicable to all types of air-dried, non-saline soil samples.

A.4.1.3 *Principle*

Soil organic matter is almost completely oxidised by a solution of potassium dichromate, sulphuric acid and orthophosphoric acid. Excess dichromate is determined by titrating with iron (II) sulphate solution. Using this method, it is the percentage of organic carbon in the soil which is determined and this is multiplied by a factor of 1.724 to give percentage organic matter. The use of this factor is based on the assumption that soil organic matter contains 58% carbon.

A.4.1.4 *Laboratory sample*

Use air-dried soil samples, for example samples pre-treated according to NR-SAS / SOP 1.

A.4.1.5 *Reagents*

Orthophosphoric acid (1.7 specific gravity)
Sulphuric acid (1.84 specific gravity)
0.167 mol/l potassium dichromate solution (RPU 14)
Iron (II) sulphate solution (RPU 15)
N-phenylanthranilic acid indicator solution (RPU 16)

A.4.1.6 *Calibration check*

Ensure dichromate dispenser gives volume of 10 ml $\pm$1 ml
Ensure sulphuric acid dispenser gives volume of 20 ml $\pm$2ml
Ensure orthophosphoric acid dispenser gives volume 10ml $\pm$1ml

A.4.1.7 *Preparation of digests*

Weigh (to 0.0001g) approximately 0.2g of air-dried soil into a 500ml conical flask (if the soil is of very low organic matter, up to 5g of sample can be used). Record this mass (W).

To each flask add, while gently swirling, in the following order

- 10ml of potassium dichromate solution
- 20ml of sulphuric acid

Allow flask to stand on a heat resistant mat for 30 minutes ± 5 minutes. Add 200ml of demineralised water, 10ml of orthophosphoric acid and 2ml of indicator solution and swirl well. Carry out a blank digest using no soil but following the same procedure.

A.4.1.8 *Determination of organic matter*

Titrate the digested soil mixture with the iron (II) sulphate solution. The end point is as the purple colour changes, via a blue colour, to green. Record the titre, which should be at least 5ml; if it is not, repeat using less soil. Titrate the digested blank with the iron (II) sulphate solution. The end point is as the purple colour changes, via a blue colour, to green. Record the titre.

A.4.1.9 *Expression of results*

The organic matter (carbon) is calculated and recorded to one decimal place.
The result for organic matter (carbon) is reported to one decimal place.

A.4.1.10 *Calculation*

Total volume, V, of potassium dichromate used to oxidise the organic matter in soil is calculated as follows:

$$V = 10x(\frac{1-y}{X})$$

Where:
y is the iron (II) sulphate titre, in ml, of the soil digest;
X is the iron (II) sulphate titre, in ml, of the blank digest.

$$\text{Organic matter content } (\%) = \frac{(0.67xV)}{W}$$

Where:
V is the volume, in ml, of potassium dichromate used to oxidise the organic matter;
W is the mass, in grams, of the sample.

A.5 TOTAL CARBON IN SOIL AND PLANT MATERIAL AND ORGANIC CARBON IN SOIL: NR-SAS / SOP 9 / VERSION 1

A.5.0.11 *Source*

This SOP is based on British Standard BS 7755 Section 3.8:1995 Determination of organic and total carbon after dry combustion (elementary analysis) which is identical to ISO 10694:1995.

A.5.0.12 *Scope*

This SOP describes a method for the determination of total and organic carbon. This SOP is applicable to all types of oven-dried soil or plant material.

A.5.0.13 *Principle*

The carbon present in the soil (plant material) is oxidised to carbon dioxide (CO_2) by heating the soil (plant material) to at least 900°C on a flow of oxygen-containing gas that is free from carbon dioxide. The amount of carbon dioxide released is then measured by a thermal conductivity detector (TCD). When the soil (plant material) is heated to a temperature of at least 900°C, any carbonates present are completely decomposed. For the determination of the organic carbon content, any carbonates present are previously removed by treating the soil with hydrochloric acid.

A.5.0.14 *Laboratory sample*

Use prepared soil or plant material, for example samples pre-treated according to NR-SAS / SOP 1 that have been dried in an oven set at 105°C for 2 hours ± 10 minutes.

A.5.0.15 *Reagents*

4 mol/l hydrochloric acid (RPU 106)

A.5.0.16 *Determination of total carbon*

Weigh (to 0.001 mg) and tightly pack into a small aluminium-foil capsule a test portion of the soil (plant material). The amount of test portion taken for analysis depends on the expected total carbon content.

Load the sample into the carousel of the automatic sample feeder. The sample mass is entered into the instrument software, align with the sample name and the matrix specific oxygen dosing. Determination of organic carbon

Weigh (to 0.001mg) into a small silver-foil capsule a test portion of the soil sample. The amount of test portion taken for analysis depends on the expected total carbon content. To this sample the 4 mol/l hydrochloric acid should be added drop by drop until any visible reaction stops. If the reaction is too vigorous, part of the sample may be lost due to the foam carrying it out of the boat. In some

cases the sample may have to be dried and the described procedure may have to be repeated in order to complete the purging of the carbonate. Finally the sample must be dried in an oven set at 90°C for 4 hours ± 15 minutes. After drying tightly pack the silver-foil capsule into a larger aluminium-foil capsule

Load the sample into the carousel of the automatic sample feeder. The sample mass is entered into the instrument software, along with the sample name and the matrix specific oxygen dosing.

B

APPENDIX TO CHAPTER 5

B.1 PARTICLE SIZE DETERMINATION

Table B.1: Results from ANOVA of proportion (%) of each soil particle size for Clapham Park in 2012. Degrees of freedom and F-values are given with significance denoted by stars: $p <= 0.001$ (***), $p <= 0.01$ (**), $p <= 0.05$ (*), $p > 0.05$ (ns). Results presented here are from three separate ANOVAs, one for each size fraction.

Term	df	Sand	Silt	Clay
Depth	1	$<0.01^{ns}$	2.40^{ns}	1.49^{ns}
Residuals	70			

B.2 BULK DENSITY AT HELEN'S WOOD

A summary of bulk density data collected from Helen's wood sampled on 16th January 2014 are included here.

Table B.2: Summary of soil bulk density data collected at Helenâs Wood near Clapham Park in January 2014. Due to the low level of replication, this data has not been included in the statistical analysis of bulk density data. Replication is based on three sampling points with three replicates taken at each depth.

	ρ_b g cm^{-3}		mc g 100 g^{-1}		
Depth (cm)	Mean	SE	Mean	SE	n
0-10	0.80	0.02	0.51	0.01	9
10-20	1.00	0.05	0.36	0.01	9
20-40	1.21	0.03	0.26	0.01	9
40-60	1.43	0.05	0.20	0.01	9

B.3 THE EFFECT OF CORE VOLUME ON SOIL BULK DENSITY

Since the volume of soil bulk density (ρ_b) samples, whilst known, was not uniform, there remained the question of whether differences in core volume resulted in a systematic bias of the experimental results.

It is clear that core volume did have an impact ($p < 0.01$) on ρ_b measurements overall (Figure B.1), but when examined at the treatment × depth level (Figure B.3), and at the level of individual sampling locations thereby reducing variation

due to soil heterogeneity: the relationships vary wildy, and there does not appear to be a systematic bias.

Since it was easier to remove a long core in a more heavily clay soil, it is likely that longer cores simply contained more silt, whilst more shallow samples were affected by a greater sand content, which tended to be lower at greater depths (Figure B.2).

```
##
## Error: depth
##          Df Sum Sq Mean Sq
## coreVol   1   22.4    22.4
## depth     2   56.4    28.2
##
## Error: Within
##                 Df Sum Sq Mean Sq F value  Pr(>F)
## coreVol          1    0.3   0.333   28.91 8.2e-08 ***
## coreVol:depth    3    0.1   0.033    2.86   0.036 *
## Residuals     2972   34.3   0.012
## ---
## Signif. codes:  0 '***' 0.001 '**' 0.01 '*' 0.05 '.' 0.1 ' ' 1
```

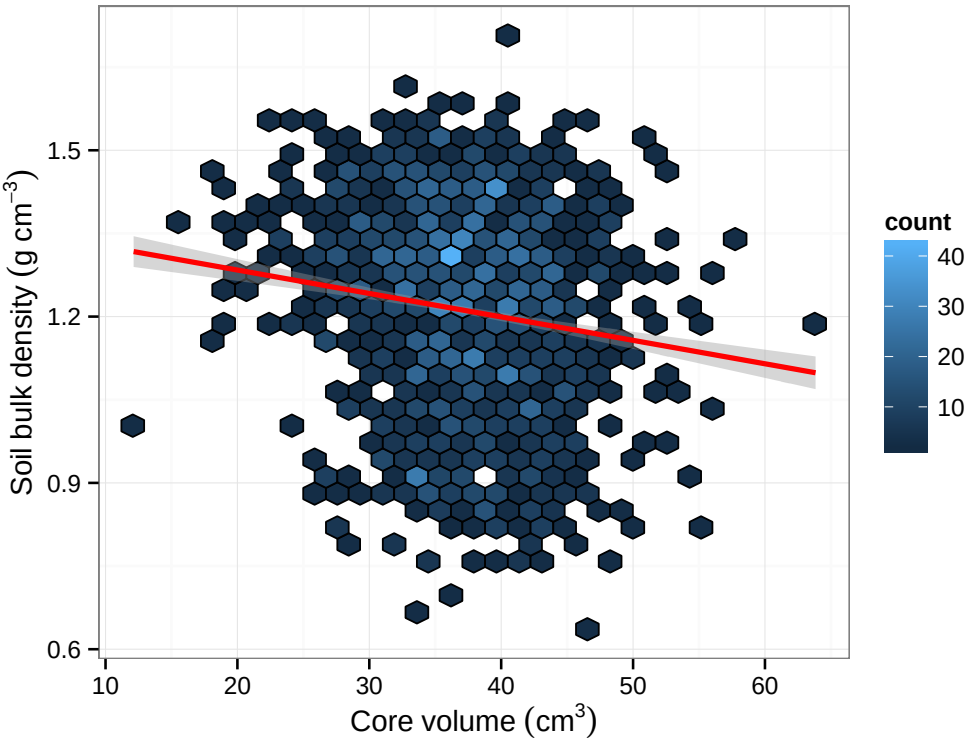

Figure B.1: Soil bulk density (g cm^{-3}) as a function of sampling core volume (cm^3) overlayed with the linear model described in the above statistical output.

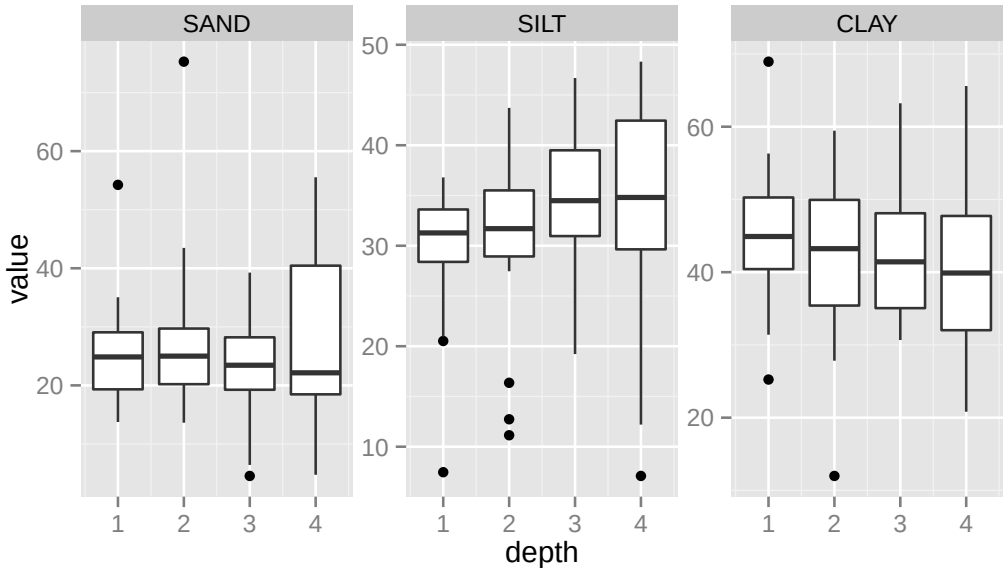

Figure B.2: Proportion (%) of each particle size classification found at each depth increment.

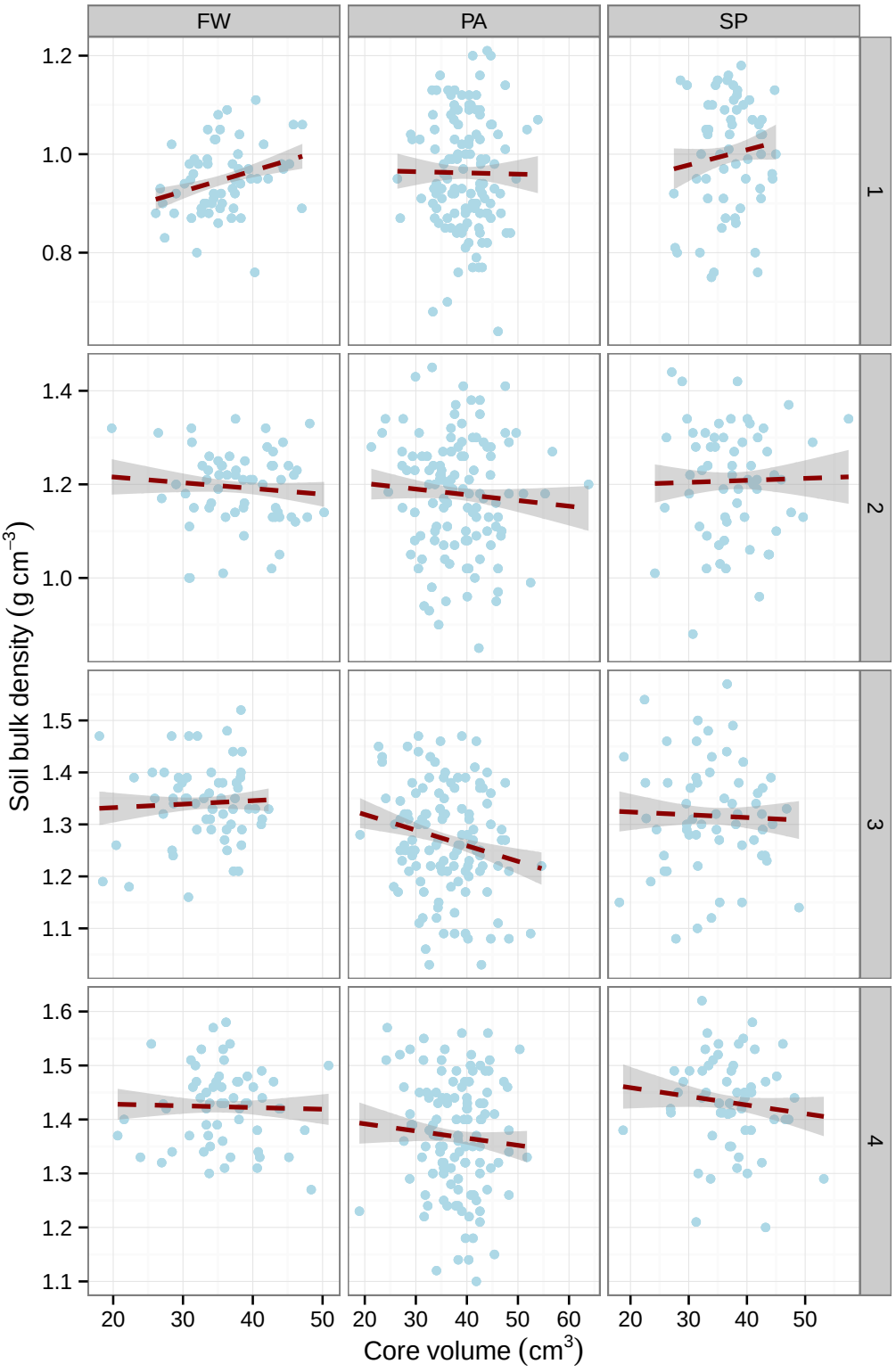

Figure B.3: Soil bulk density (g cm^{-3}) as a function of core volume (cm^3) for each treatment and depth combination. Dashed red lines show the overall relationship at the treatment × depth level. Grey shading indicates 95% confidence intervals of the regression.

B.4 PROTOCOLS AND ADDITIONAL METHODS

B.4.1 *Particle size distribution: NR-SAS / SOP 5/ Version 1*

B.4.1.1 *Source*

This SOP is based on the British Standard BS 7755 Section 5.4:1998 Determination of particle size distribution in mineral soil material - Method by sieving and sedimentation which is identical to ISO 11277:1998.

B.4.1.2 *Scope*

This SOP specifies a basic method of determining particle size distribution (PSD) applicable to a wide range of mineral soil materials, including the mineral fraction of organic soils.

This SOP does not apply to the determination of the PSD of the organic components of soil, i.e. the more or less fragile, partially decomposed, remains of plants and animals. It should also be realised that the chemical pre-treatments and mechanical handling stages in this SOP could cause disintegration of weakly cohesive particles that, from field inspection, might be regarded as primary particles, even though such primary particles could be better described as aggregates.

B.4.1.3 *Principle*

Organic matter in the soil is destroyed with hydrogen peroxide. The resulting slurry is dispersed with buffered sodium hexametaphosphate solution, and the various particle size fractions are determined by a combination of sieving and sedimentation. The latter makes use of the pipette method.

B.4.1.4 *Laboratory sample*

Use air-dried soil samples, for example samples pre-treated according to NR-SAS / SOP 1.

B.4.1.5 *Apparatus*

- Numbered, 250 ml capacity polycarbonate centrifuge bottles, complete with leak-proof caps. Check the bottles for cracks before use. Those which are badly cracked or leak must be discarded.
- Hotplate set at 100°C.
- Numbered towers of wire-mesh, brass or stainless-steel sieves. Unless otherwise specified, these will consist, in descending order, of sieves with the following apertures: 0.6 mm, 0.212 mm and 0.063 mm. At the base of the tower place is a receiver. Fewer sieves may be required on occasion, as may be others of different apertures. Record changes in sieve sizes and sieve identification numbers on the record sheet. Whatever is used, the principle is the same - coarsest at the top. The sieve sequence must always be recorded on each study. Check the fit between sieves at regular intervals. If they become

ill-fitting, mark the tower 'DO NOT USE' and report the defect to laboratory management.

B.4.1.6 *Reagents*

- 100 vol hydrogen peroxide solution - this solution looks harmless but is extremely corrosive. It causes severe burns to the skin and will destroy eyesight within seconds. Whenever handling this solution you must wear undamaged gloves and a face-mask. This solution must always be taken from a container to which a dispenser has been fitted. Never attempt to pour this solution from one container to another. Always wash out these containers prior to disposal. If any of this solution is spilt, use copious quantities of water to dilute it before any attempt is made to mop it up.
- buffered sodium hexametaphosphate dispersing solution (RPU 1)
- octan-2-ol

B.4.1.7 *Calibration check*

Ensure buffered sodium hexametaphosphate dispenser gives 20 ml $\pm$ 2 ml

B.4.1.8 *Sedimentation times*

The sedimentation time at 25°C and at a sampling depth of 9 cm is as follows.

- 0.002 mm - 6 hours 23 minutes

B.4.1.9 *Procedure for removal of organic matter*

1. Place approximately 10 ml of air-dry, <2mm soil in a labelled polycarbonate bottle, using the specially made 10 ml brass scoop.
2. Add, by measuring cylinder, 30 ml $\pm$ 1 ml of water to each soil sample bottle, and 25 ml $\pm$ 2.5 ml , by dispenser, of 100 vol hydrogen peroxide solution. Point the bottle away from yourself and others as spectacular frothing may occur.
3. Gently swirl to mix the contents. Place the bottle on a cold hotplate in a fume cupboard. Keep a careful eye on the bottle for the next few hours. If the contents show signs of vigorous frothing, add a few drops of octan-2-ol by means of a Pasteur pipette. Leave the bottle on the cold hotplate overnight.
4. Switch on the hotplate and raise the temperature to 100°C $\pm$ 2°C. Leave the bottle at this temperature for at least 2 hours. Control any frothing with a few drops of octan-2-ol. Do not allow the contents of the bottle to dry out, add more water if necessary.
5. If there appears to be incomplete decomposition of the organic matter, remove the bottle from the hotplate, allow to cool, add another 25 mm $\pm$ .5ml, of peroxide and replace on the hotplate. For most soils, one treatment should be sufficient. Do not allow the contents of the bottle to dry out, add more water if necessary. When the decomposition appears to be complete, remove the bottle from the hotplate, and allow to cool.

B.4.1.10 *Procedure for dispersal and wet sieving*

1. Balance bottle to 200 g ± 1 g by adding demineralised water. Put on the screw cap, and shake the contents of the bottle vigorously. Inspect for leaks. If there are any, transfer the contents of the bottle to a new one without visible loss of sediment. Centrifuge the bottle and contents at 2000 rpm ± 100 rpm, for at least 20 min and discard the supernatant.
2. Add, by dispenser, 20 ml ± 2 ml of buffered sodium hexametaphosphate dispersing solution to each bottle. Add, by measuring cylinder, 150 ml ±2 ml of water, cap and shake thoroughly.
3. Place the bottles on the end-over-end shaker overnight (18 hours). Remember to adjust the timer if the bottles are to be shaken over the weekend, so that the total shaking time does not exceed 18 hours.
4. Add, by dispenser, 20 ml ± 2 ml of buffered sodium hexametaphosphate dispersing solution into a weighed, to 4 d.p., glass bottle. Place the bottle and contents in the oven set at 105°C and dry overnight. Allow to cool in the desiccator and reweigh (*d*)
5. Place a large plastic funnel into one of the 500 ml measuring cylinders. Place a 0.063 mm sieve in the funnel. Choose the appropriately numbered bottle for the cylinder, and pour the contents of the bottle onto the sieve. Wash all the material out of the bottle and cap onto the sieve, and wash the material on the sieve. The gentle use of a rubber policeman can be used to keep the contents of the sieve moving. The amount of water used must not come above the cylinder graduation.
6. Very carefully wash any residue on the sieve into the appropriately numbered drying tin and dry in an oven set at 105°C ± 2°C for a minimum of four hours

B.4.1.11 *Procedure for dry sieving the sand fraction*

1. Sieve the contents of each beaker in turn through a nest of sieves on the sieve shaker for a minimum of 15 minutes.
2. Record the mass, to 4 d.p., of each full sieve and sample and then just the sieve on the results form.
3. The contents of the receiver should be returned to the cylinder for that sample, and the volume made up to 500 ml with demineralised water.

B.4.1.12 *Determination one silt and one clay fraction by pipette extraction*

1. Place the cylinders in a water bath. The water bath and cylinders need to be equilibrated to 25°C overnight, before sampling is to take place. Record this temperature using a thermometer.
2. Weigh, to 4 d.p., the masses of two sets of glass bottles according to the following scheme on the record form:

    - One set of bottles in the spaces opposite the 0.002 mm - 0.063 mm.
    - One set of bottles in the spaces opposite the <0.002 mm space.

- Stir the cylinder for approximately 30 seconds to thoroughly mix the contents, avoiding a vigorous action which might introduce air (the stirrer should not go above the level of the liquid). At the end of stirring begin timing. Immediately pipette a 25ml aliquot into the appropriate 0.002 mm - 0.063 mm bottle at a depth of 10 cm from the surface of the liquid - do not lower the pipette during sampling. This portion of sample contains silt plus clay. After the sedimentation time for a 0.002 mm particle has elapsed (6 hours 23 minutes), pipette another 25 ml aliquot into the appropriate 0.002 mm bottle, at a depth of 9 cm from the new surface of the liquid - do not lower the pipette during sampling. This portion of sample contains only clay.
- When the second round of sampling is complete, dry all the sample bottles by placing in an oven set at 105 °C) ± 2°C for a minimum of twenty four hours.
- Remove the dried bottles from the oven and cool in a desiccator. Weigh each bottle in turn, and record the weight in the appropriate place on the form.

B.4.1.13 *Expression of results*

- The Dispersant Factor (D) is calculated and recorded to four decimal places.
- The Factor (F) is calculated and recorded to four decimal places.
- The particle size fractions are calculated and recorded to two decimal places.
- The results for particle size distribution are reported to two decimal places.

B.4.1.14 *Calculation of PSD for one silt and one clay fraction*

- d = oven-dry mass of sodium hexametaphosphate dispersing solution (g)
- Z = mass of 0.002 mm-0.063 mm (pipetted sample (Silt + Clay)
- C = mass of <0.002 mm pipetted sample (Clay)
- S = Total mass of SAND (may be one or several fractions)

$$\text{Dispersant Factor } (D) = \frac{d}{20}$$

$$\text{Factor } (F) = S + ((Z - D) \times\ 20)$$

The following stage is repeated for each separate sand fraction:

$$\%\ \text{Sand} = \text{Mass of Particular Sand Fraction} \times 100F$$

$$\%\ 0.002 - 0.063\text{mm} = (Z - C) \times\ 20 \times\ 100F$$

$$\%\ < 0.002\text{mm} = (C - D) \times\ 20 \times\ 100F$$

Addition of all percentages should give 100% $\pm$ 0.2% If it doesn't, check your arithmetic. If it still doesn't, then check all your weighings. If the error is still too great, inform laboratory management. DO NOT THROW ANYTHING AWAY AS YOUR PROBLEM MIGHT IDENTIFY A MORE SERIOUS ONE.

B.4.2 *Adjustment to organic carbon determination method*

During analysis of C_o%, spurious readings were found for some samples in the three deepest increments. Soil at these depths was found to be very high in inorganic carbon, which posed problems for the detection of very low levels of organic carbon – as low as 0.5%. Furthermore, the opposite problem was found, in that the elemental analyser gave a number of zero values for organic carbon content despite showing values for nitrogen and hydrogen. All zero values were repeated until non-zero values were obtained; conversation with the elementar maintenance engineer suggested that zero values were likely a results of too low absolute levels of carbon within the sample. In order to maximise the likelihood of detecting very low values of organic carbon, whilst also completely removing all carbonates, the following procedure was adopted:

- Soil samples to be analysed were packed into the largest possible 'silver boat' available - this allowed a much larger sample to be analysed (c. 90 mg)
- Samples were treated within the silver boats with 4 mol l hydrochloric acid (RPU 106), as per NR-SAS/SOP 9/Version 1 (Appendix A.4).
- Samples were treated again with dilute hydrochloric acid (RPU 106) at approximately 2 hour intervals until thoroughly saturated, and no more fizzing occurred.
- Samples were treated with a few drops of concentrated hydrochloric acid (S.G. 1.83 - >95 %), and left for any reaction to occur (approximately 2 hours).
- Samples were dried at 90 °C) and the analysis continued as per NR-SAS/SOP 9/Version 1.

B.5 BULK DENSITY METHODS PILOT STUDY (2012)

Since there was concern that sampling with a soil corer might result in compaction, and therefore greater bulk density measurements compared to the more common ring method, a small pilot study was conducted in early July 2012.

Twelve bulk density samples at four depths were taken from the Clapham Park field site using both the ring and core methods, and the results compared. These results suggest that far from producing greater bulk densities, the core method produce significantly lower values ($p < 0.05$) than the ring method. Further replication would probably yield no significant difference, as this effect seems to have been driven by low core values at one particular depth (30 cm), but importantly, these results do not indicate increased compaction using the core method.

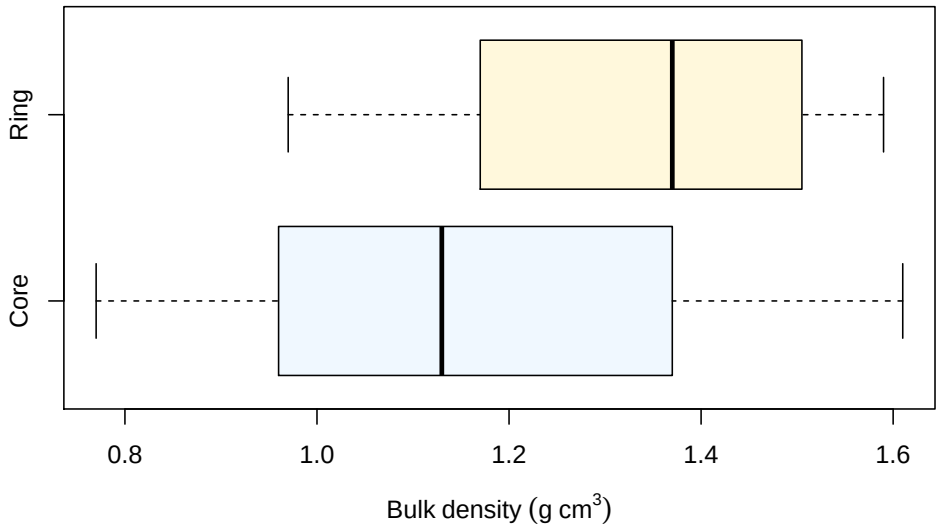

Figure B.4: Results from a pilot study of bulk density methods conducted in July 2012. Mean bulk density obtained with the core method (1.16 g cm^{-1}) were lower ($p < 0.05$) than those obtained with the ring method (1.33 g cm^{-1}).

Table B.3: Results from ANOVA of the two methods of determining soil bulk density.

	Df	Sum Sq	Mean Sq	F value	Pr(>F)
method	1	0.17	0.17	7.26	0.017
depth	3	0.88	0.29	12.76	0.000
method:depth	3	0.04	0.01	0.63	0.604
Residuals	15	0.34	0.02		

Table B.4: Summary statistics for LSD test of Soil bulk density ($g\,cm^{-3}$) × method.

	BD	std	r	LCL	UCL	Min	Max
core	1.16	0.28	11	1.06	1.26	0.77	1.61
ring	1.33	0.21	12	1.24	1.42	0.97	1.59

Table B.5: Groups of statistical similarity for Soil bulk density ($g\,cm^{-3}$) × method. Different letters indicate a significant difference $p < 0.05$.

trt	means	M
ring	1.33	a
core	1.16	b

Table B.6: Summary statistics for LSD test of Soil bulk density ($g\,cm^{-3}$) × depth.

	BD	std	r	LCL	UCL	Min	Max
15	1.22	0.22	6	1.09	1.35	0.77	1.34
30	1.33	0.19	6	1.20	1.47	1.06	1.53
5	0.96	0.10	6	0.83	1.09	0.79	1.06
50	1.52	0.08	5	1.38	1.67	1.40	1.61

Table B.7: Groups of statistical similarity for Soil bulk density ($g\,cm^{-3}$) × depth. Different letters indicate a significant difference $p < 0.05$.

trt	means	M
50	1.52	a
30	1.33	ab
15	1.22	b
5	0.96	c

C

APPENDIX TO CHAPTER 7

C.1 COARSE ROOT MODEL

The 6.4 × 10 m rooting zone was divided into concentric rings of 0.5 m ⌀ (Figure C.1), and the area within these rings calculated (Table C.1).

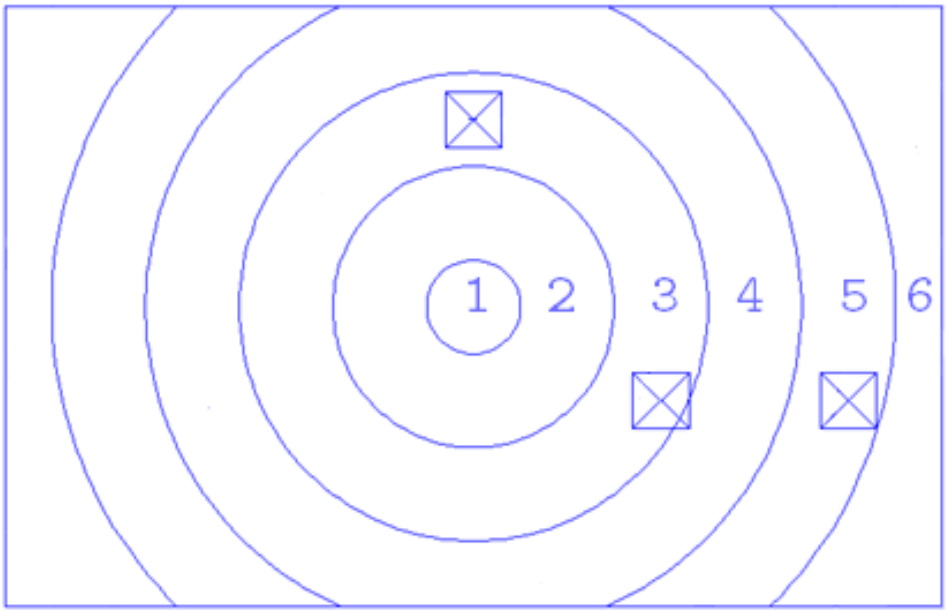

Figure C.1: Theoretical division of rooting zone. Crossed squares indicate the areas sampled for coarse root mass.

Table C.1: Measurements of theoretical rooting zones. Radius of the inside and outside edge, area and cumulative area. Note that the central root zone in Figure C.1 was not included in the coarse root model, as the rootball was extracted from this zone.

#	inner	outer	Area (m^2)	Cumulative area (m^3)
1	0	0.5	0.785	0.785
2	0.5	1.5	6.2832	7.0682
3	1.5	2.5	12.5664	19.6346
4	2.5	3.5	17.7053	37.3398
5	3.5	4.5	14.9471	52.2869
6	4.5	5.9	11.7127	63.9996

For each depth within each treatment, the mass density (kg m-3) recorded in coarse root sampling was regressed against distance using a non-linear

exponential function (Equation C.1) and the nls command in the core 'stats' package in the statistical language R (**?**).

$$\rho_m = \alpha e^{-\beta x} \tag{C.1}$$

The model coefficients established in each of these regressions were then used to predict the mass density (ρ_m) at the middle point (x) of each ring. A summary of the coefficients used in each model is included in Table **??**. The given ρ_m is then multiplied with the appropriate area given in Table C.1, and multiplied by 0.45 to account for depth. The final estimates are presented in Table C.2.

Table C.2: Coefficients used in each of the non-linear regressions as part of the coarse root model.

	Cropped		Fallow	
Depth (cm)	α	β	α	β
0-45	0.722	6.8119	0.2212	3.4305
45-90	0.7918	5.2698	0.3141	3.9089
90-135	2.324	107.0203	0.6503	1.9439

Table C.3: Results from the coarse root model. Mass density (ρ_m) in units of $\mathrm{kg\,m^{-3}}$ is given alongside the final figure for that depth stratum (m) in kg.

		Cropped		Fallow	
Depth (cm)	Distance (cm)	ρ_m	m	ρ_m	m
45	1	3.3091	9.36	2.7498	7.77
45	2	1.6075	9.09	2.2042	12.46
45	3	0.7809	6.22	1.7669	14.08
45	4	0.3794	2.55	1.4163	9.53
45	5	0.1843	0.90	1.1353	5.53
90	1	2.3874	6.75	2.8553	8.07
90	2	1.0816	6.12	2.0857	11.79
90	3	0.49	3.90	1.5236	12.14
90	4	0.222	1.49	1.1129	7.49
90	5	0.1006	0.49	0.813	3.96
135	1	10.4749	29.62	1.0145	2.87
135	2	1.0253	5.80	0.5294	2.99
135	3	0.1003	0.80	0.2763	2.20
135	4	0.0098	0.07	0.1442	0.97
135	5	0.001	0.00	0.0753	0.37

D

APPENDIX TO CHAPTER 8

D.1 LEEDS POPLAR DATA

Table D.1: Summary of diameter at breast height (D_{bh}), height and volume data used for validation of the Yield-SAFE model from the cropped treatment at the Leeds experiment (Pillbeam, D, personal communication, 2014). The final three years of height measurements were excluded, as they were inconsistent with previous measurements, and no measurements were taken in 2013 or 2014. Means are given with standard errors, and the sample size in parentheses.

Year	D_{bh}(cm)	Height (m)	Volume ($m^3\,ha^{-1}$)
		Cropped	
1993	33.7 ± 1.3 (14)	3.4 ± 0.1 (14)	0.0 ± 0.0 (14)
1994	57.8 ± 3.3 (15)	4.3 ± 0.2 (15)	0.0 ± 0.0 (15)
1995	83.9 ± 3.9 (15)	5.4 ± 0.2 (15)	0.0 ± 0.0 (15)
1996	106.5 ± 3.6 (15)	7.1 ± 0.2 (15)	0.0 ± 0.0 (15)
1997	139.9 ± 3.0 (15)	8.9 ± 0.2 (15)	0.1 ± 0.0 (15)
1998	175.9 ± 2.7 (15)	10.5 ± 0.1 (15)	0.1 ± 0.0 (15)
2000	204.3 ± 2.4 (15)	13.4 ± 0.2 (15)	0.3 ± 0.0 (15)
2001	221.3 ± 2.5 (15)	15.0 ± 0.1 (15)	0.3 ± 0.0 (15)
2005	271.9 ± 2.2 (15)	18.0 ± 0.1 (15)	0.6 ± 0.0 (15)
2006	281.7 ± 2.2 (15)	18.9 ± 0.2 (15)	0.7 ± 0.0 (15)
2007	294.3 ± 2.5 (15)	19.4 ± 0.2 (13)	0.8 ± 0.0 (13)
2008	309.3 ± 2.8 (15)	20.1 ± 0.2 (10)	0.9 ± 0.0 (10)
2009	323.9 ± 2.8 (15)	21.2 ± 0.3 (11)	1.0 ± 0.0 (11)
2010	332.7 ± 3.0 (15)		
2011	340.6 ± 3.2 (15)		
2012	346.3 ± 3.5 (15)		
2013	353.5 ± 3.8 (15)		
2014	359.1 ± 3.8 (15)		

Table D.2: Summary of diameter at breast height (D_{bh}), height and volume data used for validation of the Yield-SAFE model from the fallow treatment at the Leeds experiment (Pillbeam, D, personal communication, 2014). The final three years of height measurements were excluded, as they were inconsistent with previous measurements, and no measurements were taken in 2013 or 2014. Means are given with standard errors, and the sample size in parentheses.

Year	D_{bh}(cm)	Height (m)	Volume ($m^3\,ha^{-1}$)
		Fallow	
1993	35.8 ± 1.3 (15)	3.4 ± 0.1 (15)	0.0 ± 0.0 (15)
1994	70.8 ± 1.5 (15)	5.0 ± 0.1 (15)	0.0 ± 0.0 (15)
1995	114.5 ± 2.2 (15)	6.8 ± 0.1 (14)	0.0 ± 0.0 (14)
1996	146.1 ± 2.9 (15)	8.1 ± 0.2 (15)	0.1 ± 0.0 (15)
1997	181.1 ± 3.0 (15)	10.1 ± 0.2 (14)	0.1 ± 0.0 (14)
1998	218.3 ± 3.6 (15)	11.6 ± 0.2 (14)	0.2 ± 0.0 (14)
2000	243.7 ± 4.2 (15)	13.9 ± 0.2 (15)	0.4 ± 0.0 (15)
2001	259.8 ± 5.0 (15)	15.7 ± 0.2 (14)	0.5 ± 0.0 (14)
2005	303.5 ± 7.1 (15)	18.6 ± 0.3 (15)	0.8 ± 0.0 (15)
2006	309.4 ± 7.5 (15)	19.3 ± 0.3 (15)	0.9 ± 0.1 (15)
2007	319.5 ± 8.0 (15)	20.0 ± 0.3 (14)	0.9 ± 0.1 (14)
2008	330.1 ± 8.4 (15)	20.9 ± 0.5 (12)	1.0 ± 0.1 (12)
2009	337.4 ± 8.8 (15)	21.6 ± 0.4 (14)	1.1 ± 0.1 (14)
2010	343.0 ± 9.0 (15)		
2011	348.1 ± 9.2 (15)		
2012	351.8 ± 9.3 (15)		
2013	357.3 ± 9.4 (15)		
2014	359.9 ± 9.6 (15)		

E

APPENDIX TO CHAPTER 9

E.1 ANALYSIS OF TREE RINGS

```
##
## Error: age
##      Df Sum Sq Mean Sq
## site  1   33.5    33.5
##
## Error: age:site
##      Df Sum Sq Mean Sq
## site  6    667     111
##
## Error: age:site:tree
##           Df Sum Sq Mean Sq F value Pr(>F)
## site       6    417    69.5    0.49    0.8
## Residuals  1    142   142.3
##
## Error: age:site:tree:line
##           Df Sum Sq Mean Sq F value Pr(>F)
## site       2   1.30   0.652    1.07   0.41
## Residuals  5   3.05   0.609
##
## Error: Within
##             Df Sum Sq Mean Sq F value Pr(>F)
## site         6    172   28.62      21 <2e-16 ***
## Residuals 1509   2057    1.36
## ---
## Signif. codes:  0 '***' 0.001 '**' 0.01 '*' 0.05 '.' 0.1 ' ' 1
```

```
##   means trt  M   std   r   LCL   UCL   Min   Max
## 1 1.301  RW  f 1.133 123 1.095 1.508 0.149 6.424
## 2 1.713  VD  e 1.243 138 1.518 1.908 0.194 6.704
## 3 2.267  YN  d 1.251 354 2.145 2.389 0.282 6.142
## 4 2.373  BR cd 1.376 125 2.168 2.577 0.274 6.842
## 5 2.512  RY  c 1.210 201 2.351 2.674 0.277 5.733
## 6 3.261  MC  b 1.474 194 3.096 3.425 0.322 7.535
## 7 3.523  CP  a 1.445 402 3.409 3.637 0.591 9.107
```


E.1.1 *Analysis of tree form*

```
##
##  Pearson's Chi-squared test with simulated p-value (based on 10000
##  replicates)
##
## data:  clapham_dbh_ct
## X-squared = 17.34, df = NA, p-value = 0.006999
##
##  Pearson's Chi-squared test with simulated p-value (based on 10000
##  replicates)
##
## data:  clapham_d30_ct
## X-squared = 11.97, df = NA, p-value = 0.005699
```


F

APPENDIX TO CHAPTER 10

F.1 CALCULATING UNDERSTORY, CROP, AND BIOMASS C

F.1.1 *Silsoe silvoarable trial*

F.1.1.1 *Crop yield*

Crop yield was recorded for the cropped treatment in the agroforestry plot and for the arable control for each of the years that it was cropped. This was multiplied by an assumed 50% C content to achieve mean C values.

Table F.1: Carbon content (C ha^{-1}) from crop yields for the ten years that the site was cropped. C content was assumed to be 50%.

	Agroforestry			Arable		
Year	Mean	SE	*n*	Mean	SE	*n*
1993	0.43	0.01	48	0.33	0.03	19
1994	0.76	0.03	60	0.89	0.32	20
1995	3.25	0.05	72	3.91	0.09	11
1996	2.91	0.05	58	3.75	0.07	16
1997	2.24	0.05	72	2.71	0.10	26
1998	1.44	0.03	72	2.19	0.05	27
1999	1.06	0.03	72	1.71	0.05	27
2000	1.80	0.04	72	2.26	0.05	36
2001	–	–	–	–	–	–
2002	1.19	0.05	72	2.10	0.06	27
2003	0.67	0.01	72	1.75	0.03	6
All	1.39	0.34	10	2.16	0.35	10

F.1.2 *Clapham Park*

F.1.2.1 *Total biomass*

The trees at Clapham Park are a native broadleaf mix (Burgess et al., 2000), comprising predominantly oak (*Quercus robur*), ash (*Fraxinus excelsior*), hornbeam (*Carpinus betulus*), small-leaved lime (*Tilia cordata*), and Field maple (*Acer campestre*). In the absence of measurements of the other species, it has been assumed that the ash trees are representative of the other species also[1].

1 Alternatively one could consider the results as a 'what if' scenario, assuming only ash had been planted.

In order to calculate total biomass C storage at the Clapham Park site, the allometric equation for total aboveground C content developed in Table **??** (Equation F.1) was applied to each of the D_{bh} (mm) measurements taken in the FW[2] and PA treatments giving aboveground C (kg),

$$C_{abg} = \alpha D_{bh}^{\beta} CF \tag{F.1}$$

α = regression coefficient (-3.053)
α = regression coefficient (-3.053)
β = regression coefficient (2.124)
α = diameter at breast height ()
CF = correction factor as defined in Equation 9.8 on p. 226 (1.02)

A correction factor was not available for this equation.

Belowground biomass was calculated by applying a second allometric equation for broadleaved trees (Jenkins et al., 2011, p.51) of the same format as Equation F.1 using $\alpha = -3.83$ and $\beta = 2.12$ and D_{bh} in units of cm. Values above and belowground biomass. This equation yields belowground root dry mass in metric tonnes, and therefore was multiplied by the mean C content for ash trees (Table 9.12) of 0.483 to yield the average root C content (metric tonnes).

On a per-hectare basis, the SP blocks were found to contain significantly more biomass C than the FW treatment (Welch two-sample t-test: $t = 12.87$, $p < 0.001$, $df = 90.90$), despite containing 20 % fewer trees. This is due to the fact that trees in the SP blocks tended to have a greater D_{bh} (though were probably less tall) than trees in the FW treatment, and consequently greater above and belowground biomass according to the allometric relationships.

2 Note that only trees planted within areas with a nominal spacing of 2.5 m were used for the farm woodland treatment.

G

MISCELLANEOUS APPENDIX

G.1 CAN ROOT GROWTH INCREASE BULK DENSITY BY COMPRESSION?

Soil bulk density is defined as soil mass divided by total volume:

$$BD = \frac{Mass_s}{Volume_t}. \tag{G.1}$$

The effects that coarse roots are likely to have on this equation, is to reduce the volume available for the soil surrounding the tree. Hence, bulk density may increase as volume declines. Using Silsoe as an example, one can ask whether coarse root growth alone was sufficient to cause an increase in soil bulk density from 1.236 $g\,cm^{-1}$ in the arable control, to 1.36 $g\,cm^{-3}$, in the cropped silvoarable treatment - a change of 0.125 $g\,cm^{-1}$.
Rearranging the equation for bulk density, we can calculate the approximate mass of soil surrounding each tree, using the 'assumed rooting volume' of 10 m × 6.4 m × 1.5 m.
Hence (with $Mass_s$ in $kg\,m^{-3}$):

$$Mass_s = BD \times Volume_t \tag{G.2}$$

```
volume_total  <- 6.4 * 10 * 1.5 # assumed rooting volume (m^3)
mean_bd  <- 1.235556 * 1000  #  m^3
mass_soil  <- mean_bd * volume_total
mass_soil # kg

## [1] 118613
```

Hence, from this calculation, there are 1.1861×10^5 kg of soil in the 96 m surrounding each tree to a depth of 1.5 m.
From biomass measurements taken in 2011, we know the approximate mass of all coarse roots[1]. We can calculate the approximate volume of coarse roots, by dividing this mass by wood density (World Agroforestry Centre, n.d.). This value can then be deducted from soil volume to offer a revised soil volume for use in a new bulk density calculation.

```
wood_density <- 480 # kg m^3
 # mean of Cropped trees:
root_mass <- mean(c(105, 102, 115))
root_mass #kg fresh mass

## [1] 107.3
```

1 Very accurate measurements were taken of the rootball, whilst the remainder of the coarse roots were estimated (Chapter 7).


```
# convert to dry weight using MC%:
dry_root_mass <- root_mass  * (1 - 0.471)
# kg - already dry weight:
cr_mass <- 83.3
root_volume <- (dry_root_mass + cr_mass) / wood_density # m^3

bd_exp <- mass_soil / (volume_total - root_volume)
bd_exp <- bd_exp / 1000
bd_exp # g cm^3

## [1] 1.239
```

Taking into account the change in volume caused by the expansion of tree root growth only, one would expect the soil bulk density to increase to 1.239 $g\,cm^{-3}$, a change of just 0.0038 $g\,cm^{-1}$. Clearly therefore, it is very unlikely that the increase in root volume alone is responsible for the sort of increase in soil bulk density seen at Silsoe in 2011.
Figure G.1 shows the impact that an increase in root mass would have on soil bulk density based purely on volume changes. Since there is some uncertainty about the root mass measurements taken in 2011, root:shoot ratio has been included in the top axis.

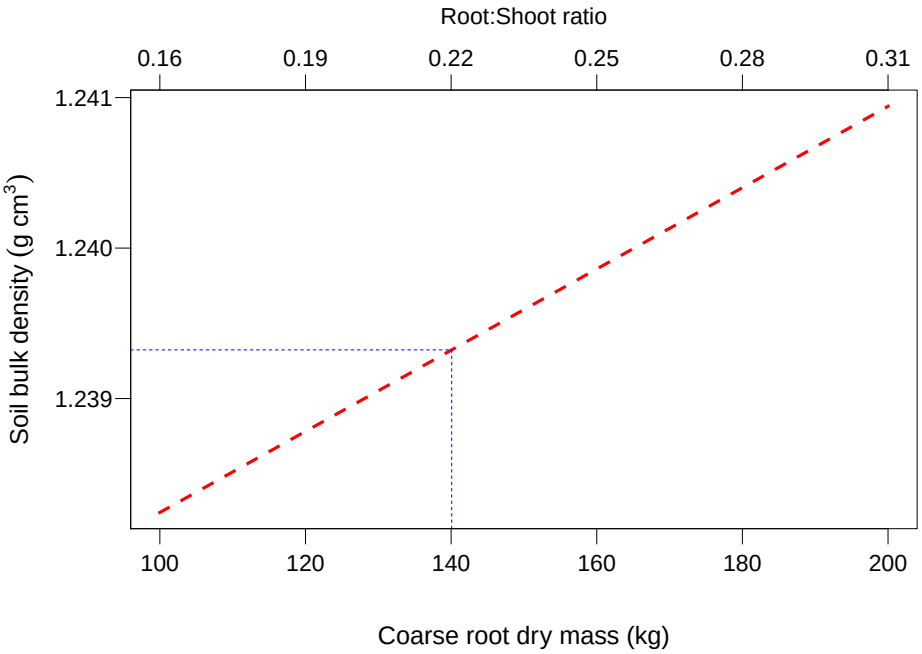

Figure G.1: Soil bulk density as a function of coarse root mass. The equivalent root:shoot ratio for trees in the crop agroforestry treatment at Silsoe in 2011 has been calculated and included in the top axis.

From the literature (Das and Chaturvedi, 2005; Friend et al., 1991; Gielen et al., 2005; Lodhiyal et al., 1995*a*; Lodhiyal and Lodhiyal, 1997; Pallardy et al., 2003; Peichl et al., 2006; Puri et al., 1994), root:shoot ratios for poplar trees

are known to vary between 0.2 and 0.3. Hence, even if our calculations have underestimated root mass, the maximum likely root mass (at a root:shoot ratio of 0.3) would still only account for an increase in bulk density of about 0.005 $g\,cm^{-1}$.

Based on these calculations therefore, soil bulk density may be expected to increase a marginal amount as a result of root growth, however this amount is relatively inconsequential, and not enough to explain values observed at Silsoe in 2011.

H

DATA SOURCES

This appendix provides a summary fo the datasets used in each chapter, and from where each originated. Abbreviation used for the attribution of data generation are incldued in Table H.1.

Table H.1: Explanation of abbreviations used in the data description table. Interns who assisted the author are indicated with a *.

Abbreviation	Full name	Organisation
MU	Matthew Upson	Cranfield University
FC*	François Clavagnier	ESITPA
AG	Andy Gregory	Rothamsted Research
IF*	Irene Friás	Universidad Politécnica de Madrid
EV	Elena Vanguelova	Forest Research
NH	N Hutton	Cranfield University
PB	Paul Burgess	Cranfield University
IS	Ian Seymour	Cranfield University
AB	Arnold Beaton	Cranfield University
SS	Simon Stranks	Cranfield University
PP	Pascal Pasturel	Cranfield University
DP	David Parsons	Leeds University
CS*	Claire Smith	_
EC*	Eleanor Chandler	_

Table H.2: List of datasets used in Chapter 4. The related files are stored in the `data/silsoe_carbon/` directory.

Filename	Year	Origin	
silsoe_coarse_root_data.csv	2011	MU, FC	Root presence data from profile pits at the Cranfield Experimental Farm at Silsoe. The data relates to six trees, and gives the presence of roots > 2 mm for 20 by 20 grid squares.

Continued on next page

Table H.2 – *Continued from previous page*

Filename	Year	Origin	Description
silsoe_fine_root_length.csv	2011	MU, FC	Fine root length and mass data collected from core samples take at Silsoe. The data relates to six trees and gives fine root length mass and density in units of mm cm^{-3} and mg cm^{-3} respectively.
fractionation_2011_data.csv	2011	MU, FC	Combined bulk density (g cm^{-3},`BD`) and organic carbon (g 100 g^{-1}, `OCC`) measurements from the Silsoe trial taken in Summer 2011 by the author and Francois Clavagnier. Fixed depth SOC (`vSOC`) and equiavelent soil mass (`MSOC`) are given in units of t C ha^{-1}.
fractionation_2011.csv	2011	AG, MU, FC	Results from Zimmermann et al. (2007) fractionations completed by Andy Gregory of Rothamsted Research on samples collected at Silsoe. The mass of each fraction (gram,`mass`) and the organic carbon content are given (g 100 g^{-1}, `value`).

Table H.3: List of datasets used in Chapter 5. The related files are stored in the `data/clapham_carbon/` directory.

Filename	Year	Origin	Description
smc_diviner.db (smc)	2013	MU	Soil moisture content data from the Clapham Park field site collected using the diviner 2000 probe. Air and water calibration readings are given alongside the actual measurement (`reading`.)

Continued on next page

Table H.3 – *Continued from previous page*

Filename	Year	Origin	Description
bd.db (bd)	2012, 2014	MU	Spatially located soil bulk density ($g\,cm^{-3}$, `BD`) and moisture content data (%, `MC`) collected at the Clapham Park field site by the author in 2012 for the pasture (PA), silvopasture (SP) and farm woodland (FW) treatments, and 2014 for the mature grazed woodland (MW).
bd_occ.db (bd_occ)	2012, 2014	MU	Spatially located dataset combining organic carbon content measurements ($g\ 100\ g^{-1}$, `OC2`), bulk density ($g\,cm^{-3}$, `BD`), moisture content (%, `MC`), and SOC (,) calculated using the equivalent soil mass method ($t\ C\ ha^{-1}$, MSOC) and fixed-depth methods ($t\ C\ ha^{-1}$, `vsoc`). `MSOC1` and `vsoc1` are the same values but calculated with an additional 13% bulk densty (see Chapter 5 for an explanation).
clapham_MW.db (BD)	2014	MU	Bulk density ($g\,cm^{-3}$, `BD`), and moisture content (%, `MC`) data from the collected from the mature grazed ash woodland, Helen's wood.
clapham_MW.db (PSD)	2014	MU, IF	Results from particle size determination (PSD) of samples collected at Helen's Wood. For an explanation of the raw data, refer to SOP 5 (Appendix: B.4.1). Sand (`sand`), silt (`silt`), and clay (`clay`) % are given.
clapham_MW.db (SOC)	2014	MU, IF	Results from C_o% determination by elementals analysis of samples collected at Helen's Wood ($g\ 100\ g^{-1}$, `OCC`).

Table H.4: List of datasets used in Chapter 6. The related files are stored in the `data/silsoe_carbon/` directory.

Filename	Year	Origin	Description
clapham_sims_summary.csv	2014	MU	Mean mean SOC and standard deviation derived from many different resampling simulation runs, from just 100 to 35 000.
FW_sim_c.csv	2014	MU	Results from 20 000 resampling simulations drawing a random sample (without replacement) from within the data collected in the Farm Woodland treatment at Clapham Park. Columns are named with the following convention: `x_y` where `x` is the statistic calculated from `y`, which is the statistic applied to each of the individual resamples. So: `max_sd` is the maximum standard deviation derived from 20 000 resampling simulations of a given length.
PA_sim_c.csv	2014	MU	Results from 20 000 resampling simulations drawing a random sample (without replacement) from within the data collected in the Pasture control at Clapham Park. Naming convention follows the above.
brown_earths_c.csv	2013	EV, MU	Results from 10 000 resampling simulations drawing a random sample (without replacement) from within the brown earth data presented by Vanguelova et al. (2013).
vanguelova.csv	2013	EV	Original coefficient of variation values for brown earths presented by Vanguelova et al. (2013).

Table H.5: List of datasets used in Chapter 7. The related files are stored in the `data/poplar_biomass/` directory.

Filename	Year	Origin	Description
poplar_hybrid_AI.csv	1995–2011	NH, PB, IS, AB, SS, PP, FC, MU	Current and mean annual increment grouped by hybrid.
poplar_crop_AI.csv	1995–2011	NH, PB, IS, AB, SS, PP, FC, MU	Current and mean annual increment grouped by crop.
final_poplar_biomass.csv	2011	MU, FC	Fresh (kg, `fresh_mass`), dry (kg, `dry_mass`), and carbon mass (kg, `carbon_mass`), moisture content (%, `MC`) and carbon content (g 100 g^{-1}, `CC`).
poplar_wood_bark_data.csv	2011	MU, FC	Thickness (mm), fresh, and dry weight (gram) of bark samples removed from poplar stem (`wood`) and branch samples from the Silsose silvoarable trial.
leaf_mc.csv	2011	MU, FC	Fresh and dry weight (g) of leaf samples collected from trees at the Silsose silvoarable trial.
poplar_carbon_content.csv	2011	MU	Results from elemental analysis of different tree and understorey tissues. Hydrogen, Nitrogen, and Carbon percentage content are given.
coarse_root_mass.csv	2011	MU	Coarse root mass density (kg m^{-3}, `mass`) from six trees at the Silsoe silvoarable trial.
coarse_root_model_output.csv	2011	MU	Output of from the coarse root model, given kg m^{-3} and kg of coarse roots for concentric rings of root area, as described in Appendix C.1.
harvested_tree_dbh_height.csv	2011	MU, FC	Measurements of D_{bh} (cm), and height (m) from the destructively sampled trees at the Silsoe silvoarable trial.

Continued on next page

Table H.5 – *Continued from previous page*

Filename	Year	Origin	Description
silsoe_coarse_root_data_summary.csv	2011	MU, FC	Root presence data with distance from the tree synthesized from silsoe_coarse_root_data.csv.

Table H.6: List of datasets used in Chapter 8. The related files are stored in the `data/poplar_yieldsafe/` directory.

Filename	Year	Origin	Description
leeds_height_dbh1.csv	1992–2014	DP	Mensuration data collected from the Leeds silvoarable network site.
leeds_agf_crop.csv	1992–2002	DP	Crop yield from each of the agroforestry blocks, cropped treatments, and hybrid areas at the Leeds silvoarable experiment. Yield is given in $\mathrm{t\,ha^{-1}}$ (`value`).
leeds_cont_crop.csv	1992–2002	DP	Crop yield from the arable control at the Leeds silvoarable experiment. Yield is given in $\mathrm{t\,ha^{-1}}$ (`value`).
agroforestry_crop_yield.csv	1992–2003	CU	Crop yield from the agroforestry component silvoarable trial at the Cranfield Experimental Farm, Silsoe. Yield is given in $\mathrm{t\,ha^{-1}}$ (`value`).
control_crop_yield.csv	1992–2003	CU	Crop yield from the arable control at the Cranfield Experimental Farm, Silsoe. Yield is given in $\mathrm{t\,ha^{-1}}$ (`value`).
AGFC1992-2022.csv	1992–2003	MU	Output from the adjusted YieldSAFE model using the cropped agroforestry scenario for the years 1992–2022. Aboveground (treeABG) and belowground (treeBG) biomass are presented in g.

Continued on next page

Table H.6 – *Continued from previous page*

Filename	Year	Origin	Description
AGFC1992-2022_fallow.csv	1992–2003	MU	Output from the adjusted YieldSAFE model using the fallow agroforestry scenario for the years 1992–2022. Aboveground (treeABG) and belowground (treeBG) biomass are presented in g.

Table H.7: List of datasets used in Chapter 9. The related files are stored in the `data/ash_biomass/` directory.

Filename	Year	Origin	Description
ash_biomass.csv	2013	MU	Summary of ash biomass data collected at several sites across Bedfordshire in 2013. D_{bh} is given in mm, height is given in cm, and weight in kg.
leaf_area.csv	2013	MU	Leaf area and mass measurements take from Clapham Park in 2013. All masses are given in g, and area in cm^2.
ash_tree_rings.csv	2013	MU	Measurements of tree ring width produced from discs cut from destructively harvested trees from woodlands in Bedfordshire. All measurements are given in mm.
ash_diameter_shrinkage.csv	2013	MU	Dataset charting the difference in diameter branch and stem sections in the round collected from destructively sampled trees. Wet (`wet_dia`) and dry diameter (`dry_dia`) after drying at 105°C are given in mm.

Continued on next page

Table H.7 – *Continued from previous page*

Filename	Year	Origin	Description
ash_wood_bark_dia_weight.csv	2013	MU	Water displacement, bark diameter, wet and dry weight for samples taken from destructively sampled ash trees in 2013. All linear measurements are given in mm, mass values are given in g, moisture content (MC1) is given as a proportion.
PSD.csv	2013	MU	Proportion (%) of each soil size classification derived from the pipette method of PSD for each of the sites at which ash trees were measured.
clapham_psd.csv	2013	MU, CS	Geospatially explicit PSD measurements taken at the Clapham Park field site. Proportion (%) of sand (large, medium, small), silt, and clay are given.
dbh_height_2012.csv	2013	MU, EC	Complete raw data from mensuration of ash trees at eight sites across Bedfordshire. All D_{bh} measurements are given in mm, height is given in cm, and spacing in metre.
ash_leaf_mc.csv	2012	MU	Ash tree leaf wet and dry weight from samples collected at Clapham Park. All weights are given in g, moisture content (`mc`) is given as a proportion of the total dry weight.
biomass_carbon.csv	2012	MU	Results from elemental analysis of tree tissues from sites Millennium Country Park (MP) and Yelnow New Wood (YN). Proportion (%) of Nitrogen, Carbon, and Hydrogen for wood and bark (`type`) tissues.

